Versatile Polymer-Based *Nanomedicines* for Drug/Gene Delivery and Cell-based Therapy Applications.

by

Diana M. Diaz Dussan

A thesis submitted in partial fulfillment of the requirements for the degree of

Doctor of Philosophy

in

CHEMICAL ENGINEERING

Department of Chemical and Materials Engineering
University of Alberta

ABSTRACT

Advances in polymer science and nanotechnology have allowed the development of biomaterials for cell-based applications, such as the delivery of a variety of drugs and genes, as well as supporting technologies, such as stem cell therapies, tissue engineering and cryopreservation. The progress in the synthesis of innovative nano-structures such as liposomes, nanocapsules, polymeric nanoparticles, hydrogels and micelles, have enabled the potential in active and passive targeting delivery as well as the development of stimuli responsive matrices. Polymers play a crucial role in this field, nonetheless various challenges must be addressed such as, improving their loading capacity to enhanced targeted delivery and controlled release in the case of nanocarriers, and in simulating the biological microenvironment, supporting cellular differentiation when using as biological matrices. Complex design of multifunctional polymeric carriers, like stimuli-responsive glycopolymer-based nanoparticles, hydrogels and nanogels, has been demonstrated as an outstanding approach for introducing advanced multiresponsive properties and targeting molecules, triggering target drug/gene delivery and "smart" release. My contributions in this thesis explored the development of leading-edge strategies for the design of glycopolymer-based nanomedicines with a central hypothesis that carbohydrate ligand molecules specific to cell-surface biomarkers will enhance the interaction of these nano-drug systems with target cells by mimicking lectin ligands and antifreeze glycoproteins inspired by nature, which will translate into an increased therapeutic index for the integrated drug/gene and offer enriched cell-therapies capabilities.

In this thesis work, we explored the use of diverse polymer chemistries and architectures to develop gene, drug delivery systems and cryopreservation agents. To achieve this, first

we explored the dynamic bond between benzoxaborole and the hydroxyl groups of the glycopolymer sugars to develop oxaborole-galactose based glycopolymers for the delivery of epidermal growth factor receptor (EFGR) siRNA to treat cervical carcinomas. This reversible interaction provided an effective release of the siRNA cargo inside the cancer cells displaying 60% gene silencing and lower cytotoxicity. Furthermore, we developed dynamic-sugar benzoxaborole polyplexes with a dual capability: a cationic segment to complex with the siRNA and an omega-end modified with an oxaborole group via thiol-ene click chemistry that responds to the acidic tumour microenvironment. This design facilitated the interaction with multiple polyplexes and release of the siRNA in a mildly acidic environment; showing enhanced gene silencing (70%) without elevating the system's cytotoxicity. Then, we decorated a Poly(glycidyl methacrylate) (PGMA)-based polymer with carbohydrate moieties for its application in gene therapy, where an optimum balance of the sugar content needed to be maintained to offer both knockdown efficiency and biocompatibility. In addition, a trehalose-based polyether was developed for cellular cryopreservation demonstrating high biocompatibility and post-thaw cell membrane integrity in cancer and normal cell lines under both controlled-rate and ultrarapid freezing protocols as well as the ability to form hydrogels as 3D cell culture scaffolds. Finally, a hypoxia-activated carbohydrate-based nanogel was explored for the delivery of Iodoazomycin Arabinoside (IAZA), a hypoxia-activated prodrug (HAP), for hypoxic cancer imaging and treatment. IAZA is a HAP that possesses structural features that enable its use as both an imaging and therapeutic agent. Thus, this novel *engineered nanoformulation* is a beyond state-of-the-art approach for theranostic management of hypoxic solid tumors. This technology delivers and provides controlled release of IAZA in physiological conditions, improving the biavailability of the drug in oxygen-deprived cancer cells and enhanced the theranostic effects

when using this nanoformulation (*nano*IAZA) in comparison to the parent drug itself. Superior therapeutic effects were observed with *nano*IAZA when used as a chemotoxic agent (*in vivo*), and in combination with external beam radiation therapy *in vitro* (as a radiosensitizer). *Nano*IAZA described here shows the promise to release IAZA selectively inside hypoxic cancer cells over a longer period, attributing to enhanced drug dose build-up, resulting in further enhancement of therapeutic effects.

The glyco-nanomedicines systems explored in this thesis, have proved to facilitate targeted delivery combined with potential chemotherapeutic treatment — in the case of *nano*IAZA as well as novel cryopreservation scaffolds with the trehalose-based hydrogels, thus offering effective multimodal vectors for biomedical management of diseases like cancer. Based on our proof-of-principle studies and results, I have made an attempt to unfold the pluripotential capability of these glyco-nanomedicines that legitimates and encourages the future design of non-viral glycopolymer-based delivery and scaffolds systems with clinical translation potential capabilities.

PREFACE

This thesis is an original work by Diana Diaz Dussan (Diaz-Dussan, D.) under the supervision of Dr. Ravin Narain (Department of Chemical & Materials Enginnering) and Dr. Piyush Kumar (Deparment of Oncology), and the collaboration of Dr. Michael Weinfeld (Deparment of Oncology) in the University of Alberta.

A portion of **chapter 1** of this thesis has been published by Diaz-Dussan, D.; Kumar, P.; Narain, R.; Engineering, M. As *Glyco-Nanomedicines and Their Applications in Cancer Treatment*, 2nd ed.; Elsevier Inc., 2020. This comprenhensive literature review is my original work.

Chapter 2 of this thesis has been published by Diaz-Dussan, D.; Nakagawa, Y.; Peng, Y.-Y. Y.; Sanchez, L. V.; Ebara, M.; Kumar, P.and Narain, R. As an original peer-reviewed research article titled "Effective and Specific Gene Silencing of Epidermal Growth Factor Receptors Mediated by Conjugated Oxaborole and Galactose-Based Polymers" in *ACS Macro Lett.* **2017**, *6* (7), 768–774. I conceived the experimental design and performed the experiments, data analysis and wrote the manuscript. Y. Nakagawa synthesized the monomers and Y-Y. Peng assisted in the polymer characterization. L. Sanchez assisted with the data collection and R. Narain and P. Kumar co-supervised the development and contributed to manuscript edits.

Chapter 3 has been published by Diaz-Dussan, D.; Peng, Y.-Y.; Kumar, P.; Narain, R. As Oncogenic Epidermal Growth Factor Receptor Silencing in Cervical Carcinoma Mediated by Dynamic Sugar-Benzoxaborole Polyplexes. *ACS Macro Lett.* **2020**, 1464–1470. First authorship was shared between Y-Y. Peng and myself. Y-Y Peng was responsible for the polymer synthesis and a part of the polymer characterization. I conducted all the biological characterization, data analysis and manuscript writing. R. Narain and P. Kumar contributed to the manuscript edits.

Chapter 4 of this thesis has been published by Chen, Y.; Diaz-Dussan, D.; Peng, Y.-Y. Y. and Narain, R. As Hydroxyl-Rich PGMA-Based Cationic Glycopolymers for Intracellular siRNA Delivery: Biocompatibility and Effect of Sugar Decoration Degree. *Biomacromolecules* **2019**, *20* (5), 2068–2074. First authorship was shared between Y.

Chen and myself. Y. Chen was responsible for the polymer synthesis and assisted in analysis and manuscript writing. I designed and conducted all biological characterization and *in vitro* experiments as well as data analysis, and contributed to the manuscript composition. Y. Peng assisted in the polymer characterization and R. Narain contributed to manuscript edits. This work was financially supported by Natural Sciences and Engineering Research Council of Canada (NSERC), the Canada Foundation for Innovation (CFI) and the Science & Technology Program of Wenzhou (Y20180230).

Chapter 5 of this thesis has been published by Diaz-Dussan, D.; Peng, Y.-Y.; Sengupta, J.; Zabludowski, R.; Adam, M. K.; Acker, J. P.; Ben, R. N.; Kumar, P. and Narain, R. As Trehalose-Based Polyethers for Cryopreservation and Three-Dimensional Cell Scaffolds. *Biomacromolecules* 2020, 21, 3, 1264–1273. I conceived the experimental design, performed the experiments, analyzed data and drafted the manuscript. Dr. Jayeeta Sengupta assisted with data collection. Y-Y. Peng and R. Zabludowski contributed to the polymer synthesis, M. K. Adam and Dr. Ben contributed by providing the dose−response curves for the ice recrystallization inhibition (IRI) activities and IRI analysis. Dr. Acker, Dr. Kumar and Dr. Narain assisted with experimental design and manuscript edits.

Chapter 6 of this thesis will be submitted for publication by Diaz-Dussan, D.; Peng, Y-Y.; Rashed, F.; Mcdonald, D.; Weinfeld, M.; Kumar, P. and Narain, R. As "Hypoxia-activated Carbohydrate-based Nanotheranostic to Manage Hypoxic Cancerous Tumours". I conceived the experimental design and performed the polymer characterization, *in vitro* and *in vivo* experiments, data analysis and writing of the manuscript. F. Rashed and Dr. D. Macdonald assisted with *in vivo* hypoxia-selective experiments and data collection. Y-Y Peng contributed with the nanogel synthesis. Dr. Weinfeld, Dr. Kumar and Dr. Narain are supervisory authors that contributed to the manuscript edits and experimental design. Financial support for this study component were provided through Alberta Innovates funded CRIO Program and CRIO Project Cancer grants (Dr. Kumar and Dr. Weinfeld). Animal experiments were conducted under the animal ethics protocol AC18239/18247 "Pharmacokinetics and Radiation Dosimetry Evaluations of Iodoazomycin Arabinofuranoside (IAZA) and Its Translation in Molecular Theranostic Management of Solid Tumors" and AC14208 "Evaluation of IAZA and its prodrugs as theranostic agents

for solid hypoxic tumors" that were approved by the Animal Ethics Committee of the Cross Cancer Institute, Edmonton, AB.

Chapter 7 contains overall discussions and conclusions. It contains sections published by Diaz-Dussan, D.; Nakagawa, Y.; Peng, Y.-Y. Y.; Sanchez, L. V.; Ebara, M.; Kumar, P.; Narain, R.; C, L. V. S.; Ebara, M.; Kumar, P.; Narain, R. As Effective and Specific Gene Silencing of Epidermal Growth Factor Receptors Mediated by Conjugated Oxaborole and Galactose-Based Polymers. *ACS Macro Lett.* **2017**, *6* (7), 768–774; Diaz-Dussan, D. Peng, Y.-Y.; Kumar, P.; Narain, R. Oncogenic Epidermal Growth Factor Receptor Silencing in Cervical Carcinoma Mediated by Dynamic Sugar-Benzoxaborole Polyplexes. *ACS Macro Lett.* **2020**, 1464–1470; Chen, Y.; Diaz-Dussan, D.; Peng, Y.-Y. Y.; Narain, R. Hydroxyl-Rich PGMA-Based Cationic Glycopolymers for Intracellular siRNA Delivery: Biocompatibility and Effect of Sugar Decoration Degree. *Biomacromolecules* **2019**, *20* (5), 2068–2074, and unpublished literature review, discussion and future studies that result from my PhD studies.

Dedicated to my beloved Parents and my loving Husband.

In memory of my Grandmother Inesita.

ACKNOWLEDGEMENTS

I have always been inspired by the complexity of interdisciplinary work. When I started my B.Eng. in Chemical Engineering, my first encounter with a project in collaboration with the Biotechnology, Mycology and Plant Pathology laboratories made me realize that my interests would be to focus on an area where chemistry and biology overlap. I decided to pursue a second major in B. Sc. Microbiology as I sought to integrate both fields through advanced coursework in molecular/cellular biology, organic chemistry and pharmaceuticals. Due to life cirscunstances I decided to explored other avenues and took a little detour from this goal and, after a brief time in the oil and gas industry, I decided to pursue my passion and embark on this academic journey under the mentorship of Dr. Ravin Narain (primary supervisor) and Dr. Piyush Kumar (co-supervisor) on developing polymeric nanomedicines and hydrogels for drug delivery, gene and cell therapy applications. Through the guidance, mentoring, and multidisciplinary expertise provided by both supervisors and mentors, I have had a great academic journey and it has been an honor to be part of such a prestigious university as it is the University of Alberta.

I would like to specially thank my supervisors, Dr. Ravin Narain and Dr. Piyush Kumar, for giving me the opportunity to combine my academic and scientific interest and their willingness to help me conceive my projects. Their confidence in my abilities eventhough I had an unconventional background allowed me to carry on with my dreams. I would also like to give my sincere thanks to Dr. Michael Weinfeld, for his mentorship in cell biology topics and for letting me work in his lab to work with human cancer cells lines. Also, I would like to thank my friends and colleagues Dr. Dawn Macdonald, and Faisal Bin Rashed for providing me with their strong insights into molecular biology and hypoxia; they have been an important resource for completing the *in vivo* studies and to bounce ideas in designing my experiments. I would also like to thank my lab mates Yi-Yang Peng, Anika Benozir Asha, Yangjun Chen and to all current and previous group members of Dr. Narain´s laboratory and the Hypoxia Canada Group that help me in addressing my multiple questions and the important collaborations that we have had.

Many, many thanks to all my family members. To my Parents, thank you for always believing in me, sometimes even more than I do, and for giving me unconditional love. To my loving Grandmother “Inesita” who inspired me to be an accomplish, independent woman, who pursued her academic goals in spite of what society would think. To my Husband, thank you for your patience and understanding during my graduate studies. For providing for our home and accepting my sometimes “unconventional” lab hours. I will love you forever.

This research was supported by the Natural Sciences and Engineering Research Council of Canada (NSERC) and Canadian Foundation for Innovation (CFI). Dr. Kumar and Dr. Weinfeld Alberta Innovates Grants: “Preclinical Theranostic Evaluations of Solid Tumors using FAZA and its Prodrugs (TEST-F): A Hypoxia-selective 'Bench to Bedside' Innovation for Cancer Management and the “Pharmacokinetic and Radiation Dosimetry Evaluations of IAZA and its Translation in Molecular Theranostic Management of Solid Tumors” and the Queen Elizabeth II and DB Robinson Graduate Scholarships awarded to me for funding a portion of my stipend. I would also like to acknowledge the funding provided for my brief travel (due to COVID-19 circunstances) as a visiting research scholar from Dr. Lingxue Kong from Deakin University and the Graduate Student Award (Faculty of Graduate Studies and Research, University of Alberta).

TABLE OF CONTENTS

List of Schemes

List of Tables

List of Figures

List of Abbreviations

AA	Ascorbic acid
ACN	Azido Conjugated Nitroimidazole
ACVA	4,4′-azobis(4-cyanovaleric acid)
AEMA	2-aminoethyl methacrylamide hydrochloride
AGA	*N*-acryloyl glucosamine
AIHS	Alberta Innovates Health Solutions
ALT	Alkaline phosphatase
AML	Acute myeloid leukaemia
ARS	Alizarin Red S
ASGPR	Asialoglycoprotein Receptor
ATRP	Atom Transfer Radical Polymerization
BSA	Bovine serum albumin
CCAC	Canadian Council of Animal Care
CD_3OD	Deuterated methanol
CDK	Cyclin-dependent kinases
CDP	Cyclodextrin-based polymer
CFA	Colony formation assays
CFI	Canada Foundation for Innovation
CNT	Carbon nanotubes
CO_2	Carbon Dioxide
CTA	Chain Transfer Agent
CTLA4	Cytotoxic T lymphocyte antigen 4
CTP	4-cyanopentanoic acid dithiobenzoate
D_2O	Deuterium oxide
DAPI	4',6-diamidino-2-phenylindole dihydrochloride
DCM	Dichloromethane
DCN	Dual-cross-link network
DEGMA	Di(ethylene glycol) methyl ethyl methacrylate
DEP	2,2- dimethacroyloxy-1-ethoxypropane

DI	Distilled
DLS	Dynamic light scattering
DMEM	Dulbecco's modified Eagle medium
DMF	N,N′-dimethylformamide
DMSO	Dimethyl Sulphoxide
DNA	Deoxyribonucleic acid
DOX	Doxorubicin
DP	Degree of Polymerization
DSC	Differential scanning calorimetry
EBiB	Ethyl α-bromoisobutyrate
EBRT	External-beam radiotherapy
ECH	Epichlorohydrin
ECM	Extracellular Matrix
EDA	Ethanediamine
EDTA	Trypsin−ethylenediaminetetraacetic acid
EGF	Epidermal growth factor
EGFR	Epidermal growth factor receptor
EPR	Enhanced permeability and retention effect
FAZA	Fluorine-18-fluoroazomycin arabinoside
FBS	Fetal bovine serum
FDA	Food and Drug Administration
FITC	Fluorescein Isothiocyanate
FMISO	Fluorine-18-fluoromisonidazole
GAEMA	2-gluconamidoethyl methacrylate
GAPMA	3-gluconaminopropyl methacrylamide
GAZ	Azomycin–Glucose Adduct
GLUT5	Glucose transporter protein
GMA	Glycidyl methacrylate
GPC	Gel Permeation Chromatography
GSH	Glutathione
HAP	Hypoxia-activated prodrug

HCl	Hydrogen Chloride
HEMA	2-hydroxyethyl methacrylate
HF	Hypoxic fraction
HIF	Hypoxia Inducible Factor
HIV	Human Immunodeficiency Virus
HOECHST	2'-[4-ethoxyphenyl]-5-[4-methyl-1-piperazinyl]-2,5'-bi-1*H*-benzimidazole trihydrochloride trihydrate
HRP	Horse radish peroxidase
IAZA	Iodoazomycin Arabinofuranoside
IGF	Insulin growth factors
IP	Intraperitonilly
IR	Ionizing radiation
IRI	Ice recrystallization inhibition
LAEMA	2-lactobionamidoethyl methacrylamide
LCST	Lower Critical Solution Temperature
LPLD	Lipoprotein lipase deficiency
MBA	N,N'-methylenebisacrylamide
MPC	2-methacryloyloxyethyl phosphorylcholine
MRI	Magnetic resonance imaging
MRT	Molecular radionuclide therapy
MTT	Thiazolyl blue tetrazolium bromide
MW	Molecular weight
NG	Nanogel
NIPAAm	Poly(N-isopropylacrylamide)
NMR	Nuclear Magnetic Resonance
NP	Nanoparticle
NSCLC	Non-squamous non-small cell lung cancer
NSERC	Natural Sciences and Engineering Research Council of Canada
OER	Oxigen Enhancment ratio
OMEM	Opti-MEM
PAMAM	Poly(amidoamine)

PBS	Phosphate buffered saline
PD1	Programmed cell death 1 pathway
PDI	Polydispersity index
PEG	Polyethylene glycol
PEGMA	Poly(ethylene glycol) methyl ether methacrylate
PEI	Polyethylenimine
PEO	Poly(ethylene oxide)
PET	Positron emission tomography
PFA	Paraformaldehyde
PGAA	Poly(glycoamidoamine)s
PGAAs	Poly(glycoamidoamine)s
PGEA	Ethanolamine (EA)-functionalized PGMA polymers
PGMA	Poly(glycidyl methacrylate)
PKN3	Protein kinase N3
PLK1	Polo-like kinase 1
PLL	Poly L-Lysine
PPIX	Protoporphyrin IX
PROH	1,2propanediol
PSMA	Prostate-specific membrane antigen
PVA	Poly(vinyl alcohol)
RAFT	Reversible Addition−Fragmentation Chain-Transfer polymerization
RISC	RNA Induced Silencing Complex
RNAi	RNA Interference
RNAm	Messenger RNA
ROP	Ring Opening Polymerization
RRM2	Ribonucleotide reductase protein
RTK	Receptor tyrosine kinase
SD	Standard deviation
SDH	Sorbitol dehydrogenase
SER	Sensitizer enhancement ratio
siRNA	Silencing RNA

SPECT	Single-photon emission computed tomography
SST	Somatostatin
TAE	Tris Acetate/EDTA Buffer
TBS	Tween 20 Buffer
TEA	Triethylamine
TEM	Transmission electron microscopy
TEST	Theranostic Evaluations of Solid Tumors
TF	Human transferrin protein
TFA	Trifluoroacetic acid
TGF	Transforming growth factor
THF	Tetrahydrofuran
TK	Tyrosine kinase
UV	Ultraviolet
VEGF	Vascular endothelial growth factor
WGA	Wheat germ agglutinin

List of Publications

Peer Reviewed Journals:

1. Zhao, J.; Diaz-Dussan, D.; Wu, M.; Peng, Y.-Y.; Wang, J.; Zeng, H.; Duan, W.; Kong, L.; Hao, X.; Narain, R. Dual-Cross-Linked Network Hydrogels with Multiresponsive, Self-Healing, and Shear Strengthening Properties. *Biomacromolecules* **2020**, https://doi.org/10.1021/acs.biomac.0c01548. Co-Author.
2. Wang, W.; Xiang, L.; Diaz-Dussan, D.; Zhang, J.; Yang, W.; Gong, L.; Chen, J.; Narain, R.; Zeng, H. Dynamic Flexible Hydrogel Network with Biological Tissue-like Self-Protective Functions. *Chem. Mater.* **2020**, *32* (24), 10545–10555. https://doi.org/10.1021/acs.chemmater.0c03526. Co-Author.
3. Diaz-Dussan, D.; Peng, Y.-Y.; Kumar, P.; Narain, R. Oncogenic Epidermal Growth Factor Receptor Silencing in Cervical Carcinoma Mediated by Dynamic Sugar-Benzoxaborole Polyplexes. *ACS Macro Lett.* **2020**, *9* (10) 1464–1470. https://doi.org/10.1021/acsmacrolett.0c00599 . First Listed Author.
4. Diaz-Dussan, D.; Peng, Y.-Y.; Sengupta, J.; Zabludowski, R.; Adam, M. K.; Acker, J. P.; Ben, R. N.; Kumar, P.; Narain, R. Trehalose-Based Polyethers for Cryopreservation and Three-Dimensional Cell Scaffolds. *Biomacromolecules* **2020**, *21* (3), 1264–1273. https://doi.org/10.1021/acs.biomac.0c00018. First Listed Author.
5. Li, T.; Huang, F.; Diaz-Dussan, D.; Zhao, J.; Srinivas, S.; Narain, R.; Tian, W.; Hao, X. Preparation and Characterization of Thermoresponsive PEG-Based Injectable Hydrogels and Their Application for 3D Cell Culture. *Biomacromolecules* **2020**, *21* (3), 1254–1263. https://doi.org/10.1021/acs.biomac.9b0174. Co-Author.
6. Wu, D.; Wang, W.; Diaz-Dussan, D.; Peng, Y.-Y.; Chen, Y.; Narain, R.; Hall, D. G. In Situ Forming, Dual-Crosslink Network, Self-Healing Hydrogel Enabled by a Bioorthogonal Nopoldiol–Benzoxaborolate Click Reaction with a Wide PH Range. *Chem. Mater.* **2019**, *31* (11), 4092–4102. https://doi.org/10.1021/acs.chemmater.9b00769. Co-Author.

7. Chen, Y.; Diaz-Dussan, D.; Peng, Y.-Y.; Narain, R. Hydroxyl-Rich PGMA-Based Cationic Glycopolymers for Intracellular SiRNA Delivery: Biocompatibility and Effect of Sugar Decoration Degree. *Biomacromolecules* **2019**, *20* (5), 2068–2074. https://doi.org/10.1021/acs.biomac.9b00274. Co-First Author.
8. Peng, Y.-Y. Y.; Diaz-Dussan, D.; Kumar, P.; Narain, R. Tumor Microenvironment-Regulated Redox Responsive Cationic Galactose-Based Hyperbranched Polymers for SiRNA Delivery. *Bioconjug. Chem.* **2019**, *30* (2), 405–412. https://doi.org/10.1021/acs.bioconjchem.8b00785. Co-First Author.
9. Peng, Y.-Y.; Diaz-Dussan, D.; Vani, J.; Hao, X.; Kumar, P.; Narain, R. Achieving Safe and Highly Efficient Epidermal Growth Factor Receptor Silencing in Cervical Carcinoma by Cationic Degradable Hyperbranched Polymers. *ACS Appl. Bio Mater.* **2018**, *1* (4), 961–966. https://doi.org/10.1021/acsabm.8b00371. Co-Author.
10. Peng, Y.-Y.; Diaz-Dussan, D.; Kumar, P.; Narain, R. Acid Degradable Cationic Galactose-Based Hyperbranched Polymers as Nanotherapeutic Vehicles for Epidermal Growth Factor Receptor (EGFR) Knockdown in Cervical Carcinoma. *Biomacromolecules* **2018**, *19* (10), 4052–4058. https://doi.org/10.1021/acs.biomac.8b01066. Co-Author.
11. Nagao, M.; Sengupta, J.; Diaz-Dussan, D.; Adam, M.; Wu, M.; Acker, J.; Ben, R.; Ishihara, K.; Zeng, H.; Miura, Y.; Narain, R. Synthesis of Highly Biocompatible and Temperature-Responsive Physical Gels for Cryopreservation and 3D Cell Culture. *ACS Appl. Bio Mater.* **2018**, *1* (2), 356–366. https://doi.org/10.1021/acsabm.8b00096. Co-Author.
12. Chen, Y.; Diaz-Dussan, D.; Wu, D.; Wang, W.; Peng, Y.-Y.; Asha, A. B.; Hall, D. G.; Ishihara, K.; Narain, R. Bioinspired Self-Healing Hydrogel Based on Benzoxaborole-Catechol Dynamic Covalent Chemistry for 3D Cell Encapsulation. *ACS Macro Lett.* **2018**, *7* (8), 904–908. https://doi.org/10.1021/acsmacrolett.8b00434. Co-Author.
13. Singhsa, P.; Diaz-Dussan, D.; Manuspiya, H.; Narain, R. Well-Defined Cationic N-[3-(Dimethylamino)Propyl]Methacrylamide Hydrochloride-Based (Co)Polymers for SiRNA Delivery. *Biomacromolecules* **2018**, *19* (1), 209–221. https://doi.org/10.1021/acs.biomac.7b01475. Co-Author.

14. Diaz-Dussan, D.; Nakagawa, Y.; Peng, Y.-Y. Y.; Sanchez, L. V.; Ebara, M.; Kumar, P.; Narain, R.; C, L. V. S.; Ebara, M.; Kumar, P.; Narain, R. Effective and Specific Gene Silencing of Epidermal Growth Factor Receptors Mediated by Conjugated Oxaborole and Galactose-Based Polymers. *ACS Macro Lett.* **2017**, *6* (7), 768–774. https://doi.org/10.1021/acsmacrolett.7b00388. First Listed Author.

Book Chapters:

1. Diaz-Dussan, D.; Kumar, P.; Narain, R.; Engineering, M. *Glyco-Nanomedicines and Their Applications in Cancer Treatment*, 2nd ed.; Elsevier Inc., 2020. https://doi.org/10.1016/B978-0-12-819475-1.00066-3. First Listed Author.
2. Peng, Y., Diaz-Dussan, D., Narain, R. Chapter 9. Thermal, mechanical, and electrical properties. *Polymer Science and Nanotechnology*; Elsevier, 2020. Pg. 179-201. ISBN 9780128168066, https://doi.org/10.1016/B978-0-12-816806-6.00009-1. Co-First author.

CHAPTER 1. GENERAL INTRODUCTION

A portion of this chapter has been published as a book chapter in Comprehensive Glycoscience 2nd edition.

Chapter 1

1.1 GLYCO-NANOMEDICINES AND THEIR APPLICATION TO CANCER TREATMENT.

Innovations in the design and development of different nanomaterials for gene/drug delivery and cell therapy applications are currently one of nanomedicine's emphasis areas. In the past few years, gene therapies and personalized nanomedicine have gained momentum as promising successful therapeutics in clinical settings with more examples of regulatory approvals[1]. Still, intracellular delivery and development of safe materials have proved to be the bottlenecks. Multiple hurdles that need to be overcome in transporting drugs/nucleic acids from the site of administration to the target cell include nuclease attack, prevention of diffusion by tightly packed cells, drug/nucleic acid instability, biological membranes, and endocytosis[2]. Transport of drugs/genetic materials to the intracellular targets is arduous due to the cargo's unfavourable pharmacokinetic properties. Nucleic acids are highly susceptible to enzymatic and chemical degradation and are rapidly cleared by the body; due to their negative charge, they are hindered from crossing cellular membranes. Controlled release in the target region in therapeutically effective doses is another challenge faced in delivering pharmaceuticals to bring the desired effect without causing any unwanted toxic reactions due to overdosing. Owing to their large surface area, nanosized systems can offer advanced control over drug release rates entering target cells with greater ease, providing protection and solubility to directed genes or pharmaceuticals, making them more soluble and resistant to proteolytic degradation in the physiological environment[3]. Although viral carriers have been typically used in clinical applications as delivery systems, a range of limitations, including immunogenicity, limited size of transgenic materials, packaging difficulties and the risk of recombination, has been observed[4]. Polymers, particularly glycopolymers, have been one of the most promising synthetic biomaterials employed to design efficient delivery vectors. Carbohydrates —the macromolecules of life—, have attracted researchers for their complex ideal structures. Main functionality of these macromolecules' in the biological system is the recognition on

the cell surface by lectins involved in cell activation and differentiation. Mimicking these units has led to a field of research that first originated in biological sciences but is now found in polymer chemistry.

Progresses in the design of polymers with different molecular weights, charge densities, targeting ligands and modifications tailoring to react to certain physiological conditions have ensured longer circulation times in the body and targeted delivery after internalization[5]. Nonetheless, presently, there is little evidence for an optimum multifunctional polymeric vector design. The US Food and Drug Administration (FDA) and the European Medicines Agency (EMA) have approved numerous nanoparticle therapeutics for clinical use. Still, most of them are liposome-based or iron-oxide colloids[6,7]. Many of these clinically approved nanoformulations are used in the treatment of various cancers. Doxil was the first approved (FDA 1995) cancer nanomedicine, and it is a polyethylene glycol (PEG) functionalized liposomal doxorubicin[8]. The only non-liposomal system currently approved is Abraxane, which is an albumin-bound paclitaxel nanoparticle[9]. Currently, all of these formulations are passively targeted, with no active targeting moieties, taking only advantage of the enhanced permeation and retention (EPR) effect to preferentially accumulate at the tumour sites and limit off-target toxicity[7]. The EPR effect states that nanoparticles' mechanism to enter solid tumours is completed through the extravasation of gaps in the endothelial lining due to the tumours compromise perfusion and leakiness. This has created some debate over the last few years due to the immune cells' potential role in the tumour microenvironment, playing essential parts in nanomedicines' accumulation, retention, and intratumoral distribution; as well as alternative nanoparticle internalization routes like active transport. In addition, the study of small animal xenograft tumour models has shown the extent of tumour heterogeneity in the EPR effect varying heavily between individuals and tumour types[10](Scheme 1-1).

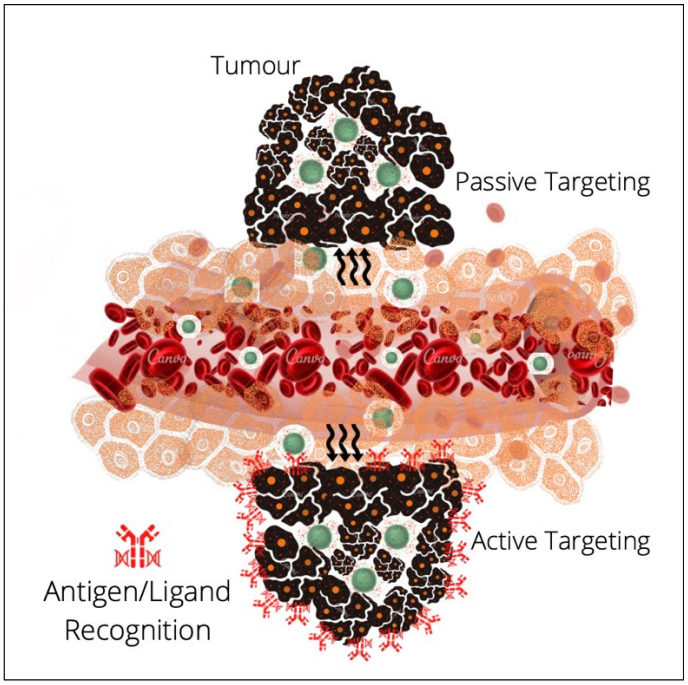

Scheme 1-1. Active and passive targeting mechanism of nanocarriers.

Active-targeting has proved to be advantageous in preclinical settings[11] and the use of polymer-based systems allows the complexation with macromolecules like carbohydrates, enhancing the function of conjugates by conferring cell recognition. The enhanced molecular recognition ability of glycoproteins and glycolipids with specific protein receptors located in the cell membrane, such as lectins, plays a crucial role in many physiological and pathological events, including cellular proliferation, cancer metastasis, intra/intercellular communication, virus and bacteria-recognition processes and adhesion. However, the study of biological phenomena at the molecular level is still in its early stages.

Controlled polymerization techniques like reversible addition-fragmentation transfer (RAFT) and chemical reactions such as ‘click’ chemistry have allowed tuning the polymers' architecture with pendant sugar moieties along the polymer backbone or at the end of the chain, which can interact with lectins through multivalent interactions,

mimicking natural polysaccharides[12]. Complex glycopolymers have been designed as delivery vectors with great success in preclinical stages[13]. Tumour microenvironment regulated glycopolymers[14] have also been explored to enhance the intra-tumoral accumulation and promote drug release at the targeted sites. Tuning the glycopolymers' structure have proved to develop efficient vehicles for systemic delivery. Cationic moieties have been reported to achieve higher gene transfection efficiencies. Still, the inherent cytotoxicity has been subdued with multiple prompt approaches, including acid degradability, to decrease the cytotoxicity while maintaining high gene knockdown[15]. Other types of cationic polymers have been developed by Xu[16–19] and Narain[20] groups by ring-opening reaction and reversible addition-fragmentation transfer polymerization (RAFT) showing optimum transfection rates. Theranostic approaches have also been intended, like branched glycopolymers, developing multi-faceted nanocarriers with several capabilities for diagnosis and therapeutic effects[21]; taking advantage of the tailored design of complex nanovehicles. Likewise, combinational approaches have been explored to attack cancer cells from different fronts to confer enhanced cytotoxicity by combining chemotherapeutic drugs, genes and activation by physical stimuli.

1.2 TYPES OF ANTICANCER NANOMEDICINES IN CLINICAL SETTINGS

As mentioned earlier, most of the applications of nanomedicines have been related to cancer treatment. Cancer is a complex disease that encompasses a cascade of dysregulated gene pathways that leads to a progressive tumorigenesis process[22]. To win the "cancer fight," many novel and combinational therapeutics have matured. Modulation of the biodistribution and target site accumulation, improving the balance between drug efficacy and toxicity are some nanomedicine's main advantages. Passive targeted delivery of anticancer nano-agents is achieved by exploiting a unique characteristic of the leaky tumour cells — the enhanced permeation and retention effect — (EPR effect), as mentioned before[23]. Solid tumours are characterized for extensive angiogenesis, hypervasculature (overexpression of the vascular endothelial growth factor (VEGF)),

defective vascular architecture, impaired lymphatic drainage and increased permeability factors such as bradykinin, nitric oxide, and peroxynitrite[24]. All of these microenvironment changes have been exploited to our advantage in tailoring anticancer medicines.

In addition to the passive targeting achieved through the EPR effect— based on size and physical properties— the nanoparticle surface can be modified with various ligands that could interact with specific receptors overexpressed on the surface of the tumour cells, revealing specificity for active targeting[25,26], as well as the ability to respond to physical stimuli (temperature, pH, etc.) to release the cargo conferring physical targeting. Nanomedicines have been used in combination with conventional pharmacological and physical treatments like chemotherapy and radiotherapy, in multimodal combination therapy regimens. Still, the relatively small number of nanomedicine products approved for clinical use and the discrepancy between the increasing number of preclinical studies has become the focus of intense debate[27]. Understating molecular cancer pathways has emerged new openings for nanomaterials aside from drug/gene delivery, including bioimaging, regulation of the immune system and the tumour microenvironment, radiosensitizers and precision medicine (Scheme 1-2). Better treatments and early diagnosis are the challenges[28].

PEGylated liposomal formulation of doxorubicin (Doxil®/Caelyx®)[8] was the first nanomedicine that received approval in 1995 for ovarian Cancer, HIV-associated Kaposi's sarcoma, and multiple myeloma. Abraxane® is another approved nanomedicine comprised of an albumin-nanoparticle-bound paclitaxel for treating advanced non-small cell lung cancer, metastatic breast cancer, and metastatic pancreatic cancer[9]. Vyxeos is a liposome-based formulation approved in 2017 by the FDA for the treatment of acute myeloid leukemia and Marqibo® is a sulfate liposomal vincristine for Philadelphia chromosome-negative acute lymphoblastic leukemia[29]. It simultaneously delivers two drugs, cytarabine and daunorubicin, to increase treatment efficacy with a lower cumulative dose[30]. In some cases these nanomedicines have become the active therapeutic ingredients[29], not merely

the delivery system; a recently approved (in 2019) radiosensitizer nanomedicine, Hensify®, is a hafnium oxide nanoparticle excited with external radiation to enhance tumour cytotoxicity for locally advanced squamous cell carcinoma. Since 1995 more than 15 nanodrugs have been developed and tested for cancer treatment that have entered the market. All of them are passive, targeting nanoparticles.

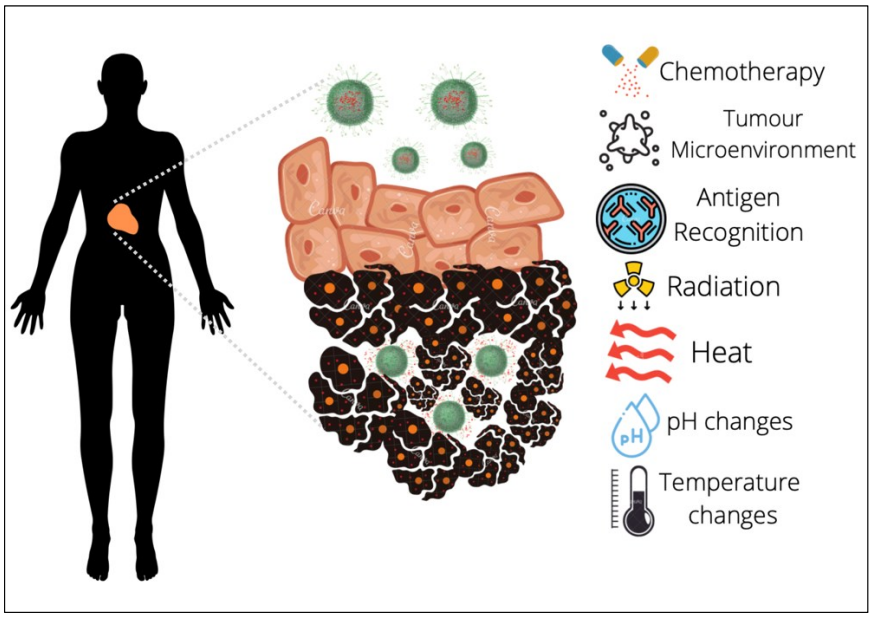

Scheme 1-2. Nanomedicine design based on physical and chemical stimuli.

1.3 OVERVIEW OF GENE DELIVERY

Almost 20 years ago, the understanding of gene regulation was revolutionized by discovering RNA interference (RNAi) in *Caenorhabditis elegans*[31] and the subsequent discovery of silencing RNA (siRNAs) in plants[32]; these two events opened a new platform for gene therapeutics. Gene therapy is the intracellular delivery of genomic materials (transgene) into specific cells to generate a therapeutic effect by correcting an existing

abnormality or providing the cells with a new function. Transfection is a method that introduces foreign nucleic acids into cells to produce genetically modified cells. The foreign nucleic acids (DNAs and RNAs) can either be transiently or stably express depending on the nature of the genetic material. For stable transfection, the transgenes are integrated into the host genome and maintain the expression after the host cells replicate. In contrast, transiently transfected genes are only expressed for a limited period of time and are not integrated into the genome[33]. Since then, target silencing of a specific gene has become a widely used technique to study gene function, and gene expression regulation has shown remarkable therapeutic potential. RNAi regulation of expression is based on the cells' defence mechanism against double-stranded RNA viruses. The process relies on blocking the translation of proteins encoded in viral messenger RNAs (mRNAs). siRNAs (silencing RNAs) are incorporated into a complex called RNA Induced Silencing Complex (RISC) that facilitates cleavage of the foreign mRNAs in the cytoplasm complementary to the built-in siRNAs, halting the target protein from being produced at a translational level. In theory, it is possible to design siRNAs (or vectors encoding them) to target any gene of interest[34] to drug the "undruggable" genome[35].

Gene silencing therapy has evolved from bench to clinic. The elucidation of the molecular pathways governing cancer development, and the encounter of RNAi— a natural post-transcriptional gene silencing mechanism— provided a new tool in the fight against cancer[36] and other diseases. Tumorigenesis is the consequence of multiple genetic and epigenetic occurrences that lead to uncontrollable cell proliferation[37]. Aberrant activation of many oncogenes due to overexpression or oncogenic mutations is often associated with cancer phenotypes, and behind this rationale is the use of silencing gene therapy. Knockdown of cancer-causing genes that compromise the malignant genetic origin has been the reasoning to develop agents that can specifically silence target genes. However, significant delivery challenges, specificity and transfection efficacy need to be overcome before nucleic acids could be used as effective therapeutic agents[38]. Naked siRNAs are

degraded in human plasma within a half-life of approximately 30 minutes[39]. Therefore, to convert siRNAs into an efficacious therapeutic, chemical modifications that prolong siRNA half-life or the design of carriers to deliver siRNA without compromising its biological activity have been implemented.

1.4 siRNA AND CANCER THERAPY

Gene expression profiling has identified distinct signatures of cancer gene expression associated with metastatic capacity and cancer prognosis. Overexpression and/or aberrant activation of specific oncogenes and tumour suppressor genes makes them suitable candidates for nucleic acid-based gene silencing therapies[36]. There are several potential strategies currently being used for targeting cancer using gene therapy including (a) expressing a gene to induce apoptosis or enhance tumour sensitivity to conventional drug/radiation therapy; (b) inserting a wild-type tumour suppressor gene to compensate for its loss/deregulation; (c) blocking the expression of an oncogene by using an antisense (RNA/DNA); and (d) enhancing the immunogenicity of the tumor to stimulate immune cell recognition[40]. Unregulated proliferation is a hallmark of cancer cells; siRNA techniques can be employed against cancer targets that govern uncontrolled cell proliferation. Some examples of these targets are cyclin-dependent kinases (CDKs)[41], insulin growth factors (IGF)[42], epidermal growth factors (EGF)[43,44] (which regulate cell cycle and cell proliferation), vascular endothelial growth factors (VEGF)[45,46] (which regulated blood vessels formation) and a large number of tumor suppressor genes including p53[47] (which regulates cell cycle and apoptosis) retinoblastoma gene Rb[48] (which regulates cell cycle and differentiation) and PTEN[49] (which regulates cell survival). Proliferation signals are generated by growth mediators like the interaction between EGF and the epidermal growth factor receptor (EGFR), an oncogenic trans-membranous receptor, which due to mutations, is overexpressed in multiple human cancers[50–53]. Somatic mutations involving EGFR lead to its constant activation, which triggers intracellular cascades promoting cell proliferation, division and survival[54]. Despite the tremendous

promises, many questions need to be solved before siRNA therapy can be used to safely and effectively treat human cancers. One of the biggest defies for siRNAs to work as therapeutic agents is delivery[34].

1.5 DESIGN CHARACTERISTICS OF VECTORS IN NANOMEDICINE

Colloidal systems and their molecular interactions have been used to create or modify materials by controlling their physical and chemical properties in the nanometer scale [55]. The basic process of gene therapy involves the transfer of a gene using a carrier known as a "vector". Essentially gene transfer vectors can be divided either into non-viral or viral-based gene transfer systems. Viruses such as adenovirus, adeno-associated virus, and lentiviruses are the most common types of vectors used in gene therapy. The viruses are genetically altered to control virulent activity in order to make them safe before their use as vectors for gene therapy but some immunogenicity and cytotoxicity has been observed in the past, and concerns about insertional mutagenesis (ectopic chromosomal integration of viral DNA that disrupts the expression of tumour suppressor gene or activates oncogenes leading to the malignant transformation of cells) are still encountered. Physical methods for gene delivery has also been employed, nevertheless, the application of these methods for gene transfer have been overlooked in the past due to their poor efficiency of delivery causing a low transient expression of their transgenes[56].

Non-viral vectors have been widely used as effective delivery vehicles. Cationic polymers and lipids that form nanosized complexes with nucleic acids are the foremost non-viral vectors use in gene delivery. Polyplexes (polymer complexes) and lipoplexes (lipid complexes) have excellent biocompatibility, low immunogenicity and have the ability to deliver large nucleic acids.

Several types of colloidal delivery systems have been developed, including biocompatible nanocarriers, such as nanoparticles, nanocapsules, micellar systems, liposomes and branched polymers, to encapsulate drugs and provide effective delivery of genetic material

(Scheme 1-3). The optimal delivery system depends on the target cells and its characteristics, duration of expression and the size of the genetic material to be incorporated, so there is no one-size-fits-all solution to gene delivery[56]. When designing a specific vector, several characteristics and functionalities need to be considered. The first requisite is the biocompatibility; reducing cell cytotoxicity and adequate clearance from the organism is one of the major challenges. Particle size is also a critical factor in the internalization process. It has been reported that sizes below 400 nm are the most suitable for accumulation in tumours through the EPR effect. This effect is based on the higher permeability of tumour vasculature relative to normal tissue (pore sizes 400–800 nm vs. 5–10 nm), which, in principle, blocks colloidal systems to enter healthy tissues, and enables crossing only in the tumour vasculature[57]. Cellular uptake of the nano-systems most often occurs through endocytosis. When the nanoparticles (NPs) reach the exterior membrane of a cell, they can interact with components of the plasma membrane or extracellular matrix and enter the cell, mainly through endocytosis. Endocytosis leads to the engulfment of NPs in membrane-bound endocytic vesicles, which fuse with early endosomes and become increasingly acidic as they mature into late endosomes. Some delivery materials respond to the low pH environment in endosomes by becoming membrane-destabilizing, thereby enabling DNA/RNA to escape from the endosomes into the cytoplasm followed by their budding and pinching off to form endocytic vesicles. To enhance the rate of cell entry, many delivery systems incorporate ligands that bind specifically to receptors on target cells to trigger receptor-mediated endocytosis. Depending on the cell type, as well as the proteins, lipids, and other molecules involved in the process, endocytosis can be classified into several types. There are five (5) main mechanisms of endocytosis: phagocytosis, clathrin-mediated endocytosis, caveolin-mediated endocytosis, clathrin/caveolae-independent endocytosis, and macropinocytosis. The last four mechanisms are also broadly defined as pinocytosis.

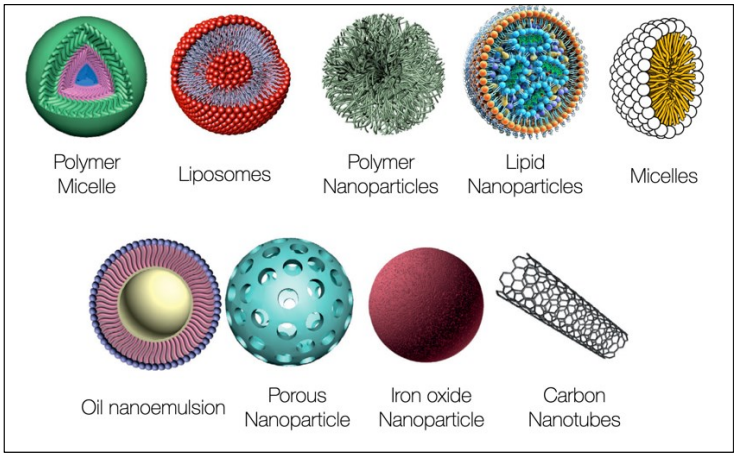

Scheme 1-3. Examples of different nanocarriers used in the nanomedicine field.

Phagocytosis occurs primarily in professional phagocytes (e.g., macrophages, monocytes, neutrophils) and dendritic cells. However, some other types of cells (e.g., fibroblasts, epithelial, and endothelial cells) also have phagocytic activity. Phagocytosis of NPs is usually initiated by opsonization. Opsonins such as immunoglobulins (i.e., antibodies), complement proteins, or other blood proteins (e.g., laminin and fibronectin) are adsorbed onto the NPs' surface followed by binding to phagocytes and ingestion[58,59]. Clathrin-mediated endocytosis is the main mechanism by which cells obtain nutrients and plasma membrane components such as cholesterol via low-density lipoproteins, (LDLs) and iron via the transferrin carrier. It is receptor dependent; clathrins assemble together, triggering the deformation of the membrane into coated pits of 100–150 nm in size. Caveolae-mediated endocytosis is a receptor-mediated cholesterol pathway. Receptors present on caveolae such as insulin receptor and epidermal growth factor receptor can also mediate caveolae-mediated endocytosis. During this process, complexes bind with the cell surface and move along the plasma membrane to caveolae invaginations. Pinocytosis is the internalization of extracellular fluid and its content by cells. Depending on the size of the cell-membrane invagination that traps the extracellular fluid it is called micro- or macropinocytosis[60].

Although these mechanisms have been studied, an improved understanding of both endosomal release and intracellular trafficking of the polyplexes is still needed and could help in understanding the molecular mechanisms of cell-nanoparticle interactions and aid in the design of effective delivery systems.

Another significant parameter that mediates the cellular internalization is the surface charge and surface chemistry. There are two types of intermolecular interactions among nucleic acids/drugs and colloidal biological systems: non-specific and specific interactions. Non-specific interactions are related to van der Waals, structural, hydrophobic and electrostatic forces. Charged nanocarriers can interact with liquids in the medium, creating an electric double-layer force. The combination between this electric force and the van der Waals force is called the DLVO force. This force can be either attractive or repulsive, depending on the distance and nature of the surfaces. Positively charged particles may interact electrostatically with negatively charged components of the plasma membrane's outer leaflet, and subsequently, are internalized by cells, possibly through clathrin-mediated endocytosis. Negatively-charged vectors may be internalized through the caveolae-mediated endocytotic pathway[55]. Specific interactions can be receptor-ligand interactions, cell-protein interactions and other complex biological interactions that can cause specific uptake of the nanocomplexes by the cell[61].

Cationic polymers such as Poly L-Lysine (PLL), poly (ethyleneamine) (PEI) and cationic liposomes such as Lipofectamine, especially the last two, have become gold standards as non-viral vectors for gene delivery. Electrostatic forces between the cationic primary amines of polymers or the positively charged nitrogen in the head groups of the liposomes govern the interactions with the anionic phosphate backbone of the nucleic acids leading to the formation of condensed polyplexes and lipoplexes[62]. Interaction of the polyplexes with the nucleic acid cargo is calculated by the molar ratio of nitrogen's able to be protonated in the polymer repeated unit divided by the ratio of each nucleotide base phosphate (typically termed N/P ratio). In the case of primary, secondary, or tertiary amines,

the charged state of the amines varies in the physiological pH range from about 4.5 to 7, but for polycations whose charge centers remain positively charged throughout this pH range (i.e., pK a > ~8.5), such as quaternary ammonium, amidine, or guanidinium groups the charge ratio is more accurate[63]. Polymer complexes can address several issues, such as 1) protect the nucleic acids from enzymatic and non-enzymatic degradation[64], 2) ensure rapid clearance[65,66], 3) modify interactions with blood components[67,68], 4) enhance cellular uptake[58,69], and 5) increase the drug/gene's half-life in the cytoplasm[65,70]. The efficiency of these vectors, among other properties, depends on the degree of polymerization (DP), molecular weight (MW), branching and charged density. Both PLL and PEI are synthesized by ring-opening polymerization (ROP), exhibiting poor control over molecular weights and high polydispersity. PEI has shown a transfection efficiency comparatively higher than most non-viral carriers, but its non-biodegradability, toxicity and non-specific interactions pose problems for clinical applications[71]. Similarly, Lipofectamine, a liposome-based delivery system, has provided high transfection efficiencies *in vitro* and *in vivo,* but toxicity and off-target silencing remain significant issues[72].

1.6 GLYCOPOLYMERS TARGETED DELIVERY OF GENES AND CHEMOTHERAPEUTIC AGENTS.

Recent advances in polymer chemistry have enabled the design of drug/gene delivery systems using glycopolymers[73,74]. The glycopolymer carrier's size and properties affect the drug/gene delivery behaviour. Desirable functions such as hydrophilicity/water solubility and biodegradability, confer a significant advantage in terms of safety. Besides, controlling the degradability have yield glycopolymers with diverse molecular weights, and conjugation with different ligands have afforded several architectures for precise applications. This design plasticity allows glycopolymers to be used as carriers to deliver various drugs (proteins, DNA, RNA, small molecule drugs, and radiotherapeutic drugs) in multiple formulations. Moreover, anchoring different sugar derivatives on the polymer's chain allows multivalency interactions between the cell surface lectins and the sugar chains

regulating cell internalization, triggering the activation of metabolic and molecular cascades regulated by the genes or drugs delivered. These interactions could inhibit cell differentiation, proliferation and malignant transformation of cancer cells.

The first reported glucose methacrylate derivative (3-O-methacryloxyl-1,2,5,6-di-O-isoproylidine-D-glucoside glycopolymer was reported by Ohno *et al*[75] synthesized by atom transfer radical polymerization (ATRP). Narain[76] and Armes'[77] groups had synthesized sugar methacrylate glycopolymers by atom-transfer radical polymerization (ATRP) with different macroinitiators like poly(ethylene oxide) (PEO), poly (propylene oxide), and poly (ε-caprolactone), enabling to polymerize glycopolymers of 2-lactobionamidoethyl methacrylate (LAEMA) and 2-gluconamidoethyl methacrylate (GAEMA). Armes group has synthesized assorted self-assembled glycopolymers with amphiphilic nature and investigated the glycopolymers' self-assembling properties, using block polymers with galactose methacrylate and hydrophobic methacrylate segments[77]. Hydrophobic segments in the glycopolymers chain can be used to encapsulate hydrophobic medicines, such as doxorubicin, a first-line chemotherapeutic agent in treating some cancers, including soft tissue sarcomas, ovarian, lung and multiple myeloma[78].

McCormick *et al.*[79] reported the first synthesis of 2-Methacryloxyethyl glucosides prepared by reversible-addition fragmentation transfer polymerization (RAFT). Since then, various bulky monomers have been used for the polymerization of Polyacrylamide, Polymethacrylate, Polyvinyl ester, Polyacrylate, and Polyvinyl triazole with Galactose, Mannose, and N- acetylglucosamine, including simple linear glycopolymer structures with this method. Glycopolymers with well-defined architectures that exhibit enhanced biocompatibility, tissue-specific targeting, and colloidal stability have been developed by Reineke[80] and Narain[81] groups by RAFT. Some of the advantages of this technique are that various monomers can be used, and easy modification is achieved through the polymer terminal thiocarbonyl group of the RAFT reagent (Scheme 1-4), allowing useful variations, including Au−S bond formation[82]. Glycopolymer carriers with complex architectures pose

essential features to achieve intracellular delivery by mimicking naturally occurring polysaccharides, enhancing blood biocompatibility and promoting carbohydrate-specific recognition[83]. Diblock copolymer architectures composed of both a cationic block, such as N-(2-aminoethyl) methacrylamide (AEMA) and a hydrophilic block, such as poly (ethylene glycol) (PEG), have increased the colloidal stability of the polyplexes to prevent aggregation. The cationic block encapsulates the DNA/RNA/drug in the core, while the hydrophilic shell provides a steric repulsion to inhibit aggregation and resist clearance by the immune system. A delicate balance between the hydrophilic and hydrophobic residues need to be met to increase the cellular uptake of the nanocomplexes and ensure significant release of the cargo; in this case, carbohydrate blocks serve as the hydrated shell to enhance the colloidal stability while allowing the complex to interact with carbohydrate receptors on the cell surfaces to promote tissue- and organ-specific delivery without hindering the interaction and binding to the cell membrane[80]. Poly(glycoamidoamine)s (PGAAs), a novel class of carbohydrate-based polymers, have also been manufactured by Reineke *et al*. by step-growth polymerization of linear monosaccharides with linear ethyleneamines, creating a poly(ethyleneimine) (PEI) analogue with decreased charge density and increased hydrophilic character making it more biocompatible than PEI[84]. Kiessling studied glycopolymers' binding to lectins with different DPs showing considerable increase in the binding affinities with high DP glycopolymers[82,85]. Higher DP glycopolymers can crosslink lectins and showed a larger binding affinity because of the enthalpy gain with multiple binding, as shown in figure 1-1. Other architectures such as multi-arm star-shaped glycopolymers composed of D-Mannose acrylamide have been homo- and copolymerized with Poly(N-isopropylacrylamide) (NIPAAm) showing dendritic cell-specific intercellular adhesion with two different human lectins (DC-SIGN and MBL)[86].

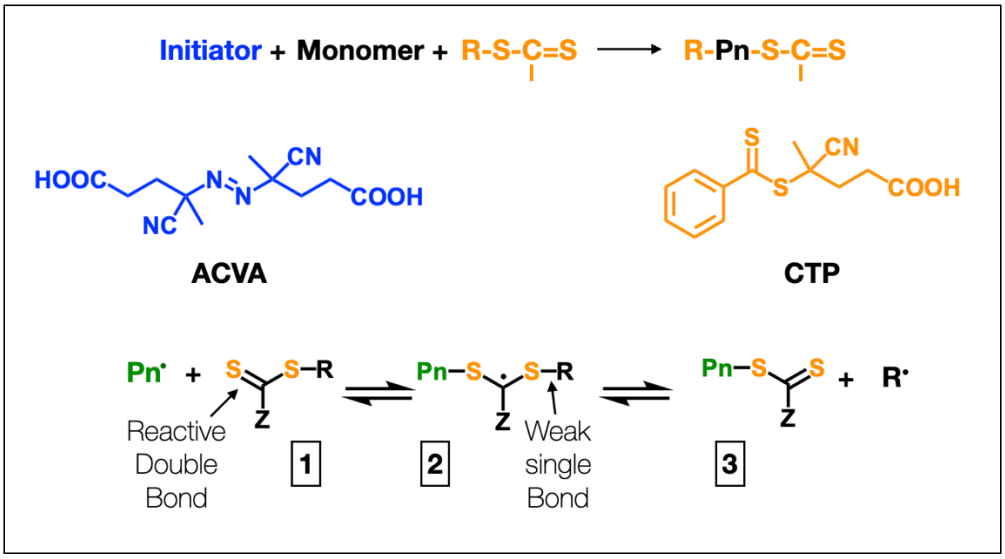

Scheme 1-4. RAFT Process. A dead polymer (Pn•) is activated by an initiator. An initial RAFTagent (1) is converted into a polymeric macro-RAFT agent (3) by sequential insertion of monomer units into a C=S bond. The effectiveness of a RAFT agent depends on the monomer being polymerized and is determined by the properties of the radical leaving group R• and the activating group Z. Modified from *Chem. - An Asian J.* **2013**, *8* (8), 1634–1644[87].

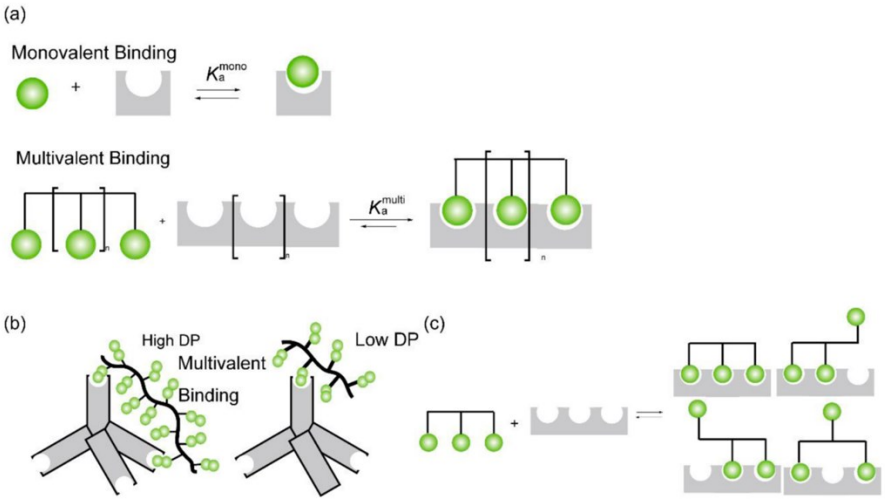

Figure 1-1. Glycopolymer interactions with lectins. Reprinted with permission from (1) Sapsford, K. E.; Algar, W. R.; Berti, L.; Gemmill, K. B.; Casey, B. J.; Oh, E.; Stewart, M. H.; Medintz, I. L.; Chem. Rev. **2013**, 113 (3), 1904–2074. https://doi.org/10.1021/cr300143v. Copyright © 2013, American Chemical Society.

Wang *et al*. reported a drug delivery system based on the glycopolymers' interaction with the asialoglycoprotein receptor (ASGPR) to deliver doxorubicin (DOX) to HepG2 (liver) cells via ASGPR interaction[88]. This strategy is used for active targeting to hepatocytes, which overexpress the ASGPR, which can recognize and bind to galactose or N-acetylgalactosamine residues[89]. Morell and colleagues first discovered the ASGPR when studying the metabolism of ceruloplasmin in 1968. This receptor is conserved across species and highly expressed in hepatocytes (~ 500,000 copies/cell). The binding of ligands depends on Ca^{2+}, the position of terminal galactose residues and optimum pH conditions[90]. The ligands' interaction mechanism with ASGPR has been thoroughly investigated, elucidating the facilitated uptake and clearance of circulating glycoproteins with exposed

terminal galactose and N-acetylgalactosamine, glycans via clathrin-mediated endocytosis[91] (scheme 1-5).

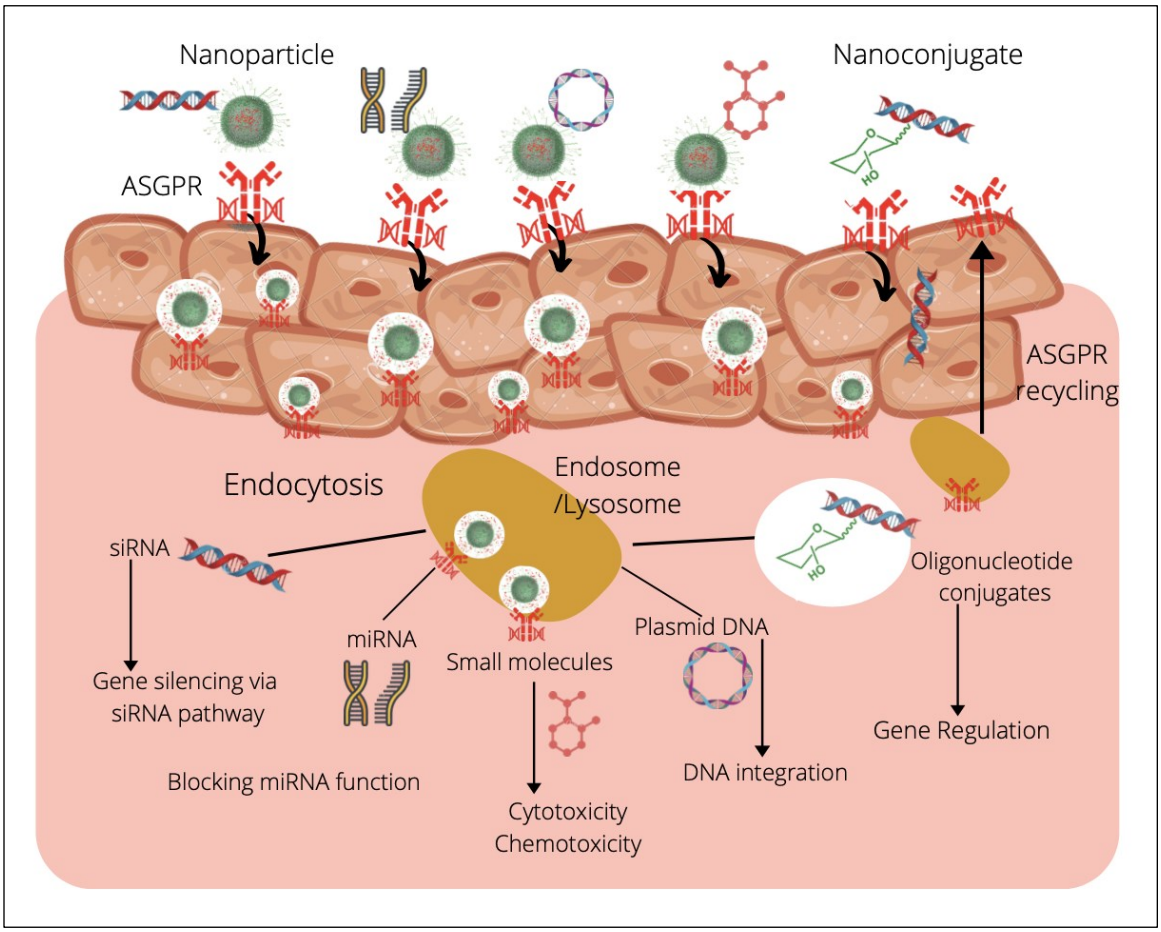

Scheme 1-5. ASGPR-mediated gene and drug delivery to hepatocytes. Galactose-decorated nanoparticles and oligonucleotides loading siRNA, miRNA, Plasmid DNA, small molecules; are recognized by ASGPR, which triggers endocytosis via the clathrin-mediated pathway. Then, the payloads escape from the endosome/lysosome and further mediate gene silencing, block the miRNA function, cause mRNA degradation or DNA integration. Moreover, galactose- conjugates can also be used for liver-targeted delivery of chemo/cytotoxicity small molecules. The exact mechanism for galactose-conjugate

escaping from the endosome/lysosome is still under study. Meanwhile, ASGPR will be recycled to the cell surface to mediate the subsequent internalization. Modified from Huang, Y. Preclinical and Clinical Advances of GalNAc-Decorated Nucleic Acid Therapeutics. *Mol. Ther. - Nucleic Acids* **2017**, *6* (March), 116–132. https://doi.org/10.1016/j.omtn.2016.12.003.

1.7 STIMULI-RESPONSIVE GENE DELIVERY SYSTEMS

Narain and co-workers prepared well-defined cationic glycopolymers of known molecular weights, narrow polydispersity, and novel architectures by RAFT polymerization. They studied the effect of small sugars (glucose and galactose residues) on gene expression efficacies. Various diblocks and random copolymers and hyperbranched glycopolymers have shown enhanced DNA/RNA transfection. Interestingly, gene expression is less dependent on sugar residues and the cationic content, and the degree of polymerization (DP) of copolymers dominated their biological effect[92,93]. The "proton sponge" effect suggests that polymers that can buffer against the endosomal pH yield higher transfection efficiencies by increasing the osmotic enlargement of the endosome, which leads to vesicle rupture and release of the nucleic acid cargo into the cytoplasm[94]. Many proton-accepting groups, including primary, secondary, and tertiary amines, can achieve endosomal escape by causing an influx of chloride and water into the endosome upon increased protonation in an acidified environment.

A cationic segment's conjugation to the glycopolymer is important for complexation with DNA and RNA for gene delivery[59]. Delivery of smaller polynucleotides like siRNA is more defiant than larger nucleic acids (DNA) due to the possible formation of non-stable complexes that can dissociate upon contact with the polyanionic cell surface. Some amphiphilic polymers, such as poly-alkyl-carboxylic acids and polyvinyl ethers, seem to enhance endosomal escape due to their hydrophobic nature. Galactose-based glycopolymers P(LAEMA-*b*-AEMA) have shown high transfection efficiencies and

specific epidermal growth factor receptor (EGFR) knockdown in HeLa cells[59,92]. But one limitation seen is cell toxicity, which increases as the AEMA block lengths decrease[95].

Hyperbranched cationic glycopolymers bearing pendant glucose and galactose residues have succeeded in glycotargeting —a technique for delivering nucleic acids via receptor-mediated endocytosis due to the interactions between cell-surface lectins and carbohydrate vectors—[96]. The nucleic acids' complexation with the glycosylated polymers can be achieved either directly by a covalent linkage or by non-covalent immobilization (H-bonding, electrostatic interactions)[97]. Zhang *et al.* prepared a hyperbranched poly[2-(α-D-mannopyranosyloxy) ethyl methacrylate-co- N, N'-methylenebisacrylamide] (HPManEMA-co-MBA), showing affinity to Concanavalin A and demonstrating low cytotoxicity, thus exhibiting potential for biomedical applications as drug/gene delivery systems[98]. Redox-sensitive and pH-dependent chemical groups have also enhanced the proton sponge effect when added to polymers[99]. Peng *et al*. manufactured acid degradable cationic galactose-based hyperbranched polymers with an acid degradable cross-linker, 2,2-dimethacroyloxypropane (DEP), to allow the breakdown of the polymer in an acidic environment to lower the cytotoxicity. The addition of DEP cross-linker[100] —a pH-sensitive ketal-based cross-linker— has shown to endorse lower cytotoxicity and high gene silencing (95%)[15] (Figure 1-2). Complexation of nucleic acids with a reducible cationic, disulphide-containing polymer such as poly (disulphide amine) can improve transfection and gene silencing compared with non-redox sensitive analogues as a result of the quick disassembly of the complexes under reductive intracellular conditions[101]. Thioketal-based nanoparticles have also been formulated due to their sensitivity to reactive oxygen species in inflammatory tissues. These oxidative-responsive vectors have exhibited the capability to deliver TNFα–siRNA to the sites of intestinal inflammation[101].

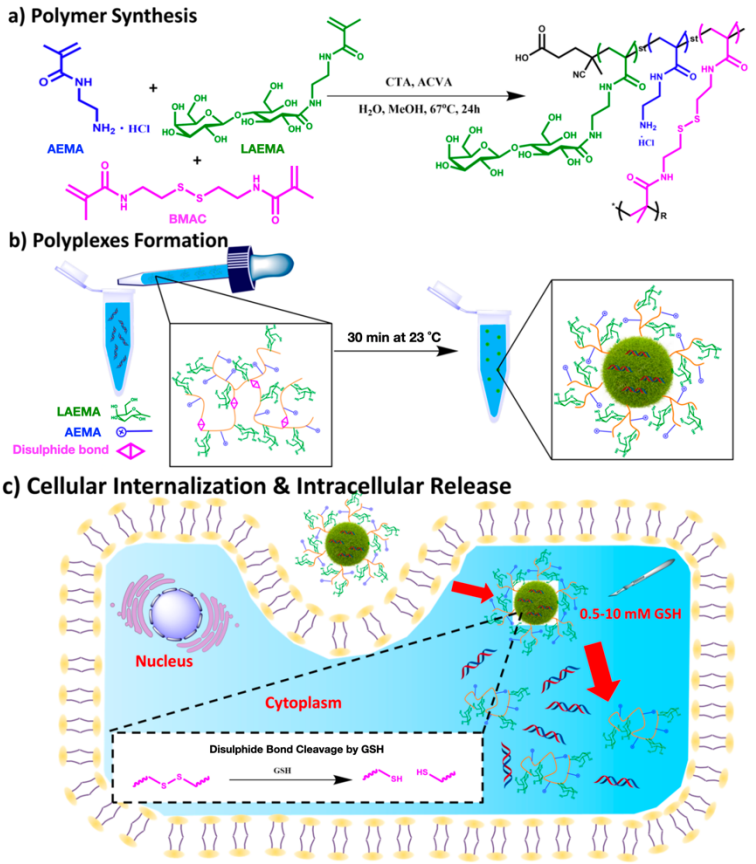

Figure 1-2. Redox-Responsive Galactose-based and Cationic Hyperbranched polymers (P(LAEMA-*st*-AEMA-*st*-BMAC) via RAFT polymerization; (b) Formation of polyplexes via electrostatic interaction between redox-responsive Galactose-based Cationic Hyperbranched polymers and siRNA; (c) Intracellular release of siRNA via degradation of polyplexes due to the cleavage of disulphide bonds in the presence of GSH in the cytoplasm. Reprinted with permission from *Bioconjug. Chem.*, **30**, 405–412 (2019) http://pubs.acs.org/doi/10.1021/acs.bioconjchem.8b00785. Copyright © 2019, American Chemical Society.

Many recent reports described the use of sugars, proteins, or antibodies attached to the polyplexes' surface binding to upregulated receptors on cells[102]. Research is being focused on modifying existing structures with these molecules to lower the toxicity. Lactose moieties bind to hepatocytes through ASGPRs receptors, improved transfection efficiency in glyconanogels and nanoparticles of LAEMA/AEMA[83]. Targeting polyplex delivery to liver hepatocytes has been examined by Kunath *et al*. by substituting B-PEI with galactose groups to target ASGPRs. The PEI amino groups had a galactose substitution degree of 3.5%, 9.7% and 31%, and at N/P of 5 (3.5%), the expression was nearly the same as that obtained with unsubstituted PEI. However, some expression was still noticed in ASGPR-negative cells, suggesting that this system is not yet optimized for hepatocyte targeting[103]. Poly(lysine)-PEG vehicles have also been studied in hepatocellular carcinomas[104]. Hydrophilic PEG moieties sterically hinder interactions with the neighbouring NPs or serum proteins and blood components by creating a hydrated cloud around the NP. Unfortunately, the use of PEG to enhance circulation time has other consequences. The steric hindrance and stealth properties can prevent intended cellular uptake and reduce transfection efficiency. Furthermore, there is still a fraction of serum proteins that can adhere to the vehicle even after PEGylation.

1.8 STIMULI-RESPONSIVE DRUG DELIVERY SYSTEMS

Some polymeric materials exhibit a temperature transition state, where they become hydrophilic or hydrophobic depending on the temperature. These thermoresponsive systems are generally made of poly(N-isopropyl acrylamide) (PNIPAAm), and other amphiphilic block copolymers with AB type or ABA type, whose thermosensitive behavior is adjusted by shifting the hydrophilic/hydrophobic balance in its backbone such as Poly(EVEOVE): poly(2-ethoxy) ethoxyethyl vinyl ether (EOEOVE); PDMA: poly(N,N-dimethylaminoethyl methacrylate); PCIPAAm: poly(2-carboxyisopropylacrylamide);

PEO: poly(ethylene oxide); PPO: poly(propylene oxide); DM-b-CD: heptakis (2,6-di-Omethyl)-b-cyclodextrin; PHB: Poly[(R)-3-hydroxybutyrate]; PLGA: poly(DL-lactic acid-co-glycolic acid)[105] and poly(γ-2-(2-(2-methoxyethoxy)-ethoxy)ethoxy-ε-caprolactone)-b-poly(γ-octyloxy-ε-caprolactone)[101]. Stenzel group has investigated glycopolymer brushes composed of *N*-acryloyl glucosamine (AGA) and NIPAAm using RAFT polymerization showing temperature-responsive properties for drug delivery[106]. Tuning the nature and the composition of the copolymers so that the transition temperature is close to body temperature has proved useful for local administration. Designed at the molecular level, the lower critical solution temperature (LCST) of PNIPAAm can be adjusted to around the physiological temperature of 37ºC by introducing a hydrophilic co-monomer, such as dimethylacrylamide (DMAAm) or acrylic acid (AAc)[105]. Encapsulation of the drugs can be made through electrostatic interactions or to avoid limitations related to physical drug entrapment like uncontrolled burst release or poor drug loading; some drugs can be covalently linked to the nanoparticles or nanogels. The release of the encapsulated drug can be modulated by the degree of crosslinking of the polymer network and the hydrodynamic size[107].

Another type of stimuli-responsive polymers responds to changes in environmental pH. Glycopolymers having an amino group or carboxylic acid group can react to pH fluctuations. The ionic strength of those groups varies between amine and ammonium ion or carboxylic acid and carboxylate. Two main strategies are used: the first one is by using polymers (polyacids or polybases) with ionizable groups that undergo conformational and/or solubility changes depending on the pH, and the second one is to add acid-sensitive bonds to the polymeric design systems whose cleavage enables the release of molecules and the modification of the charge of the polymer or the exposure to ligands. Anticancer drug-delivery systems have exploited a slight difference in pH between healthy tissues (~7.4) and solid tumours' extracellular environment (6.5–7.2). This pH difference is mainly a consequence of dysregulated angiogenesis in fast-growing tumours, shifting towards a glycolytic metabolism due to lack of oxygen, leading to acidic metabolites[108]. Liu *et al*.

reported a pH-responsive micelle formed in acidic condition with a block copolymer of poly (2-(diethylamino)ethyl methacrylate)-co-(3-O-methacryloy-glucopyranose)) via RAFT polymerization[109]. A galactose-based glycopolymer, poly(N-(prop-2-enoyl)-β-D-galactopyranosylamine)-*b*-poly(N-isopropyl acrylamide) pGal-*b*-pNIPAA/doxorubicin (DOX) (GND NPs) showed enhanced cellular uptake to HepG2 cells mediated by the ASGPR, resulting in anti-tumour efficacy in vitro and were observed to be rapidly disintegrated under acidic conditions resulting in an increased release of DOX. Moreover, GND NPs exerted higher anti-tumour effects than free DOX on a transgenic zebrafish TO(KrasG12V) model *in vivo*[110].

Tumour microenvironment-regulated polymers have also been developed to interact with the different molecules involved in cell metabolism. Jin *et al*. reported glucose-responsive carriers with phenylboronic acid form particles for insulin delivery in diabetic patients[111]. Polymer redox-sensitivity can be attained using disulphide bonds, prone to rapid cleavage by glutathione (GSH). The different concentrations of GSH can then trigger the cytosolic release of drugs found in extracellular (~2–10 μM) and intracellular (~2–10 mM) compartments and in tumour tissues. Wu *et al*. proposed (GSH)-responsive core crosslinking galactose-based glycopolymer-drug conjugates (GPDs) NPs with both redox-responsive and pH-sensitive characteristics to target DOX release in cancer cells with high GSH concentrations. A disulphide bond was introduced to the side-chain via a dynamic covalent boronate ester bond between galactose moieties and phenylboronic acid, which exhibits pH-regulated characteristics[112].

1.9 NANOGELS AS NOVEL DELIVERY VEHICLES

Nanogels are one of these “smart” delivery systems due to their stimuli-responsive properties, loading capacity, high stability, cationic/anionic functionalization, and responsiveness to environmental factors (ionic strength, pH, and temperature sensitivity). Nanogels are defined as an aqueous dispersion of hydrogel particles formed by physically

and/or chemically cross-linked, hydrophilic and hydrophobic polymer networks of nanoscale size[113]. Loading biological agents to these vehicles is usually achieved spontaneously through electrostatic, van-der Waals and/or hydrophobic interactions between the agent and the polymer matrix. Nanogels are thermoresponsive materials; they become either soluble or insoluble at a specific transition temperature. When the transition is from a soluble to a less soluble state, this temperature is the LCST. The first phase of this separation is when individual polymer chains undergo an intramolecular collapse due to the loss of water molecules and increased intramolecular hydrogen bonding and hydrophobic forces. This is followed by intermolecular aggregation of collapsed chains and phase separation. Thermo-responsive nanogels with an LCST closed to 37–39ºC have been developed such that in the normal tissues, they are in their hydrophilic swollen state, but in the tumour environment (which is often 1–2ºC warmer than normal tissue), they collapsed and become hydrophobic releasing the encapsulated agent effectively (Scheme 1-6). This thermal change has been functional to enhance drug delivery by improving drug release and higher tumoral uptake[114] .

Addition of stimuli-sensitive monomers or functional biomolecules can lead to versatile macromolecules use as delivery vehicles. For instance, to reduce interaction with serum proteins and extend circulation times, the nanocarrier surface can be modified with hydrophilic inert polymers, such as poly(ethylene glycol) PEG[115]. To enhance site-specific delivery, the nanogel surface can also be decorated with biospecific targeting groups, such as glycopolymeric gold nanoparticles[116], galactose or N-glucosamine molecules that mediate cellular interactions with lectins such as asialoglycoprotein receptors[117] improving cellular uptake in targeted cells.

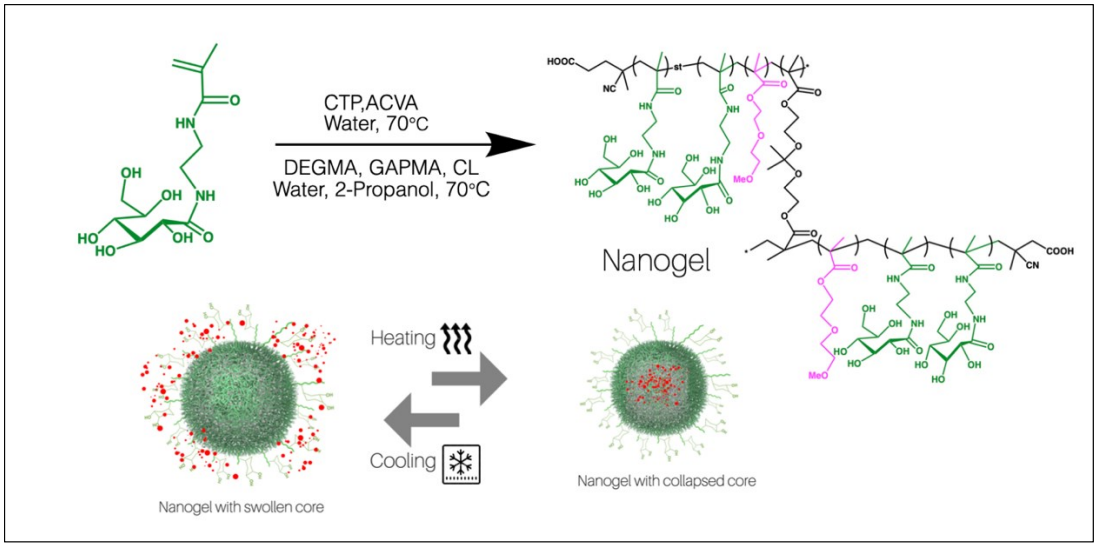

Scheme 1-6. Synthesis of Galactose-Decorated Nanogels and the Encapsulation of pharmaceuticals within the Thermosensitive Nanogel Core.

1.10 NANOTHERANOSTIC GLYCOPOLYMER COMPOUNDS

Nanotheranostic agents combine the advantages of treatment and diagnosis in a single nanoscale carrier. Identifying small tumours requires whole-body imaging techniques that are sometimes not feasible. The major therapeutic challenge is to ensure early clinical diagnosis, to determine tumour heterogeneity and phenotypic diversity due to the cell expansion process and the presence of cells with metastatic potential and multidrug resistance[118,119]. The integration of imaging methods with nanomedicine have led to more efficient preclinical developments, clinical translation and improved therapeutic outcomes.

Polymers such as polyethylene glycol (PEG), poly(D, L-lactic acid), poly(D, L-glycolic acid), and poly(ε-caprolactone) have been approved for clinical use in nanoformulations[28]. Labelling nanomedicines to be tracked using nuclear imaging techniques requires the incorporation of different agents: magnetic resonance imaging (MRI) contrast agents, radioactive agents for radionuclide imaging via positron emission tomography (PET) or

single-photon emission computed tomography (SPECT), fluorescent agents for fluorescent imaging, and nano/microbubbles for ultrasound imaging. Photodynamic therapy (PDT) offers potential applications in the clinic for the treatment of deep-seated tumours. Proposed PDT nanoparticles have a diagnostic capability under Computed Tomography (CT) or MRI[120]. Lu *et al*. designed a glycopolymer-porphyrin conjugate via a thiol-ene coupling reaction of poly(2-(methacrylamido) glucopyranose) (PMAG) and protoporphyrinogen. Porphyrin compounds are one of the most common photosensitizers used in PDT. The glyco-modification of porphyrin proved to increase its water solubility and enable targeted PDT against tumour cells, due to the specific interaction of glycopolymers with lectin receptors, over-expressed in malignant cells. The glyco-particles showed enhanced affinity toward ConA lectin and *in vitro* studies showed enhanced cytotoxic effects against chronic myelogenous leukemia (CML) K562 cells that over-expressed GLUTs (GLUT1) receptors[121]. Another glycopolymer architecture evaluated for PDT therapeutics is a star-shaped glycopolymer bearing galactose residues modified with 5,10,15,20-Tetrakis[4-(2-hydroxyethoxy)phenyl] porphyrin photosensitizer by atom transfer radical polymerization (ATRP). This construct has proved to be an effective photosensitizer for potential use in photodynamic therapy[122]. A cathepsin B-responsive biodegradable branched glycopolymers designed as theranostic nanomedicines have significantly enhanced therapeutic indexes and strengthened contrast of MRI at tumour sites. A degradable gadolinium-based branched glycopolymers conjugated to paclitaxel through a cathepsin B responsive linker had shown an extended circulation time, enhanced accumulation in tumours, and excellent biocompatibility enhancing imaging contrast up to 24 h post-injection and showing superior antitumor efficacy with more than 90% tumour inhibition[21].

Optical imaging-guided chemo-photothermal combination therapy has recently emerged as a potential treatment strategy—this non-invasive and high sensitivity personalized precision treatment— aids in diagnostic accuracy and synergistic effects with chemotherapeutic drugs. NIR-II, a longer-wavelength of 1300−1400 nm, has been reported

to achieve a higher signal-to-background ratio. Combination therapy to achieve excellent physiological stability, high drug loading and controlled drug release by exploiting boronic acid-catechol conjugates has been widely used. Chen *et al*. designed a NIR-II dye-based multifunctional telechelic glycopolymers conjugate displaying stimuli-responsive properties with inherent stability under neutral conditions and acid-induced cleavage in the acidic tumour microenvironment for controlled drug release, which not only exhibits strong fluorescence emission for NIR-II but also serves as a photothermal agent for photothermal therapy (PTT)[123].

1.11 NANOPARTICLE-BASED COMBINATIONAL THERAPY OF DRUGS AND GENES

Cancers are treated mainly with a combination of surgery, radiotherapy, chemotherapy and/ or immunotherapy depending on their location, stage and grade. However, clinical trials are generally designed for evaluation in monotherapy settings. At first gene therapy was focussed on monogenic diseases, more than 1,500 diseases are known to be caused by a single defective gene — hereditary diseases such as severe combined immunodefficiency (SCID), hemophilia, or cystic fibrosis. However as gene therapy has evolved, it has shifted away from monogenic diseases, toward diseases like cancer, where multiple genes are dysregulated[124]. In 2003, Gendicine in China became the world's first gene therapy to treat head and neck cancer approved for commercial production. After 12 years, more 30,000 patients have exhibited significantly higher response rates when combined with chemotherapy and radiotherapy. In addition, Gendicine has been successfully applied to treat various other cancer types and different stages of disease[47].

Sometimes synergistic effects are observed in nanomedicines when combined with conventional anticancer drugs or other treatment modalities. Using the pharmacological distribution of nanomedicines depends more on vascular perfusion and permeability than small molecule drugs, delivering higher amounts of drugs and for prolonged periods, thereby beneficially affecting locally applied physical combination therapies or been able

to specifically respond to locally applied physical triggers[125]. Cancer nanomedicines combined well with locally confined treatment modalities, such as radiotherapy, ultrasound and hyperthermia, increase accumulation and penetration, improving radio/chemotherapy outcomes. Co-delivery of two drugs with different biodistribution profiles has also been exploited in combination therapy. Combination therapy with nanoparticle albumin-bound paclitaxel (Abraxane) has induced unprecedented therapeutic responses enhancing accumulation at the tumour site in triple-negative breast cancer patients[126] when adding targeting ligands like CD44 receptor [127,128], folate[129,130], or epidermal growth factor[14,51,131,132], among others.

Zhang and colleagues developed a co-delivery system based on a N-succinyl chitosan–poly-L-lysine–palmitic acid (NSC–PLL–PA) polymer. The hydrophilic chitosan-based shell was designed to increase the micelle's half-life and decrease the cationic backbone's toxicity, PLL. The hydrophobic core was used to encapsulate DOX, and the cationic moiety was designed to entrap the negatively charged siRNA electrostatically. The triblock polymer micelle co-delivering DOX and siRNA (DOX–siRNA-micelle) was devised to downregulate P-glycoprotein expression, one of the major energy-dependent efflux transporters that contribute to multidrug resistance to help exert synergistic therapeutic effects[133].

The combination of nanomedicines with immune checkpoint inhibitors has been of particular interest for immunomodulation since nanoparticle formulations of cytotoxic drugs tend to be less toxic to the bone marrow than free drugs[134]. Filipova *et al.* developed a multivalent poly-LacNAc (Galβ4GlcNAc)-derived oligosaccharides with N-(2-hydroxypropyl) methacrylamide (HPMA) copolymers to act as potential inhibitors of extracellular and intracellular galectin-3 (Gal-3). This lectin has a vital role in cancer development and progression by interacting with immune cells (T lymphocytes and macrophages), leading to apoptosis. In macrophages, higher expression of Gal-3 is related to M2-like form activation, which supports tumour growth and angiogenesis. Moreover,

intracellular Gal-3 can increase tumour cells' resistance to chemotherapeutic treatment with apoptosis-inducing agents such as arsenic trioxide, cisplatin and doxorubicin[135].

1.12 GLYCO-POLYMER CONJUGATES

Poor pharmacokinetics is a particular problem for many drugs. Ringsdorf introduced in the mid-1970s a simple model for the polymeric development of drugs. According to his model, a polymer backbone should contain three types of groups: a targeting moiety, a solubilizing moiety and, a cleavable linker to attach the drug to be delivered. Combinations of polymer-bound drugs or polymer conjugates that contain drugs covalently linked is a recent strategy employed in the field. In the case of glycopolymers, the carbohydrate moieties may act as both the solubilizing and targeting moiety by specific targeting to a lectin on the surface of the tissue[136]

Targeted delivery of a drug payload to cancer cells is mediated via the EPR effect, but in some cases, active targeting is used to mediate ligand-receptor specific interactions. Every cell's surface contains carbohydrates in the form of polysaccharides, glycoproteins, glycolipids, and/or other glycoconjugates. These naturally occurring glycoconjugates have been found to play essential roles as recognition sites involved in biological functions[137]. Coupling of ligands to the nanoparticle's surface for active targeting of nano-based drugs is a biomimetic approach with similar (or even superior) functions to those of natural glycoconjugates. Complex carbohydrates and carbohydrate-based polymers require sugar ligands to be anchored on the nanoparticle's external surface by chemical modification. Developments in controlled polymerization have made possible to design glycopolymers with precise structures. Amphiphilic glycopolymer conjugates are capable of assembling into well-defined nanostructures such as micelles. The valency and architecture defined the lectin binding to complex polyvalent glycopolymers. Due to their structure, linear glycopolymers can produce intra- and intermolecular clusters caused by the hydroxyl groups' hydrogen bonding on the carbohydrate moieties and/or hydrophobic interactions

from the polymer backbone[138]. Hashida *et al*. synthesized galactosylated poly[L-glutamic acid] (PLGA) polymers by reaction with ethylenediamine, followed by 2-imino-2-methoxyethyl 1-thiogalactoside. This polymer was reacted with vitamin K5 to generate a galactosyl-PLGA-vitamin K conjugate, which showed anti-hemorrhagic effects and a significant reduction in prothrombin 2, 3 and 4 h after treatment in comparison to a 4-hour treatment with vitamin K5 alone[117]. DOX, has also been conjugated in a biocompatible glycoblock copolymer onto multi-walled carbon nanotubes (CNTs) with two different ends functionalized poly(1-O-methacryloyl-b-D- fructopyranose-b-(2-methacryloxyethoxy))benzaldehyde glycoblock copolymers, which were synthesized via RAFT polymerization, by either non-covalent or covalent tethering. CNTs were coated with the glycoblock copolymers and folic acid to obtain an efficient drug delivery platform for dual-targeting[139]. Haddleton *et al*. and Stenzel *et al*. synthesized different glycomonomers utilizing copper-catalyzed azide-alkyne cycloaddition (CuAAC) click reaction for receptor-mediated targeting to specific tissues or cells for the delivery of therapeutics including glucose transporter protein (GLUT5) and folic acid receptors (FR) in breast cancer[139].

Crossing the blood-brain barrier (BBB) is another major impediment. This highly selective semipermeable endothelial cell layer prevents non-selective crossing of solutes from the circulating blood into the central nervous system's extracellular fluid, allowing only small molecules to diffuse between the bloodstream and the cerebral tissues. Anticancer drugs are usually cytotoxic; thus, targeted delivery and accurate dose control is required to destroy the tumour without disrupting healthy cells. Glycosylation has recently been shown to effectively enable peptides, proteins, and nanoparticles to cross the BBB selectively [136]. Gliomas have been found to have intact BBB during the first stage, which allows for the design of nanocarriers to exploit active transport using targeting ligands on the surface. A hybrid, peptide decorated Glycol chitosan-based nanomicelle conjugated to a biocompatible aliphatic long-chain fatty acid (stearic acid) to impart amphiphilicity and a

specific brain targeting short peptide sequence with BBB targeting ability; has demonstrated efficacy in crossing the BBB for delivering a hydrophobic drug (Curcumin) model in brain; with the potential of these nanomicelles to be used as drug delivery vehicles in glioma therapy[140].

Covalent conjugation of carbohydrates, peptides, and polyamines to oligonucleotides for nucleic acid therapeutics targeted delivery has also been reported. Nair *et al.* described siRNA's conjugation to N-acetylgalactosamine (GalNAc), a highly efficient ligand for the ASGPR receptor. This was done by solid-phase oligonucleotide synthesis in deprotection conditions. This siRNA-conjugate achieved a 5-fold improvement in efficacy over the parent design *in vivo* in hepatocyte carcinomas. As mentioned earlier, galactose and GalNAc glycans are internalized via clathrin-mediated endocytosis through the ASGPR receptor overexpressed in hepatocytes. This result showed that conjugates improved the pharmacokinetics and systemic stability relative to the unconjugated siRNAs[141]. This nanoformulation is currently studied in multiple clinical trials by Alnylam Pharmaceuticals as a promising siRNA drug development for genetic medicines, cardio-metabolic diseases, and hepatic infectious diseases[91].

A new class of nanosized polymeric nanoparticles called single-chain nanoparticles (SCNPs) has been developed. A readily accessible technique that intramolecularly crosslinks a single polymer chain to form nanoparticles below 10 nm in diameter[142] has proved to be effective in viral mimicry. Light-induced fluorescent glyco single-chain nanoparticles (glyco-SCNPs) coated onto nanodiamonds were developed from single-chain acetylated mannose-based methacrylate monomers[143]. These SCNPs had fluorescent, water-soluble, and bioactive properties inspired by glycoprotein spikes on viruses. Glycopolymers for biomimicry of virus capsid proteins, conjugated with click chemistry and novel architectures — like glycodendrimers prepared dendritic sialosides with poly (amidoamine) (PAMAM) dendrimer backbones[144] have provided a novel glyco-synthetic

platform for viral mimicry use in cancer immunotherapy to activate viral defence signalling in cancer[145]

Crosslinked 3D network structures have also been developed as novel nanocarriers. Hydrogels and nanogels offer homogeneous encapsulation of cells and bioactive molecules by mirroring their native extracellular matrix (ECM) microenvironment. The use of "click" chemistry has been employed as a powerful and advantageous strategy to provide high selectivity and specificity. Wu *et al.* developed a dual-crosslink network hydrogel composed of 5-methacrylamido-1,2-benzoxaborole (MAAmBO), with poly(ethylene glycol) methyl ether methacrylate (PEGMA). The binding affinity of MAAmBO with nopoldiol and a range of diols (LAEMA, GAEMA, D-glucose, D-fructose, Cathecol and Capecitabine) was studied. This design involved benzoxaborolate formation with both sugar and nopoldiol to confer bioorthogonality, acid/polyol resistance, fast gelation, mild crosslinking reaction, and self-healing properties under a wide pH range of the hydrogel network (Figure 1-3)[146]. Soft carbohydrate-modified "clickable" nanogels composed of poly(*N*-vinylcaprolactam), PNVCL, were surface-functionalized with different glucose and maltose ligands by Siirilä *et al*[147]. The glucose and maltose bearing nanogels were thermoresponsive, and a study of the interactions with a model lectin, Con A, was done to address the carbohydrate recognition for thermoresponsive drug delivery applications.

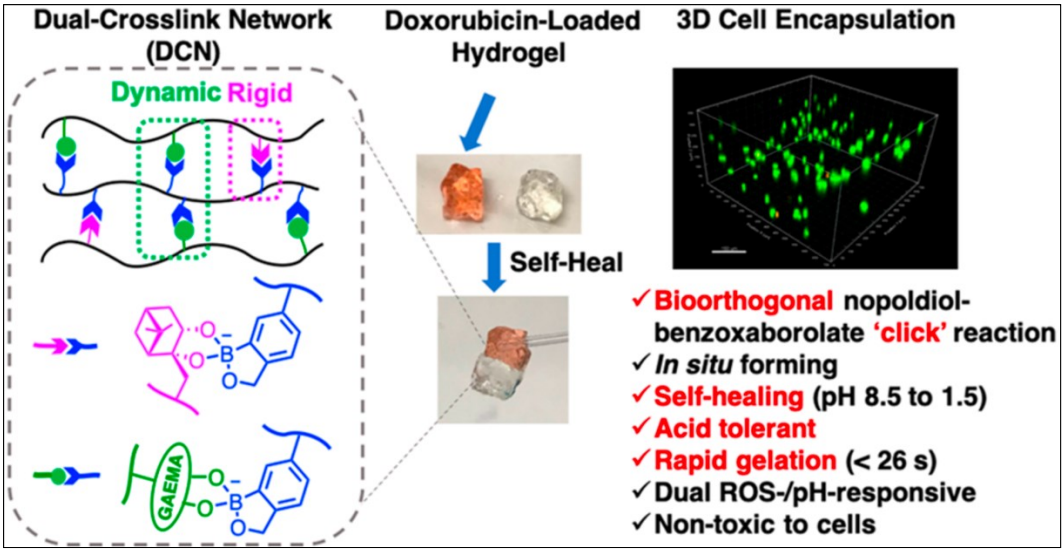

Figure 1-3. Graphic illustration of the design and preparation of benzoxaborolate-based single and dual-cross-link network (DCN) hydrogels for doxorubicin delivery. Reprinted with permission from *Chem. Mater.*, 2019, 31, 11, 4092–4102. https://doi.org/10.1021/acs.chemmater.9b00769. Copyright © 2019, American Chemical Society.

1.13 TYPES OF ANTICANCER NANOMEDICINES IN CLINICAL SETTINGS

The first therapeutic clinical trial of a gene therapeutic agent was in 1990 in two patients with adenosine deaminase (ADA) deficiency where transfection was conducted *ex vivo*. In 1999 some challenges were faced in the gene therapy field when a patient with a deficiency of ornithine transcarbamylase, died in a clinical trial after administration of an adenoviral vector to the liver[148]. Later, a few patients with severe combined immunodeficiency developed leukemia due to mutagenic retroviral insertion. These incidents have laden the broad clinical application of gene therapy[149] and have driven the development of safer non-viral gene transfer vectors. As of March 2018, almost 2600 gene therapy clinical trials have been completed, are ongoing or have been approved worldwide. The majority are in phase I and phase I/II but an increasing proportion of trials are now entering later stages. There

were also reports of the first successful clinical trials using immunotherapy approaches, using chimeric antigen receptor (CAR) T cells to target tumour-associated cell-surface antigens and new genome editing technologies like clustered regularly interspaced short palindromic repeats, (CRISPR). The approval of Glybera, a nanomedicine for the treatment of hereditary lipoprotein lipase deficiency (LPLD), a rare genetic disease and posterior withdrawal, showed the higher cost of the development of personalized medicine. In the past few years, nanomedicines with a more widely and sustainable applicability have found broader interest. In Table 1-1, we showed the undergoing clinical trials in 2020 using nanomedicines for cancer treatment and their applications. It is worth noting that combinational therapies are being explored extensively by using current chemotherapeutic agents combined with gene therapy and other pharmaceuticals. Metallic/Carbon nanoparticles have also received some interest in combination with polymers; quantum dots carrying PEG amine (Qdots-PEG-NH_2) conjugated with somatostatin (SST) and loaded with Cetuximab for breast cancer are currently explored[150].

Albumin-bound Paclitaxel, an FDA recently approved solvent-free formulation of paclitaxel for the treatment of metastatic breast cancer, has now been the most investigated nanoparticle in multiple controlled studies (Table 1-2). In patients with non-squamous non-small cell lung cancer (NSCLC) (NCT00616967), in combination with Pertuzumab and Trastuzumab, in HER-2 positive breast cancer (NCT01730833), in combination with Gemcitabine and Wee inhibitor in pancreatic cancers (NCT02194829) and hepatobiliary tumours (NCT04060472).

Table 1-1. Nanoparticle Clinical Trials until 2020 divided by their application—data obtained from ClinicalTrials.gov.

Application	NCT Number	Title	Phases	URL
Imaging	NCT04138342	Topical Fluorescent Nanoparticles Conjugated Somatostatin Analog for Suppression and Bioimaging Breast Cancer	Phase 1	https://ClinicalTrials.gov/show/NCT04138342

Combination with Gene therapy	NCT03323398	Dose Escalation and Efficacy Study of mRNA 2416 for Intratumoral Injection Alone and in Combination With Durvalumab for Patients With Advanced Malignancies	Phase 1 Phase 2	https://ClinicalTrials.gov/show/NCT03323398
	NCT02766699	A Study to Evaluate the Safety, Tolerability and Immunogenicity of EGFR(V)-EDV-Dox in Subjects With Recurrent Glioblastoma Multiforme (GBM)	Phase 1	https://ClinicalTrials.gov/show/NCT02766699
	NCT03739931	Dose Escalation Study of mRNA-2752 for Intratumoral Injection to Patients With Advanced Malignancies	Phase 1	https://ClinicalTrials.gov/show/NCT03739931
Metallic/ Carbon Nanoparticles	NCT03550001	Carbon Nanoparticles as Lymph Node Tracer in Rectal Cancer After Neoadjuvant Radiochemotherapy	Not Applicable	https://ClinicalTrials.gov/show/NCT03550001
	NCT04482803	Targeted Biopsy of Carbon Nanoparticles Labelled Axillary Node for cN+ Breast Cancer	Not Applicable	https://ClinicalTrials.gov/show/NCT04482803
	NCT01895829	Ferumoxytol - Iron Oxide Nanoparticle Magnetic Resonance Dynamic Contrast Enhanced MRI	Early Phase 1	https://ClinicalTrials.gov/show/NCT01895829
	NCT04261777	Ferumoxtran-10-enhanced MRI in Prostate Cancer Patients	Phase 3	https://ClinicalTrials.gov/show/NCT04261777
Combination with Chemotherapy/ Radiotherapy	NCT03531827	Combining CRLX101, a Nanoparticle Camptothecin, With Enzalutamide in People With Progressive Metastatic Castration Resistant Prostate Cancer Following Prior Enzalutamide Treatment	Phase 2	https://ClinicalTrials.gov/show/NCT03531827
	NCT01455389	TUSC2-nanoparticles and Erlotinib in Stage IV Lung Cancer	Phase 1|Phase 2	https://ClinicalTrials.gov/show/NCT01455389
	NCT02769962	Trial of CRLX101, a Nanoparticle Camptothecin With Olaparib in People With Relapsed/Refractory Small Cell Lung Cancer	Phase 1|Phase 2	https://ClinicalTrials.gov/show/NCT02769962
	NCT02975882	Nanoparticle Albumin-Bound Rapamycin, Temozolomide, and Irinotecan Hydrochloride in Treating Pediatric Patients With Recurrent or Refractory Solid Tumors	Phase 1	https://ClinicalTrials.gov/show/NCT02975882
	NCT03308604	AGuIX Gadolinium-based Nanoparticles in Combination With Chemoradiation and Brachytherapy	Phase 1	https://ClinicalTrials.gov/show/NCT03308604
	NCT02788981	Abraxane® With or Without Mifepristone for Advanced, Glucocorticoid Receptor-Positive, Triple-Negative Breast Cancer	Phase 2	https://ClinicalTrials.gov/show/NCT02788981
	NCT02805894	NBTXR3 Nanoparticles and EBRT or EBRT With Brachytherapy in the Treatment of Prostate Adenocarcinoma	Phase 1|Phase 2	https://ClinicalTrials.gov/show/NCT02805894
	NCT04486833	TUSC2-nanoparticles (GPX-001) and Osimertinib in Patients With Stage IV Lung Cancer Who Progressed on Osimertinib Alone	Phase 1|Phase 2	https://ClinicalTrials.gov/show/NCT04486833

	NCT02010567	Neoadjuvant Chemoradiotherapy With CRLX-101 and Capecitabine for Rectal Cancer	Phase 1|Phase 2	https://ClinicalTrials.gov/show/NCT02010567
	NCT03825328	A Trial of NS/GEMOX Chemotherapy in Patients With Untreated Pancreatic Cancer (HZ-NS/GEMOX-PC)	Phase 2	https://ClinicalTrials.gov/show/NCT03825328
	NCT03660930	Nanoparticle Albumin-Bound Rapamycin and Pazopanib Hydrochloride in Treating Patients With Advanced Nonadipocytic Soft Tissue Sarcomas	Phase 1|Phase 2	https://ClinicalTrials.gov/show/NCT03660930
	NCT04310007	Testing the Addition of the Pill Chemotherapy, Cabozantinib, to the Standard Immune Therapy Nivolumab Compared to Standard Chemotherapy for Non-small Cell Lung Cancer	Phase 2	https://ClinicalTrials.gov/show/NCT04310007
	NCT03181100	Atezolizumab With Chemotherapy in Treating Patients With Anaplastic or Poorly Differentiated Thyroid Cancer	Phase 2	https://ClinicalTrials.gov/show/NCT03181100
	NCT04264143	CED of MTX110 Newly Diagnosed Diffuse Midline Gliomas	Phase 1	https://ClinicalTrials.gov/show/NCT04264143
	NCT03961698	Evaluation of IPI-549 Combined With Front-line Treatments in Pts. With Triple-Negative Breast Cancer or Renal Cell Carcinoma (MARIO-3)	Phase 2	https://ClinicalTrials.gov/show/NCT03961698
	NCT02716038	Neoadjuvant MPDL3280A, Nab-paclitaxel and Carboplatin (MAC) in NSCLC	Phase 2	https://ClinicalTrials.gov/show/NCT02716038
	NCT02930902	Pembrolizumab and Paricalcitol With or Without Chemotherapy in Patients With Pancreatic Cancer That Can Be Removed by Surgery	Phase 1	https://ClinicalTrials.gov/show/NCT02930902
	NCT03003546	Nab-paclitaxel/Rituximab-coated Nanoparticle AR160 in Treating Patients With Relapsed or Refractory B-Cell Non-Hodgkin Lymphoma	Phase 1	https://ClinicalTrials.gov/show/NCT03003546
	NCT04514497	Testing the Addition of an Anti-cancer Drug, BAY 1895344, to Usual Chemotherapy for Advanced Stage Solid Tumors, With a Specific Focus on Patients With Small Cell Lung Cancer, Poorly Differentiated Neuroendocrine Cancer, and Pancreatic Cancer	Phase 1	https://ClinicalTrials.gov/show/NCT04514497
	NCT04316091	A Phase I Clinical Trial of Neoadjuvant Chemotherapy With/Without SPIONs/SMF for Patients With Osteosarcoma	Phase 1	https://ClinicalTrials.gov/show/NCT04316091
	NCT03566199	MTX110 by Convection-Enhanced Delivery in Treating Participants With Newly-Diagnosed Diffuse Intrinsic Pontine Glioma	Phase 1|Phase 2	https://ClinicalTrials.gov/show/NCT03566199
	NCT03337087	Liposomal Irinotecan, Fluorouracil, Leucovorin Calcium, and Rucaparib in Treating Patients With Metastatic Pancreatic, Colorectal, Gastroesophageal, or Biliary Cancer	Phase 1|Phase 2	https://ClinicalTrials.gov/show/NCT03337087

	NCT03907475	Durvalumab in Combination With Chemotherapy in Treating Patients With Advanced Solid Tumors, (DURVAStudydy)	Phase 2	https://ClinicalTrials.gov/show/NCT03907475
	NCT03736720	Liposomal Irinotecan, Fluorouracil and Leucovorin in Treating Patients With Refractory Advanced High Grade Neuroendocrine Cancer of Gastrointestinal, Unknown, or Pancreatic Origin	Phase 2	https://ClinicalTrials.gov/show/NCT03736720
Combination with Immunotherapy	NCT02620865	Bispecific Antibody Armed Activated T-cells With Aldesleukin and Sargramostim in Treating Patients With Locally Advanced or Metastatic Pancreatic Cancer	Phase 1|Phase 2	https://ClinicalTrials.gov/show/NCT02620865
	NCT03942068	Apatinib With albumin-bound Paclitaxel in Patients With Platinum-resistant Recurrent Ovarian Cancer	Phase 2	https://ClinicalTrials.gov/show/NCT03942068
	NCT04221828	Trial of NanoPac Focal Therapy for Prostate Cancer	Phase 2	https://ClinicalTrials.gov/show/NCT04221828
	NCT03463265	ABI-009 (Nab-Rapamycin) in Recurrent High Grade Glioma and Newly Diagnosed Glioblastoma	Phase 2	https://ClinicalTrials.gov/show/NCT03463265
Polymeric Nanoparticles	NCT03774680	Targeted Polymeric Nanoparticles Loaded With Cetuximab and Decorated With Somatostatin Analogue to Colon Cancer	Phase 1	https://ClinicalTrials.gov/show/NCT03774680
	NCT04167969	The Use of Nanoparticles to Guide the Surgical Treatment of Prostate Cancer	Phase 1	https://ClinicalTrials.gov/show/NCT04167969
	NCT02106598	Targeted Silica Nanoparticles for Real-Time Image-Guided Intraoperative Mapping of Nodal Metastases	Phase 1|Phase 2	https://ClinicalTrials.gov/show/NCT02106598
	NCT04094077	Evaluating AGuIX® Nanoparticles in Combination With Stereotactic Radiation for Brain Metastases	Phase 2	https://ClinicalTrials.gov/show/NCT04094077
	NCT04484909	NBTXR3 Activated by Radiation Therapy for the Treatment of Locally Advanced or Borderline-Resectable Pancreatic Cancer	Phase 1	https://ClinicalTrials.gov/show/NCT04484909
	NCT03818386	Radiotherapy of Multiple Brain Metastases Using AGuIX®	Phase 2	https://ClinicalTrials.gov/show/NCT03818386
	NCT04314895	Trial of NanoPac Intratumoral Injection in Lung Cancer	Phase 2	https://ClinicalTrials.gov/show/NCT04314895
	NCT02740985	A Phase 1 Clinical Study of AZD4635 in Patients With Advanced Solid Malignancies	Phase 1	https://ClinicalTrials.gov/show/NCT02740985
	NCT03217838	Safety, Tolerability, Pharmacokinetics, and Efficacy of AZD2811 Nanoparticles as Monotherapy or in Combination in Acute Myeloid Leukemia Patients.	Phase 1	https://ClinicalTrials.gov/show/NCT03217838
	NCT03020017	NU-0129 in Treating Patients With Recurrent Glioblastoma or Gliosarcoma Undergoing Surgery	Early Phase 1	https://ClinicalTrials.gov/show/NCT03020017

	NCT04137653	Treatment of Triple-negative Breast Cancer With albumin-bound Paclitaxel as Neoadjuvant Therapy: a Prospective RCT	Phase 3	https://ClinicalTrials.gov/show/NCT04137653
	NCT00609791/NCT01620190	Paclitaxel Albumin-Stabilized Nanoparticle Formulation in Treating Patients of Different Ages With Metastatic Breast Cancer and Treated Advanced Non-small Cell Lung Cancer	Phase 2	https://ClinicalTrials.gov/show/NCT00609791/ https://ClinicalTrials.gov/show/NCT01620190
	NCT01463072	Nab-Paclitaxel in Treating Older Patients With Locally Advanced or Metastatic Breast Cancer	Phase 2	https://ClinicalTrials.gov/show/NCT01463072

Table 1-2. Some of the NAB-Paclitaxel applications in clinical trials 2020. Data obtained from ClinicalTrials.gov.

Application	Type of Cancer	Phases	NCT Number	URL
NAB-Paclitaxel in combination with chemotherapeutic agents	Breast	Phase 4	NCT03799679/NCT03799692	https://ClinicalTrials.gov/show/NCT03799679
	Pancreatic	Phase 2	NCT03636308	https://ClinicalTrials.gov/show/NCT03636308
	Pancreatic	Phase 1	NCT02336087	https://ClinicalTrials.gov/show/NCT02336087
	HER-2 (+) Breast	Phase 2	NCT01730833	https://ClinicalTrials.gov/show/NCT01730833
	IIIB/IIIC or IV NSCLC	Phase 3	NCT00616967	https://ClinicalTrials.gov/show/NCT04033354
	Breast	Phase 2	NCT01525966	https://ClinicalTrials.gov/show/NCT00616967
	Melanoma	Phase 1	NCT02020707	https://ClinicalTrials.gov/show/NCT02020707
	Pancreatic	Phase1 Phase 2	NCT02194829	https://ClinicalTrials.gov/show/NCT02194829
	Head and Neck	Phase 1	NCT01847326	https://ClinicalTrials.gov/show/NCT01847326
	Oropharyngeal	Phase 2	NCT02258659	https://ClinicalTrials.gov/show/NCT02258659
	Non-Hodgkin Lymphoma	Phase 1	NCT03003546	https://ClinicalTrials.gov/show/NCT03003546
	Hepatobiliary	Phase 2 Phase 3	NCT04060472	https://ClinicalTrials.gov/show/NCT04060472

The field of nanomedicines has had numerous advances over the past few decades, shifting towards personalized approaches that are sometimes highly resource-demanding and time-intensive. In preclinical settings, nanomedicines have inhibited tumour growth and prolonged survival in increasing amounts compared to conventional drugs, but only reduced side effects improvements have been seen in clinical practice. However, reducing the devastating side effects has become equally important to improve patients' quality of life during treatment[151]. The first clinical trial that used a targeted glyconanoparticle-delivery system (clinical trial NCT00689065) was a PEGylated cyclodextrin-based polymer (CDP) with a human transferrin protein (TF) targeting ligand and RNA M2 subunit of ribonucleotide reductase protein (RRM2) siRNA called CALAA-01[152] in 2010. Several glycopolymer-based vectors have been developed since then. Still, the FDA has approved none for gene/drug therapy applications because most of these systems have been less efficient than viral vectors or parent drug counterparts.

1.14 SUCCESSFUL DELIVERY/APPLICATION: FUTURE POTENTIAL CANDIDATES

1.14.1 Exploiting Immunomodulation

Cancer immunotherapy is a rapidly evolving treatment modality that generates more sustanined and robust anticancer effects[153]. The delivery of molecular adjuvants and cancer-associated antigens or cancer-specific neoantigens, immunostimulatory agents to antitumour immune cells and gene therapeutic oligonucleotides like DNA, short hairping RNA (shRNA) or silencing RNA (siRNA); seems to be a far more efficient tactic to eradicate cancerous tumours than delivery of conventional cytotoxic drugs[154]. Co-delivery of multiple nucleic acid and peptide therapeutics for cancer immunomodulation is the new venture in the battle against cancer[155]. Engineering cancer immunotherapies using nanomaterials (immunoengineering) delivers a remarkable platform that could potentially

avoid autoimmunity against healthy tissues (due to target delivery), and provide synergistic effects due to co-delivery of adjuvants and neoantigens of interest to stimulate the tumour immune-environment[156](Scheme 1-7).

Cancer immunotherapy attempts to exploit the specificity of the immune system to treat tumours[157]. The molecular identification of human cancer-specific antigens has allowed the development of antigen-specific immunotherapies[158]. Dendritic cells (DCs) are known to act as adjuvants and after decades of research, it is now clear that DCs are key for the immune system, owing to their ability to control both immune tolerance and immunity[159]. Vaccination strategies involving DCs have been developed due to these special properties; the goal of DC vaccination is to induce tumour-specific effector T cells that can reduce the tumour mass and can induce immunological memory to control tumour metastasis and relapse[159]. Activation of DCs is critical for the stimulation of immunity[160]; a promising strategy for reprogramming DC function is through the use of silencing RNA (siRNA)[159,161]. Oligodeoxynucleotides (ODN) containing unmethylated CpG motifs has been utilized as a potent adjuvant due to the activation of immature DCs via Toll-like receptor (TLR) 9[162,163]. This adjuvant is reported to play an essential role in both the initiation of an immune response and ending the pre-existing immune tolerance[164]. Therapeutic targeting of the immune system has marked successes in cancer treatment. Blockade of checkpoint inhibitors, like the programmed cell death 1 (PD1) pathway, co-treatment with antibodies that target immune cells like cytotoxic T lymphocyte antigen 4 (CTLA4) and CAR T cell therapy for leukemias and lymphomas, has shown some modest progress. New immune therapeutics have focussed on enhancing the adaptive responses through immunostimulatory pathways, but safety issues have hindered successful therapeutic implementation.

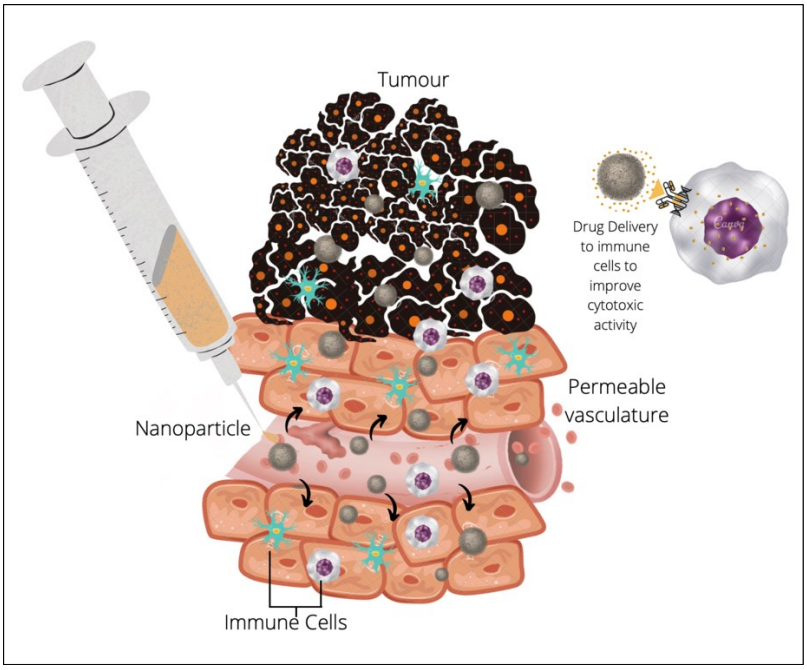

Scheme 1-7. Immunomodulation through nanomedicines.

1.14.2 Exploiting Tumour Hypoxia

Exploiting hypoxia features is another strategy implemented to develop novel therapeutics that turn malignant tumour cell characteristics into an advantage. Hypoxic-cancerous tumours are invasive and metastatic. Genetic changes associated with hypoxia impair oxygen and drug delivery (chemotherapy), leading to ineffective targeting and undesirable resistance to radiotherapy, causing therapy failures[165] (Scheme 1-8). Radiation-resistant cells might arise from differences in the distributions of the initial ionization events, leading to variances in spatial clustering of damage from the free radicals that are the ultimate cause of cell death[166]. Hypoxia is one of the main biological factors that has been shown to affect the outcome of radiotherapy[167]. Clinical use of adjuvant chemotherapeutic agents concomitant with radiotherapy has proved to be successful against malignant tumours by aiding in the destruction of radio-resistant populations acting as radiosensitizers[168]. Nonetheless, a synergistic combination of therapies could suffer major

drawbacks —one being the lack of selectivity, which leads to severe side effects and limited efficacy, the other is the occurrence/selection of drug resistance[169]. Radiotherapy remains one of the most important cancer management modes to date, with approximately 50% of patients undergoing radiotherapy for treatment or palliative purposes[170]. Radiotherapy is the use of ionizing-radiations to eradicate any malignant tumours simply by delivering suitably high doses of radiation. In practice, the total dose administered is limited by the biologic consequences for normal tissues irradiated along with the tumour tissue. A balance between radiation-induced complications in normal tissue and the tumour control must be met for an effective therapeutic outcome. Therefore, in planning a course of radiation therapy, the goal is to optimize the therapeutic ratio as much as possible by shifting the tumour control towards lower radiation doses for the same biological effect[171]. The biggest challenge and limitation of radiotherapy is toxicity caused to healthy cells around and near the tumour due to the exposure to high energy radiation beams. Therefore, radiosensitizers are intended to solve this problem by enhancing sensitivity of tumour cell to the killing effects of external beam radiotherapy while having minimal effect on normal healthy tissues. One approach for radiosensitizing cells explores the elimination of tolerant DNA damage-induced cell death via inactivation of pro-survival signalling cascades (e.g. phosphatidylinositol-3 kinases (PI3K/AKT), nuclear factor-kB (NF-kB), and mitogen-activated protein kinase (MAPK))[172]. DNA repair mechanisms maintain the genomic stability of an organism. Tumour-specific DNA repair defects drive genomic instability and ultimately radiation-resistant; loss of function mutations in gene modulating DNA damage response (DDR), precisely double-stranded breaks (DSBs) provide a number of rare, syndromic conditions including ataxia-telangiectasia (ATM), Bloom's syndrome, Fanconi anemia, Rothmund–Thomson syndrome, Werner syndrome and Nijmegen breakage syndrome, all of which cause extreme radiosensitivity; a feature currently explored as an opportunity for radioresistant cells therapeutics[173]. Poly(ADP-ribose) polymerase (PARP) protein inhibitors involved in single-stranded base repair (SSB) are potent radiosensitizers. The absence of PARP-1 and PARP-2 results in hypersensitivity to

ionizing radiation and alkylating agents; however, whether this is due exclusively to impaired DNA damage responses or whether tumour re-oxygenation contributes to this radiosensitization via the vasoactive effects of the PARP inhibitors remains to be determined[174]. The combination of chemotherapeutic drugs with radiotherapy has been seen as beneficial in the treatment of many solid tumours. Integration of cisplatin into DNA or RNA in close proximity to a radiation-induced single-strand break can act synergistically to make the defect significantly more challenging to repair, and agents that affect nucleotide metabolism, such as fluoropyrimidines and gemcitabine, among others, inhibit the repair of radiation-induced DNA damage, producing cytotoxicity to tumour cells[168].

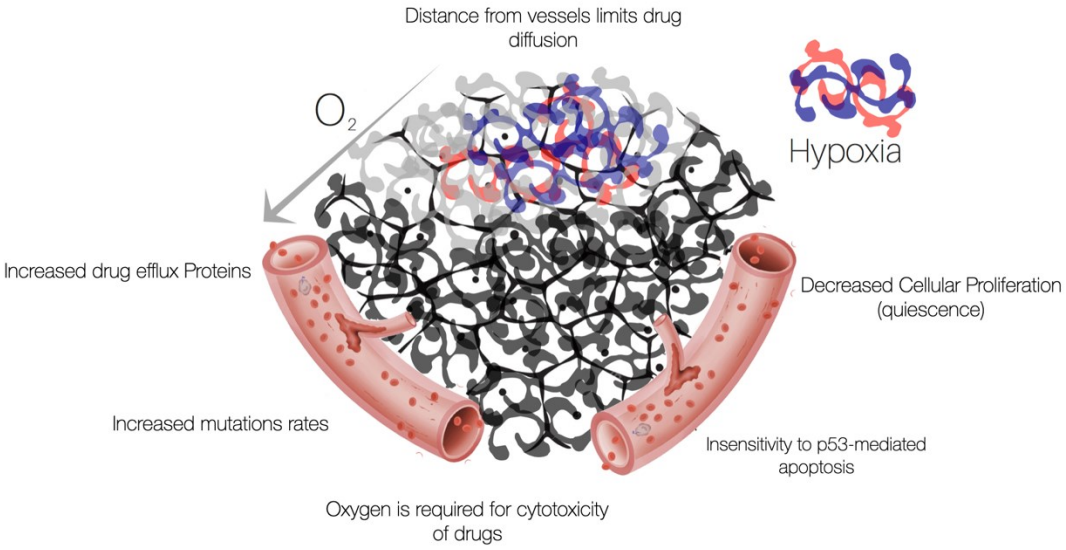

Scheme 1-8. Tumour Hypoxia and the consequences. Adapted from Muz, B.; de la Puente, P.; Azab, F.; Azab, A. K. The Role of Hypoxia in Cancer Progression, Angiogenesis, Metastasis, and Resistance to Therapy. *Hypoxia* **2015**, *3*, 83.

Oxygen is the ultimate radiosensitizer; it acts as a radiosensitizer by forming peroxides in different biomolecules such as DNA, "fixing" the radiation damage. Evidence of the high efficacy of oxygen required low oxygen concentration to achieve maximum sensitization of fully anoxic cells (about 0.5% pO_2 compared to physioxic conditions). Cells situated beyond the diffusion distance of oxygen (70 μm)[171] within tumours exhibited a clonogenic and radioresistant phenotype. Aberrant tumour vasculature, and rapid growth of solid tumours facilitates the creation of regions with low oxygen tensions. Hypoxia is known to alter cancer cell metabolism and contributes to therapy resistance by inducing cell quiescence and stimulating complex cell signalling networks, including the HIF, PI3K, MAPK, RAS, mTOR and NFκB pathways involved in tumour blood vessel formation, metastasis, and development of resistance to chemo/radio therapy[175]. Tissue normoxia or physoxia is the oxygenation in healthy tissues, which varies widely between the organs due to the extent of the blood vessels network and metabolic activity. Oxygen concentration in humans ranges between approximately 9.5% pO_2 in the renal cortex to 3.4% pO_2 in the brain. It is generally accepted that hypoxic tumour tissues are, on an average, between 1%–2% pO_2 and below physoxia levels in that particular tissue[176].

The potential gain of radiosensitizing hypoxic cells is huge: severely hypoxic cells typically require two to three times higher radiation doses for a killing effect when compared with well-oxygenated cells; this is referred to as the oxygen enhancement ratio (OER). A way to modulate the microenvironment to improved radiotherapy is by targeting hypoxia using prodrugs to induce tumour-specific toxicity, which are selectively activated under bioreductive conditions. Hypoxia-exclusive cytotoxicity requires one-electron reduction of a prodrug to a radical much toxic than superoxide. Electron mimicking radiosensitizers such as nitroimidazoles have been studied since the 1960s. The most popular nitroimidazole-based compound is misonidazole; however, in Phase I clinical trials it was found to cause dose-limiting efficacy neuropathies[177]. Pimonidazole was another drug that showed enhanced efficacy in vitro and good tumour uptake, but despite these

features is was not found effective in clinical trials as a radiosensitizer and was later used as a tracer for hypoxia diagnosis[178]. 5-Nitroimidazoles, like nimorazoles, are effective in several clinical trials and have been used for the treatment of head and neck cancers in Denmark[179]. Several positron emission tomography (PET) tracers, including fluorine-18-fluoromisonidazole ([^{18}F]FMISO)[180] and fluorine-18-fluoroazomycin arabinoside ([^{18}F]FAZA)[181,182] and the single-photon emission computed tomography (SPECT) agent iodine-123-iodoazomycin arabinoside ([^{123}I]IAZA)[183,184] have found extensive clinical use in hypoxia detection in cancer imaging[185]. Nonetheless, poor performance of nitroimidazoles as in vivo radiosensitizers, when used in conjunction with X-ray treatment, has been attributed to their inability to achieve radiosensitizing concentrations at dose-limiting neurotoxicities[186]. Additionally, agents that allow tumour shrinkage has been explored for treating resistant hypoxic regions by increasing perfusion and oxygenation in these areas; for examples paclitaxel[187], and EGFR inhibitors[188] have shown remarkable benefits as a synergistic combination for hypoxic targeted therapies.

Nanotechnology can potentiate radiotherapy by specifically delivering radionuclides or radiosensitizers into novel nanoparticles (NPs) designed to reach target tumours, therefore enhancing the efficacy while alleviating radiotherapy's toxicity. NPs have proven to be ideal delivery vehicles due to adjusting the kinetics, body distribution, and drug release of these particular drugs[189]. A noteworthy approach is some of these NPs themselves have a radiosensitizing nature; apart from contributing to therapeutic efficacy, they can also be used as diagnostic agents, therefore, being used in both therapy and diagnosis, giving scope for theranostic application. The abnormal vasculatures in tumours help extend the radiotherapeutics' retention time through the enhanced permeation retention effect (EPR). Aberrant blood vessels branching and leaky arterial walls allow nanoparticles to penetrate the tumour and easily disrupt lymphatic vessels, making tumours inefficient in drainage enhancing nanoparticle retention time[23,190]. Many radiopharmaceuticals exhibit fast renal clearance causing short circulation time in blood for tumor dose build up, thus compromising its therapeutic effect. Opsonization by the mononuclear phagocyte system

(MPS) is another elimination mechanism observed. Conversely, through loading or conjugation to nanocarriers, radioisotopes can escape from these biological purging. Nanoparticles such as liposomes, micelles, or polymeric complex are usually more than >10 nm, which significantly decreases the renal clearance, and the surface of nanoparticles produces steric hindrance, which prevents the adsorption of opsonins. These particular characteristics help prolong the half-life of radiotherapeutic agents in the physiological environment[191].

1.15 GLYCOPOLYMERS USED FOR CELL THERAPIES AND CRYOPRESERVATION

Understanding the behaviour of cells and the water-ice interphase has led to the ability to cryopreserve cells[192]. Despite these advances, the use of "conventional" cryopreservation approaches are not always optimum, as new challenges are faced. The requirement for even higher post-thaw cell viabilities is becoming imperative, particularly in cases where a limited number of valuable cells are available such as hematopoietic stem cells for the treatment of patients with hematologic cancers, such as leukemia and lymphoma, and congenital or acquired diseases of the hematopoietic system such as sickle cell disease [193–197] . Mazur developed the two-factor hypothesis of freezing injury to explain cells' survival when subjected to cryogenic temperatures (Fig. 1-4); very fast cooling rates supercool the intracellular environment, typically causing intracellular freezing. Cooling cells slower than the optimal rate in the presence of ice results in the osmotic dehydration of cells and solute toxicity[198], as originally argued by Lovelock (Fig. 1-5A). These osmotic stresses alone may be severe enough to cause lethal injury changes, such as Meryman's stated in his "minimal critical volume" hypothesis[199]. Moreover, mechanical action of the extracellular ice is likely to "seed" nucleation within cells and to directly injure cell membranes by compressing cells together (unfrozen fraction hypothesis)[200] (Fig. 1-5B). During optimal cooling, cells experience a hypertonic environment and have time to sufficiently dehydrate before irreversible injury appears. Difficulties in designing

cryopreservation protocols may arise from these variables' complex interactions; thus, cooling rates that are low enough to avoid intracellular ice formation (IIF) may be slow and induce damage from solution effects (Fig. 1-5C). Many of the cryobiology successes derive from manipulating these variables, using controlled freezing and rewarming protocols, along with cryoprotective agents (CPAs)[201,202]. Successful cryopreservation depends mainly on the permeability of cells to water and CPAs and their tolerance concentration limits[203]. In essence, based on our understanding of the established principles of cell injury and survival during the freezing process[192,198], macromolecular antifreezers are designed to modulate ice formation and growth[204].

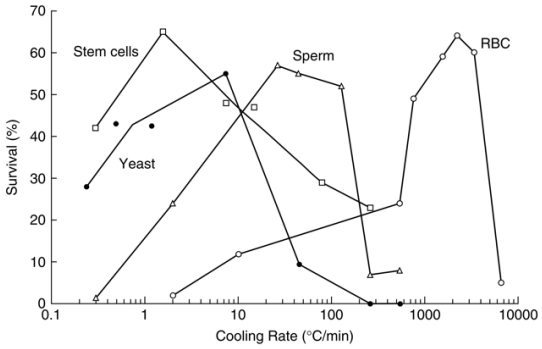

Figure 1-4. Survival of mouse marrow stem cells, yeast, mouse sperm, and human red cells as a function of cooling rate. We pointed out that cell survival plots vs. cooling rates usually exhibit an inverted U, which indicates that an injury occurring at high cooling rates has a different genesis than that occurring during slow cooling. Mazur explains this with the two-factor hypothesis theory; in general, solution effects are responsible for injury when cooling is slower than optimal and intracellular freezing is responsible for injury when cooling is faster than optimal. The optimum rate is the one that its slow enough to prevent IIF and yet is rapid enough to minimize the amount of time that the cells are exposed to solution effects[198].

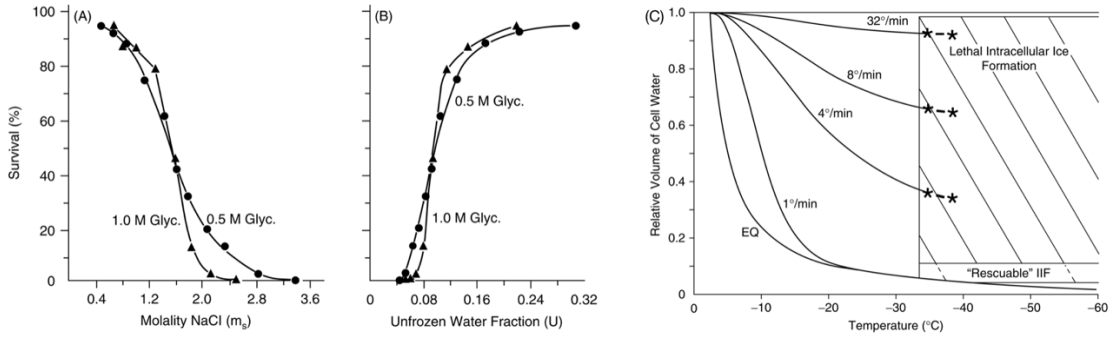

Figure 1-5. Survival of human red cells (percentage unhemolyzed) (A) as a function of the molality of NaCl to which they are exposed after being frozen at 1.7 °C/min to various sub-zero temperatures while suspended in solutions of 0.5 or 1.0 M glycerol in isotonic saline, and (B) as a function of the fraction of water that remains unfrozen at those temperatures. Thawing was rapid. (C) Kinetics of water loss from mouse ova as a function of the cooling rate during freezing in 1 M dimethyl sulfoxide (DMSO) or glycerol. The vertical solid line at –33°C is the median ice nucleation temperature observed by Rall *et al*. (1983) for eight-cell mouse embryos. It is proposed that a cell that enters the nucleation zone still containing 10% or more of its isotonic water volume and with that water supercooled 2°C or more will undergo IIF. Modified from [205,206].

A more recent cryopreservation approach involves the use of polymers mimicking antifreeze proteins (AFPs) and antifreeze glycoproteins (AFGPs). Custom-tailored mono- and disaccharides have exhibited moderate ice recrystallization inhibition (IRI) activity, and this has ultimately facilitated the discovery of several carbohydrate-based ice recrystallization inhibitors with IRI activity[207]. The accumulation of internal sugars or mixtures of sugars, such as trehalose, sucrose, and raffinose, is one of the complex physiological adaptations that allow some organisms to survive drying stress[201,208–210]. These sugars are believed to play a significant role in stabilizing membranes, proteins, and other key cellular structures. One of the major advantages of these sugars is their high glass

transition temperature (T_g) compared with conventional cryoprotectants (CPAs), such as dimethyl sulfoxide (DMSO), ethylene glycol (EG), and 1,2-propanediol (PROH). Sugars also deliver their protection by stabilizing lipid membranes through hydrogen bonding (water replacement hypothesis); by preventing aggregations of intracellular proteins, and acting as osmolytes against osmotic stresses[211]. Besides, its non-toxic nature has the potential to infuse freeze-thawed cells directly into patients without the requirement of further steps involved in the removal of traditional CPAs[212].

Until recently, sugars have been used as extracellular additives due to the cell membranes' impermeability. In recent years, several groups overcame this barrier by using different approaches such as thermotropic lipid-phase transition[213], reversible poration[214], transfection[215] and microinjection[216]. Gibson and Knight *et al*. studied the IRI activity of various synthetic polymers like poly-L-histidine, poly-L-hydroxyproline, poly(2-aminoethyl methacrylate), poly-L-lysine, poly-L-glutamic acid, polyethylene glycol (PEG) and polyvinyl alcohol (PVA)[207]. Glycopolymers have been recently used as cryoprotectants. Gibson and coworkers have synthesized amphipathic glycopolymers that mimic the three-dimensional structure of AFGPs. The hydrophobic/hydrophilic arrangement of the carbohydrate-based glycopolymers is known to influence their IRI activity and ice nucleation[217]. Addition of different sugars into the polymer backbone has also been studied. Carbohydrate hydration has a strong effect on IRI activity. Galactose is a highly hydrated carbohydrate that allows the disruption of water molecules in the quasi-liquid layer from a more disordered to an ordered ice crystal lattice, resulting in ice recrystallization inhibition[207]. C-linked methyl esters conjugated to galactose have also been explored as cryoprotectants[218]. Inclusion of trehalose for cryopreservation has displayed enhance cell viability of fetal skin cells, fibroblasts and mammalian germ cells, spermatozoa and oocytes after cryopreservation[210,219]. The mechanism of trehalose action is to stabilize cell membranes by interacting with the phospholipids, reducing cell osmotic stress on the cryopreserved cells. Multiple studies have confirmed the effectiveness of trehalose in cryopreservation or drying of mammalian cells, including primary human

hepatocyte cryopreservation[220] as well as preservation of red blood cells[221], hematopoietic cells and embryonic stem cells[210], but its high molecular weight limits its permeability. This is why designing glycopolymers that improve the permeability properties of trehalose is of great interest.

1.16 CONCLUSION

In conclusion, designing complex synthetic linear and branched glycostructures to mimic naturally existing glycans is the main reason why glycopolymers have been exploited as carbohydrate-based systems in biological and medical applications. Even though considerable advances in recent years have brought hope to the carbohydrate field and many research groups have contributed to innovations in the synthesis of complex architectures, biological research on glycopolymers' interactions lags far behind other synthetic polymers. There are still intricated mechanisms that need to be elucidated to understand the low-affinity binding of carbohydrate-selective interactions to provide sufficient target cell recognition and to improve the engineering of these glyco-nanomedicines.

1.17 PROJECT OVERVIEW AND RATIONALE.

This thesis pursued the central hypothesis that novel glycopolymer architectures can enhance the therapeutic index of chemotherapeutic drugs and genes when using as delivery vehicles, as well as improve cell therapy strategies for cryopreservation by taking advantage of the specific cell-surface interactions with the carbohydrate moieties and the mimetic capability with natural glycoproteins and glycans.

In this project, we have developed glycopolymer vectors for siRNA therapy for the treatment of cervical carcinomas, exploiting the dynamic oxaborole-diol interactions of methacrylamide benzoxaborole (MAAmBO) and exploring the biocompatibility and effect

of sugar decoration degree in poly(glycidyl methacrylate) (PGMA), 2-methacryloyloxyethyl phosphorylcholine (MPC) and 2-hydroxyethyl methacrylate (HEMA) polymers with 2-lactobionamidoethyl methacrylamide (LAEMA) and 2-amino-ethyl methacrylamide hydrochloride (AEMA) glycopolymer designs. These delivery systems have demonstrated effectiveness in the knockdown of epidermal growth factor receptors (EGFR) —an overexpressed oncogene in cervical cancers— offering improved target-oriented delivery, bio-distribution and biocompatibility enhancing the therapeutic efficacy. Furthermore, to our knowledge, the use of oxaborole-glycopolymer combination is novel and has not been used as gene targeting agents.

The versatility of colloidal systems has been implemented as a current strategy to revolutionize pharmaceutical therapy. Its high biocompatibility and sustained-release properties make them excellent candidates for drug delivery and imaging, used for early diagnosis of various diseases. The lack of successful approaches has long impeded the use of non-viral drug delivery systems in cancer treatment. Clinically relevant biomedical applications of bioconjugates to deliver anticancer drugs offer a highly innovative opportunity for *multimodal* (imaging, chemotherapy, radiosensitization and molecular radiotherapy [MRT]) molecular theranosis (therapy+diagnosis) of solid hypoxic tumours. Developing novel stimuli-responsive carbohydrate-based nanogels with statistical glycopolymers of 2-lactobionamidoethyl methacrylamide (LAEMA) with 2-aminoethylmethacrylamide hydrochloride (AEMA) and thermosensitive di(ethylene-glycol) methyl ethyl methacrylate (DEGMA), —where glycotargeting abilities, hydrodynamic size and core composition have played key roles in enhancing drug-loading capacity and time-controlled release of anticancer drugs— provides a unique platform to address this problem. Alongside, proof-of-principle studies in our group have confirmed that the encapsulated form of Iodoazomycin Arabinofuranoside (IAZA)[222] —a clinical radiopharmaceutical for imaging and diagnosis of hypoxic tumors[183] that in hypoxic microenvironment initiates bioreductive activation generating cytotoxic intermediates to facilitate hypoxia-specific chemotherapeutic effects- improved the bioavailability of IAZA

in hypoxic cancer cells and enhanced its radiosensitization potential *in vitro*[114]. The proposed research evaluated an *engineered nanoformulation* of this encapsulated form (nanoIAZA) to deliver IAZA in oxygen-deprived cancer cells and evaluated the enhancement in theranostic effects from nanoIAZA by exploring its chemo-sensitizing effect on hypoxic cancerous tumours and showing enhanced pharmacokinetic distribution over a more extended period which would further enhance the therapeutic effects of IAZA *in vivo*. This study led to an innovative opportunity for nanocarriers in treating hypoxic solid tumours by optimizing drug target delivery, combined with potential treatment and imaging features of IAZA overcoming chemotherapy resistance problems, and offering effective multimodal management of hypoxic cancerous tumours. This could translate into improved patient care, reduction in mortality and reduced health care costs associated with the management of hypoxic cancer[54]. To date, there is no report on the development of *nano*IAZA and its use as a potential multimodal nanotheranostic in hypoxic cancer management.

Likewise, a novel cryoprotective agent for cell therapy cryopreservation applications has been developed. The capability to slowdown ice growth and recrystallization is compulsory in the cryopreservation of cells and tissues to avoid injuries associated with the physical and chemical responses of freezing and thawing. Cryoprotective agents (CPAs) have been used to restrain cryoinjury and improve cell survival. Still, some of these compounds pose greater risks for the clinical application of cryopreserved cells due to their inherent toxicity. Trehalose is known for its unique physicochemical properties and its interaction with the plasma membrane phospholipids, reducing cell osmotic stress and stabilizing the cryopreserved cells. Nonetheless, there has been a shortage of relevant studies on the synthesis of trehalose-based CPAs. We hereby report the synthesis and evaluation of a trehalose-based polymer and hydrogel and its use as a cryoprotectant and three-dimensional (3D) cell scaffold for cell encapsulation and organoid production. High post-thaw cell membrane integrity and post-thaw cell plating efficiencies were achieved after

24 h of incubation with skin fibroblast, HeLa (cervical), and PC3 (prostate) cancer cell lines under both controlled rate and ultrarapid freezing protocols. Furthermore, the ability to form hydrogels as 3D cell scaffolds encourages the use of these novel polymers to develop cell organoids and cryopreservation platforms.

In summary, this thesis demonstrates the design and characterization of complex glycopolymer architectures for the safety and anti-tumour delivery efficacy of EGFR siRNA and a radiosensitizer pharmaceutical IAZA in cervical, prostate and head & neck cancer *in vitro* models as well as the chemosensitizing *in vivo* therapeutic potential of *nanoIAZA* in a head & neck tumour xenograft. Negligible additional toxicity was seen with the novel glycopolymer vectors both in vitro and in vivo, which would encourage us to pursue further pharmaceuticals and gene encapsulation strategies to better target diseases with these nanomedicines and reduce the concomitant normal tissue toxicity of these therapeutics.

1.18 REFERENCES

(1) Anguela, X. M.; High, K. A. Entering the Modern Era of Gene Therapy. *Annu. Rev. Med.* **2019**, *70* (1), 273–288. https://doi.org/10.1146/annurev-med-012017-043332.

(2) Wong, J. K. L.; Mohseni, R.; Hamidieh, A. A.; MacLaren, R. E.; Habib, N.; Seifalian, A. M. Will Nanotechnology Bring New Hope for Gene Delivery? *Trends Biotechnol.* **2017**, *35* (5), 434–451. https://doi.org/10.1016/j.tibtech.2016.12.009.

(3) Ahmed, M.; Narain, R. Glycopolymer Bioconjugates. In *Engineered Carbohydrate-Based Materials for Biomedical Applications: Polymers, Surfaces, Dendrimers, Nanoparticles, and Hydrogels*; 2011; pp 167–188.

(4) Deng, W.; Chen, W.; Clement, S.; Guller, A.; Zhao, Z.; Engel, A.; Goldys, E. M. Controlled Gene and Drug Release from a Liposomal Delivery Platform Triggered by X-Ray Radiation. *Nat. Commun.* **2018**, *9* (1), 1–11.

https://doi.org/10.1038/s41467-018-05118-3.

(5) Kandil, R.; Merkel, O. M. Recent Progress of Polymeric Nanogels for Gene Delivery. *Curr. Opin. Colloid Interface Sci.* **2019**, *39*, 11–23. https://doi.org/10.1016/j.cocis.2019.01.005.

(6) Anselmo, A. C.; Mitragotri, S. Nanoparticles in the Clinic: An Update. *Bioeng. Transl. Med.* **2019**, *4* (3), 1–16. https://doi.org/10.1002/btm2.10143.

(7) Anselmo, A. C.; Mitragotri, S. Nanoparticles in the Clinic. *Bioeng. Transl. Med.* **2016**, *1* (1), 10–29. https://doi.org/10.1002/btm2.10003.

(8) Barenholz, Y. Doxil® - The First FDA-Approved Nano-Drug: Lessons Learned. *J. Control. Release* **2012**, *160* (2), 117–134. https://doi.org/10.1016/j.jconrel.2012.03.020.

(9) Miele, E. E.; Spinelli, G. P.; Miele, E. E.; Tomao, F.; Tomao, S. Albumin-Bound Formulation of Paclitaxel (Abraxane® ABI-007) in the Treatment of Breast Cancer. *Int. J. Nanomedicine* **2009**, *4* (1), 99–105. https://doi.org/10.2147/ijn.s3061.

(10) Shi, Y.; van der Meel, R.; Chen, X.; Lammers, T. The EPR Effect and beyond: Strategies to Improve Tumor Targeting and Cancer Nanomedicine Treatment Efficacy. *Theranostics* **2020**, *10* (17), 7921–7924. https://doi.org/10.7150/thno.49577.

(11) Abdul Karim, A.; Dou, Q.; Li, Z.; Loh, X. J. Emerging Supramolecular Therapeutic Carriers Based on Host-Guest Interactions. *Chem. - An Asian J.* **2016**, *00*, 0–0. https://doi.org/10.1002/asia.201501434.

(12) Muñoz-Bonilla, A.; Fernández-García, M. Glycopolymeric Materials for Advanced Applications. *Materials (Basel).* **2015**, *8* (5), 2276–2296. https://doi.org/10.3390/ma8052276.

(13) Yilmaz, G.; Becer, C. R. Glycopolymer Code: Programming Synthetic Macromolecules for Biological Targeting. *Macromol. Chem. Phys.* **2020**, *221* (7), 1–3. https://doi.org/10.1002/macp.202000006.

(14) Peng, Y.-Y. Y.; Diaz-Dussan, D.; Kumar, P.; Narain, R. Tumor Microenvironment-Regulated Redox Responsive Cationic Galactose-Based Hyperbranched Polymers for SiRNA Delivery. *Bioconjug. Chem.* **2019**, *30* (2), 405–412. https://doi.org/10.1021/acs.bioconjchem.8b00785.

(15) Peng, Y.-Y.; Diaz-Dussan, D.; Kumar, P.; Narain, R. Acid Degradable Cationic Galactose-Based Hyperbranched Polymers as Nanotherapeutic Vehicles for Epidermal Growth Factor Receptor (EGFR) Knockdown in Cervical Carcinoma. *Biomacromolecules* **2018**, *19* (10), 4052–4058. https://doi.org/10.1021/acs.biomac.8b01066.

(16) Xu, F. J. Versatile Types of Hydroxyl-Rich Polycationic Systems via O-Heterocyclic Ring-Opening Reactions: From Strategic Design to Nucleic Acid Delivery Applications. *Progress in Polymer Science*. 2018. https://doi.org/10.1016/j.progpolymsci.2017.09.003.

(17) Qi, M.; Duan, S.; Yu, B.; Yao, H.; Tian, W.; Xu, F.-J. PGMA-Based Supramolecular Hyperbranched Polycations for Gene Delivery. *Polym. Chem.* **2016**, *7* (26), 4334–4341. https://doi.org/10.1039/C6PY00759G.

(18) Li, R. Q.; Wu, Y.; Zhi, Y.; Yang, X.; Li, Y.; Xua, F. J.; Du, J. PGMA-Based Star-Like Polycations with Plentiful Hydroxyl Groups Act as Highly Efficient MiRNA Delivery Nanovectors for Effective Applications in Heart Diseases. *Adv. Mater.* **2016**. https://doi.org/10.1002/adma.201602319.

(19) Sun, Y.; Hu, H.; Yu, B.; Xu, F. J. PGMA-Based Cationic Nanoparticles with Polyhydric Iodine Units for Advanced Gene Vectors. *Bioconjug. Chem.* **2016**. https://doi.org/10.1021/acs.bioconjchem.6b00509.

(20) Chen, Y.; Diaz-Dussan, D.; Peng, Y.-Y. Y.; Narain, R. Hydroxyl-Rich PGMA-Based Cationic Glycopolymers for Intracellular SiRNA Delivery: Biocompatibility and Effect of Sugar Decoration Degree. *Biomacromolecules* **2019**, *20* (5), 2068–2074. https://doi.org/10.1021/acs.biomac.9b00274.

(21) Cai, H.; Xiang, Y.; Zeng, Y.; Li, Z.; Zheng, X.; Luo, Q.; Zhu, H.; Gong, Q.; Gu, Z.; Liu, Y.; Zhang, H.; Luo, K. Cathepsin B-Responsive and Gadolinium-Labeled Branched Glycopolymer-PTX Conjugate-Derived Nanotheranostics for Cancer Treatment. *Acta Pharm. Sin. B* **2020**. https://doi.org/10.1016/j.apsb.2020.07.023.

(22) Knox, S. S. From "omics" to Complex Disease: A Systems Biology Approach to Gene-Environment Interactions in Cancer. *Cancer Cell Int.* **2010**, *10*, 1–13. https://doi.org/10.1186/1475-2867-10-11.

(23) Matsumura, Y.; Maeda, H. A New Concept for Macromolecular Therapeutics in Cancer Chemotherapy: Mechanism of Tumoritropic Accumulation of Proteins and the Antitumor Agent Smancs. *Cancer Res.* **1986**, *46* (8), 6387–6392. https://doi.org/10.1021/bc100070g.

(24) Maeda, H.; Wu, J.; Sawa, T.; Matsumura, Y.; Hori, K. Tumor Vascular Permeability and the EPR Effect in Macromolecular Therapeutics: A Review. *J. Control. Release* **2000**, *65* (1–2), 271–284. https://doi.org/10.1016/S0168-3659(99)00248-5.

(25) Silva, V. L.; Al-Jamal, T. Exploiting the Cancer Niche: Tumor-Associated Macrophages and Hypoxia as Promising Synergistic Targets for Nano-Based Therapy. *J. Control. Release* **2017**, *253*, 82–96. https://doi.org/10.1016/j.jconrel.2017.03.013.

(26) Panariti, A.; Miserocchi, G.; Rivolta, I. The Effect of Nanoparticle Uptake on Cellular Behavior: Disrupting or Enabling Functions? *Nanotechnol. Sci. Appl.* **2012**, *5* (1), 87–100. https://doi.org/10.2147/NSA.S25515.

(27) van der Meel, R.; Sulheim, E.; Shi, Y.; Kiessling, F.; Mulder, W. J. M.; Lammers, T. Smart Cancer Nanomedicine. *Nat. Nanotechnol.* **2019**, *14* (11), 1007–1017. https://doi.org/10.1038/s41565-019-0567-y.

(28) Luk, B. T.; Zhang, L. Current Advances in Polymer-Based Nanotheranostics for Cancer Treatment and Diagnosis. *ACS Appl. Mater. Interfaces* **2014**, *6* (24), 21859–21873. https://doi.org/10.1021/am5036225.

(29) Germain, M.; Caputo, F.; Metcalfe, S.; Tosi, G.; Spring, K.; Åslund, A. K. O.; Pottier, A.; Schiffelers, R.; Ceccaldi, A.; Schmid, R. Delivering the Power of Nanomedicine to Patients Today. *J. Control. Release* **2020**, *326* (July), 164–171. https://doi.org/10.1016/j.jconrel.2020.07.007.

(30) Alfayez, M.; Kantarjian, H.; Kadia, T.; Ravandi-Kashani, F.; Daver, N. CPX-351 (Vyxeos) in AML. *Leuk. Lymphoma* **2020**, *61* (2), 288–297. https://doi.org/10.1080/10428194.2019.1660970.

(31) Fire, A.; Xu, S.; Montgomery, M. K.; Kostas, S. A.; Driver, S. E.; Mello, C. C. Potent and Specific Genetic Interference by Double-Stranded RNA in Caenorhabditis Elegans. *Nature* **1998**, *391* (6669), 806–811. https://doi.org/10.1038/35888.

(32) Hamilton, A. J.; Baulcombe, D. C. A Species of Small Antisense RNA in Posttranscriptional Gene Silencing in Plants. *Science (80-.).* **1999**, *286* (5441), 950-2. https://doi.org/10.1126/science.286.5441.950.

(33) Kim, T. K.; Eberwine, J. H. Mammalian Cell Transfection: The Present and the Future. *Anal. Bioanal. Chem.* **2010**, *397* (8), 3173–3178. https://doi.org/10.1007/s00216-010-3821-6.

(34) Davidson, B. L.; McCray, P. B. Current Prospects for RNA Interference-Based Therapies. *Nat. Rev. Genet.* **2011**, *12* (5), 329–340. https://doi.org/10.1038/nrg2968.

(35) Dang, C. V.; Reddy, E. P.; Shokat, K. M.; Soucek, L. Drugging the "undruggable" Cancer Targets. *Nat. Rev. Cancer* **2017**, *17* (8), 502–508. https://doi.org/10.1038/nrc.2017.36.

(36) Song, C.-Z. Gene Silencing Therapy Against Cancer. In *Gene Therapy for Cancer*; Humana Press: Totowa, NJ, 2007; pp 185–196. https://doi.org/10.1007/978-1-59745-222-9_11.

(37) Hanahan, D.; Weinberg, R. A.; Pan, K. H.; Shay, J. W.; Cohen, S. N.; Taylor, M. B.; Clarke, N. W.; Jayson, G. C.; Eshleman, J. R.; Nowak, M. A.; al., et. Hallmarks of Cancer: The Next Generation. *Cell* **2011**, *144* (5), 646–674. https://doi.org/10.1016/j.cell.2011.02.013.

(38) Devi, G. R. SiRNA-Based Approaches in Cancer Therapy. *Cancer Gene Ther.* **2006**, *13* (9), 819–829. https://doi.org/10.1038/sj.cgt.7700931.

(39) de Fougerolles, A.; Vornlocher, H. P.; Maraganore, J.; Lieberman, J. Interfering with Disease: A Progress Report on SiRNA-Based Therapeutics. *Nat. Rev. Drug Discov.* **2007**, *6* (6), 443–453. https://doi.org/10.1038/nrd2310.

(40) Emdad, L.; Sarkar, D.; Fisher, P. B. Gene Therapies for Cancer: Strategies, Challenges and Successes. *HHS Public Access* **2016**, *230* (2), 259–271. https://doi.org/10.1002/jcp.24791.Gene.

(41) Senderowicz, A. M. Inhibitors of Cyclin-Dependent Kinase Modulators for Cancer Therapy. In *Advances in Targeted Cancer Therapy*; Birkhäuser-Verlag: Basel, 2005; pp 183–206. https://doi.org/10.1007/3-7643-7414-4_8.

(42) Talebpour Amiri, F.; Fadaei Fathabadi, F.; Mahmoudi Rad, M.; Piryae, A.; Ghasemi, A.; Khalilian, A.; Yeganeh, F.; Mosaffa, N. The Effects of Insulin-Like Growth Factor-1 Gene Therapy and Cell Transplantation on Rat Acute Wound Model. *Iran. Red Crescent Med. J.* **2014**, *16* (10), 1–7.

https://doi.org/10.1177/0269881103017001687.

(43) Normanno, N.; De Luca, A.; Bianco, C.; Strizzi, L.; Mancino, M.; Maiello, M. R.; Carotenuto, A.; De Feo, G.; Caponigro, F.; Salomon, D. S. *Epidermal Growth Factor Receptor (EGFR) Signaling in Cancer*; Elsevier, 2006; Vol. 366, pp 2–16. https://doi.org/10.1016/j.gene.2005.10.018.

(44) Perez, R.; Crombet, T.; Leon, J. de; Moreno, E. A View on EGFR-Targeted Therapies from the Oncogene-Addiction Perspective. *Front. Pharmacol.* **2013**, *4*, 53. https://doi.org/10.3389/fphar.2013.00053.

(45) Lee, S.-Y. Y.; Yang, C.-Y. Y.; Peng, C.-L. L.; Wei, M.-F. F.; Chen, K.-C. C.; Yao, C.-J. J.; Shieh, M.-J. J. A Theranostic Micelleplex Co-Delivering SN-38 and VEGF SiRNA for Colorectal Cancer Therapy. *Biomaterials* **2016**, *86*, 92–105. https://doi.org/10.1016/j.biomaterials.2016.01.068.

(46) Koide, H.; Yoshimatsu, K.; Hoshino, Y.; Lee, S.-H.; Okajima, A.; Ariizumi, S.; Narita, Y.; Yonamine, Y.; Weisman, A. C.; Nishimura, Y.; Oku, N.; Miura, Y.; Shea, K. J. A Polymer Nanoparticle with Engineered Affinity for a Vascular Endothelial Growth Factor (VEGF165). *Nat. Chem.* **2017**, *9* (7), 715–722. https://doi.org/10.1038/nchem.2749.

(47) Zhang, W.-W.; Li, L.; Li, D.; Liu, J.; Li, X.; Li, W.; Xu, X.; Zhang, M. J.; Chandler, L. A.; Lin, H.; Hu, A.; Xu, W.; Lam, D. M.-K. The First Approved Gene Therapy Product for Cancer Ad- *P53* (Gendicine): 12 Years in the Clinic. *Hum. Gene Ther.* **2018**. https://doi.org/10.1089/hum.2017.218.

(48) Goodwin, E. C.; DiMaio, D. Repression of Human Papillomavirus Oncogenes in HeLa Cervical Carcinoma Cells Causes the Orderly Reactivation of Dormant Tumor Suppressor Pathways. *Proc. Natl. Acad. Sci. U. S. A.* **2000**, *97* (23), 12513–12518. https://doi.org/10.1073/pnas.97.23.12513.

(49) Tanaka, M.; Rosser, C. J.; Grossman, H. B. PTEN Gene Therapy Induces Growth Inhibition and Increases Efficacy of Chemotherapy in Prostate Cancer. *Cancer Detect. Prev.* **2005**. https://doi.org/10.1016/j.cdp.2004.07.006.

(50) Xu, X. C.; Abuduhadeer, X.; Zhang, W. B.; Li, T.; Gao, H.; Wang, Y. H. Knockdown of RAGE Inhibits Growth and Invasion of Gastric Cancer Cells. *Eur. J. Histochem.* **2013**, *57* (4), 36. https://doi.org/10.4081/ejh.2013.e36.

(51) Diaz-Dussan, D.; Nakagawa, Y.; Peng, Y.-Y. Y.; Sanchez, L. V.; Ebara, M.; Kumar, P.; Narain, R.; C, L. V. S.; Ebara, M.; Kumar, P.; Narain, R. Effective and Specific Gene Silencing of Epidermal Growth Factor Receptors Mediated by Conjugated Oxaborole and Galactose-Based Polymers. *ACS Macro Lett.* **2017**, *6* (7), 768–774. https://doi.org/10.1021/acsmacrolett.7b00388.

(52) Ciardiello, F.; De Vita, F. Epidermal Growth Factor Receptor (EGFR) Inhibitors in Cancer Therapy. In *Advances in Targeted Cancer Therapy*; Birkhäuser Basel: Basel, 2005; pp 93–115. https://doi.org/10.1007/3-7643-7414-4_5.

(53) Nicholson, R. .; Gee, J. M. .; Harper, M. . EGFR and Cancer Prognosis. *Eur. J. Cancer* **2001**, *37*, 9–15. https://doi.org/10.1016/S0959-8049(01)00231-3.

(54) Young, S. W. S.; Stenzel, M.; Jia-Lin, Y. Nanoparticle-SiRNA: A Potential Cancer Therapy? *Crit. Rev. Oncol. Hematol.* **2016**, *98*, 159–169. https://doi.org/10.1016/j.critrevonc.2015.10.015.

(55) Beija, M.; Salvayre, R.; Viguerie, N.; Marty, J.-D. D.; Lauth-de Viguerie, N.; Marty, J.-D. D.; Viguerie, N.; Marty, J.-D. D. Colloidal Systems for Drug Delivery: From Design to Therapy. *Trends Biotechnol.* **2012**, *30* (9), 485–496. https://doi.org/10.1016/j.tibtech.2012.04.008.

(56) Ramamoorth, M.; Narvekar, A. Non Viral Vectors in Gene Therapy - An Overview. *J. Clin. Diagnostic Res.* **2015**, *9* (1), GE01–GE06.

https://doi.org/10.7860/JCDR/2015/10443.5394.

(57) Abulateefeh, S. R.; Spain, S. G.; Aylott, J. W.; Chan, W. C.; Garnett, M. C.; Alexander, C. Thermoresponsive Polymer Colloids for Drug Delivery and Cancer Therapy. *Macromol. Biosci.* **2011**, *11* (12), 1722–1734. https://doi.org/10.1002/mabi.201100252.

(58) Behzadi, S.; Serpooshan, V.; Tao, W.; Hamaly, M. A.; Alkawareek, M. Y.; Dreaden, E. C.; Brown, D.; Alkilany, A. M.; Farokhzad, O. C.; Mahmoudi, M. Cellular Uptake of Nanoparticles: Journey inside the Cell. *Chem. Soc. Rev.* **2017**, *46* (14), 4218–4244. https://doi.org/10.1039/c6cs00636a.

(59) Thapa, B.; Narain, R. *Mechanism, Current Challenges and New Approaches for Non Viral Gene Delivery*; Elsevier Ltd., 2016. https://doi.org/10.1016/B978-0-08-100520-0.00001-1.

(60) Adjei, I. M.; Sharma, B.; Labhasetwar, V. Nanoparticles: Cellular Uptake and Cytotoxicity. In *Nanomaterial, Advances in Experimental Medicine and Biology*; Chen, Y., Capco, D. G., Eds.; 2014; Vol. 811. https://doi.org/10.1007/978-94-017-8739-0.

(61) Ali, F., Huang, J., & Hongbo, Z. Properties and Characterization of Biomaterials. In *Chemistry of Bioconjugates*; Narain, R., Ed.; Jon Wiley & Sons, 2013; pp 427–428. https://doi.org/doi:10.1142/9789812700858_0005.

(62) Dalby, B.; Cates, S.; Harris, A.; Ohki, E. C.; Tilkins, M. L.; Price, P. J.; Ciccarone, V. C. Advanced Transfection with Lipofectamine 2000 Reagent: Primary Neurons, SiRNA, and High-Throughput Applications. *Methods* **2004**, *33* (2), 95–103. https://doi.org/10.1016/j.ymeth.2003.11.023.

(63) Reineke, T. M.; Davis, M. E. *Nucleic Acid Delivery via Polymer Vehicles*; Elsevier B.V., 2012; Vol. 9. https://doi.org/10.1016/B978-0-444-53349-4.00239-9.

(64) Fihurka, O.; Sanchez-Ramos, J.; Sava, V. Optimizing Nanoparticle Design for Gene Therapy: Protection of Oligonucleotides from Degradation Without Impeding Release of Cargo. *Nanomed Nanosci Res* **2018**, *2* (6), 139–148. https://doi.org/10.29011/2577-1477.100055.

(65) Alexis, F.; Pridgen, E.; Molnar, L. K.; Farokhzad, O. C. Factors Affecting the Clearance and Biodistribution of Polymeric Nanoparticles. In *Molecular Pharmaceutics*; 2008. https://doi.org/10.1021/mp800051m.

(66) Michelle Longmire, Peter L. Choyke, M.D., and Hisataka Kobayashi, M.D., P. . Clearance Properties of Nano-Sized Particles and Molecules as Imagin Agents: Consideration and Caveats. **2012**, *3* (5), 703–717. https://doi.org/10.2217/17435889.3.5.703.Clearance.

(67) Zelepukin, I. V.; Yaremenko, A. V.; Yuryev, M. V.; Mirkasymov, A. B.; Sokolov, I. L.; Deyev, S. M.; Nikitin, P. I.; Nikitin, M. P. Fast Processes of Nanoparticle Blood Clearance: Comprehensive Study. *J. Control. Release* **2020**, *326*, 181–191. https://doi.org/10.1016/J.JCONREL.2020.07.014.

(68) Narain, R.; Wang, Y.; Ahmed, M.; Lai, B. F. L.; Kizhakkedathu, J. N. Blood Components Interactions to Ionic and Nonionic Glyconanogels. *Biomacromolecules* **2015**, *16* (9), 2990–2997. https://doi.org/10.1021/acs.biomac.5b00890.

(69) Foroozandeh, P.; Aziz, A. A. Insight into Cellular Uptake and Intracellular Trafficking of Nanoparticles. *Nanoscale Res. Lett.* **2018**, *13*. https://doi.org/10.1186/s11671-018-2728-6.

(70) Kadam, R. S.; Bourne, D. W. A.; Kompella, U. B. Nano-Advantage in Enhanced Drug Delivery with Biodegradable Nanoparticles: Contribution of Reduced Clearance. *Drug Metab. Dispos.* **2012**, *40* (7), 1380–1388. https://doi.org/10.1124/dmd.112.044925.

(71) Kafil, V.; Omidi, Y. Cytotoxic Impacts of Linear and Branched Polyethylenimine Nanostructures in A431 Cells. *Bioimpacts* **2011**, *1* (1), 23–30. https://doi.org/10.5681/bi.2011.004.

(72) Zhong, Y.-Q.; Wei, J.; Fu, Y.-R.; Shao, J.; Liang, Y.-W.; Lin, Y.-H.; Liu, J.; Zhu, Z.-H. Toxicity of Cationic Liposome Lipofectamine 2000 in Human Pancreatic Cancer Capan-2 Cells. *Nan Fang Yi Ke Da Xue Xue Bao* **2008**, *28* (11), 1981–1984.

(73) Bono, N.; Ponti, F.; Mantovani, D.; Candiani, G. Non-Viral in Vitro Gene Delivery: It Is Now Time to Set the Bar! *Pharmaceutics* **2020**, *12* (2). https://doi.org/10.3390/pharmaceutics12020183.

(74) Mastrobattista, E.; Hennink, W. E. Polymers for Gene Delivery: Charged for Success. *Nat. Mater.* **2011**. https://doi.org/10.1038/nmat3209.

(75) Ohno, K.; Tsujii, Y.; Miyamoto, T.; Fukuda, T.; Goto, M.; Kobayashi, K.; Akaike, T. Synthesis of a Well-Defined Glycopolymer by Nitroxide-Controlled Free Radical Polymerization. *Macromolecules* **1998**. https://doi.org/10.1021/ma971329g.

(76) Adokoh, C. K.; Quan, S.; Hitt, M.; Darkwa, J.; Kumar, P.; Narain, R. Synthesis and Evaluation of Glycopolymeric Decorated Gold Nanoparticles Functionalized with Gold-Triphenyl Phosphine as Anti-Cancer Agents. *Biomacromolecules* **2014**, *15* (10), 3802–3810. https://doi.org/10.1021/bm5010977.

(77) Ladmiral, V.; Semsarilar, M.; Canton, I.; Armes, S. P. Polymerization-Induced Self-Assembly of Galactose-Functionalized Biocompatible Diblock Copolymers for Intracellular Delivery. *J. Am. Chem. Soc.* **2013**. https://doi.org/10.1021/ja407033x.

(78) Kasper, B. The Challenge of Finding New Therapeutic Avenues in Soft Tissue Sarcomas. *Clin. Sarcoma Res.* **2019**, *9* (1), 1–5. https://doi.org/10.1186/s13569-019-0115-4.

(79) Lowe, A. B.; Sumerlin, B. S.; McCormick, C. L. The Direct Polymerization of 2-

Methacryloxyethyl Glucoside via Aqueous Reversible Addition-Fragmentation Chain Transfer (RAFT) Polymerization. *Polymer (Guildf).* **2003**. https://doi.org/10.1016/j.polymer.2003.08.039.

(80) Van Bruggen, C.; Hexum, J. K.; Tan, Z.; Dalal, R. J.; Reineke, T. M. Nonviral Gene Delivery with Cationic Glycopolymers. *Acc. Chem. Res.* **2019**. https://doi.org/10.1021/acs.accounts.8b00665.

(81) Ahmed, M.; Narain, R. Progress of RAFT Based Polymers in Gene Delivery. *Prog. Polym. Sci.* **2013**, *38* (5), 767–790. https://doi.org/10.1016/j.progpolymsci.2012.09.008.

(82) Miura, Y.; Hoshino, Y.; Seto, H. Glycopolymer Nanobiotechnology. *Chem. Rev.* **2016**, *116* (4), 1673–1692. https://doi.org/10.1021/acs.chemrev.5b00247.

(83) Quan, S.; Kumar, P.; Narain, R. Cationic Galactose-Conjugated Copolymers for Epidermal Growth Factor (EGFR) Knockdown in Cervical Adenocarcinoma. *ACS Biomater. Sci. Eng.* **2016**, *2* (5), 853–859. https://doi.org/10.1021/acsbiomaterials.6b00085.

(84) Reineke, T. M. Poly(Glycoamidoamine)s: Cationic Glycopolymers for DNA Delivery. *J. Polym. Sci. Part A Polym. Chem.* **2006**, *44* (24), 6895–6908. https://doi.org/10.1002/pola.21697.

(85) Miura, Y. Design and Synthesis of Well-Defined Glycopolymers for the Control of Biological Functionalities. *Polym. J.* **2012**, *44* (7), 679–689. https://doi.org/10.1038/pj.2012.4.

(86) Monaco, A.; Beyer, V. P.; Napier, R.; Becer, C. R. Multi-Arm Star Shaped Glycopolymers with Precisely Controlled Core Size and Arm Length. *Biomacromolecules* **2020**. https://doi.org/10.1021/acs.biomac.0c00838.

(87) Moad, G.; Rizzardo, E.; Thang, S. H. RAFT Polymerization and Some of Its

Applications. *Chem. - An Asian J.* **2013**, *8* (8), 1634–1644. https://doi.org/10.1002/asia.201300262.

(88) Wang, Y.; Zhang, X.; Yu, P.; Li, C. Glycopolymer Micelles with Reducible Ionic Cores for Hepatocytes-Targeting Delivery of DOX. *Int. J. Pharm.* **2013**. https://doi.org/10.1016/j.ijpharm.2012.12.001.

(89) Thapa, B.; Kumar, P.; Zeng, H.; Narain, R. Asialoglycoprotein Receptor-Mediated Gene Delivery to Hepatocytes Using Galactosylated Polymers. *Biomacromolecules* **2015**, *16* (9), 3008–3020. https://doi.org/10.1021/acs.biomac.5b00906.

(90) Roggenbuck, D.; Mytilinaiou, M. G.; Lapin, S. V.; Reinhold, D.; Conrad, K. Asialoglycoprotein Receptor (ASGPR): A Peculiar Target of Liver-Specific Autoimmunity. *Autoimmun. Highlights* **2012**, *3* (3), 119–125. https://doi.org/10.1007/s13317-012-0041-4.

(91) Huang, Y. Preclinical and Clinical Advances of GalNAc-Decorated Nucleic Acid Therapeutics. *Mol. Ther. - Nucleic Acids* **2017**, *6* (March), 116–132. https://doi.org/10.1016/j.omtn.2016.12.003.

(92) Ahmed, M.; Deng, Z.; Liu, S.; Lafrenie, R.; Kumar, A.; Narain, R. Cationic Glyconanoparticles: Their Complexation with DNA, Cellular Uptake, and Transfection Efficiencies. *Bioconjug. Chem.* **2009**, *20* (11), 2169–2176. https://doi.org/10.1021/bc900350c.

(93) Ahmed, M.; Deng, Z.; Narain, R. Study of Transfection Efficiencies of Cationic Glyconanoparticles of Different Sizes in Human Cell Line. *ACS Appl. Mater. Interfaces* **2009**, *1* (9), 1980–1987. https://doi.org/10.1021/am900357x.

(94) Holban, A. M.; Grumezescu, A. M.; Frère, A.; Evrard, B.; Mottet, D.; Piel, G. Polymeric Nanoparticles as SiRNA Drug Delivery System for Cancer Therapy: The Long Road to Therapeutic Efficiency. In *Nanoarchitectonics for Smart Delivery and*

Drug Targeting; 2016; pp 503–540. https://doi.org/10.1016/B978-0-323-47347-7.00018-5.

(95) Smith, A. E.; Sizovs, A.; Grandinetti, G.; Xue, L.; Reineke, T. M. Diblock Glycopolymers Promote Colloidal Stability of Polyplexes and Effective PDNA and SiRNA Delivery under Physiological Salt and Serum Conditions. *Biomacromolecules* **2011**, *12* (8), 3015–3022. https://doi.org/10.1021/bm200643c.

(96) Wadhwa*, M. S.; Rice*, K. G. Receptor Mediated Glycotargeting. *J. Drug Target.* **2003**, *11* (5), 255–268. https://doi.org/10.1080/10611860310001636557.

(97) Ahmed, M.; Narain, R. *Synthetic Cationic Glycopolymers for Gene Delivery*; Elsevier Ltd., 2016. https://doi.org/10.1016/B978-0-08-100520-0.00004-7.

(98) Zhang, Y.; Wang, B.; Zhang, Y.; Zheng, Y.; Wen, X.; Bai, L.; Wu, Y. Hyperbranched Glycopolymers of 2-(α-D-Mannopyranose) Ethyl Methacrylate and N, N'-Methylenebisacrylamide: Synthesis, Characterization and Multivalent Recognitions with Concanavalin A. *Polymers (Basel).* **2018**, *10* (2). https://doi.org/10.3390/polym10020171.

(99) Li, Y.; Gao, J.; Zhang, C.; Cao, Z.; Cheng, D.; Liu, J.; Shuai, X. Stimuli-Responsive Polymeric Nanocarriers for Efficient Gene Delivery. *Top. Curr. Chem.* **2017**, *375* (2), 27. https://doi.org/10.1007/s41061-017-0119-6.

(100) Peng, Y.-Y.; Diaz-Dussan, D.; Vani, J.; Hao, X.; Kumar, P.; Narain, R. Achieving Safe and Highly Efficient Epidermal Growth Factor Receptor Silencing in Cervical Carcinoma by Cationic Degradable Hyperbranched Polymers. *ACS Appl. Bio Mater.* **2018**, *1* (4), 961–966. https://doi.org/10.1021/acsabm.8b00371.

(101) Mura, S.; Nicolas, J.; Couvreur, P. Stimuli-Responsive Nanocarriers for Drug Delivery. *Nat. Mater.* **2013**, *12* (11), 991–1003. https://doi.org/10.1038/nmat3776.

(102) Nakamura, Y.; Mochida, A.; Choyke, P. L.; Kobayashi, H. Nanodrug Delivery: Is

the Enhanced Permeability and Retention Effect Sufficient for Curing Cancer? *Bioconjug. Chem.* **2016**, *27* (10), 2225–2238. https://doi.org/10.1021/acs.bioconjchem.6b00437.

(103) Kunath, K.; von Harpe, A.; Fischer, D.; Kissel, T. Galactose-PEI–DNA Complexes for Targeted Gene Delivery: Degree of Substitution Affects Complex Size and Transfection Efficiency. *J. Control. Release* **2003**, *88* (1), 159–172. https://doi.org/10.1016/S0168-3659(02)00458-3.

(104) Oishi, M.; Nagasaki, Y.; Nishiyama, N.; Itaka, K.; Takagi, M.; Shimamoto, A.; Furuichi, Y.; Kataoka, K. Enhanced Growth Inhibition of Hepatic Multicellular Tumor Spheroids by Lactosylated Poly(Ethylene Glycol)-SiRNA Conjugate Formulated in PEGylated Polyplexes. *ChemMedChem* **2007**. https://doi.org/10.1002/cmdc.200700076.

(105) Wang, B.; Shao, P.; Wang, Y.; Li, J.; Zhang, Y. The Application of Thermosensitive Nanocarriers in Controlled Drug Delivery. *J. Nanomater.* **2011**, *2011*. https://doi.org/10.1155/2011/389640.

(106) Pearson, S.; Allen, N.; Stenzel, M. H. Core-Shell Particles with Glycopolymer Shell and Polynucleoslde Core via RAFT: From Micelles to Rods. *J. Polym. Sci. Part A Polym. Chem.* **2009**. https://doi.org/10.1002/pola.23275.

(107) Schmidt, J. J.; Rowley, J.; Hyun, J. K. Hydrogels Used for Cell-Based Drug Delivery. *J. Biomed. Mater. Res. - Part A* **2008**, *87* (4), 1113–1122. https://doi.org/10.1002/jbm.a.32287.

(108) Yalcin, A.; Telang, S.; Clem, B.; Chesney, J. Regulation of Glucose Metabolism by 6-Phosphofructo-2-Kinase/Fructose-2,6-Bisphosphatases in Cancer. *Experimental and Molecular Pathology*. 2009, pp 174–179. https://doi.org/10.1016/j.yexmp.2009.01.003.

(109) Liu, L. I.; Zhang, J.; Wenhui, L. V.; Luo, Y. A. N.; Wang, X. Well-Defined Ph-Sensitive Block Glycopolymers via Reversible Addition-Fragmentation Chain Transfer Radical Polymerization: Synthesis, Characterization, and Recognition with Lectin. *J. Polym. Sci. Part A Polym. Chem.* **2010**. https://doi.org/10.1002/pola.24119.

(110) Li, J.; Zhang, Y.; Cai, C.; Rong, X.; Shao, M.; Li, J.; Yang, C.; Yu, G. Collaborative Assembly of Doxorubicin and Galactosyl Diblock Glycopolymers for Targeted Drug Delivery of Hepatocellular Carcinoma. *Biomater. Sci.* **2020**, *8* (1), 189–200. https://doi.org/10.1039/c9bm01604j.

(111) Jin, X.; Zhang, X.; Wu, Z.; Teng, D.; Zhang, X.; Wang, Y.; Wang, Z.; Li, C. Amphiphilic Random Glycopolymer Based on Phenylboronic Acid: Synthesis, Characterization, and Potential as Glucose-Sensitive Matrix. *Biomacromolecules* **2009**. https://doi.org/10.1021/bm8010006.

(112) Wu, J.; Yuan, J.; Ye, B.; Wu, Y.; Xu, Z.; Chen, J.; Chen, J. Dual-Responsive Core Crosslinking Glycopolymer-Drug Conjugates Nanoparticles for Precise Hepatocarcinoma Therapy. *Front. Pharmacol.* **2018**, *9* (JUL), 1–12. https://doi.org/10.3389/fphar.2018.00663.

(113) Sultana, F.; Manirujjaman; Imran-Ul-Haque; Arafat, M.; Sharmin, S. An Overview of Nanogel Drug Delivery System. *J. Appl. Pharm. Sci.* **2013**. https://doi.org/10.7324/JAPS.2013.38.S15.

(114) Quan, S.; Wang, Y.; Zhou, A.; Kumar, P.; Narain, R. Galactose-Based Thermosensitive Nanogels for Targeted Drug Delivery of Iodoazomycin Arabinofuranoside (IAZA) for Theranostic Management of Hypoxic Hepatocellular Carcinoma. *Biomacromolecules* **2015**, *16* (7), 1978–1986. https://doi.org/10.1021/acs.biomac.5b00576.

(115) Gary, D. J.; Min, J. Bin; Kim, Y.; Park, K.; You-Yeon, W. The Effect of N/P Ratio

on the In Vitro and In Vivo Interaction Properties of PEGylated Poly(2-(Dimethylamino)Ethyl Methacrylate)-Based SiRNA Complexes. *Macromol. Biosci.* **2014**, *71* (11), 3831–3840. https://doi.org/10.1158/0008-5472.CAN-10-4002.BONE.

(116) Blasco, E.; Sims, M. B.; Goldmann, A. S.; Sumerlin, B. S.; Barner-Kowollik, C. 50th Anniversary Perspective: Polymer Functionalization. *Macromolecules* **2017**, *50* (14), 5215–5252. https://doi.org/10.1021/acs.macromol.7b00465.

(117) Hashida, M.; Hirabayashi, H.; Nishikawa, M.; Takakura, Y. Targeted Delivery of Drugs and Proteins to the Liver via Receptor-Mediated Endocytosis. *J. Control. Release* **1997**, *46* (1–2), 129–137. https://doi.org/10.1016/S0168-3659(96)01577-5.

(118) Gupta, S.; Gupta, M. K. Possible Role of Nanocarriers in Drug Delivery against Cervical Cancer. *Nano Rev. Exp.* **2017**, *8* (1), 1335567. https://doi.org/10.1080/20022727.2017.1335567.

(119) Moselhy, J.; Srinivasan, S.; Ankem, M. K.; Damodaran, C. Natural Products That Target Cancer Stem Cells. *Anticancer Res.* **2015**, *35* (11), 5773–5788.

(120) Sun, Y.; Hu, H.; Zhao, N.; Xia, T.; Yu, B.; Shen, C.; Xu., F. J. Multifunctional Polycationic Photosensitizer Conjugates with Rich Hydroxyl Groups for Versatile Water-Soluble Photodynamic Therapy Nanoplatforms. *Biomaterials* **2017**. https://doi.org/10.1016/j.biomaterials.2016.11.055.

(121) Lu, J.; Zhang, W.; Yuan, L.; Ma, W.; Li, X.; Lu, W.; Zhao, Y.; Chen, G. One-Pot Synthesis of Glycopolymer-Porphyrin Conjugate as Photosensitizer for Targeted Cancer Imaging and Photodynamic Therapy. *Macromol. Biosci.* **2014**, *14* (3), 340–346. https://doi.org/10.1002/mabi.201300451.

(122) Ma, Z.; Liu, H.; Peng, Z.; Xuan, Y.; Rivera, E.; Zhu, X. X. Star-Shaped Glycopolymers with a Porphyrin Core: Synthesis, Singlet Oxygen Generation, and

Photodynamic Therapy. *ACS Appl. Polym. Mater.* **2020**, *2* (6), 2477–2484. https://doi.org/10.1021/acsapm.0c00451.

(123) Chen, S.; Sun, B.; Miao, H.; Wang, G.; Sun, P.; Li, J.; Wang, W.; Fan, Q.; Huang, W. NIR-II Dye-Based Multifunctional Telechelic Glycopolymers for NIR-IIa Fluorescence Imaging-Guided Stimuli-Responsive Chemo-Photothermal Combination Therapy. *ACS Mater. Lett.* **2020**, *2* (2), 174–183. https://doi.org/10.1021/acsmaterialslett.9b00480.

(124) McCain, J. The Future of Human Gene Therapy. *Biotechnol. Healthc.* **2005**, *22* (3), 113–142. https://doi.org/10.1016/S0098-2997(01)00004-8.

(125) Arruebo, M.; Vilaboa, N.; Sáez-Gutierrez, B.; Lambea, J.; Tres, A.; Valladares, M.; González-Fernández, Á. Assessment of the Evolution of Cancer Treatment Therapies. *Cancers (Basel).* **2011**, *3* (3), 3279–3330. https://doi.org/10.3390/cancers3033279.

(126) Cyprian, F. S.; Akhtar, S.; Gatalica, Z.; Vranic, S. Targeted Immunotherapy with a Checkpoint Inhibitor in Combination with Chemotherapy: A New Clinical Paradigm in the Treatment of Triple-Negative Breast Cancer. *Bosn. J. basic Med. Sci.* **2019**, *19* (3), 227–233. https://doi.org/10.17305/bjbms.2019.4204.

(127) Yoshida, G. J.; Saya, H. Therapeutic Strategies Targeting Cancer Stem Cells. *Cancer Sci.* **2016**, *107* (1), 5–11. https://doi.org/10.1111/cas.12817.

(128) Wang, H.; Agarwal, P.; Zhao, S.; Xu, R. X.; Yu, J.; Lu, X.; He, X. Hyaluronic Acid-Decorated Dual Responsive Nanoparticles of Pluronic F127, PLGA, and Chitosan for Targeted Co-Delivery of Doxorubicin and Irinotecan to Eliminate Cancer Stem-like Cells. *Biomaterials* **2015**, *72*, 74–89. https://doi.org/10.1016/j.biomaterials.2015.08.048.

(129) Huang, Y.; Luo, Y.; Zheng, W.; Chen, T. Rational Design of Cancer-Targeted BSA

Protein Nanoparticles as Radiosensitizer to Overcome Cancer Radioresistance. *ACS Appl. Mater. Interfaces* **2014**, *6* (21), 19217–19228. https://doi.org/10.1021/am505246w.

(130) Lee, J. Y.; Termsarasab, U.; Park, J. H.; Lee, S. Y.; Ko, S. H.; Shim, J. S.; Chung, S. J.; Cho, H. J.; Kim, D. D. Dual CD44 and Folate Receptor-Targeted Nanoparticles for Cancer Diagnosis and Anticancer Drug Delivery. *J. Control. Release* **2016**. https://doi.org/10.1016/j.jconrel.2016.06.021.

(131) Singhsa, P.; Diaz-Dussan, D.; Manuspiya, H.; Narain, R. Well-Defined Cationic N-[3-(Dimethylamino)Propyl]Methacrylamide Hydrochloride-Based (Co)Polymers for SiRNA Delivery. *Biomacromolecules* **2018**, *19* (1), 209–221. https://doi.org/10.1021/acs.biomac.7b01475.

(132) Ahmed, M.; Wattanaarsakit, P.; Narain, R. Cationic Glyco-Nanogels for Epidermal Growth Factor Receptor (EGFR) Specific SiRNA Delivery in Ovarian Cancer Cells. *Polym. Chem.* **2013**, *4* (13), 3829–3836. https://doi.org/10.1039/c3py00425b.

(133) Zhang, C. G.; Zhu, W. J.; Liu, Y.; Yuan, Z. Q.; Yang, S. Di; Chen, W. L.; Li, J. Z.; Zhou, X. F.; Liu, C.; Zhang, X. N. Novel Polymer Micelle Mediated Co-Delivery of Doxorubicin and P-Glycoprotein SiRNA for Reversal of Multidrug Resistance and Synergistic Tumor Therapy. *Sci. Rep.* **2016**, *6* (March), 1–12. https://doi.org/10.1038/srep23859.

(134) Zhang, H. Onivyde for the Therapy of Multiple Solid Tumors. *Onco. Targets. Ther.* **2016**, *9*, 3001–3007. https://doi.org/10.2147/OTT.S105587.

(135) Filipová, M.; Bojarová, P.; Rodrigues Tavares, M.; Bumba, L.; Elling, L.; Chytil, P.; Gunár, K.; Křen, V.; Etrych, T.; Janoušková, O. Glycopolymers for Efficient Inhibition of Galectin-3: In Vitro Proof of Efficacy Using Suppression of T Lymphocyte Apoptosis and Tumor Cell Migration. *Biomacromolecules* **2020**. https://doi.org/10.1021/acs.biomac.0c00515.

(136) Spain, S. G.; Cameron, N. R. A Spoonful of Sugar: The Application of Glycopolymers in Therapeutics. *J. Mater. Chem. C* **2015**, *3*, 10715–10722. https://doi.org/10.1039/b000000x.

(137) Ahmed M. Eissa; Cameron, N. R. Glycopolymer Conjugates. In *Advances in Polymer Science*; 2013; Vol. 253, pp 71–114. https://doi.org/10.1007/12_2012_177.

(138) Yilmaz, G.; Becer, C. R. Glycopolymer Code Based on Well-Defined Glycopolymers or Glyconanomaterials and Their Biomolecular Recognition. *Front. Bioeng. Biotechnol.* **2014**, *2* (OCT), 1–18. https://doi.org/10.3389/fbioe.2014.00039.

(139) Omurtag Ozgen, P. S.; Atasoy, S.; Zengin Kurt, B.; Durmus, Z.; Yigit, G.; Dag, A. Glycopolymer Decorated Multiwalled Carbon Nanotubes for Dual Targeted Breast Cancer Therapy. *J. Mater. Chem. B* **2020**, *8* (15), 3123–3137. https://doi.org/10.1039/c9tb02711d.

(140) Meenu Vasudevan, S.; Ashwanikumar, N.; Vinod Kumar, G. S. Peptide Decorated Glycolipid Nanomicelles for Drug Delivery across the Blood-Brain Barrier (BBB). *Biomater. Sci.* **2019**, *7* (10), 4017–4021. https://doi.org/10.1039/c9bm00955h.

(141) Nair, J. K.; Willoughby, J. L. S.; Chan, A.; Charisse, K.; Alam, M. R.; Wang, Q.; Hoekstra, M.; Kandasamy, P.; Kelin, A. V.; Milstein, S.; Taneja, N.; Oshea, J.; Shaikh, S.; Zhang, L.; Van Der Sluis, R. J.; Jung, M. E.; Akinc, A.; Hutabarat, R.; Kuchimanchi, S.; Fitzgerald, K.; Zimmermann, T.; Van Berkel, T. J. C.; Maier, M. A.; Rajeev, K. G.; Manoharan, M. Multivalent N -Acetylgalactosamine-Conjugated SiRNA Localizes in Hepatocytes and Elicits Robust RNAi-Mediated Gene Silencing. *J. Am. Chem. Soc.* **2014**, *136* (49), 16958–16961. https://doi.org/10.1021/ja505986a.

(142) Park, H.; Walta, S.; Rosencrantz, R. R.; Körner, A.; Schulte, C.; Elling, L.; Richtering, W.; Böker, A. Micelles from Self-Assembled Double-Hydrophilic PHEMA-Glycopolymer-Diblock Copolymers as Multivalent Scaffolds for Lectin

Binding. *Polym. Chem.* **2016**. https://doi.org/10.1039/c5py00797f.

(143) Wuest, K. N. R.; Lu, H.; Thomas, D. S.; Goldmann, A. S.; Stenzel, M. H.; Barner-Kowollik, C. Fluorescent Glyco Single-Chain Nanoparticle-Decorated Nanodiamonds. *ACS Macro Lett.* **2017**. https://doi.org/10.1021/acsmacrolett.7b00659.

(144) Roy, R. Syntheses and Some Applications of Chemically Defined Multivalent Glycoconjugates. *Curr. Opin. Struct. Biol.* **1996**, *6* (5), 692–702. https://doi.org/10.1016/S0959-440X(96)80037-6.

(145) Gonzalez-Cao, M.; Karachaliou, N.; Santarpia, M.; Viteri, S.; Meyerhans, A.; Rosell, R. Activation of Viral Defense Signaling in Cancer. *Ther. Adv. Med. Oncol.* **2018**, *10*, 175883591879310. https://doi.org/10.1177/1758835918793105.

(146) Wu, D.; Wang, W.; Diaz-Dussan, D.; Peng, Y.-Y.; Chen, Y.; Narain, R.; Hall, D. G. In Situ Forming, Dual-Crosslink Network, Self-Healing Hydrogel Enabled by a Bioorthogonal Nopoldiol–Benzoxaborolate Click Reaction with a Wide PH Range. *Chem. Mater.* **2019**, *31* (11), 4092–4102. https://doi.org/10.1021/acs.chemmater.9b00769.

(147) Siirilä, J.; Hietala, S.; Ekholm, F. S.; Tenhu, H. Glucose and Maltose Surface-Functionalized Thermoresponsive Poly(N-Vinylcaprolactam) Nanogels. *Biomacromolecules* **2020**, *21* (2), 955–965. https://doi.org/10.1021/acs.biomac.9b01596.

(148) Lehrman, S. Virus Treatment Questioned after Gene Therapy Death. *Nature* **1999**. https://doi.org/10.1038/43977.

(149) Thomas Carroll. Introduction to Gene Therapy. *Eur. Soc. Cell Gene Ther.* **2011**, 1–7. https://doi.org/10.1007/978-3-0348-0402-8_1.

(150) Abdellatif, A. A. H.; Abdelhafez, W. A.; Sarhan, H. A. Somatostatin Decorated

Quantum Dots for Targeting of Somatostatin Receptors. *Iran. J. Pharm. Res.* **2018**, *17* (2), 513–524. https://doi.org/10.22037/ijpr.2018.2189.

(151) The Two Directions of Cancer Nanomedicine. *Nat. Nanotechnol.* **2019**, *14* (12), 1083. https://doi.org/10.1038/s41565-019-0597-5.

(152) Davis, M. E.; Zuckerman, J. E.; Choi, C. H. J.; Seligson, D.; Tolcher, A.; Alabi, C. A.; Yen, Y.; Heidel, J. D.; Ribas, A. Evidence of RNAi in Humans from Systemically Administered SiRNA via Targeted Nanoparticles. *Nature* **2010**, *464* (7291), 1067–1070. https://doi.org/10.1038/nature08956.

(153) Gotwals, P.; Cameron, S.; Cipolletta, D.; Cremasco, V.; Crystal, A.; Hewes, B.; Mueller, B.; Quaratino, S.; Sabatos-Peyton, C.; Petruzzelli, L.; Engelman, J. A.; Dranoff, G. Prospects for Combining Targeted and Conventional Cancer Therapy with Immunotherapy. *Nat. Rev. Cancer* **2017**, *17* (5), 286–301. https://doi.org/10.1038/nrc.2017.17.

(154) Velpurisiva, P.; Gad, A.; Piel, B.; Jadia, R.; Rai, P. Nanoparticle Design Strategies for Effective Cancer Immunotherapy. *J. Biomed.* **2017**, *2* (2), 64–77. https://doi.org/10.7150/jbm.18877.Nanoparticle.

(155) Zhu, G.; Zhang, F.; Ni, Q.; Niu, G.; Chen, X. Efficient Nanovaccine Delivery in Cancer Immunotherapy. *ACS Nano* **2017**, *11* (3), 2387–2392. https://doi.org/10.1021/acsnano.7b00978.

(156) Zhu, G.; Mei, L.; Vishwasrao, H. D.; Jacobson, O.; Wang, Z.; Liu, Y.; Yung, B. C.; Fu, X.; Jin, A.; Niu, G.; Wang, Q.; Zhang, F.; Shroff, H.; Chen, X. Intertwining DNA-RNA Nanocapsules Loaded with Tumor Neoantigens as Synergistic Nanovaccines for Cancer Immunotherapy. *Nat. Commun.* **2017**, *8* (1). https://doi.org/10.1038/s41467-017-01386-7.

(157) Luo, M.; Samandi, L. Z.; Wang, Z.; Chen, Z. J.; Gao, J. Synthetic Nanovaccines for

Immunotherapy. *J. Control. Release* **2017**. https://doi.org/10.1016/j.jconrel.2017.03.033.

(158) Sathiyajith, C. W. Nanovaccines for Cancer Immunotherapy. *Int. J. Vaccines Vaccin.* **2017**, *4* (4). https://doi.org/10.15406/ijvv.2017.04.00085.

(159) Palucka, K.; Banchereau, J. Cancer Immunotherapy via Dendritic Cells. *Nat. Rev. Cancer* **2012**, *12* (4), 265–277. https://doi.org/10.1038/nrc3258.

(160) Jiang, T.; Chen, X.; Zhou, W.; Fan, G.; Zhao, P.; Ren, S.; Zhou, C.; Zhang, J. Immunotherapy with Dendritic Cells Modified with Tumor-Associated Antigen Gene Demonstrates Enhanced Antitumor Effect Against Lung Cancer. *Transl. Oncol.* **2017**, *10* (2), 132–141. https://doi.org/10.1016/j.tranon.2016.12.002.

(161) Kranz, Lena M. Diken, M.; Haas, Heinrich. Kreiter, S. Systemic RNA Delivery to Dendritic Cells Exploits Antiviral Defence for Cancer Immunotherapy. *Nat* **2016**, *534*.

(162) Miconnet, I.; Koenig, S.; Speiser, D.; Krieg, A.; Guillaume, P.; Cerottini, J.-C.; Romero, P. CpG Are Efficient Adjuvants for Specific CTL Induction Against Tumor Antigen-Derived Peptide. *J. Immunol.* **2002**, *168* (3), 1212–1218. https://doi.org/10.4049/jimmunol.168.3.1212.

(163) Jahrsdörfer, B.; Weiner, G. J. CpG Oligodeoxynucleotides as Immunotherapy in Cancer. *Update on Cancer Therapeutics*. 2008, pp 27–32. https://doi.org/10.1016/j.uct.2007.11.003.

(164) Naves, L. B.; Dhand, C.; Venugopal, J. R.; Rajamani, L.; Ramakrishna, S.; Almeida, L. Nanotechnology for the Treatment of Melanoma Skin Cancer. *Prog. Biomater.* **2017**, *6* (1–2), 13–26. https://doi.org/10.1007/s40204-017-0064-z.

(165) Bristow, R. G.; Hill, R. P. Hypoxia and Metabolism. Hypoxia, DNA Repair and Genetic Instability. *Nat. Rev. Cancer* **2008**, *8* (3), 180–192.

https://doi.org/10.1038/nrc2344.

(166) Wardman, P. Chemical Radiosensitizers for Use in Radiotherapy. *Clin. Oncol.* **2007**, *19* (6), 397–417. https://doi.org/10.1016/j.clon.2007.03.010.

(167) Begg, A. C.; Stewart, F. A.; Vens, C. Strategies to Improve Radiotherapy with Targeted Drugs. *Nat. Rev. Cancer* **2011**, *11* (4), 239–253. https://doi.org/10.1038/nrc3007.

(168) Seiwert, T. Y.; Salama, J. K.; Vokes, E. E. The Concurrent Chemoradiation Paradigm—General Principles. *Nat. Clin. Pract. Oncol.* **2007**, *4* (2), 86–100. https://doi.org/10.1038/ncponc0714.

(169) Schultz, R. M. *Advances in Targeted Cancer Therapy (Progress in Drug Research)*; Herrling, P. L., Matter, A., Schultz, R. M., Eds.; Birkhäuser Basel: Basel, 2005. https://doi.org/10.1007/3-7643-7414-4.

(170) Cleary, J.; Gelband, H.; Wagner, J. Cancer: Disease Control Priorities. *Dis. Control Priorities 3rd Ed.* **2015**, 1–363. https://doi.org/10.1017/CBO9781107415324.004.

(171) Zeman, E. M. *Biologic Basis of Radiation Oncology*, Thrid Edit.; Elsevier Inc., 2011. https://doi.org/10.1016/B978-1-4377-1637-5.00001-8.

(172) Kunz-Schughart, L. A.; Dubrovska, A.; Peitzsch, C.; Ewe, A.; Aigner, A.; Schellenburg, S.; Muders, M. H.; Hampel, S.; Cirillo, G.; Iemma, F.; Tietze, R.; Alexiou, C.; Stephan, H.; Zarschler, K.; Vittorio, O.; Kavallaris, M.; Parak, W. J.; Mädler, L.; Pokhrel, S. Nanoparticles for Radiooncology: Mission, Vision, Challenges. *Biomaterials* **2017**, *120*, 155–184. https://doi.org/10.1016/j.biomaterials.2016.12.010.

(173) Lord, C. J.; Ashworth, A. The DNA Damage Response and Cancer Therapy. *Nature* **2012**, *481* (7381), 287–294. https://doi.org/10.1038/nature10760.

(174) Pernin, V.; Mégnin-Chanet, F.; Pennaneach, V.; Fourquet, A.; Kirova, Y.; Hall, J. Inhibiteurs de PARP et Radiothérapie : Rationnel et Perspectives Pour Une Utilisation En Clinique. *Cancer/Radiothérapie* **2014**, *18* (8), 790–798. https://doi.org/10.1016/j.canrad.2014.05.012.

(175) Muz, B.; de la Puente, P.; Azab, F.; Luderer, M.; Azab, A. K. The Role of Hypoxia and Exploitation of the Hypoxic Environment in Hematologic Malignancies. *Mol. Cancer Res.* **2014**, *12* (10).

(176) Muz, B.; de la Puente, P.; Azab, F.; Azab, A. K. The Role of Hypoxia in Cancer Progression, Angiogenesis, Metastasis, and Resistance to Therapy. *Hypoxia* **2015**, *3*, 83. https://doi.org/10.2147/HP.S93413.

(177) Chapman, J Donald; Lee, Jane; Meeker, B. E. Keynote Address: Cellular Reduction of Nitroimidazole Drugs: Potential for Selective Chemotherapy and Diagnosis of Hypoxic Cells. *Int. J. Radiat. Oncol. Biol. Phys.* **1989**, *16* (4), 911–917. https://doi.org/10.1016/0360-3016(89)90886-9.

(178) Watts, M. E.; Dennis, M. F.; Roberts, I. J.; Wattst, M. E. International Journal of Radiation Biology Radiosensitization by Misonidazole, Pimonidazole and Azomycin and Intracellular Uptake in Human Tumour Cell Lines Radiosensitization by Misonidazole, Pimonidazole and Azomycin and Intracellular Uptake in Human Tu. *Int. J. Radiat. Biol. INT . J . RADIAT . BIOL* **1990**, *57* (3), 361–372. https://doi.org/10.1080/09553009014552461.

(179) Overgaard, J.; Hansen, H. S.; Overgaard, M.; Bastholt, L.; Berthelsen, A.; Specht, L.; Lindeløv, B.; Jørgensen, K. A Randomized Double-Blind Phase III Study of Nimorazole as a Hypoxic Radiosensitizer of Primary Radiotherapy in Supraglottic Larynx and Pharynx Carcinoma. Results of the Danish Head and Neck Cancer Study (DAHANCA) Protocol 5-85. *Radiother. Oncol.* **1998**, *46* (2), 135–146. https://doi.org/10.1016/S0167-8140(97)00220-X.

(180) Lawrentschuk, N.; Poon, A. M. T.; Foo, S. S.; Putra, L. G. J.; Murone, C.; Davis, I. D.; Bolton, D. M.; Scott, A. M. Assessing Regional Hypoxia in Human Renal Tumours Using 18F-Fluoromisonidazole Positron Emission Tomography. *BJU Int.* **2005**, *96* (4), 540–546. https://doi.org/10.1111/j.1464-410X.2005.05681.x.

(181) Kumar, P.; Stypinski, D.; Xia, H.; McEwan, A. J. B.; Machulla, H.-J. J.; Wiebe, L. I. Fluoroazomycin Arabinoside (FAZA): Synthesis, 2H and 3H-Labelling and Preliminary Biological Evaluation of a Novel 2-Nitroimidazole Marker of Tissue Hypoxia. *J. Label. Compd. Radiopharm.* **1999**, *42* (1), 3–16. https://doi.org/10.1002/(SICI)1099-1344(199901)42:1<3::AID-JLCR160>3.0.CO;2-H.

(182) Wiebe, L. I. PET Radiopharmaceuticals for Metabolic Imaging in Oncology. *Int. Congr. Ser.* **2004**, *1264*, 53–76. https://doi.org/10.1016/j.ics.2003.12.102.

(183) Reischl, G.; Dorow, D. S.; Cullinane, C.; Katsifis, A.; Roselt, P.; Binns, D.; Hicks, R. J. Imaging of Tumor Hypoxia with [124I]IAZA in Comparison with [18F]FMISO and [18F]FAZA–First Small Animal PET Results. *J Pharm Pharm Sci Publ Can Soc Pharm Sci Société Can Des Sci Pharm* **2007**, *10* (2), 203–211.

(184) Stypinski, D.; McQuarrie, S. A.; Wiebe, L. I.; Tam, Y. K.; Mercer, J. R.; McEwan, A. J. Dosimetry Estimations for 123I-IAZA in Healthy Volunteers. *J. Nucl. Med.* **2001**, *42* (9), 1418–1423.

(185) Kumar, P.; Elsaidi, H. R. H.; Zorniak, B.; Laurens, E.; Yang, J.; Bacchu, V.; Wang, M.; Wiebe, L. I. Synthesis and Biological Evaluation of Iodoglucoazomycin (I-GAZ), an Azomycin–Glucose Adduct with Putative Applications in Diagnostic Imaging and Radiotherapy of Hypoxic Tumors. *ChemMedChem* **2016**, 1638–1645. https://doi.org/10.1002/cmdc.201600213.

(186) Dische, S. Chemical Sensitizers for Hypoxic Cells: A Decade of Experience in Clinical Radiotherapy. *Radiother. Oncol.* **1985**, *3* (2), 97–115.

https://doi.org/10.1016/S0167-8140(85)80015-3.

(187) Milas, L.; Hunter, N.; Mason, K. a; Milross, C.; Peters, L. J. Tumor Reoxygenation as a Mechanism of Taxol-Induced Enhancement of Tumor Radioresponse. *Acta Oncol.* **1995**, *34* (3), 409–412. https://doi.org/10.3109/02841869509093999.

(188) Krause, M.; Ostermann, G.; Petersen, C.; Yaromina, A.; Hessel, F.; Harstrick, A.; Van Der Kogel, A. J.; Thames, H. D.; Baumann, M. Decreased Repopulation as Well as Increased Reoxygenation Contribute to the Improvement in Local Control after Targeting of the EGFR by C225 during Fractionated Irradiation. In *Radiotherapy and Oncology*; 2005; Vol. 76, pp 162–167. https://doi.org/10.1016/j.radonc.2005.06.032.

(189) Parveen, S.; Misra, R.; Sahoo, S. K. Nanoparticles: A Boon to Drug Delivery, Therapeutics, Diagnostics and Imaging. *Nanomedicine Nanotechnology, Biol. Med.* **2012**, *8* (2), 147–166. https://doi.org/10.1016/j.nano.2011.05.016.

(190) Maeda, H.; Wu, J.; Sawa, T.; Matsumura, Y.; Hori, K. Tumor Vascular Permeability and the EPR Effect in Macromolecular Therapeutics: A Review. *Journal of Controlled Release*. 2000, pp 271–284. https://doi.org/10.1016/S0168-3659(99)00248-5.

(191) Mi, Y.; Shao, Z.; Vang, J.; Kaidar-Person, O.; Wang, A. Z. Application of Nanotechnology to Cancer Radiotherapy. *Cancer Nanotechnol.* **2016**, *7* (1), 11. https://doi.org/10.1186/s12645-016-0024-7.

(192) Hubel, A.; Skubitz, A. P. N. Principles of Cryopreservation. In *Biobanking of Human Biospecimens*; Springer International Publishing: Cham, 2017; pp 1–21. https://doi.org/10.1007/978-3-319-55120-3_1.

(193) Boldt, J. Current Results with Slow Freezing and Vitrification of the Human Oocyte. *Reprod. Biomed. Online* **2011**, *23* (3), 314–322.

https://doi.org/10.1016/j.rbmo.2010.11.019.

(194) Mazur, P.; Seki, S.; Pinn, I. L.; Kleinhans, F. W.; Edashige, K. Extra- and Intracellular Ice Formation in Mouse Oocytes. *Cryobiology* **2005**, *51* (1), 29–53. https://doi.org/10.1016/j.cryobiol.2005.04.008.

(195) Li, Y.; Ma, T. Bioprocessing of Cryopreservation for Large-Scale Banking of Human Pluripotent Stem Cells. *Biores. Open Access* **2012**, *1* (5), 205–214. https://doi.org/10.1089/biores.2012.0224.

(196) Sultani, A. B.; Marquez-Curtis, L. A.; Elliott, J. A. W.; McGann, L. E. Improved Cryopreservation of Human Umbilical Vein Endothelial Cells: A Systematic Approach. *Sci. Rep.* **2016**, *6* (September), 1–14. https://doi.org/10.1038/srep34393.

(197) Pacchiarotti, J.; Ramos, T.; Howerton, K.; Greilach, S.; Zaragoza, K.; Olmstead, M.; Izadyar, F. Developing a Clinical-Grade Cryopreservation Protocol for Human Testicular Tissue and Cells. *Biomed Res. Int.* **2013**, *2013*, 1–10. https://doi.org/10.1155/2013/930962.

(198) Fuller, B. J.; Lane, N.; Benson, E. E. *Life in the Frozen State*; Boca Raton, Fla: CRC Press, 2004.

(199) Meryman, H. T. T. Osmotic Stress as a Mechanism of Freezing Injury. *Cryobiology* **1971**, *8* (5), 489–500. https://doi.org/10.1016/0011-2240(71)90040-X.

(200) Mazur, P.; Cole, K. W. Influence of Cell Concentration on the Contribution of Unfrozen Fraction and Salt Concentration to the Survival of Slowly Frozen Human Erythrocytes. *Cryobiology* **1985**, *22* (6), 509–536. https://doi.org/10.1016/0011-2240(85)90029-X.

(201) Chen, G.; Yue, A.; Ruan, Z.; Yin, Y.; Wang, R.; Ren, Y.; Zhu, L. Comparison of the Effects of Different Cryoprotectants on Stem Cells from Umbilical Cord Blood. *Stem Cells Int.* **2016**, *2016*, 1–7. https://doi.org/10.1155/2016/1396783.

(202) Baboo, J.; Kilbride, P.; Delahaye, M.; Milne, S.; Fonseca, F.; Blanco, M.; Meneghel, J.; Nancekievill, A.; Gaddum, N.; Morris, G. J. The Impact of Varying Cooling and Thawing Rates on the Quality of Cryopreserved Human Peripheral Blood T Cells. *Sci. Rep.* **2019**, *9* (1), 1–13. https://doi.org/10.1038/s41598-019-39957-x.

(203) Kashuba Benson, C. M.; Benson, J. D.; Critser, J. K. An Improved Cryopreservation Method for a Mouse Embryonic Stem Cell Line. *Cryobiology* **2008**, *56* (2), 120–130. https://doi.org/10.1016/j.cryobiol.2007.12.002.

(204) Biggs, C. I.; Bailey, T. L.; Ben Graham; Stubbs, C.; Fayter, A.; Gibson, M. I. Polymer Mimics of Biomacromolecular Antifreezes. *Nat. Commun.* **2017**, *8* (1), 1–11. https://doi.org/10.1038/s41467-017-01421-7.

(205) Mazur, P.; Rigopoulos, N. Contributions of Unfrozen Fraction and of Salt Concentration to the Survival of Slowly Frozen Human Erythrocytes: Influence of Warming Rate. *Cryobiology* **1983**, *20* (3), 274–289. https://doi.org/10.1016/0011-2240(83)90016-0.

(206) Mazur, P. Equilibrium, Quasi-Equilibrium, and Nonequilibrium Freezing of Mammalian Embryos. *Cell Biophys.* **1990**, *17* (1), 53–92. https://doi.org/10.1007/BF02989804.

(207) Balcerzak, A. K.; Capicciotti, C. J.; Briard, J. G.; Ben, R. N. Designing Ice Recrystallization Inhibitors: From Antifreeze (Glyco)Proteins to Small Molecules. *RSC Adv.* **2014**, *4* (80), 42682–42696. https://doi.org/10.1039/c4ra06893a.

(208) Crowe, J. H.; Crowe, L. M.; Chapman, D. Preservation of Membranes in Anhydrobiotic Organisms: The Role of Trehalose. *Science (80-.).* **1984**, *223* (4637), 701–703. https://doi.org/10.1126/science.223.4637.701.

(209) Sola-Penna, M.; Meyer-Fernandes, J. R. Stabilization against Thermal Inactivation Promoted by Sugars on Enzyme Structure and Function: Why Is Trehalose More

Effective than Other Sugars? *Arch. Biochem. Biophys.* **1998**, *360* (1), 10–14. https://doi.org/10.1006/abbi.1998.0906.

(210) Buchanan, S. S.; Gross, S. A.; Acker, J. P.; Toner, M.; Carpenter, J. F.; Pyatt, D. W. Cryopreservation of Stem Cells Using Trehalose: Evaluation of the Method Using a Human Hematopoietic Cell Line. *Stem Cells Dev.* **2004**, *13* (3), 295–305. https://doi.org/10.1089/154732804323099226.

(211) Eroglu, A. Cryopreservation of Mammalian Oocytes by Using Sugars: Intra- and Extracellular Raffinose with Small Amounts of Dimethylsulfoxide Yields High Cryosurvival, Fertilization, and Development Rates. *Cryobiology* **2010**, *60* (706), 1–14. https://doi.org/10.1016/j.cryobiol.2009.07.001.Cryopreservation.

(212) Yang, J.; Cai, N.; Zhai, H.; Zhang, J.; Zhu, Y.; Zhang, L. Natural Zwitterionic Betaine Enables Cells to Survive Ultrarapid Cryopreservation. *Sci. Rep.* **2016**, *6* (October), 1–9. https://doi.org/10.1038/srep37458.

(213) Beattie, G. M.; Crowe, J. H.; Lopez, A. D.; Cirulli, V.; Ricordi, C.; Hayek, A. Trehalose: A Cryoprotectant That Enhances Recovery and Preserves Function of Human Pancreatic Islets after Long-Term Storage. *Diabetes* **1997**, *46* (3), 519–523. https://doi.org/10.2337/diab.46.3.519.

(214) Eroglu, A.; Russo, M. J.; Bieganski, R.; Fowler, A.; Cheley, S.; Bayley, H.; Toner, M. Intracellular Trehalose Improves the Survival of Cryopreserved Mammalian Cells. *Nat. Biotechnol.* **2000**, *18* (2), 163–167. https://doi.org/10.1038/72608.

(215) Guo, N.; Puhlev, I.; Brown, D. R.; Mansbridge, J.; Levine, F. Trehalose Expression Confers Desiccation Tolerance on Human Cells. *Nat. Biotechnol.* **2000**, *18* (2), 168–171. https://doi.org/10.1038/72616.

(216) Eroglu, A.; Toner, M.; Toth, T. L. Beneficial Effect of Microinjected Trehalose on the Cryosurvival of Human Oocytes. *Fertil. Steril.* **2002**, *77* (1), 152–158.

https://doi.org/10.1016/S0015-0282(01)02959-4.

(217) Graham, B.; Fayter, A. E. R.; Houston, J. E.; Evans, R. C.; Gibson, M. I. Facially Amphipathic Glycopolymers Inhibit Ice Recrystallization. *J. Am. Chem. Soc.* **2018**, *140* (17), 5682–5685. https://doi.org/10.1021/jacs.8b02066.

(218) Chaytor, J. L.; Ben, R. N. Assessing the Ability of a Short Fluorinated Antifreeze Glycopeptide and a Fluorinated Carbohydrate Derivative to Inhibit Ice Recrystallization. *Bioorg. Med. Chem. Lett.* **2010**, *20* (17), 5251–5254. https://doi.org/10.1016/J.BMCL.2010.06.148.

(219) Lee, Y. A.; Kim, Y. H.; Kim, B. J.; Kim, B. G.; Kim, K. J.; Auh, J. H.; Schmidt, J. A.; Ryu, B. Y. Cryopreservation in Trehalose Preserves Functional Capacity of Murine Spermatogonial Stem Cells. *PLoS One* **2013**, *8* (1). https://doi.org/10.1371/journal.pone.0054889.

(220) Katenz, E.; Vondran, F. W. R.; Schwartlander, R.; Pless, G.; Gong, X.; Cheng, X.; Neuhaus, P.; Sauer, I. M. Cryopreservation of Primary Human Hepatocytes: The Benefit of Trehalose as an Additional Cryoprotective Agent. *Liver Transplant.* **2007**, *13* (1), 38–45. https://doi.org/10.1002/lt.20921.

(221) Holovati, J. L.; Gyongyossy-Issa, M. I. C.; Acker, J. P. Effects of Trehalose-Loaded Liposomes on Red Blood Cell Response to Freezing and Post-Thaw Membrane Quality. *Cryobiology* **2009**, *58* (1), 75–83. https://doi.org/10.1016/j.cryobiol.2008.11.002.

(222) Mannan, R. H.; Somayaji, V. V; Lee, J.; Mercer, J. R. 1-(5-Iodo-5-Deoxy-b-D-Arabinofuranosyl)-2-Nitroimidazole (Iodoazomycin Arabinoside:IAZA), a Novel Marker of Tissue Hypoxia. *Nucl. Med. Biol.* **1991**, *32*, 1764–1770.

CHAPTER 2. EFFECTIVE AND SPECIFIC GENE SILENCING OF EPIDERMAL GROWTH FACTOR RECEPTORS MEDIATED BY CONJUGATED OXABOROLE AND GALACTOSE-BASED POLYMERS.

The content of this chapter was published in

Journal of *ACS Macro Letters*

Chapter 2

2.1 INTRODUCTION

Gene silencing therapy has evolved from 'bench-to-clinic' due to innovative advances in nanotechnology. The elucidation of molecular pathways governing cancer growth in combination with the discovery of RNA interference (RNAi) —a natural mechanism of post-transcriptional gene silencing— provided a new tool in the fight against cancer by targeting the undruggable genome[1]. Tumorigenesis in humans is the consequence of multiple genetic and epigenetic events that lead to uncontrollable cell proliferation[2]. Aberrant activation of many oncogenes due to overexpression and/or oncogenic mutations is often associated with cancer phenotypes, and behind this rationale is the use of silencing gene therapy. Knockdown of cancer-causing genes that compromise its malignant state has prompted the development of agents that can specifically silence target genes; nonetheless, major challenges of delivery, specificity and efficacy need to be overcome before siRNAs can be used as an effective therapeutic agent. Naked siRNAs are degraded in human plasma with a half-life of approximately 30 minutes[3]. To transform siRNAs into a successful therapeutic agent, two main strategies are used: 1) perform chemical modifications that prolong siRNA half-life, and 2) design of carriers to deliver siRNA without threatening its biological activity. Narain and co-workers have synthesized glycopolymers and nanogels of 2-lactobionamidoethyl methacrylamide (LAEMA) and 2-aminoethyl methacrylamide hydrochloride (AEMA) that demonstrate efficient siRNA knockdown *in vitro*, however some toxicity challenges in these nanocarriers have yet to be overcome. Studies have demonstrate that high dosages of silencing molecules could have a toxic effect, probably due to the associated toxicity of the delivery system; highlighting the importance of finding a biocompatible vehicle that is safe and effective[4–7]. Current research explored the feasibility of delivering siRNA using an oxaborole and galactose-based polymeric complex to downregulate epidermal growth factor receptor (EGFR) proteins that cause aberrant cell growth in cervical cancer cells[8].

Gene expression profiling has identified distinct signatures of gene expression that are associated with metastatic capacity and prognosis of cancer. Overexpression and/or aberrant activation of specific oncogenes and tumor suppressor genes makes them suitable

candidates for nucleic acid-based gene-silencing therapies[1]. siRNA systems can be employed against cancer targets that govern uncontrolled cell proliferation. Some examples of these targets are cyclin-dependent kinases (CDKs), insulin growth factors (IGF), vascular endothelial growth factors (VEGF), protein kinase N3 (PKN3), polo-like kinase 1 (PLK1) and epidermal growth factors (EGF)[9]. Lipid nanoparticle-based delivery system containing therapeutic siRNA targeting PLK1 and PKN3 are currently in phase I/II clinical trial for the treatment of neuroendocrine and pancreatic cancers tumors, respectively[10,11]. Unregulated proliferation is a hallmark of cancer cells; proliferation signals are generated by growth mediators, as the interaction between epidermal growth factors (EGF) and EGFR (an oncogenic tyrosine-kinase trans-membranous receptor) which due to mutations are overexpressed in multiple human cancers[12,13]. These somatic mutations associated with EGFR, lead to its constant activation, stimulating various signaling pathways, including Ras-MAPK, PI3K-AKT, Src, and STAT3, which promote cell proliferation, differentiation, cell motility, survival[14,15] and radioresistance[16]. Increased EGFR expression was found to act as a strong prognostic indicator, associated with reduced remission or overall survival rates in head and neck, ovarian, esophageal, bladder and cervical cancers [17]. Therefore, EGFR-targeting shows great potential in the treatment of the latter types of cancer. Despite the tremendous promises of siRNA therapy, many challenges need to be addressed before it can be used to treat human cancers safely and effectively; the biggest task is to find an appropriate mode for its effective delivery[18,19].

Electrostatic forces between the cationic primary amines of polymers or the positively charged nitrogen in the head groups of the liposomes governs the interactions with the anionic phosphate backbone of the nucleic acids, thus controlling the formation of condensed polyplexes (polyionic complexes) or lipoplexes[20]. siRNA molecules are too large and strongly hydrophilic to diffuse across cell membranes alone. The complexation with these materials have proved to enhance cellular uptake and increase half-life in cytoplasm of the nucleotides by guarding them against enzymatic and non-enzymatic degradation, evading the immune system, and avoiding non-specific interactions with serum proteins; thus preventing rapid clearance and allowing extravasation from blood

vessels[21]. The efficiency of these polymeric vectors depends on the degree of polymerization (DP), molecular weight (MW), branching and charged density, among other properties. Cationic polymers such as polyethylenimine (PEI) and cationic liposomes such as Lipofectamine have become gold standards as non-viral vectors for gene delivery. PEI has shown relatively higher transfection efficiencies than most non-viral carriers, but its non-biodegradability, toxicity and non-specific interactions pose problems for clinical applications[22,23]. Analogously, lipofectamine has provided high transfection efficiencies *in vitro* and *in vivo* but still toxicity at higher doses and off-target silencing remain to be significant concerns[24,25]. Delivery of smaller polynucleotides like siRNA is more defiant than larger nucleic acids (DNA) due to the possible formation of non-stable complexes that can dissociate upon contact with the polyanionic cell surface. Alternative carriers that pose important features to achieve this purpose are glycopolymers which mimic naturally occurring polysaccharides, increasing blood biocompatibility and promoting carbohydrate-specific recognition[7]. Reineke and Narain's groups have evaluated cationic glycopolymers gene delivery efficacy in relation to synthetic parameters, such as molecular weights, cationic content, degree of polymerization and architectures. It has been reported that an increase in amine content at a fixed DP leads to increase in gene expression[26,27]. Galactose-based glycopolymers of 2-aminoethyl methacrylamide hydrochloride (AEMA), 2-lactobionamidoethyl methacrylamide (LAEMA), P(LAEMA-*b*-AEMA) have shown high transfection efficiencies and specific EGFR knockdown in HeLa cells[6,7]. Longer AEMA block length has shown to promote higher binding affinity and stable polyplex formation at higher weight/weight (w/w) ratios ($\cong 100$[7]), but one limitation is cell toxicity which increases as the AEMA block lengths of the copolymer increases[28]. Therefore, we proposed a biocompatible and efficient nanocarrier from the conjugation of an oxaborole polymer poly(N-isopropylacrylamide-*st*-5-methacrylamido-1,2-benzoxaborole) P(NIPAm-*st*-AAm-*st*-MAAmBO) and a galactose-based polymer P(LAEMA-*b*-AEMA) that displayed minimal cytotoxicity, while providing a stable complex to protect siRNA from dissociation and bestowing higher transfection efficiencies (Scheme 2-1).

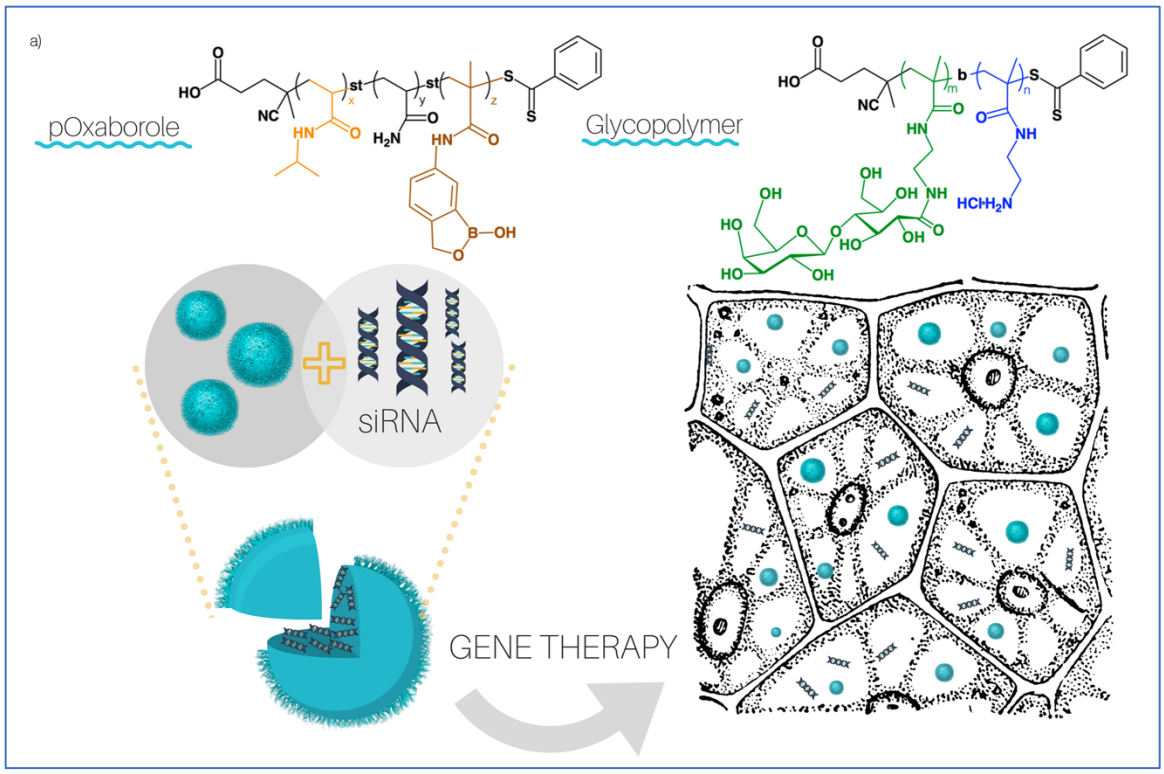
a)
pOxaborole
Glycopolymer
siRNA
GENE THERAPY

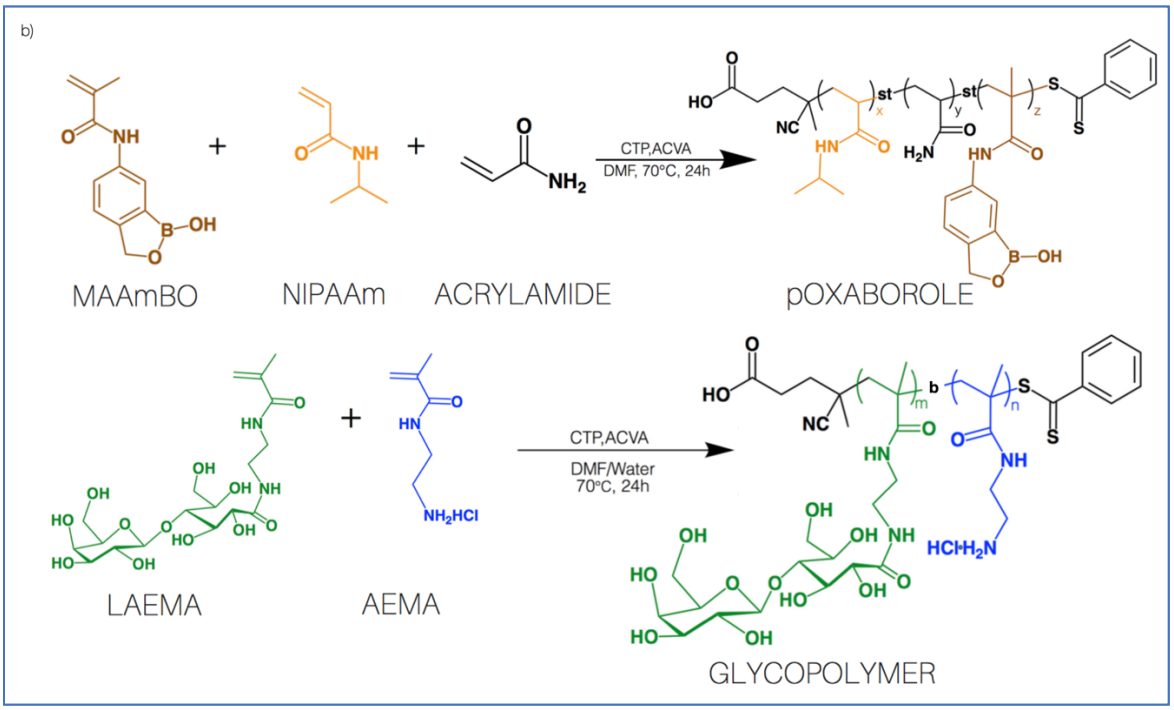
b)
MAAmBO
NIPAAm
ACRYLAMIDE
CTP,ACVA
DMF, 70°C, 24h
pOXABOROLE
LAEMA
AEMA
CTP,ACVA
DMF/Water
70°C, 24h
GLYCOPOLYMER

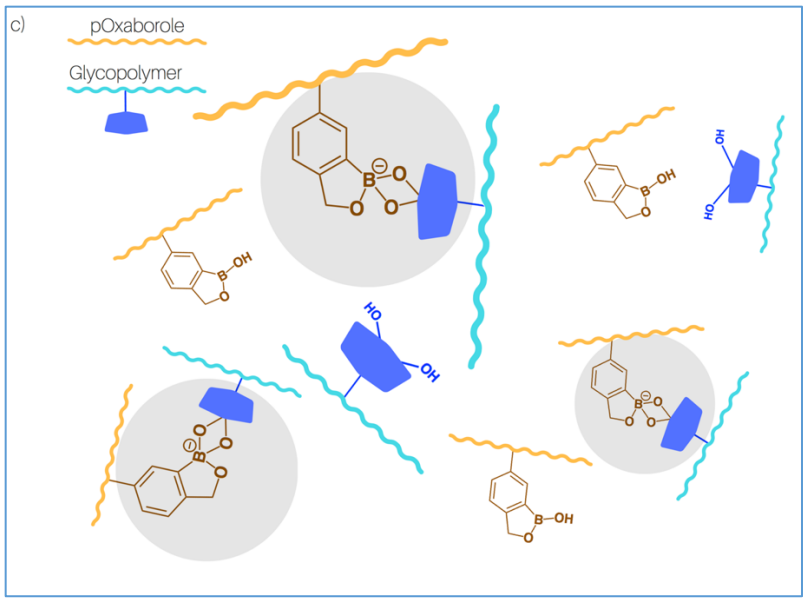

Scheme 2-1. (a) Representation of the polyplex formation by the interactions between the pOxaborole and glycopolymer with EGFR siRNA and its use for gene therapy. (b) Synthesis of pOxaborole (P(NIPAAm-*st*-AAm-*st*-MAAmBO)) and glycopolymer (P(LAEMA-*b*-AEMA)) by RAFT polymerization[29]. (c) Complexation of pOxaborole and glycopolymer via boronic-diol interaction.

2.2 MATERIALS & METHODS

2.2.1 Materials. The organic solvents were purchased from Caledon Laboratories Ltd. (Georgetown, Canada). 2-Aminoethyl methacrylamide hydrochloride (AEMA), 2-lactobionamidoethyl methacrylamide (LAEMA), and the chain transfer agent, cyanopentanoic acid dithiobenzoate (CTP), were synthesized in the laboratory according to previously reported protocols[1]. The initiator, 4,4′-azobis(cyanovaleric acid) (ACVA), was obtained from Sigma-Aldrich (Oakville, Canada). DMEM media, Opti-MEM (OMEM), 0.25% trypsin−EDTA, fetal bovine serum (FBS) and Streptomycin (5000 μg mL^{-1})-Penicillin (5000 U mL^{-1}) were obtained from Gibco. Lipofectamine was purchased from Invitrogen Control EGFR siRNA−FITC conjugate, human EGFR-specific small interfering RNA (EGFR siRNA) sc-29301 Sense: CUCUGGAGGAAAAGAAAGU.

Antisense: ACUUUCUUUUCCUCCAGAG; and primary antibody (rabbit polyclonal EGFR specific IgG sc-03-G) and FITC-conjugated control siRNA were purchased from Santa Cruz Biotechnology. (HRP)-conjugated secondary antibody (Anti-rabbit IgG, W4011) was purchased from Promega Corporation.

2.2.2 Synthesis of pOxaborole-Glycopolymer complexes.

2.2.2.1 Cationic Glycopolymers Synthesis. Cationic glycopolymers were prepared as described in a previously reported procedure [2] In a typical synthesis of a block copolymer, AEMA macroCTA is synthesized using 4,4′-azobis(4-cyanovaleric acid) (ACVA) as the initiator and 4-cyanopentanoic acid dithiobenzoate (CTP) as the chain transfer agent (CTA). AEMA monomer was first dissolved in double distilled water followed by the addition of CTP and ACVA in N,N′-dimethylformamide (DMF) solution. After degassing with nitrogen for 30 min, the polymerization was carried out at 70°C for 6 h. The reaction was stopped in liquid nitrogen and the resulting polymer was isolated after precipitation in acetone. The residual monomer was removed by washing twice the solids with 2-propanol. The macroCTA, P-(AEMA), was used to prepare the P(LAEMA-*b*-AEMA) copolymer. LAEMA was first mixed with P(AEMA) solution in double distilled water and ACVA in DMF solution was subsequently added. After purging with nitrogen, the polymerization was achieved in an oil bath at 70°C for 24h. The diblock copolymer P(LAEMA-*b*-LAEMA) was obtained after precipitation in acetone followed by three washes with methanol to remove residual monomer. Gel permeation chromatography (GPC) and nuclear magnetic resonance (NMR) was used to determine molecular weight and composition of the glycopolymers respectively.

2.2.2.2 Synthesis of MAAmBO. 5-Amino-2-hydroxymethylphenylboronic acid HCl salt (5.0 g, 26.95 mmol) was dissolved in 2N NaOH aqueous solution (20 mL), and the mixture was cooled down to 0 ^{o}C. After 15 min stirring, methacryloyl chloride (5.5 mL, 56.5 mmol) was added dropwise to the solution, and the reaction mixture was stirred for 3h, and following neutralized by dripping 1N HCl aqueous solutions with an ice bath. The pale pink precipitate was collected by filtration and washed with 0.01N HCl aqueous solution

twice, the liquid components were removed by high vacuum pumping and finally, a white powder was obtained (96% yield).

2.2.2.3 Synthesis of P(NIPAAm-st-AAm-st-MAAmBO). Varying molar ratios of NIPAAm, AAm, MAAmBO, CTP, and ACVA were dissolved in *N*,*N*-dimethylformamide (DMF). After degassing with nitrogen gas for 30 min in an ice/methanol bath (-30^{o}C), the mixture was allowed to polymerize for 24 h at 70 °C. The resulting P(NIPAAm-st-AAm-st-MAAmBO) was purified by re-precipitation using diethyl ether.

2.2.3 Preparation of pOxaborole-Glycopolymer-siRNA Polyplexes. EGFR-siRNA/control-siRNA (25 µg) was diluted in 250 µL of OMEM and complexed with pOxaborole- glycopolymers (in OMEM media) at a weight/weight (w/w) ratio of 10. The mixture was incubated at room temperature (23 °C) for 30 min.

2.2.4 Characterization of Polymers and pOxaborole-Glycopolymer-siRNA complexes. The hydrodynamic size and charge of the pOxaborole-Glycopolymer-siRNA complexes were determined using ZetaPlus-Zeta Potential Analyzer (Brookhaven Instruments Corporation). The pOxaborole-Glycopolymer-siRNA complexes were formulated at w/w ratio of 10 in water and OMEM media. The polyplexes stability of oxaborole-glycopolymer-siRNA polyplexes was also evaluated in the presence and absence of serum proteins in OMEM after 48 h. The net charge of the polyplexes was determined in nanopure water.

2.2.5 Agarose Gel Electrophoresis. The polyplexes were formulated in OMEM at varying polymer/siRNA ratios, as described above. The polyplexes were loaded in 1% agarose gel containing 1µg/mL ethidium bromide in 1X Tris Acetate/EDTA (TAE) buffer. The gel was run for 45 minutes at 130 V and illuminated with UV light and the DNA bands were visualized using UV transilluminator.

2.2.6 In vitro polyplexes evaluations for EGFR knockdown

2.2.6.1 Cell Culture. HeLa cells (cervical cancer) were cultured in DMEM medium containing 10% fetal bovine serum (FBS) and 1% antibiotic (50 units of penicillin, 50 µg streptomycin) in a humidified atmosphere at 37°C and 5% CO_2. At about 80% confluency,

the cells were subcultured by detaching with 0.25% trypsin-EDTA and were cultured twice per week.

2.2.6.2 Cytotoxicity of the pOxaborole-Glycopolymer complexes. Proliferation (MTT) assay was performed to determine the inherent toxicity of the complexes in HeLa cells by staining with dimethyl thiazol dyes for metabolically viable cells. IC_{50} values will be calculated with GraphPad Prism software. Cytotoxicity post-transfection will be done by Janus Green assay after 48 h of incubation.

2.2.7 Transfection of EGFR-siRNA. HeLa cells were seeded into 60 mm plates at a cell density of 10^5 cells per plate. The polyplexes were prepared in OMEM (in the absence/presence of serum proteins), and 500 µL of the polyplexes/lipofectamine mixture (EGFR siRNA/control siRNA) was added per plate. After incubation for 6 h, the media was removed and replaced with 2 mL of DMEM media containing with 10% fetal bovine serum (FBS). The EGFR knockdown efficacy was characterized after 48h of cell growth.

2.2.8 EGFR Knockdown Western Blot Evaluation. Harvesting of cells was done in RiPa buffer supplemented with a protease inhibitor and the protein concentrations were determined using a Bradford protein assay kit (Bio-Rad). Eluates were then run on a SDS-PAGE denaturing gel, transferred to a nitrocellulose membrane (0.45 um), and visualized by probing with EGFR-1005 sc-03 antibody (Santa Cruz) and a streptavidin horse radish peroxidase (HRP) anti-rabbit conjugate. The amount of EGFR protein expression was quantified using ImageJ image analysis.

2.2.9 Fluorescent Labeling of pOxaborole-glycopolymers. The polyplexes are fluorescently labeled with fluorescein isothiocyanate (FITC) control-siRNA. After overnight incubation, the media was removed and replaced with FITC-labeled siRNA-pOxaborole-glycopolymer at a w/w ratio of 10 in OMEM and subsequently incubated for 3 h in a humidified atmosphere at 37°C and 5% CO_2.

2.2.10 Cellular uptake of polyplexes. Confocal Fluorescence Microscopy and Flow cytometry. HeLa cells were cultured as mentioned above, trypsinized, and seeded onto glass coverslips in 10 mm plate at a density of 1000 cells per plate. After overnight incubation, the media was removed and replaced FITC-control siRNA polyplexes at a w/w

ratio of 10 in OMEM and subsequently incubated for 3 h in a humidified atmosphere at 37°C and 5% CO_2. After removal of the media and washing with 1× PBS (three times), the cells were stained with (1:10000) DAPI dye dissolved in PBS for 1h and fixed with 4% Paraformaldehyde for 15 min at 37°C. Visualization using a confocal microscope at 490 nm emission spectra for FITC was done. For flow cytometry, HeLa cells were trypsinized and subsequently seeded into 60 mm well plate at a density of $1x10^6$ cells per plate. After incubation overnight, the cells were treated with the oxaborole-glycopolymer-FITC-labeled control siRNA complexes for 3 h at a w/w ratio of 10 in OMEM. After the media was removed and washed with 1 × PBS at pH 7.4 (three times), the cells were trypsinized and centrifuged at 1200 rpm. The pellet was re-suspended in 1× PBS buffer and cells were characterized using a BD FACS dual laser flow cytometer (Cross Cancer Institute).

2.3 RESULTS & DISCUSSION

Oxaborole based copolymer, P(NIPAAm$_{290}$-*st*-AAm$_{63}$-*st*-MAAmBO$_9$) (MAAmBO content: 9 mol %, M_n = 90,000 gmol^{-1}, M_w/M_n = 1.54) was synthesized by the RAFT polymerization, a technique that is capable of synthesizing well-defined polymers with advanced architectures and allowing design customization of complex carbohydrate groups[28,30]. Varying molar ratios of NIPAAm, AAm, MAAmBO were used. P(NIPAAm) shows temperature-responsive properties with a lower critical solution temperature (LCST) of 32 °C and interactions of the MAAmBO residues with hydroxyl groups of the sugars that allowed cross-linking of the polymer chains in a reversible manner as a function of temperature, and the presence of free glucose. Copolymerization of NIPAAm with MAAmBO leads to the formation of a copolymer with temperature, pH and glucose-responsive properties[31]. Synthesis of P(LAEMA-*b*-AEMA) polymers was carried out using the same conditions as previously reported[32]. The properties of these polymers are shown in Table 2-1. Polymer compositions were evaluated by ^{1}H-NMR (Figure 2S1, 2S2, 2S3, 2S4), P(LAEMA$_{20}$-*b*-AEMA$_{47}$) was denoted as Glycopolymer 1 (**G1**) and P(LAEMA$_8$-*b*-AEMA$_{24}$) as Glycopolymer 2 (**G2**). Boron NMR (Figure 2S5) was run to confirm the presence of boron (^{11}B) in the conjugated polymers. As illustrated in Figure 2S5,

pOxaborole P(NIPAAm$_{294}$-*st*-AAm$_{63}$-*st*-MAAmBO$_9$) revealed a single ^{11}B peak at 19.5 ppm, the binding between pOxaborole and the glycopolymers was indicated by the two small peaks at 10.9 and 10.5 ppm as previously reported[33]. Molecular weights (MW) were determined by gel permeation chromatography (GPC) displaying molecular weights of 17 and 8 kDa for the glycopolymers and 90 kDa for the oxaborole polymer with low MW distributions.

Table 2-1. Characterization of oxaborole and galactose-based polymers by Gel Permeation Chromatography and Zeta Potential analysis.

Polymer	M_n (g/mol)	M_w/M_n	Zeta Potential (mV)
G1 P(LAEMA$_{20}$-*b*-AEMA$_{47}$)	17 K	1.15	+36.52 ± 1.5
G2 P(LAEMA$_8$-*b*-AEMA$_{24}$)	8 K	1.43	+52.95 ± 1.06
pOxaborole P(NIPAAm$_{294}$-st-AAm$_{63}$-st-MAAmBO$_9$)	90 K	1.54	-6.39 ± 0.55

Our group has previously reported that mixing of P(NIPAAm-*st*-MAAmBO) with glycopolymers such as P(GAPMA) and P(LAEMA) spontaneously form cross-linked structures[31]. Due to the interesting biological properties of glycopolymers (biocompatibility, target specificity, solubility and ability to facilitate receptor-mediated uptake), conjugated oxaborole-glycopolymer complexes could be excellent vehicles for delivering drugs and genes, while minimizing cell toxicity. Preparation of oxaborole polymer-glycopolymer-siRNA polyplexes was achieved by complexing 10 nM siRNA in OMEM media (in the absence and presence of serum). At a w/w ratio of polymer to siRNA of 10 complexations were evidenced by agarose gel electrophoresis (Figure 2S6). Electrostatic interactions between the cationic glycopolymers and the negative charge siRNA guarantee the complex formation and the addition of the oxaborole polymer provides a superior level of stability, assuring nucleic acid protection and increasing

physiological stability. Analysis by dynamic light scattering (DLS) and Zeta potential revealed small hydrodynamic sizes (~200 nm) and almost neutral charge of these conjugated polyplexes (Figure 2-1a). These diameters assure high potential for prolonged blood systemic circulation since they are large enough to avoid uptake in the liver but small enough to avoid filtration in the spleen[34]. Nanoparticle surface charge can be tailored to prolong circulation lifetime and selectively enhance accumulation at specific sites; neutral and slightly negative surface charges have been shown to reduce the adsorption of the serum proteins resulting in longer circulation half-lives[35]. The nearly neutral charge of the complexes seems to be the influence, perhaps by a higher density of sugar motifs on the polyplex surface, enhancing biocompatibility and potentially promoting targeted uptake. The presence of serum seemed to have an impact on the size of the nanoparticles making them relatively smaller in comparison to the polyplexes formed in the absence of serum, as has been previously reported[4,36]. Stability analysis of the polyplexes was performed in a time-dependent manner. The size of polyplexes with both statistical glycopolymers increased after incubation in media (in the presence and absence of serum proteins) at 22 °C for 6 h due to possible aggregation of polyplexes, but its size remained nearly unaffected after 6 h (~300 nm) showing stable complexes (Figure 2-1b).

a)

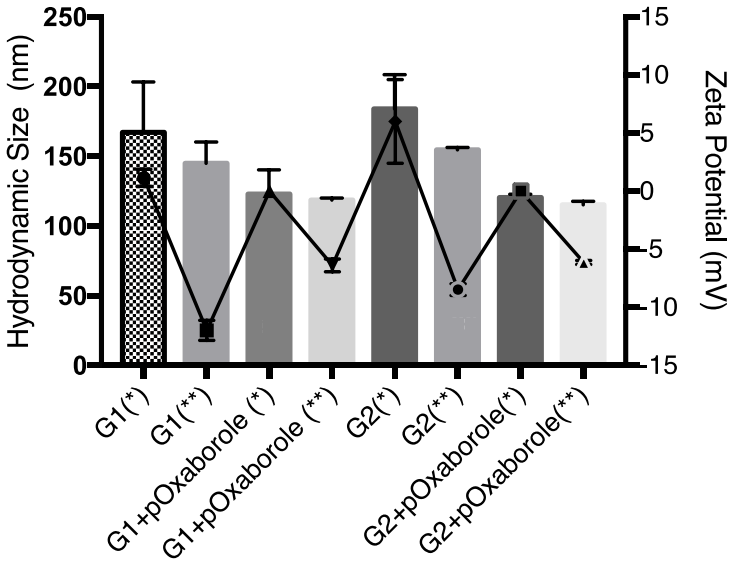

b)

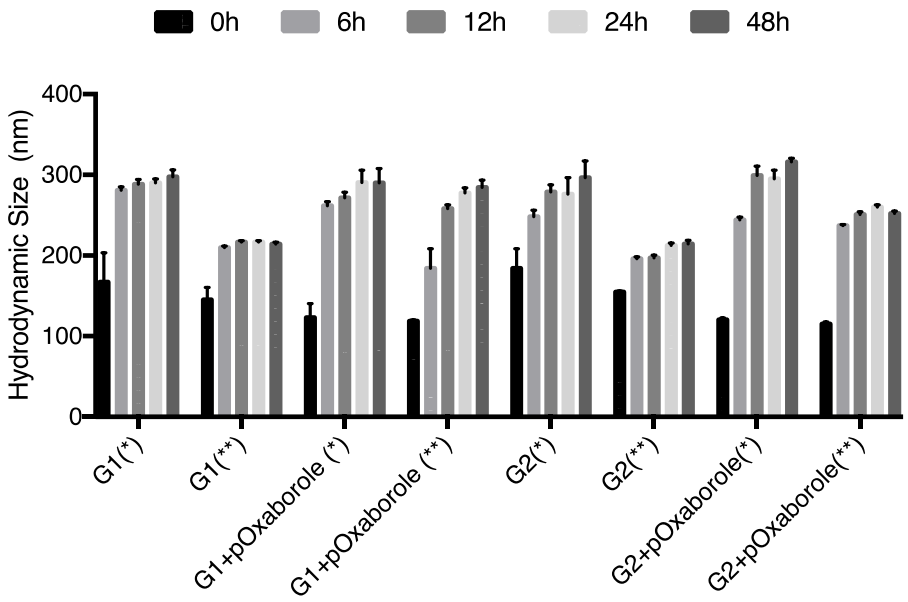

Figure 2-1. (a) Characterization of the oxaborole polymer-glycopolymer-siRNA polyplexes size and charges by dynamic light scattering (DLS) and Zeta potential instrumentation. Electrostatic interactions between the cationic glycopolymers and the negative charge siRNA guarantee the complex formation and the addition of the oxaborole polymer provides a superior level of stability. (b) Polyplexes sizes and stability as evidenced by DLS analysis in OMEM media in the absence (*) and presence (**) of serum. G1: P(LAEMA$_{20}$-*b*-AEMA$_{47}$), G2: P(LAEMA$_{8}$-*b*-AEMA$_{24}$) and pOxaborole: P(NIPAAm$_{294}$-st-AAm$_{63}$-st-MAAmBO$_{9}$).

One major impediment to the development of siRNA therapeutics is the delivery of the drug into the cytoplasm; avoidance of many challenges such as phagocytic uptake, enzymatic degradation by nucleases, triggering of the immune response and the hydrophobic plasma membrane barrier need to be overcome. Several transporters in the plasma membrane are able to internalize small molecule therapeutics however for larger oligonucleotides, such as siRNA being negatively charged and prone to degradation, requires a delivery vehicle[37]. Due to the high metabolic demands stimulated by rapid

proliferation, cancer cells overexpressed sugar receptors[34], potentially enhancing targeted uptake of nanoparticles decorated with sugar motifs such as glucose and galactose. Cellular uptake of nanoparticles has been hypothesized to be mediated by numerous pathways of endocytosis as well as direct penetration through the membrane[38]; the buffering capacity of nanoparticles activates the proton pump raising the osmotic pressure inside the endosome allowing the escape of the siRNA[39]. Regardless of the uptake mechanism, imaging studies with fluorescently labeled fluorescein isothiocyanate (FITC)-control siRNA have shown that oxaborole-glycopolymers complexes are being localized towards the cytoplasm (Figure 2-2). To further measure cellular retention and siRNA uptake efficacy, flow cytometry was implemented. The greater fluorescence intensity of siRNA labeled-oxaborole glycopolymer 2 conjugate (green) compared to the control (orange) (Figure 2-3) corroborates that this gene delivery vehicle successfully prevents polynucleotides from enzymatic degradation by avoiding rapid clearance by the reticuloendothelial system and degradation by cytosolic enzymes[28]. This demonstrates the competence of this nanovector in delivering siRNA without compromising its integrity and revealing its ability to boost endosomal escape, or possibly non-endocytic unidentified mechanisms of intracellular uptake.

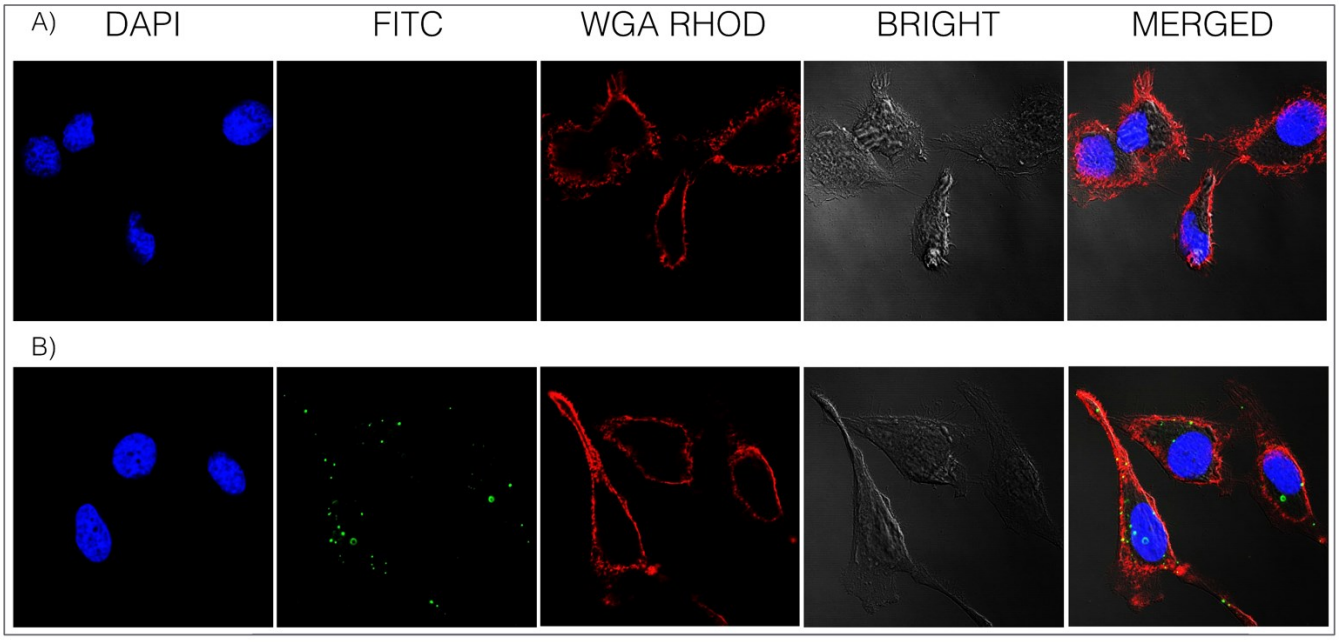

Figure 2-2. Cellular uptake of pOxaborole+Glycopolymer 2 complexed with FITC-control siRNA at w/w ratio of 10 after 3 h incubation; imaged using confocal fluorescence microscopy. Cellular membrane was stained with wheat germ agglutinin, tetramethylrhodamine (WGA-Rhodamine) dye and the cell's nucleus was stained with 4',6-diamidino-2-phenylindole dihydrochloride (DAPI).

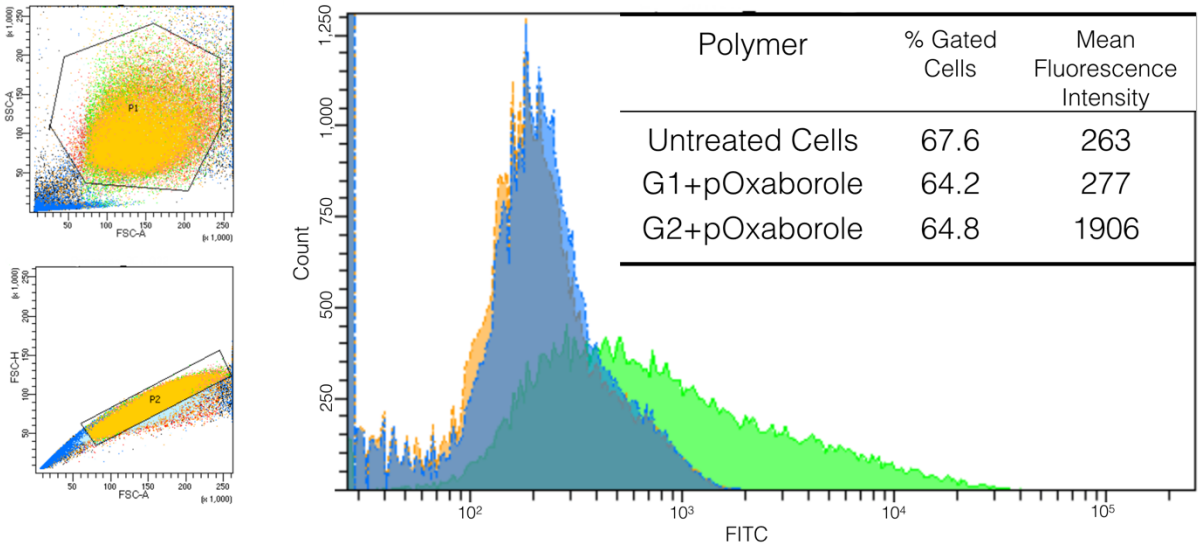

Figure 2-3. Flow cytometry analysis of cellular uptake of FITC-labelled complexes as compared to untreated cells (orange color); G1+pOxaborole (blue color) and G2+pOxaborole (green color). HeLa cells were incubated for 3 h.

Expression of EGFR is significantly related to chemosensitivity in many cancers[40]. Preclinical studies have suggested that blockade of EGFR results in a setback of chemoresistance in many tumor types[41]. To determine if our nanocomplex exerts targeted delivery of EGFR siRNA to cervical cancer cells, knockdown efficiencies were evaluated by immunoblotting and effective silencing of EGFR was seen for G2+pOxaborole polymer (Figure 2-4 a, b, c). On the other hand, glycopolymer 1 complex was also evaluated, but lower gene knockdown was observed (<30%) (Figure 2S7). We hypothesized that lesser cellular retention of G1+pOxaborole complex could translate to inferior gene silencing due

to stronger interactions between the AEMA residues and the polynucleotides that prevent disassembly of the complex hampering siRNA release in the cytosol.

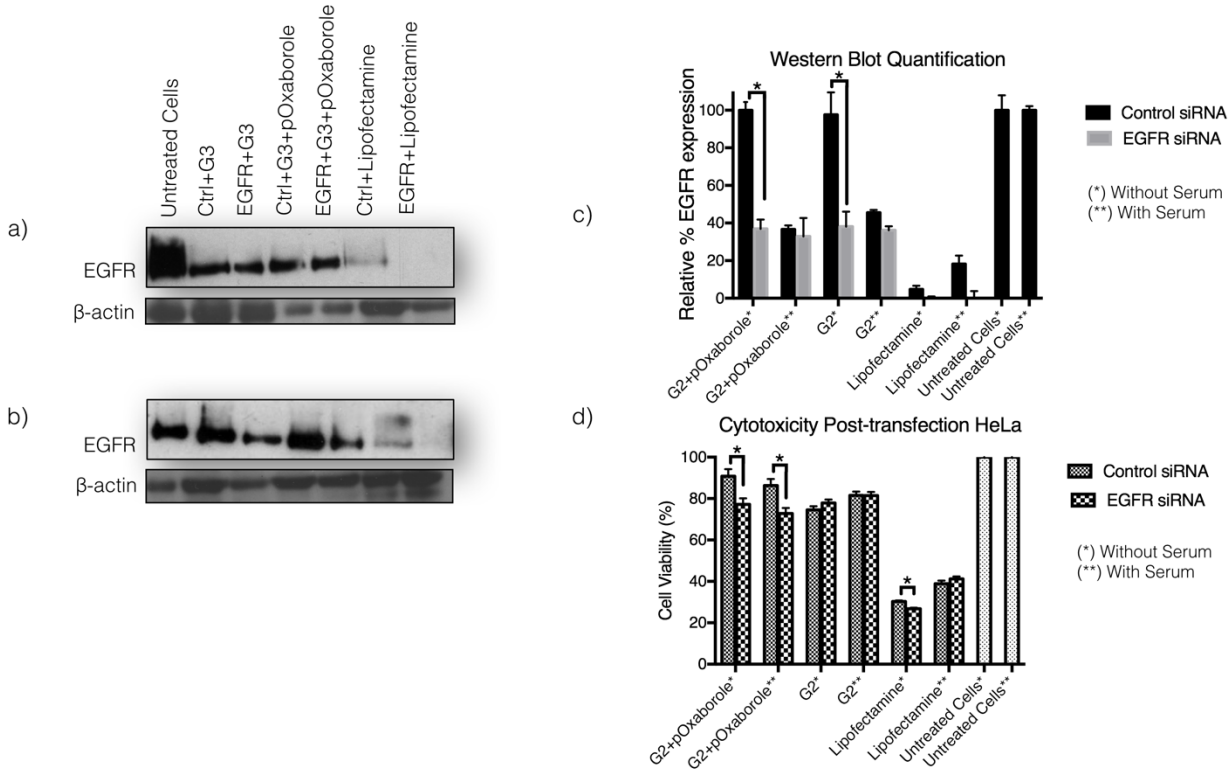

Figure 2-4. EGFR knockdown with G2 and G2+pOxaborole complex in HeLa cells in the (a) presence and (b) absence of the serum. HeLa cells were transfected with either control or EGFR siRNA for 48 h and cell lysates were subjected to immunoblot analysis using indicated antibodies; (c) Western Blot quantification was done by ImageJ analysis (d) Cell viability was assessed by Janus Green assay 48h post-transfection, with error bars representing S.D. (versus control siRNA *P<0.01).

Interestingly, the presence of serum proteins seems to promote off-target knockdown of EGFR proteins control siRNA (ctrl-siRNA) in both the glycopolymer alone (G2) and the conjugated complex (G2+pOxaborole) however gene knockdown efficiency of EGFR siRNA remains unaffected as evidenced in previous studies done with glycopolymer-based

carriers[27]. Although Lipofectamine shows lower EGFR expression (<20%) than the conjugated complex (40%), off-target silencing was observed in the presence and absence of serum proteins.

Cell toxicity seems to be related to the glycopolymer composition; higher AEMA content appears to be linked with higher toxicity, but the conjugation with oxaborole polymers appears to significantly decrease glycopolymer intrinsic toxicity at higher concentrations (Figure 2S8); probably by sheltering the amine residues on the nanoparticle surface preventing direct contact with the cell membrane. For the oxaborole-glycopolymer complexes, lower toxicity was exhibited 48 h post-transfection (Figure 2-4d and 2S7d). It is hypothesized that the higher cell viability may be associated with the charge shielding along the statistical galactose-polymer surface conferred by the oxaborole polymer, likewise this could offer further benefits in its pharmacokinetic profile *in vivo*. Decreased cell viability with Lipofectamine (<40%) was observed in contrast, and the cell toxicity was negligible for the G2+pOxaborole complex (<15%) (Figure 2-4d).

This novel oxaborole-galactose-based polymer has attested to be an effective vehicle for siRNA delivery by enriching gene knockdown in the presence and absence of serum proteins. Moreover, incorporation of oxaborole polymer increases the biocompatibility of the delivery system, nonetheless higher molar ratios of the AEMA residues in the statistical glycopolymers have shown to contribute to lower EGFR silencing and higher cellular toxicity as compared to lower AEMA ratios. The versatility of this therapeutic property, which appears to be due to the sequence-specificity of siRNA formulations, shows the potential use of this conjugate to silence the expression of additional targeted proteins. Further studies will focus on targeting different oncogenes and evaluating their biological response *in vivo* for the successful clinical implementation of nanoparticle-mediated siRNA silencing.

2.4 REFERENCES

(1) Song, C.-Z. Gene Silencing Therapy Against Cancer. In *Gene Therapy for Cancer*; Humana Press: Totowa, NJ, 2007; pp 185–196.

(2) Hanahan, D.; Weinberg, R. A.; Pan, K. H.; Shay, J. W.; Cohen, S. N.; Taylor, M. B.; Clarke, N. W.; Jayson, G. C.; Eshleman, J. R.; Nowak, M. A.; et al. Hallmarks of Cancer: The Next Generation. *Cell* **2011**, *144* (5), 646–674 DOI: 10.1016/j.cell.2011.02.013.

(3) de Fougerolles, A.; Vornlocher, H.-P.; Maraganore, J.; Lieberman, J. Interfering with disease: a progress report on siRNA-based therapeutics. *Nat. Rev. Drug Discov.* **2007**, *6* (6), 443–453 DOI: 10.1038/nrd2310.

(4) Ahmed, M.; Deng, Z.; Liu, S.; Lafrenie, R.; Kumar, A.; Narain, R. Cationic glyconanoparticles: Their complexation with DNA, cellular uptake, and transfection efficiencies. *Bioconjug. Chem.* **2009**, *20* (11), 2169–2176 DOI: 10.1021/bc900350c.

(5) Deng, Z.; Ahmed, M.; Narain, R. Novel well-defined glycopolymers synthesized via the reversible addition fragmentation Chain transfer process in aqueous media. *J. Polym. Sci. Part A Polym. Chem.* **2009**, *47* (2), 614–627 DOI: 10.1002/pola.23187.

(6) Ahmed, M.; Wattanaarsakit, P.; Narain, R. Cationic glyco-nanogels for epidermal growth factor receptor (EGFR) specific siRNA delivery in ovarian cancer cells. *Polym Chem* **2013**, *4* (13), 3829–3836 DOI: 10.1039/C3PY00425B.

(7) Quan, S.; Kumar, P.; Narain, R. Cationic Galactose-Conjugated Copolymers for Epidermal Growth Factor (EGFR) Knockdown in Cervical Adenocarcinoma. *ACS Biomater. Sci. Eng.* **2016**, *2* (5), 853–859 DOI: 10.1021/acsbiomaterials.6b00085.

(8) Normanno, N.; De Luca, A.; Bianco, C.; Strizzi, L.; Mancino, M.; Maiello, M. R.; Carotenuto, A.; De Feo, G.; Caponigro, F.; Salomon, D. S. Epidermal growth factor receptor (EGFR) signaling in cancer. *Gene* **2006**, *366* (1), 2–16 DOI: 10.1016/j.gene.2005.10.018.

(9) Heidenreich, O. Targeting Oncogenes with siRNAs. In *Methods in Molecular Biology, siRNA and miRNA Gene Silencing*; 2009; Vol. 487, pp 221–242.

(10) Lam, J. K. W.; Chow, M. Y. T.; Zhang, Y.; Leung, S. W. S. siRNA Versus miRNA

as Therapeutics for Gene Silencing. *Mol. Ther. Nucleic Acids* **2015**, *4* (9), e252 DOI: 10.1038/mtna.2015.23.

(11) Aleku, M.; Schulz, P.; Keil, O.; Santel, A.; Schaeper, U.; Dieckhoff, B.; Janke, O.; Endruschat, J.; Durieux, B.; Roder, N.; et al. Atu027, a Liposomal Small Interfering RNA Formulation Targeting Protein Kinase N3, Inhibits Cancer Progression. *Cancer Res.* **2008**, *68* (23), 9788–9798 DOI: 10.1158/0008-5472.CAN-08-2428.

(12) Xu, X. C.; Abuduhadeer, X.; Zhang, W. B.; Li, T.; Gao, H.; Wang, Y. H. Knockdown of RAGE inhibits growth and invasion of gastric cancer cells. *Eur. J. Histochem.* **2013**, *57* (4), 36 DOI: 10.4081/ejh.2013.e36.

(13) Ciardiello, F.; De Vita, F. Epidermal growth factor receptor (EGFR) inhibitors in cancer therapy. In *Advances in Targeted Cancer Therapy*; Birkhäuser Basel: Basel, 2005; pp 93–115.

(14) Young, S. W. S.; Stenzel, M.; Jia-Lin, Y. Nanoparticle-siRNA: A potential cancer therapy? *Crit. Rev. Oncol. Hematol.* **2016**, *98*, 159–169 DOI: 10.1016/j.critrevonc.2015.10.015.

(15) Yun, U.-J.; Sung, J. Y.; Park, S.-Y.; Ye, S.-K.; Shim, J.; Lee, J.-S.; Hibi, M.; Bae, Y.-K.; Kim, Y.-N. Oncogenic role of rab escort protein 1 through EGFR and STAT3 pathway. *Cell Death Dis.* **2017**, *8* DOI: 10.1038/cddis.2017.50.

(16) Noordhuis, M. G.; Eijsink, J. J. H.; Hoor, K. A. Expression of Epidermal Growth Factor Receptor (EGFR) and Activated EGFR Predict Poor Response to (Chemo) radiation and Survival in Cervical Cancer Expression of Epidermal Growth Factor Receptor (EGFR) and and Survival in Cervical Cancer. *Clin. Cancer Res.* **2009**, *15* (23), 7389–7397 DOI: 10.1158/1078-0432.CCR-09-1149.

(17) Nicholson, R. .; Gee, J. M. .; Harper, M. . EGFR and cancer prognosis. *Eur. J. Cancer* **2001**, *37*, 9–15 DOI: 10.1016/S0959-8049(01)00231-3.

(18) Davidson, B. L.; McCray, P. B. Current prospects for RNA interference-based

therapies. *Nat. Rev. Genet.* **2011**, *12* (5), 329–340 DOI: 10.1038/nrg2968.

(19) Gavrilov, K.; Saltzman, W. M. Therapeutic siRNA: Principles, challenges, and strategies. *Yale J. Biol. Med.* **2012**, *85* (2), 187–200.

(20) Dalby, B.; Cates, S.; Harris, A.; Ohki, E. C.; Tilkins, M. L.; Price, P. J.; Ciccarone, V. C. Advanced transfection with Lipofectamine 2000 reagent: primary neurons, siRNA, and high-throughput applications. *Methods* **2004**, *33* (2), 95–103 DOI: 10.1016/j.ymeth.2003.11.023.

(21) Kanasty, R.; Dorkin, J. R.; Vegas, A.; Anderson, D. Delivery materials for siRNA therapeutics. *Nat. Mater.* **2013**, *12* (11), 967–977 DOI: 10.1038/nmat3765.

(22) Kafil, V.; Omidi, Y. Cytotoxic impacts of linear and branched polyethylenimine nanostructures in a431 cells. *Bioimpacts* **2011**, *1* (1), 23–30 DOI: 10.5681/bi.2011.004.

(23) Xu, H.; Ma, H.; Yang, P.; Zhang, X.; Wu, X.; Yin, W.; Wang, H.; Xu, D. Targeted polymer-drug conjugates: Current progress and future perspective. *Colloids Surfaces B Biointerfaces* **2015**, *136*, 729–734 DOI: 10.1016/j.colsurfb.2015.10.001.

(24) Zhong, Y.-Q.; Wei, J.; Fu, Y.-R.; Shao, J.; Liang, Y.-W.; Lin, Y.-H.; Liu, J.; Zhu, Z.-H. Toxicity of cationic liposome Lipofectamine 2000 in human pancreatic cancer Capan-2 cells. *Nan Fang Yi Ke Da Xue Xue Bao* **2008**, *28* (11), 1981–1984.

(25) Cardarelli, F.; Digiacomo, L.; Marchini, C.; Amici, A.; Salomone, F.; Fiume, G.; Rossetta, A.; Gratton, E.; Pozzi, D.; Caracciolo, G. The intracellular trafficking mechanism of Lipofectamine-based transfection reagents and its implication for gene delivery. *Sci. Rep.* **2016**, *6* (1), 25879 DOI: 10.1038/srep25879.

(26) Xue, L.; Ingle, N. P.; Reineke, T. M. Highlighting the role of polymer length, carbohydrate size, and nucleic acid type in potency of glycopolycation agents for pDNA and siRNA delivery. *Biomacromolecules* **2013**, *14* (11), 3903–3915 DOI: 10.1021/bm401026n.

(27) Ahmed, M.; Narain, R. The effect of polymer architecture, composition, and molecular weight on the properties of glycopolymer-based non-viral gene delivery systems. *Biomaterials* **2011**, *32* (22), 5279–5290 DOI: 10.1016/j.biomaterials.2011.03.082.

(28) Smith, A. E.; Sizovs, A.; Grandinetti, G.; Xue, L.; Reineke, T. M. Diblock Glycopolymers Promote Colloidal Stability of Polyplexes and Effective pDNA and siRNA Delivery under Physiological Salt and Serum Conditions. *Biomacromolecules* **2011**, *12* (8), 3015–3022 DOI: 10.1021/bm200643c.

(29) Thapa, B.; Kumar, P.; Zeng, H.; Narain, R. Asialoglycoprotein receptor-mediated gene delivery to hepatocytes using galactosylated polymers. *Biomacromolecules* **2015**, *16* (9), 3008–3020 DOI: 10.1021/acs.biomac.5b00906.

(30) Moad, G.; Chong, Y. K.; Postma, A.; Rizzardo, E.; Thang, S. H. Advances in RAFT polymerization: The synthesis of polymers with defined end-groups. *Polymer (Guildf).* **2005**, *46* (19 SPEC. ISS.), 8458–8468 DOI: 10.1016/j.polymer.2004.12.061.

(31) Kotsuchibashi, Y.; Agustin, R. V. C.; Lu, J.-Y. Y.; Hall, D. G.; Narain, R. Temperature, pH, and glucose responsive gels via simple mixing of boroxole- and glyco-based polymers. *ACS Macro Lett.* **2013**, *2* (3), 260–264 DOI: 10.1021/mz400076p.

(32) Ahmed, M.; Deng, Z.; Narain, R. Study of transfection efficiencies of cationic glyconanoparticles of different sizes in human cell line. *ACS Appl. Mater. Interfaces* **2009**, *1* (9), 1980–1987 DOI: 10.1021/am900357x.

(33) Jiang, K.; Wang, Y.; Thakur, G.; Kotsuchibashi, Y.; Naicker, S.; Narain, R.; Thundat, T. Rapid and Highly Sensitive Detection of Dopamine Using Conjugated Oxaborole-Based Polymer and Glycopolymer Systems. *ACS Appl. Mater. Interfaces* **2017**, *9* (18), 15225–15231 DOI: 10.1021/acsami.7b04178.

(34) Petros, R. A.; DeSimone, J. M. Strategies in the design of nanoparticles for therapeutic applications. *Nat. Rev. Drug Discov.* **2010**, *9* (8), 615–627.

(35) Blanco, E.; Shen, H.; Ferrari, M. Principles of nanoparticle design for overcoming biological barriers to drug delivery. *Nat. Biotechnol.* **2015**, *33* (9), 941–951 DOI: 10.1038/nbt.3330.

(36) Ahmed, M.; Ishihara, K.; Narain, R. Calcium mediated formation of phosphorylcholine-based polyplexes for efficient knockdown of epidermal growth factor receptors (EGFR) in HeLa cells. *Chem. Commun.* **2014**, *50* (22), 2943 DOI: 10.1039/c4cc00181h.

(37) Peer, D. Nanotechnology for the delivery of therapeutic nucleic acids. *Nanotechnol. Deliv. Ther. Nucleic Acids* **2013** DOI: 10.4032/9789814411059.

(38) Sahay, G.; Alakhova, D. Y.; Kabanov, A. V. Endocytosis of nanomedicines. *J. Control. Release* **2010**, *145* (3), 182–195 DOI: 10.1016/j.jconrel.2010.01.036.

(39) Sahay, G.; Querbes, W.; Alabi, C.; Eltoukhy, A.; Sarkar, S.; Zurenko, C.; Karagiannis, E.; Love, K.; Chen, D.; Zoncu, R.; et al. Efficiency of siRNA delivery by lipid nanoparticles is limited by endocytic recycling. *Nat Biotech* **2013**, *31* (7), 653–658.

(40) Satpathy, M.; Mezencev, R.; Wang, L.; McDonald, J. F.; Sood, A. K. Targeted in vivo delivery of EGFR siRNA inhibits ovarian cancer growth and enhances drug sensitivity. *Sci. Rep.* **2016**, *6* (1), 36518 DOI: 10.1038/srep36518.

(41) Dickerson, E. B.; Blackburn, W. H.; Smith, M. H.; Kapa, L. B.; Lyon, L. A.; McDonald, J. F. Chemosensitization of cancer cells by siRNA using targeted nanogel delivery. *BMC Cancer* **2010**, *10* (1), 10 DOI: 10.1186/1471-2407-10-10.

Chapter 2

CHAPTER 3. ONCOGENIC EPIDERMAL GROWTH FACTOR RECEPTOR (EGFR) SILENCING IN CERVICAL CARCINOMA MEDIATED BY DYNAMIC SUGAR-BENZOXABOROLE POLYPLEXES.

The content of this chapter was published in

Journal of *ACS Macro Letters*

3.1 INTRODUCTION

Worldwide, one of the most common malignancies in women with respect to both incidence and mortality is cervical carcinoma. Nearly half of Canadians are expected to receive a diagnosis of cancer in their lifetime[1]. Decades of cancer research have contributed to the elucidation of some of the complex molecular mechanisms implicated in the pathogenesis of this disease. Shifting of cancer therapies towards novel genetic treatments against cancer that include counteracting or replacing a malfunctioning gene within the affected cells. The identification of different driver genes of cancer has been possible due to wide-ranging genomic profiling. Some of these "target" genes are successfully deactivated by small inhibiting molecules but the majority (70–80%) are considered to be "non-druggable" on the protein level. Additionally, when using protein inhibitors some negative side effects are seen due to off-target responses. As a result, increasing interest has been shown in the potential application of silencing RNAs (siRNAs) and other small regulatory RNAs in the treatment of cancer[2]. In cervical carcinoma, overexpression of the epidermal growth factor receptor (EGFR) gene has been detected in 70-90% of patients and has also been associated with poor prognosis of the disease[3]. EGFR is encoded by the c-ErbB1 proto-oncogene on chromosome 7p and is a member of a class of cell cycle regulatory molecules, the growth factor receptor family of protein tyrosine kinases (TKs). The glycoprotein receptor is activated when its ligand binds to the extracellular domain and it has the capability to interact with several ligands such as EGF, transforming growth factor (TGF)[4], amphiregulin[5], and heparin-binding EGF[6]. Activation of EGFR cues into cell growth, differentiation, resistance to apoptosis, cell cycle progression and angiogenesis. EGFR-based therapy is now being used for head and neck squamous cell carcinoma, colorectal carcinoma and non-small-cell lung carcinoma[7].

Delivering new genetic information into the target cell without disrupting other important molecular regulatory mechanisms is still highly challenging due to the intricate cellular and tissue barriers. To drive proficient therapeutic effects, the number of targeted cells must be large enough to setback the disorder, escape the immune system and be able to transmit the gene modification to their progeny to withstand some benefits. In the past two decades, numerous gene-therapy trials have been conducted targeting inherited

diseases, cancer and chronic infections, nonetheless only a few testified clinical benefits have been observed; the main reason being severe adverse events related to the vectors[8]. Narain and collaborators have made significant contributions to the synthesis of several glycopolymer-based vectors, by reversible addition−fragmentation chain transfer (RAFT) polymerization[9–11]. Carbohydrate-based polymers have shown unique characteristics supporting specific cell recognition and high stability in physiological environment enhancing blood biocompatibility[12,13]. It has also been reported that cationic moieties are needed to achieve the targeted outcome, but they cause inherent cytotoxicity. Therefore, multiple approaches have been explored, including acid degradability in galactose-based hyperbranched cationic polymers composed of 2-lactobioamidoethyl methacrylamide [LAEMA] and 2-aminoethyl methacrylamide hydrochloride [AEMA][14], that were able to reduce the cytotoxicity while maintaining high gene knockdown (60%). Along the same lines, the use of 2,2- dimethacroyloxy-1-ethoxypropane (DEP) cross-linker[15], a lower molecular weight (MW), pH sensitive ketal-based cross-linker, has been suggested to demonstrate lower cytotoxicity and high gene silencing (95%). Furthermore, tumour microenvironment regulated vectors have also been explored to enhance intra-tumoral accumulation and promote drug release at the targeted sites. Glutathione (GSH) regulated galactose-based hyperbranched polymers (HRRP) composed of LAEMA and AEMA[16] showed 85% EGFR silencing in cervical (HeLa) cancer cells without compromising the biocompatibility of the system[16]. Likewise, PGMA polymers have been studied by Xu[17–20] and Narain[21] groups by developing cationic polymers by ring-opening reaction of PGMA with ethanolamine and a lactobionic acid-derived aminosaccharide (Lac-NH_2). It has also shown that higher sugar content improved the biocompatibility of the polymers, but it also seemed to be detrimental for the knockdown capability. Oxaborole-based polymers are another class of gene delivery vectors owing to their stimuli-responsive features, where the methacrylamide benzoxaborole (MAAmBO) residues with the hydroxyl groups of the glycopolymer sugars allowed reversable cross-linking of the polymer chains as a function of temperature, pH and the presence of free glucose. This reversible interaction has shown to provide effective release of the siRNA cargo inside the cancer cells displaying 60% gene silencing[22]. In this study, a different approach has been pursued by using boron chemistry. A short benzoxaborole-glycopolymer polyplex composed of AEMA and 2-

methacryloyloxyethyl phosphorylcholine (MPC) and 2-hydroxyethyl methacrylate (HEMA) has been synthesized. MPC has a zwitterionic structure, and its polymer derivatives are known to be highly biocompatible and nontoxic[23]. HEMA, like MPC, is a hydrophilic polymer that resists protein absorption[24]; it is biocompatible in nature and possesses tunable mechanical properties specially used for the elaboration of polymer gels and matrices. Lower biodegradability of this material limits its application in the biological field[25], however combining the reversible responsiveness of the oxaborole motifs and the cationic glycopolymer capabilities seemed to overcome this issue and provided effective knockdown of the EGFR receptors in cervical carcinomas.

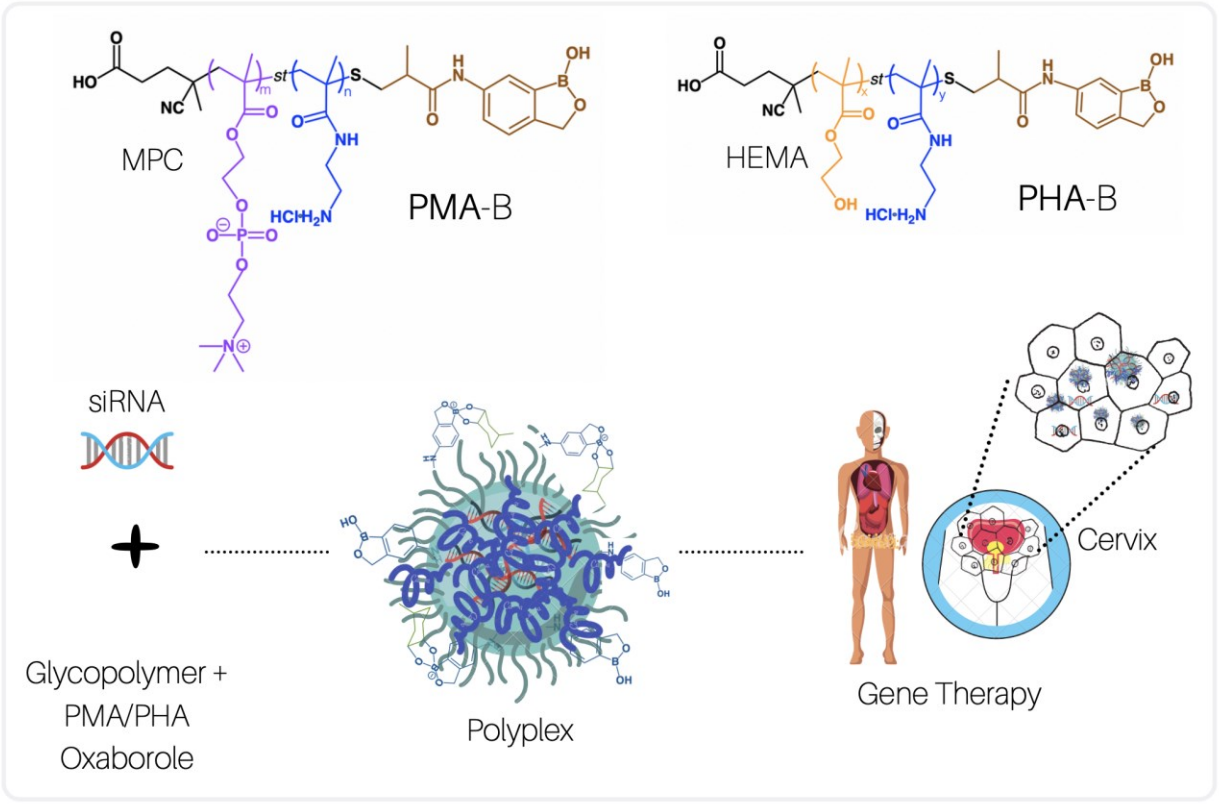

Scheme 3-1. Dynamic Sugar-Benzoxaborole polymers (PMA-B: (MPC-st-AEMA-MAAmBO)) and (PHA-B:(HEMA-st-AEMA-MAAmBO)) synthesized by RAFT polymerization.

3.2 EXPERIMENTAL SECTION

3.2.1 Materials

2-Methacryloyloxyethyl phosphorylcholine (MPC) was a gift from Dr. Ishihara's lab (Tokyo University, Japan). Hydroxyl methacrylate (HEMA), 4,4'Azobis (4-cyanovaleric acid) (ACVA), 1-amino-2-propanol, thiazolyl blue tetrazolium bromide (MTT) and Alizarin Red S (ARS) were purchased from Sigma-Aldrich (Oakville, Canada). 2-Aminoethylmethacrylamide hydrochloride (AEMA)[1], 5-methacrylamido-1,2benzoxaborole (MAAmBO)[2,3], 2-lactobionamidoethyl methacrylamide (LAEMA)[4] and 4-cyano-4-(thiobenzoylthio) pentanoic acid (CTP)[5] were prepared according to previously reported procedures). EGFR-specific siRNA sc-29301 Sense: CUCUGGAGGAAAAGAAAGU. Antisense: ACUUUCUUUUCCUCCAGAG; EGFR-(A-10) sc-373746 antibody (Santa Cruz) DMEM medium, penicillin, fetal bovine serum (FBS), and trypsin-EDTA, 0.25% were ordered from Gibco. Methanol, tetrahydrofuran (THF) and dimethylformamide (DMF) were purchased from Caledon Laboratories Ltd. (Georgetown, Canada).

3.2.2. Polymer Characterization.

A TSK-Gel G5000PWxl column from Tosoh Bioscience and conventional gel permeation chromatography (GPC) system were used to obtain the average molecular weights (M_n) and polydispersity (M_w/M_n) of the polymers. 0.5 M sodium acetate/0.5 M acetic acid buffer was used as eluent for the system at a flow rate of 0.5 ml/min. Monodisperse Pullulan standards (M_w=5,900-404,000 Da) was utilized to make a calibration curve. ^{1}H NMR spectra of the copolymers were recorded on a Varian 500 MHz spectrometer, and CD_3OD was used as the solvent. Fluorescence spectrums were measured by SpectraMax® i3x.

3.2.3 Preparation of P(HEMA-st-AEMA) (PHA) via RAFT polymerization.

In brief, HEMA (413 mg, 3.17 mmole), AEMA (522 mg, 3.17 mmole), CTP (40mg, 0.143 mmole), and ACVA (10mg, 35.7 μmole) were dissolved into methanol. The mixture was degassed with nitrogen gas for a half hour and subsequently heated to 67 °C and reacted for 20 hours. The polymers were precipitated into THF. The polymer was

precipitated into acetone and redispersed into THF for three-time for purifying the polymers.

3.2.4 Preparation of P(MPC-st-AEMA) (PMA) via RAFT polymerization.

592 mg MPC (2.0 mmole), 332mg AEMA (2.0 mmole), 40mg CTP (0.143 mmole), and 10 mg ACVA(35.7 μmole) were dissolved into methanol and the sample was purged with nitrogen gas for 30 min. Then, the polymerization was conducted at 67^{o}C for 20 hours. The polymer was precipitated into acetone and redispersed into methanol. The process was repeated three times. The cleavage of dithioester group was same as PHA.

3.2.5 Preparation of P(LAEMA) (PL) via RAFT polymerization.

921 mg LAEMA was dissolved into 1.5 mL of deionized water and mixed with 0.5 mL DMF that pre-dissolved 10 mg CTP and 2.5 mg ACVA. The mixture was degassed with nitrogen gas for 30 min and subsequently reacted at 67 °C for 20 hours. The resulted polymers were precipitated into acetone and washed with methanol three times.

3.2.6 Preparation of thiol end-functionalized PHA (PHA-SH) and PMA (PMA-SH) via aminolysis.

Dithioester group of the RAFT polymer was cleaved via aminolysis by using 1-amino-2-propanol in methanol under nitrogen environment at 23 °C for 4 hours. The resulted polymers were purified by precipitated into acetone and washed three times with acetone.

3.2.7 Preparation of oxaborole End-Functionalized PHA (PHA-B) and PMA (PMA-B) via thiol-ene click chemistry.

The reaction was carried out by adjusting the method that reported in literature[6]. Briefly, 3.0 equivalent mole of MAAmBO and 1.0 equivalent mole of ACVA were dissolved into a minimum amount of DMF and mixed M9-SH/H9-SH (1.0 equivalent mole of thiol group) that dispersed into a minimum amount of deionized water. The mixture was reacted under an oxygen-free environment at 70 °C for 20 hours. Acetone was used to precipitate and wash the modified polymer.

3.2.8 ARS assay for studying Boron-Carbohydrate interaction.

Fluorescence spectrums of samples were measured by SpectraMax® i3x in a standard 96 well plate, and the excitation was set to 475 nm. The different samples used are summarized in Table 3-1.

Table 3-1. Samples used for ARS assay.

	0.05mM ARS (µL)	10mg/mL PHA-B/PMA-B (µL)	10 mg/mL PL (µL)	pH 7.4 PBS (µL)
ARS alone	10.0	0.0	0.0	90.0
PMA-B + ARS	10.0	10.0	0.0	80.0
PMA-B + ARS + PLAEMA	10.0	10.0	10.0	70.0
PHA-B + ARS	10.0	10.0	0.00	80.0
PHA-B + ARS + PLAEMA	10.0	10.0	10.0	70.0

3.2.9 Polyplex confirmation by Agarose Gel Electrophoresis. The polyplexes were formulated in OMEM at varying polymer/siRNA ratios of 5, 25 and 50 and loaded in 1% agarose gel containing 1µg/mL ethidium bromide in 1X Tris Acetate/EDTA (TAE) buffer. The gel was run for 45 minutes at 130 V and illuminated with UV light and the DNA bands were visualized using UV transilluminator (Fig. S3).

3.2.10 Cell Culture. DMEM medium containing 10% fetal bovine serum (FBS) and 1% antibiotic (50 units of penicillin, 50 µg streptomycin) was used to culture HeLa cells (cervical cancer) in a humidified atmosphere at 37 °C and 5% CO_2. The cells were sub-cultured twice per week when reaching 80% confluency.

3.2.11 Cytotoxicity Evaluation of the dynamic sugar-benzoxaborole polymers and polyplexes. Cytotoxicity post-transfection was done by Janus Green assay after 48 h of incubation. A proliferation (MTT) assay was also done to evaluate the inherent toxicity of the polymers prior to complexation with the siRNA to determine the metabolically viable cells and if cellular functions were compromised related to metabolic activity after 72 h of incubation.

3.2.12 Cell Transfection with EGFR-siRNA. Cells were cultured into 60 mm plates at a cell density of 10^5 cells per plate. A mixture in OMEM of the polyplexes/lipofectamine with the EGFR siRNA/control siRNA (w/w:25) was added per plate. After incubation for 6 h, the media was removed and replaced with 2 mL of DMEM media containing with 10% fetal bovine serum (FBS). Protein quantification was done after 48 h of incubation by

Western Blot. RiPa buffer supplemented with a protease inhibitor was used to harvest the cells and the protein concentrations were determined using a Bradford protein assay kit (Bio-Rad). An SDS-PAGE denaturing gel was run and then transfer to a nitrocellulose membrane (0.45 um). EGFR-(A-10) sc-373746 antibody (Santa Cruz) and visualized by probing with and a streptavidin horse radish peroxidase (HRP) anti-mouse conjugate sc-516102. EGFR protein expression was quantified using ImageJ image analysis.

3.2.13 Fluorescent polyplexes Labeling of sugar-benzoxaborole polymers. The polymers were incubated with fluorescein isothiocyanate (FITC) control-siRNA. A w/w ratio of 25 in OMEM was used to evaluate the cellular uptake of the polyplexes after 3 h in a humidified atmosphere at 37 °C and 5% CO_2.

3.2.14 Cellular uptake of the polyplexes by Confocal Fluorescence Microscopy. The cells were cultured as mentioned above and seeded onto glass coverslips in a 10 mm plate at a density of 10^3 cells per plate. After overnight incubation, the FITC-control siRNA polyplexes at a w/w ratio of 25 in OMEM were added and subsequently incubated for 3 h in a humidified atmosphere at 37 °C and 5% CO_2. The media was the removed and the cells were wash three times with 1× PBS. Cell staining was done with (1:10000) HOECHST dye dissolved in PBS for 1h and fixed with 4% Paraformaldehyde for 15 min at 37 °C, and WGA Rhodamine for the cell membrane for 7 min. Visualization using a confocal microscope at 490 nm emission spectra for FITC was done.

3.2.15 Polymer synthesis and modification. RAFT polymerization allows the preparation of well-defined and low molecular weight distribution polymers, so this technique was chosen. In here, AEMA was selected for its cationic units to interact with negatively charged siRNA to form the polyplexes. MPC and HEMA are biocompatible and decreased the cationic distribution among the resulted polyplexes, therefore they were chosen to reduce the cytotoxicity of the resulted polymer. The method for preparing benzoxaborole (MAAmBO) functionalizaed P(HEMA-*st*-AEMA) (**PHA-B)** and P(MPC-*st*-AEMA) (**PMA-B**) is shown in Scheme 3-1. Table 3-2 summarized the molecular weight (M_n) and polydispersity (M_w/M_n) of the prepared polymers. P($LAEMA_{43}$) (**PL**) formed a dynamic bond with the polyplexes at pH 7.4 via boron-carbohydrate interaction which acts as a holder of the polyplexes (Scheme 3-2 D).

Table 3-2. Molecular weight (M_n), and polydispersity (M_w/M_n) of PHA, PMA and PL.

Sample	Composition	M_n (kDa)	M_w/M_n
PHA	P(HEMA$_{12}$-*st*-AEMA$_{10}$)	3.3	1.39
PMA	P(MPC$_{15}$-*st*-AEMA$_{12}$)	6.5	1.26
PL	P(LAEMA$_{43}$)	20.2	1.12

3.3 RESULTS & DISCUSSION

Prior to thiol-ene click chemistry, the omega-end of the polymer needed to be thiol-end functionalized. The thiol group was modified via aminolysis (Scheme 3-2B). The disappearance of the signal between 7 and 8 ppm in ^{1}H NMR spectrum of the product, which is the region for benzene group, (Figure 3S1A and 3S1B) confirmed the modification. ACVA was used as a thermal radical initiator to conduct thiol-ene click chemistry. Figure 3S2A and 3S2B illustrate the ^{1}H NMR of PMA-B and PHA-B (polymers modified with oxaborole). The existence of the characteristic peak of benzoxaborole suggested that the modification was successful.

Boron-carbohydrate interaction. The polyplexes were prepared by incubating PMA-B/PHA-B with siRNA via electrostatic interaction and subsequent conjugation of the polyplexes with PL to afford a macromolecule that can interact with multiple polyplexes and release them in acidic environment. Alizarin Red S **(**ARS) is a common agent used in studying boron-carbohydrate interactions[26]. ARS alone has a low fluorescence, but after binding with benzoxaborole the fluorescence significantly increases (Scheme 3-2E). Figure 3-1A and 3-1B clearly showed this behavior as the fluorescence intensity increased significantly in the presence of (**PMA**-B) or (**PHA**-B). Addition of the competitive agent, PL, led to an increase in amount of free ARS and a reduction of the fluorescence intensity as PL compete with ARS in forming dynamic bonds with benzoxaborole. LAEMA has slightly higher binding constant in comparison to catechol group (ARS) as illustrated by Wu and her colleagues in studying the conversion of benzoxaborolate in the presence of LAEMA (61.5%) ad catechol (57.3%) at pH 7.4 by ^{1}H NMR[27]. Based on the results, it is

evident that numerous chains of PMA-B and PHA-B can interact with PL to form a dynamic bond via boron-carbohydrate interaction. Thus, the advantage of this strategy lies in its facile engineering process to design a non-viral vector that can target various carcinomas as the system can be divided into two parts: a cationic segment that interacts with siRNA and a targeting segment; in this case, the targeting segment possesses diol or sugar units and a cationic segment having the oxaborole group. Cancer cells are known to display deregulated sugar transporters, augmenting sugar uptake and consumption. EGFR overexpression revealed a surprising link in maintaining sugar uptake by cells through the SGLT1 stabilization, promoted by the EGFR-SGLT1 interaction[28]. Moreover, the system can be combined easily at physiological environment and separated at mild acidic environment like inside the endosome.

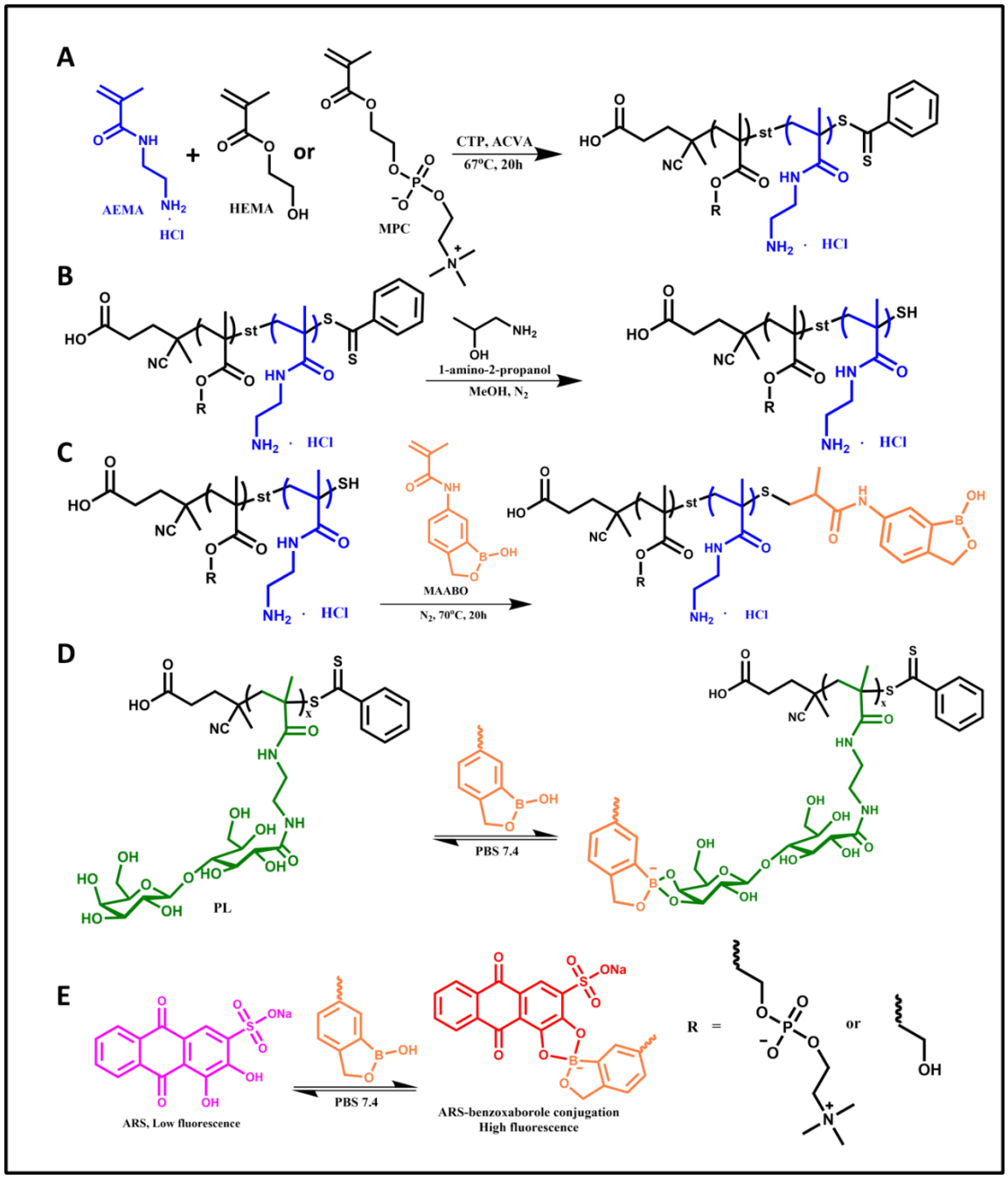

Scheme 3-2. Preparation of PHA and PMA via RAFT polymerization (A). Thiol-end functionalization of PHA-SH and PMA-SH via aminolysis (B). Thiol-ene click chemistry to modify omega end of polymer to an oxaborole group (C). (D) Mechanism of the dynamic bond formation between LAEMA and MAAmBO via boron-carbohydrate interaction and (E) ARS displacement assay.

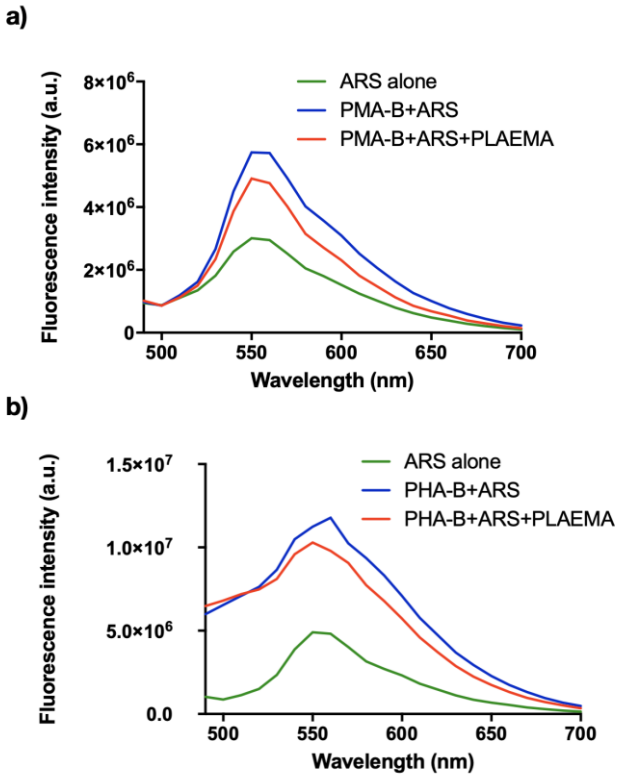

Figure 3-1. Fluorescence intensity of ARS alone, ARS in the existence of PMA a)/ PHA b), and competition of PLAEMA in PBS, pH=7.4, excitation: 475 nm.

Successful functionalization of polymers and nanosystems for the targeted delivery of siRNA against EGFR has a number of advantages such as the protection of the siRNA cargo from bloodstream degradation, augmentation of gene stability, targeted gene delivery, decreased toxic side effects, and improved bioavailability of the nucleic acids. Research in the past few years demonstrate that nanoscale gene delivery systems have boosted gene therapy specificity, reduced systemic toxicity, provide advance absorption rates, and have offered protection for active agents from biological and chemical degradation[29]. However, a persistent impediment to the clinical application of RNA therapy is the development of procedures that can competently target delivery of therapeutic RNAs *in vivo*. Entry into the target cells is challenging for many nanomaterial applications. The cell membrane presents a barrier to macromolecules, where intracellular uptake is orchestrated by a series of events that coordinates the function of lipids and proteins of the plasma membrane[30]. To evaluate

the cellular internalization of the sugar-benzoxaborole polyplexes fluorescence microscopy was used. In this case the siRNAs were labeled with a fluorescent probe fluorescein isothiocyanate (FITC). In Figure 3-2, we observed the cellular uptake of PL, PL+PMA-B and PL+PHA-B polyplexes. Largely, the transport of nanocarriers such as nanoparticles from the cell surface to the lysosomal vesicles occurs with a process known as endocytosis. Other critical parameters controlling the uptake of polyplexes is their surface properties (Fig. 3S4). Zeta potential and hydrodynamic size affect the opsonization and interactions with cellular membrane receptors that facilitate endocytosis. Functionalization with sterically shielding polymers, such as hydrophilic MPC and HEMA, can repel opsonization by preventing or minimizing protein adsorption to their surface. After 12 h incubation in DMEM media with serum the polyplexes did not change the hydrodynamic size showing high stability (Fig. 3S4b). In figure 3-2, we observed the polyplexes being internalized into HeLa cells after 3 h of incubation. (FITC)-control siRNA polyplexes localization has shown that the short sugar-benzoxaborole polymer complexes are being internalized and are located inside the cell cytoplasm.

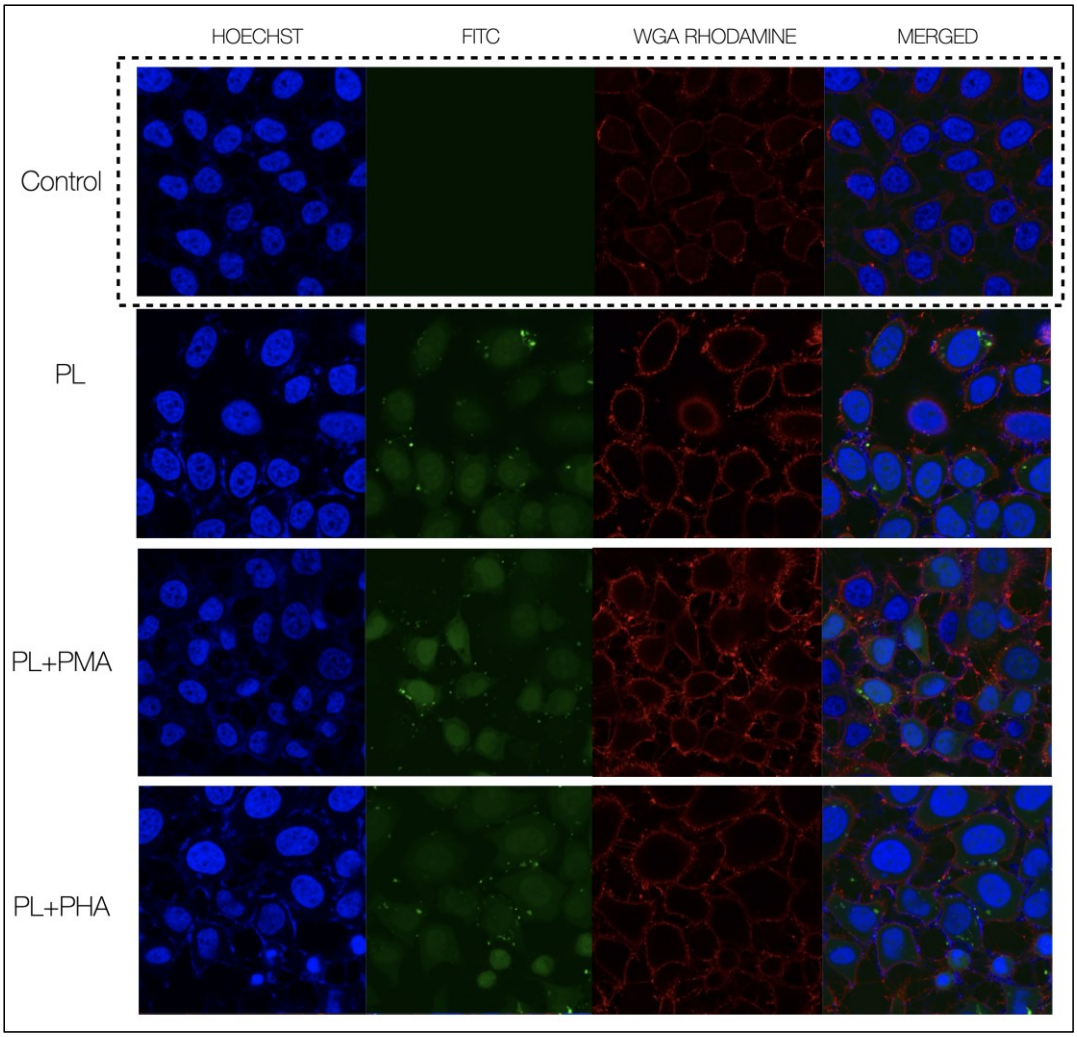

Figure 3-2. Cellular uptake of short dynamic sugar-benzoxaborole polyplexes with FITC-control siRNA at w/w ratio of 25 after 3 h incubation; imaged using confocal fluorescence microscopy. Cellular membrane was stained with wheat germ agglutinin, tetramethylrhodamine (WGA-Rhodamine) dye and the cell's nucleus was stained with 2'-[4-ethoxyphenyl]-5-[4-methyl-1-piperazinyl]-2,5'-bi-1*H*- benzimidazole trihydrochloride trihydrate (HOECHST).

The opportunity to understand key cellular biology pathways involved in the pathogenesis of cancer and the effective cellular uptake of the polyplexes and their intracellular trafficking provided a conduit to study the EFGR knockdown efficacies of these polyplexes. EGFR protein expression was quantified by western blot. In Figure 4-3b, the

protein quantification was determined after 48 h incubation with the polyplexes in absence of serum proteins and compared to the standard vector lipofectamine. Based on our results, both PL+PMA-B and PL+PHA-B exhibit knockdown of EGFR in a range of 60% and 70% respectively. As observed earlier, off target knockdown was seen with the vector lipofectamine (30%) and less than 15% with the short sugar-oxaborole polymers. p(HEMA) have been commercialized as a bulk material for the development and production of biomedical devices such as catheters, dental adhesives, implantable drug delivery systems, and contact and intraocular lenses. Some of the attributes of this polymer include a high-water retention capacity, broad biocompatibility and resemblance with living soft tissues, which are more inert to normal biological processes. MPC-containing polymeric materials are used as anti-fouling agents because the external surface of cellular membranes is rich in phospholipids possessing zwitterion headgroups, particularly phosphatidylcholine. Hence, MPC-modified biomaterials are likely to mimic cell membranes and be highly biocompatible. Nonspecific adsorption of protein and other biomolecules plays a significant part in the development of undesirable biological responses, including inflammation, blood clotting, biofilm formation, cell adhesion, bacterial adhesion, and bacterial infection. The functionalization of HEMA or the biomembrane mimicking zwitterionic polymer (MPC) utilizing a second hydrophilic monomer such as AEMA which interacts with the polynucleotides through the primary amine is one tactic to develop such “protein-resistant” materials. The multivalency of glycopolymers like LAEMA augments the molecular interactions with lectins and cells by the “glycoside cluster effect”, improving the cellular uptake of the polyplexes. This highly hydrophilic and uncharged moiety may help to reduce the positive charge density of AEMA controlling the electrostatic interactions with the cell membrane and increasing the cellular compatibility[9,31]. These zwitterionic polymers are recognized as the next-generation of antifouling biomaterials largely due to their ability to form a hydration shell via electrostatic interactions[32].

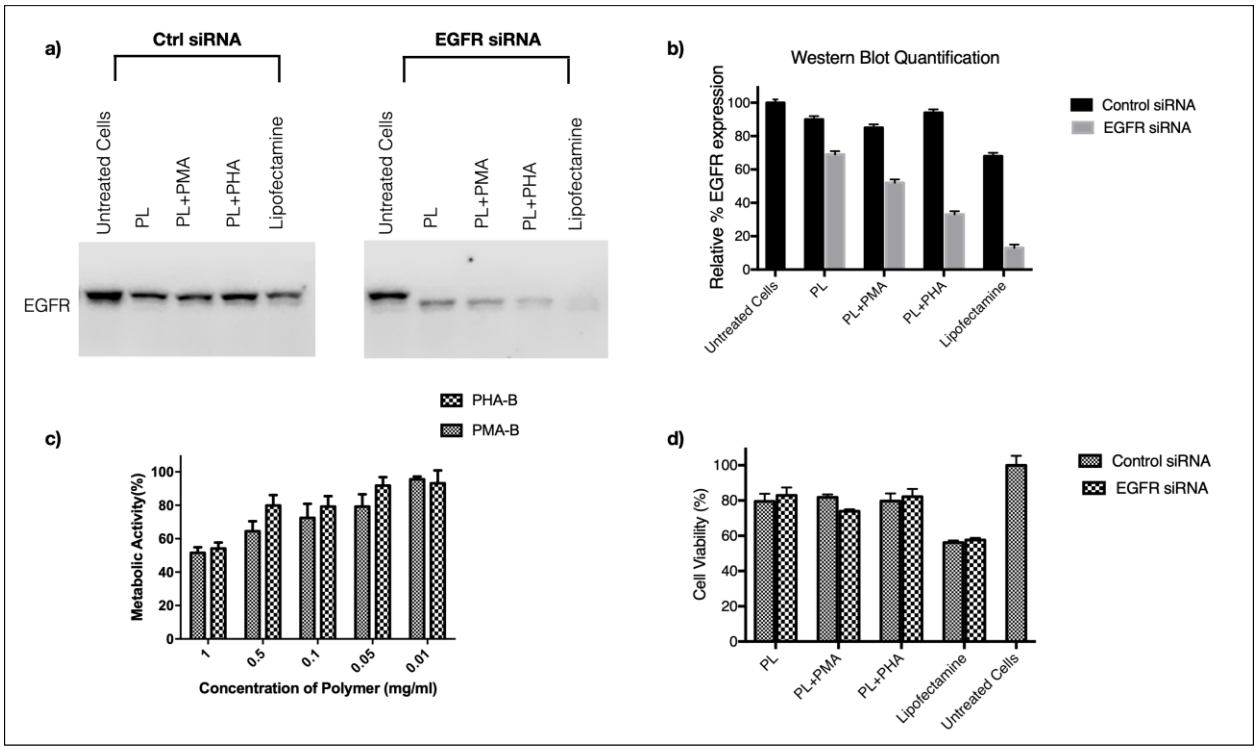

Figure 3-3. (a) EGFR knockdown of the short sugar-oxaborole complexes in HeLa cells in the absence of serum. HeLa cells were transfected with either control or EGFR siRNA for 48 h and cell lysates were subjected to immunoblot analysis using indicated antibodies. (b) Western Blot quantification was done by ImageJ analysis. (c) Polymer cytotoxicity related to metabolic activity with MTT assay in HeLa cells after 72 h incubation. (d) Cytotoxicity post-transfection in HeLa cells after 48 h of incubation with the short sugar-benzoxaborole polyplexes. Cell viability was assessed by Janus Green assay 48h post-transfection, —error bars representing S.D.

The use of carbohydrate-based polymer complexes seems to be advantageous as they are found essentially in all living organisms and their application does not exhibit toxic effects owing to their intrinsic biocompatibility and biodegradability that ensure safe therapies[33]. Due to their cationic nature, cationic polymers like AEMA can formed electrostatic interactions with negatively charged membranes in both the extracellular and intracellular spaces and complex with negatively charged proteins in the intracellular space disrupting

signaling pathways, resulting in apoptosis. The biocompatibility is influenced by different properties of the polymers like the molecular weight, charge density and type of the cationic functionalities[31]. Higher AEMA content appears to be interrelated with higher toxicity, but the functionalization with MAAmBO polymer and MPC/HEMA appears to significantly decrease the glycopolymer intrinsic toxicity after 48 h of transfection with the polyplexes as shown in Figure 3-3d. Normal metabolic activity in HeLa cells after the incubation with PMA-B and PHA-B were obtained according to the MTT assay (Figure 3-3c). In contrast a higher cytotoxicity was observed with the vector Lipofectamine.

Herein, we demonstrate that the combination of the glycopolymer p(LAEMA) with hydrophilic and zwitterionic MPC and HEMA moieties is a feasible methodology for developing functional biomaterials with dual capabilities of directing responsive ligands like oxaborole and cationic groups that interact with the negatively charge siRNA with enhanced resistance to protein adsorption and effective polynucleotide delivery. The complexation with the oxaborole polymers increases the biocompatibility of the delivery system by the tunable properties provided by this motif and sugar regulation.

3.4 REFERENCES

(1) Brenner, D. R.; Weir, H. K.; Demers, A. A.; Ellison, L. F.; Mhsc, C. L.; Shaw, A.; Turner, D.; Woods, R. R.; Smith, L. M. Projected Estimates of Cancer in Canada in 2020. **2020**, *192* (9), 199–205. https://doi.org/10.1503/cmaj.191292.

(2) Satpathy, M.; Mezencev, R.; Wang, L.; McDonald, J. F. Targeted in Vivo Delivery of EGFR SiRNA Inhibits Ovarian Cancer Growth and Enhances Drug Sensitivity. *Sci. Rep.* **2016**, *6* (June), 1–9. https://doi.org/10.1038/srep36518.

(3) Kim, Y. T.; Park, S. W.; Kim, J. W. Correlation between Expression of EGFR and the Prognosis of Patients with Cervical Carcinoma. *Gynecol. Oncol.* **2002**, *87* (1), 84–89. https://doi.org/10.1006/gyno.2002.6803.

(4) Fisher, D. A.; Lakshmanan, J. Metabolism and Effects of Epidermal Growth Factor and Related Growth Factors in Mammals. *Endocr. Rev.* **1990**.

https://doi.org/10.1210/edrv-11-3-418.

(5) Shoyab, M.; Plowman, G. D.; McDonald, V. L.; Bradley, J. G.; Todaro, G. J. Structure and Function of Human Amphiregulin: A Member of the Epidermal Growth Factor Family. *Science (80-.).* **1989**. https://doi.org/10.1126/science.2466334.

(6) Higashiyama, S.; Abraham, J.; Miller, J.; Fiddes, J.; Klagsbrun, M. A Heparin-Binding Growth Factor Secreted by Macrophage-like Cells That Is Related to EGF. *Science (80-.).* **1991**. https://doi.org/10.1126/science.1840698.

(7) Schrevel, M.; Gorter, A.; Kolkman-Uljee, S. M.; Trimbos, J. B. M. Z.; Fleuren, G. J.; Jordanova, E. S. Molecular Mechanisms of Epidermal Growth Factor Receptor Overexpression in Patients with Cervical Cancer. *Mod. Pathol.* **2011**, *24* (5), 720–728. https://doi.org/10.1038/modpathol.2010.239.

(8) Naldini, L. Gene Therapy Returns to Centre Stage. *Nature* **2015**, *526* (7573), 351–360. https://doi.org/10.1038/nature15818.

(9) Ahmed, M.; Narain, R. Progress of RAFT Based Polymers in Gene Delivery. *Prog. Polym. Sci.* **2013**, *38* (5), 767–790. https://doi.org/10.1016/j.progpolymsci.2012.09.008.

(10) Ahmed, M.; Narain, R. Carbohydrate-Based Materials for Targeted Delivery of Drugs and Genes to the Liver. *Nanomedicine (Lond)* **2015**, *10* (14), 2263–2288. https://doi.org/10.2217/nnm.15.58.

(11) Deng, Z.; Ahmed, M.; Narain, R. Novel Well-Defined Glycopolymers Synthesized via the Reversible Addition Fragmentation Chain Transfer Process in Aqueous Media. *J. Polym. Sci. Part A Polym. Chem.* **2009**, *47* (2), 614–627. https://doi.org/10.1002/pola.23187.

(12) Narain, R.; Wang, Y.; Ahmed, M.; Lai, B. F. L.; Kizhakkedathu, J. N. Blood Components Interactions to Ionic and Nonionic Glyconanogels. *Biomacromolecules* **2015**, *16* (9), 2990–2997. https://doi.org/10.1021/acs.biomac.5b00890.

(13) Smith, A. E.; Sizovs, A.; Grandinetti, G.; Xue, L.; Reineke, T. M. Diblock Glycopolymers Promote Colloidal Stability of Polyplexes and Effective PDNA and SiRNA Delivery under Physiological Salt and Serum Conditions. *Biomacromolecules* **2011**, *12* (8), 3015–3022. https://doi.org/10.1021/bm200643c.

(14) Peng, Y.-Y.; Diaz-Dussan, D.; Kumar, P.; Narain, R. Acid Degradable Cationic Galactose-Based Hyperbranched Polymers as Nanotherapeutic Vehicles for Epidermal Growth Factor Receptor (EGFR) Knockdown in Cervical Carcinoma. *Biomacromolecules* **2018**, *19* (10), 4052–4058. https://doi.org/10.1021/acs.biomac.8b01066.

(15) Peng, Y.-Y.; Diaz-Dussan, D.; Vani, J.; Hao, X.; Kumar, P.; Narain, R. Achieving Safe and Highly Efficient Epidermal Growth Factor Receptor Silencing in Cervical Carcinoma by Cationic Degradable Hyperbranched Polymers. *ACS Appl. Bio Mater.* **2018**, *1* (4), 961–966. https://doi.org/10.1021/acsabm.8b00371.

(16) Peng, Y.-Y. Y.; Diaz-Dussan, D.; Kumar, P.; Narain, R. Tumor Microenvironment-Regulated Redox Responsive Cationic Galactose-Based Hyperbranched Polymers for SiRNA Delivery. *Bioconjug. Chem.* **2019**, *30* (2), 405–412. https://doi.org/10.1021/acs.bioconjchem.8b00785.

(17) Xu, F. J. Versatile Types of Hydroxyl-Rich Polycationic Systems via O-Heterocyclic Ring-Opening Reactions: From Strategic Design to Nucleic Acid Delivery Applications. *Progress in Polymer Science*. 2018. https://doi.org/10.1016/j.progpolymsci.2017.09.003.

(18) Qi, M.; Duan, S.; Yu, B.; Yao, H.; Tian, W.; Xu, F.-J. PGMA-Based Supramolecular Hyperbranched Polycations for Gene Delivery. *Polym. Chem.* **2016**, *7* (26), 4334–4341. https://doi.org/10.1039/C6PY00759G.

(19) Li, R. Q.; Wu, Y.; Zhi, Y.; Yang, X.; Li, Y.; Xua, F. J.; Du, J. PGMA-Based Star-Like Polycations with Plentiful Hydroxyl Groups Act as Highly Efficient MiRNA Delivery Nanovectors for Effective Applications in Heart Diseases. *Adv. Mater.* **2016**. https://doi.org/10.1002/adma.201602319.

(20) Sun, Y.; Hu, H.; Yu, B.; Xu, F. J. PGMA-Based Cationic Nanoparticles with Polyhydric Iodine Units for Advanced Gene Vectors. *Bioconjug. Chem.* **2016**. https://doi.org/10.1021/acs.bioconjchem.6b00509.

(21) Chen, Y.; Diaz-Dussan, D.; Peng, Y.-Y. Y.; Narain, R. Hydroxyl-Rich PGMA-Based Cationic Glycopolymers for Intracellular SiRNA Delivery: Biocompatibility and Effect of Sugar Decoration Degree. *Biomacromolecules* **2019**, *20* (5), 2068–2074. https://doi.org/10.1021/acs.biomac.9b00274.

(22) Diaz-Dussan, D.; Nakagawa, Y.; Peng, Y.-Y. Y.; Sanchez, L. V.; Ebara, M.; Kumar, P.; Narain, R.; C, L. V. S.; Ebara, M.; Kumar, P.; Narain, R. Effective and Specific Gene Silencing of Epidermal Growth Factor Receptors Mediated by Conjugated Oxaborole and Galactose-Based Polymers. *ACS Macro Lett.* **2017**, *6* (7), 768–774. https://doi.org/10.1021/acsmacrolett.7b00388.

(23) Nagao, M.; Sengupta, J.; Diaz-Dussan, D.; Adam, M.; Wu, M.; Acker, J.; Ben, R.; Ishihara, K.; Zeng, H.; Miura, Y.; Narain, R. Synthesis of Highly Biocompatible and Temperature-Responsive Physical Gels for Cryopreservation and 3D Cell Culture. *ACS Appl. Bio Mater.* **2018**, *1* (2), 356–366. https://doi.org/10.1021/acsabm.8b00096.

(24) Kumari, J.; Kumar, A. Development of Polymer Based Cryogel Matrix for Transportation and Storage of Mammalian Cells. *Sci. Rep.* **2017**, *7* (December 2016), 1–13. https://doi.org/10.1038/srep41551.

(25) Barui, A. *Synthetic Polymeric Gel*; Elsevier Ltd, 2018. https://doi.org/10.1016/b978-0-08-102179-8.00003-x.

(26) Springsteen, G.; Wang, B. Alizarin Red S. as a General Optical Reporter for Studying the Binding of Boronic Acids with Carbohydrates. *Chem. Commun.* **2001**. https://doi.org/10.1039/b104895n.

(27) Wu, D.; Wang, W.; Diaz-Dussan, D.; Peng, Y.-Y.; Chen, Y.; Narain, R.; Hall, D. G. In Situ Forming, Dual-Crosslink Network, Self-Healing Hydrogel Enabled by a Bioorthogonal Nopoldiol–Benzoxaborolate Click Reaction with a Wide PH Range.

Chem. Mater. **2019**, acs.chemmater.9b00769. https://doi.org/10.1021/acs.chemmater.9b00769.

(28) Aparicio, L. A.; Calvo, M. B.; Figueroa, A.; Pulido, E. G.; Campelo, R. G. Potential Role of Sugar Transporters in Cancer and Their Relationship with Anticancer Therapy. *Int. J. Endocrinol.* **2010**, *2010*. https://doi.org/10.1155/2010/205357.

(29) Gupta, S.; Gupta, M. K. Possible Role of Nanocarriers in Drug Delivery against Cervical Cancer. *Nano Rev. Exp.* **2017**, *8* (1), 1335567. https://doi.org/10.1080/20022727.2017.1335567.

(30) Panariti, A.; Miserocchi, G.; Rivolta, I. The Effect of Nanoparticle Uptake on Cellular Behavior: Disrupting or Enabling Functions? *Nanotechnol. Sci. Appl.* **2012**, *5* (1), 87–100. https://doi.org/10.2147/NSA.S25515.

(31) Singhsa, P.; Diaz-Dussan, D.; Manuspiya, H.; Narain, R. Well-Defined Cationic N-[3-(Dimethylamino)Propyl]Methacrylamide Hydrochloride-Based (Co)Polymers for SiRNA Delivery. *Biomacromolecules* **2018**, *19* (1), 209–221. https://doi.org/10.1021/acs.biomac.7b01475.

(32) Vales, T. P.; Jee, J. P.; Lee, W. Y.; Cho, S.; Lee, G. M.; Kim, H. J.; Kim, J. S. Development of Poly (2-Methacryloyloxyethyl Phosphorylcholine)-Functionalized Hydrogels for Reducing Protein and Bacterial Adsorption. *Materials (Basel).* **2020**, *13* (4). https://doi.org/10.3390/ma13040943.

(33) Salatin, S.; Yari Khosroushahi, A. Overviews on the Cellular Uptake Mechanism of Polysaccharide Colloidal Nanoparticles. *J. Cell. Mol. Med.* **2017**, *21* (9), 1668–1686. https://doi.org/10.1111/jcmm.13110.

CHAPTER 4. HYDROXYL-RICH PGMA-BASED CATIONIC GLYCOPOLYMERS FOR INTRACELLULAR siRNA DELIVERY: BIOCOMPATIBILITY AND EFFECT OF SUGAR DECORATION DEGREE.

The content of this chapter was published in

Journal of *Biomacromolecules*

4.1 INTRODUCTION

Protein tyrosine kinase receptors have been implicated in human cancer since the avian erythroblastosis tumor virus initiated the encoding of an aberrant form of the epidermal growth factor receptor (EGFR).[1] EGFR is the first receptor tyrosine kinase (RTK) identified, and the first one linked to cancer. Thus, EGFR has been the most intensively studied among all RTKs.[2] In the human genome, the ErbB receptor family (ErbB, is derived from the name of a viral oncogene, erythroblastic leukemia viral oncogene)[3] or the EGFR family includes the EGFR or ErbB1/Her1, ErbB2/Her2, ErbB3/ Her3, and ErbB4/Her4. The ErbB receptor signaling is activated by homo- or heterodimerization after binding to soluble ligands like EGF growth factors that promote receptor activation.[4] Activated ErbB receptors stimulate signaling cascades, including the Ras-Raf-Mek-ERK, PI3K-Akt-mTOR, STAT, and Src pathways.[5] Governing of these diverse signaling networks by ErbB receptors, regulate many critical cellular processes, such as cell proliferation, cell differentiation, cell survival, cell metabolism, cell migration, and cell cycle that contribute to tumor carcinogenesis.[4,6] ErbB receptors exhibit various types of alterations; the most common ones are gene amplification leading to EGFR overexpression and constitutive EGFR activation due to self-production of EGF-related growth factors by the tumor cells. Structural rearrangements that cause in-frame deletions in the extracellular domain of the EGFR receptor are also frequent in some carcinomas.[4] Gene therapy has been proposed as an innovative strategy for cancer treatment by delivering of genetic materials, either RNA or DNA, into specific human tissues or cells to replace faulty genes, substitute absent genes, silence malfunctioning gene expression, or introduce new genes to restore cellular functions.[7] Tumor heterogeneity of cancerous cells is the main obstacle for effective cancer treatment; therefore, targeting genomic alterations that drive tumor formation such as tumor suppressor genes and oncogenes like EGFR is a promising strategy to target this disease.[8] In spite of significant development in the field of gene therapy, still further optimization is required to achieve effective therapeutic results. Vector designing is one of the key factors for future outcomes among gene therapy. Suitable vectors are required for optimized gene delivery and expression, but current vectors have some limitations such as associated cytotoxicity and off- target effects. Aminated poly(glycidyl methacrylate)

(PGMA) polymers have drawn much attention as a promising gene delivery system.[9] PGMA can react readily and irreversibly with nucleophilic groups such as −NH2,providing effective condensation capacity of nucleotides such as DNA or RNA.[10–15] Recently, ethanolamine (EA)-functionalized PGMA polymers (PGEA) have been extensively studied for gene therapy by Xu's group,[9,16–20] exhibiting high transfection efficiency and low toxicity in different cell lines. The nonionic hydroxyl groups confer hydrophilicity to the polymer, and the cationic secondary amine bestows the cationic charged and buffering capacity to complex with and further release nucleic acids. Moreover, hydroxyl-rich PGEA-grafted carbohydrates have been developed by Xu's group to achieve both high gene transfection efficiency and excellent biocompatibility.[17] However, little attention has been paid to the exploration of PGEA decorated with small sugar molecules for gene delivery. Our group[21–28] together with several other groups[29–33] have been focusing on the development of cationic glycopolymers as effective gene delivery vehicles. The transfection efficacy by these cationic glycopolymers is found to be related to different parameters, such as molecular weights, cationic content, and architectures.[21,22] Optimization of these carriers by increasing the amine content has led to increase in gene expression, and addition of sugar moieties provides higher affinity and further improvement of cellular uptake.[26] The most studied cationic glycopolymers were usually synthesized by copolymerzation between sugar monomers and amine methacrylates/methacrylamides. Benefiting from the high reactivity of PGMA, grafting with sugar molecules bearing reactive amine groups can thus induce novel hydroxyl-rich PGMA-based cationic glycopolymers, which can probably combine the advantages of both kinds of polymers for gene delivery. Herein, we first synthesized a lactobionic acid-derived sugar molecule containing one amine group: N-(2-aminoethyl)-O-β- D-galactopyranosyl-(1 → 4)-D-gluconamide (denoted as Lac-NH2). To investigate the effect of sugar decoration degree on gene transfection efficiency, Lac-NH2 and ethanolamine with different feed ratios were applied to react with epoxy groups of PGMA. The resultant cationic polymers with sugar decoration degrees of 0, 9, and 33% were used to form polyplexes with EGFR siRNA. The siRNA condensation ability, size and charge of polyplexes, cytotoxicity, and transfection performance were studied in detail. We found

that cationic PGMA-based glycopolymer with sugar decoration degree of 9% exhibited great potential as a gene delivery vector due to its satisfactory balance between EGFR knockdown efficiency and biocompatibility (Scheme 4-1)

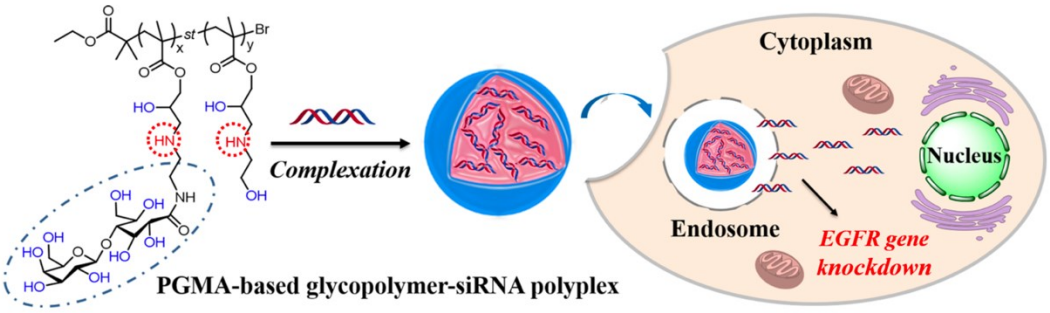

Scheme 4-1. Schematic Illustration of Galactose-Decorated PGMA-Based Polycations for EGFR Gene Knockdown in HeLa Cells.

4.2 EXPERIMENTAL SECTION

4.2.1. Materials. Copper(I) bromide (CuBr), 2,2′ -bipyridyl (bpy),glycidyl methacrylate (GMA), ethyl α-bromoisobutyrate (EBiB), lactobionic acid, ethanediamine (EDA), ethanolamine (EA), triethylamine (TEA), and trifluoroacetic acid (TFA) were purchased from Sigma-Aldrich. Streptomycin (10 mg/mL), penicillin (10 000 U/mL), Dulbecco's modified Eagle medium (DMEM)/F12 media, Opti-MEM (OMEM), 0.25% trypsin−ethylenediaminetetraacetic acid (EDTA), and fetal bovine serum (FBS) were obtained from Gibco. Lipofectamine 2000 was purchased from Invitrogen. Control siRNA, human EGFR-specific siRNA sc-29301 Sense: CUCUGGAGGAAAAGAAAGU. Antisense: ACUUUCUUUUCCUCCAGAG; primary antibody (rabbit polyclonal EGFR-specific IgG IgG sc-03-G), and fluorescein isothiocyanate (FITC)-conjugated control siRNA were purchased from Santa Cruz Biotechnology. (3,3′ ,5,5′ -Tetramethylbenzidine) (HRP)-conjugated secondary antibody (antirabbit IgG W4011) was purchased from Promega Corporation. The organic solvents, including anhydrous dimethylsulfoxide (DMSO), anhydrous methanol, dichloromethane (DCM), diethyl ether, and acetone, were purchased from Caledon Laboratories Ltd. (Georgetown, Canada) and used without further purification.

4.2.2. Instrumentation. ^{1}H NMR spectra were recorded using a Bruker Avance III HD 500 MHz spectrometer. $CDCl_3$ or D_2O was used as a solvent. The molecular weight and polydispersity of the polymers were determined by gel permeation chromatography (GPC). Aqueous phase GPC34 with two Waters Ultrahydogel linear WAT011545 columns and Viscotek model 270 dual detector and organic phase GPC35 with I-MBLMW-3078 and I-MBHMW-3078 columns and Viscotek model 250 dual detector were applied for detecting PGEA/PGEL and PGMA, respectively. Sodium acetate (0.50 M)/0.50 M acetic acid buffer and DMF with 10 mM LiBr were used accordingly as eluent, and the flow rate was set at 1.0 mL/min.

4.2.3. Synthesis of PGMA via Atom Transfer Radical Polymerization (ATRP). PGMA was synthesized using EBiB as initiator and CuBr/bpy as catalyst as previously reported.[36] Typically, GMA (2.13 g, 15 mmol) and EBiB (48.8 mg, 0.25 mmol) were dissolved in 4 mL of DMSO, and the mixture was added into a 50 mL flask. After degassing for 20 min by nitrogen, CuBr (36 mg, 0.25 mmol) and bpy (78 mg, 0.5 mmol) in 300 μL of DMSO were injected into the flask with a syringe. The solution was further degassed for 10 min and allowed to stir at room temperature for 4 h. The reaction was then terminated by exposure to air. Crude product was obtained by precipitation into methanol for three times. The precipitate was further dried in vacuum overnight to give pure PGMA.

4.2.4. Synthesis of N-(2-Aminoethyl)-O-β-D-galactopyranosyl-(1 → 4)-D-gluconamide (Lac-NH2). Lac-NH2 was synthesized according to published literatures with minor modification (Scheme 3-2a).[37,38]First, lactobionic lactone was synthesized from lactobionic acid as previously reported in our group.[39] Briefly, lactobionic acid (10.0 g) and a catalyst amount of TFA was dissolved in anhydrous methanol (150 mL) at 70 °C, followed by vacuum distillation. This process was repeated for three times to ensure complete conversion of the acid to lactone. Subsequently, the obtained lactobionic lactone was directly dissolved in 50 mL of anhydrous methanol at 70 °C and dropwise added into 20 times excess of EDA solution in 30 mL of anhydrous DMSO. The mixed solution was allowed to react at 70 °C for 2 h and kept stirring at room temperature overnight. Afterward, the solution was poured into excess amount of DCM to precipitate the crude product. The

precipitate was filtered and washed with acetone, followed by vacuum drying to give Lac-NH2.

4.2.5. Synthesis of PGMA-Based Cationic Glycopolymers. The cationic polymers were synthesized via ring-opening reaction between epoxy groups of PGMA and amino groups of EA or Lac-NH2. The EA-functionalized PGMA, namely, PGEA, was synthesized as previously reported.[18] Briefly, PGMA (100 mg) was dissolved in 5 mL of anhydrous DMSO in a 50 mL flask, followed by addition of 30 times excess of EA (1.29 g). The mixture was degassed by nitrogen for 10 min, put in an oil bath of 80 °C, and kept stirring for 1 h. Afterward, the solution was precipitated into excess diethyl ether to get a crude polymer product. The product was further dialyzed against deionized (DI) water for 2 days and freeze-dried to give pure PGEA. For the synthesis of cationic glycopolymers, both EA and Lac-NH2 were used to react with PGMA (Scheme 4-2b). Typically, PGMA (100 mg) was dissolved in 5 mL of DMSO, followed by the addition of Lac-NH2 (282 mg) and EA (172 mg) to reach a designed molar ratio of epoxy/Lac-NH2/EA to be 1:1:4. The mixture was degassed for 10 min and stirred at 40 °C overnight. The solution was further heated up to 80 °C for 1 h to complete the ring-opening reaction. Afterward, the solution was precipitated into excess diethyl ether, and the precipitate was dialyzed against DI water for 2 days. The PGMA-based cationic glycopolymer was obtained by lyophilization and named as PGEL-1. Similarly, cationic glycopolymer with higher sugar ratio, namely, PGEL-2, was obtained by changing the molar ratio of epoxy/Lac-NH2/EA to be 1:3:2

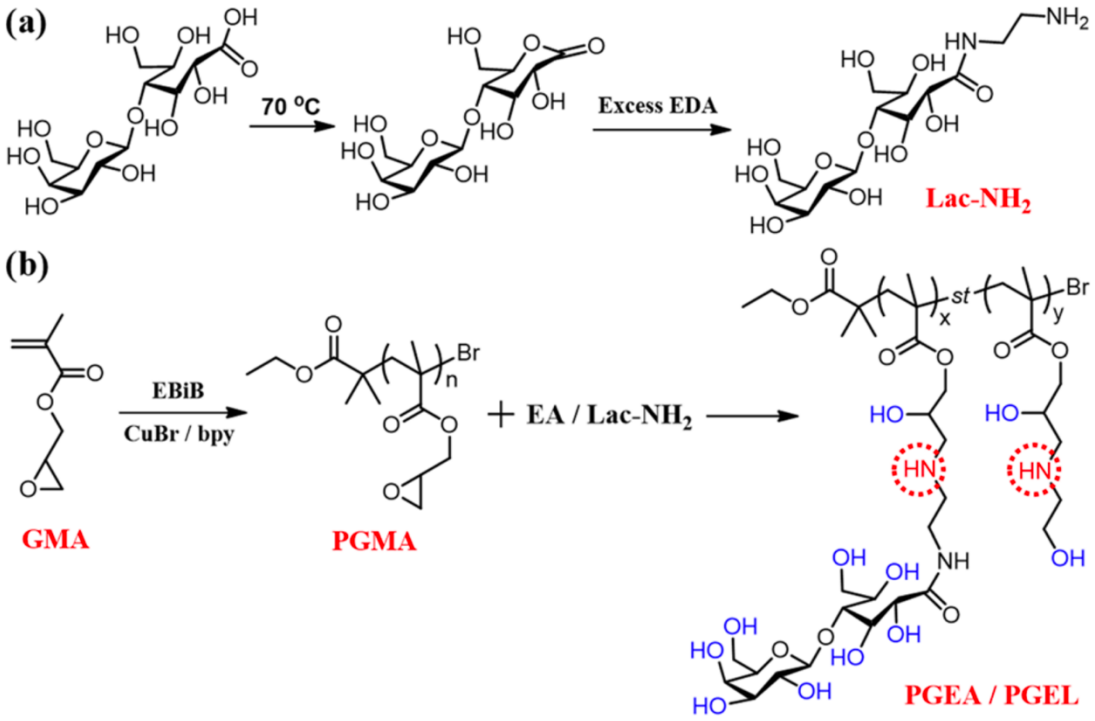

Scheme 4-2. Synthetic Routes for (a) Lac-NH2 and (b) PGMA-Based Cationic Polymers (PGEA or PGEL).

4.2.6. Preparation of Glycopolymer−siRNA Polyplexes. EGFR- siRNA/control-siRNA (0.1 mg/mL in OMEM) was complexed with the designed amount of PGEA/PGEL polymers in OMEM media. The cationic polymer/siRNA ratio was expressed as the molar N/P ratio of nitrogen (N) in PGEA/PGEL to phosphate (P) in siRNA. The mixture was incubated at room temperature for 30 min. Fluorescent-labeled polyplexes were prepared using the same method except for the incubation with FITC-labeled control-siRNA.

4.2.7. Agarose Gel Electrophoresis. The polyplexes with different N/P ratios of 1, 2, 5, and 10 were used to evaluate the ability of cationic PGEA/PGEL to condense with siRNA. The polyplexes were loaded in 1% agarose gel containing 1 μg/mL ethidium bromide in 1× Tris acetate/EDTA (TAE) buffer. The gel was run for 45 min at 130 V and illuminated with UV light, and the siRNA bands were visualized using UV transilluminator.[40]

4.2.8. Characterization of Cationic Glycopolymer−siRNA Complexes. The hydrodynamic size and charge of the cationic glycopolymer−siRNA complexes were determined using

ZetaPlus- Zeta Potential Analyzer (Brookhaven Instruments Corporation) at a scattering angle θ=90 °C. The polycation−siRNA complexes (0.16 μg of control-siRNA) were formulated at an N/P ratio of 40 in a mixture of water and OMEM media (in total 5% FBS). The size of the polyplexes was evaluated in the presence of serum proteins in OMEM. The net charge of the polyplexes was determined in deionized water.

4.2.9. Cell Culture. HeLa cells (cervical cancer) were cultured in DMEM medium containing 10% FBS and 1% antibiotic (50 units of penicillin, 50 μg of streptomycin) in a humidified atmosphere at 37°C and 5% CO2. At about 80% confluency, the cells were subcultured by detaching with 0.25% trypsin−EDTA, twice per week.[25]

4.2.10. Cytotoxicity of the Polycations and Polyplexes After Transfection. 10000 HeLa cells per well were seeded in 96-well tissue culture plates in duplicates and were allowed to adhere overnight. The medium was then removed, and the fresh medium containing varying concentrations of polymers was added. The cells were incubated for 48 h with the polymers. Metabolic activity assay (MTT) was performed to determine the inherent toxicity of the cationic polymers in HeLa cells by staining with dimethyl thiazol dyes for metabolically viable cells. The plate was read at 570 nm using TECAN. IC50 values were calculated with GraphPad Prism software.[28]Cytotoxicity after transfection was done by incubating the cells with polyplexes at an N/P ratio of 40 for 6 h followed by change in medium and additional 48 h of incubation.

4.2.11. Transfection of EGFR-siRNA. To determine the expression of the EGFR gene, HeLa cells were cultured in 60 mm plates (105 cells/well) and incubated for 24 h prior to polyplex exposure. Polyplexes (0.25 μg of EGFR-siRNA/control-siRNA) with an N/P ratio of 40 were prepared immediately before transfection. As positive control, polyplexes formed with Lipofectamine 2000 (1:1 w/w) were prepared. After incubation with the polyplexes for 6 h, the medium was replaced with 2 mL of DMEM containing 10% FBS. After 48 h, the cells were washed with 500 μL of phosphate-buffered saline (PBS) and treated with lysis buffer.

4.2.12. EGFR Knockdown Western Blot Evaluation. Protein lysates were harvested using the radioimmunoprecipitation assay buffer (RiPa) supplemented with protease inhibitor,

and the protein concentrations were determined using a Bradford protein assay kit (Bio-Rad). Lysates were resolved on a sodium dodecyl sulfate polyacrylamide gel electrophoresis denaturing gel and transferred to a nitrocellulose membrane (0.45 μm). Membranes were blocked in 5% nonfat milk containing 0.1% Tween 20 (TBS-T) for 1 h at room temperature and incubated overnight with EGFR-1005 sc-03 antibody (Santa Cruz) at 4 °C. Secondary antibodies coupled to horseradish peroxidase were visualized using streptavidin horse radish peroxidase (HRP) antirabbit conjugate. The amount ofEGFR protein expression was quantified using ImageJ image software analysis.[40]

4.2.12. Cellular Uptake of Polyplexes. HeLa cells (1×10^5) were seeded in 35 mm tissue culture plates containing sterilized 18×18 cm^2 glass coverslips. The cells were allowed to grow overnight, and the medium was removed and replaced with FITC-labeled control-siRNA polyplexes at an N/P ratio of 40 in OMEM and subsequently incubated for 6 h. Then, the cells were washed three times with 1 × PBS, fixed in 4% paraformaldehyde for 15 min at 37 °C, and washed again three times with 1 × PBS. The fixed cells were stained with DAPI (1:10 000 dilution in PBS) for 60 min, and the cell membrane was stained with WGA-rhodamine dye before mounting them on glass slides. The prepared slides were kept at 4 °C until imaged. Images were obtained with a Plan-Apochromat 40×/1.3 Oil DIC lens on a Zeiss 710 confocal microscope using Zen 2011 software.

4.3 RESULTS AND DISCUSSION

4.3.1. Synthesis and Characterization of Lac-NH2. Ethanolamine has been widely used for the synthesis of hydroxyl-rich PGEA polymers for condensation with DNA or RNA. In this study, we proposed to use amino-functionalized saccharide to create novel cationic PGMA-based glycopolymers containing large number of hydroxyl groups for gene delivery. Lactobionic acid based glycopolymers have been extensively studied by our group for many biomedical applications including gene/drug delivery vehicles[24−26,41,42] and hydrogels.[35,43] Moreover, lactobionic acid functionalized nanosystems have been widely accepted to exhibit hepatoma-targeting capability due to the specific recognition with asialoglycoprotein receptor (ASGPR).[44] Therefore, here we introduced amino-functionalized lactobionic acid Lac-NH2 by the reaction between EDA and lactobionic

lactone. As shown in the ^{1}H NMR spectrum in Figure 4S1, all typical peaks for sugar and aminoethyl groups can be clearly observed. The ratio between sugar protons and aminoethyl protons were calculated and found to be close to that in its chemical structure, which confirmed the successful synthesis of Lac-NH2.

4.3.2. Synthesis and Characterization of PGMA-Based Cationic Polymers. PGMA with a targeted degree of polymerization (DP) of 60 was synthesized by ATRP using EBiB as an initiator. For the polymerization of PGMA, both RAFT and ATRP can be used. We chose to use ATRP as described by Xu, *et. al*[17–20,46] for gene delivery applications.The chemical structure of PGMA was evaluated by ^{1}H NMR as shown in Figure 4S2. The typical peaks (δ 2.63, 2.85, and 3.24 ppm) for the epoxy ring of PGMA can be clearly observed. The DP of GMA was determined to be around 40 by comparing the peak integral of epoxy ring with that of EBiB. The molecular weight (Mn) and polydispersity index were further measured by GPC (Figure 4S3) using polystyrene as a standard to be 18.2 kDa and 1.28, respectively. Ethanolamine and Lac-NH2 of different feed ratios were then applied to react with epoxy groups of PGMA to obtain cationic polymers with different sugar content. The detailed information of these three polymers is summarized in Table 4-1. The chemical structure of these three polymers are confirmed by 1H NMR in Figure 4-1. The spectrum of PGEA with 0% sugar decoration was consistent with previous studies.[18] With increasing Lac-NH2 feed ratio, higher sugar residues were observed in the spectrum. The sugar content of PGEL-1 and PGEL-2 was calculated to be 9 and 33%, respectively. The molecular weights (Mn) of these three hydrophilic polymers were further determined by aqueous GPC using pullulan as a standard to be 16.8, 17.5, and 17.9 kDa, respectively, with a similar PDI of ∼1.5. The Mn values of these derived polymers were found to be lower than that of the starting PGMA, which can be explained by the different mobile phases and different standards used for the measurement of these polymers as GPC gives relative Mn values to the standards. The number of hydroxyl groups per polymer chain was calculated to be 80, 105.2, and 172.4 for PGEA, PGEL-1, and PGEL-2, respectively.

Table 4-1. Summary of Synthetic Conditions, Molecular Weights, and Chemical Composition Determined for PGMA-Based Cationic Glycopolymers with Different Sugar-Grafting Ratios, Determined by GPC and ^{1}H NMR.

	feed ratio epoxy/Lac-NH_2/EA	M_n (GPC; g/mol)	M_w (GPC; g/mol)	PDI (GPC)	Lac mol % (^{1}H NMR)	number of −OH groups per chain
PGEA	1:0:30	16.8k	25.6k	1.52	0%	80
PGEL-1	1:1:4	17.5k	25.3k	1.44	9%	105.2
PGEL-2	1:3:2	17.9k	25.9k	1.44	33%	172.4

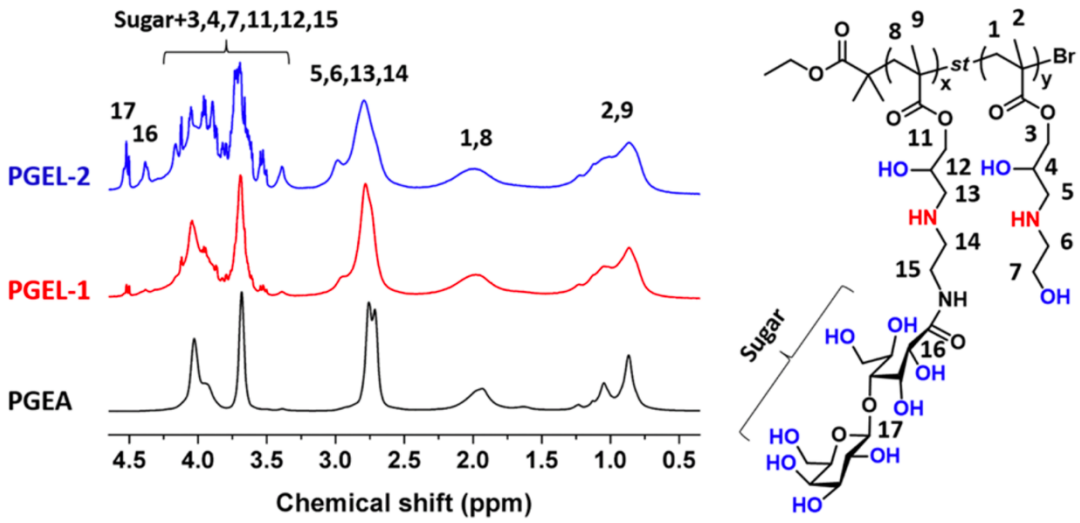

Figure 4-1. 1H NMR spectra of cationic polymers with different sugar compositions.

hydroxyl groups per polymer chain was calculated to be 80, 105.2, and 172.4 for PGEA, PGEL-1, and PGEL-2, respectively.

4.3.3 Characterization of Polycation/siRNA Complexes by Electrophoretic Mobility Assay. The successful condensation of siRNA by the cationic polymers is required for effective gene delivery systems. The capability of hydroxyl-rich PGEA and PGEL vectors to condense siRNA was confirmed by agarose gel electrophoresis. Figure 4-2 shows the gel retardation results of the various polycation/siRNA complexes with increasing N/P ratios of 1, 2, 5, and 10 in comparison to uncomplexed siRNA. PGEA, PGEL-1, and PGEL-2 exhibited similar condensation capabilities, with siRNA completely condensed at the N/P ratio of 5 and above

4.3.4. Hydrodynamic Size and ζ-Potential of Polyplexes. The size and charge of these polyplexes (N/P ratio = 40) were measured by dynamic light scattering and ζ-potential at room temperature. As shown in Figures 4-3 and 4S4, smaller size and lower ζ-potential values were found for polyplexes formed by polycations with higher hydroxyl amount, i.e., polymers with higher sugar content. For example, the hydrodynamic size and ζ-potential for PGEA/siRNA complex were 81.1 ± 22.9 nm (PDI = 0.302) and 19.73 ± 0.84 mV, respectively. However, in the case of polyplexes based on PGEL-2, which have 2 times more hydroxyl groups than PGEA, the numbers were correspondingly decreased to be only 43.3 ± 7.0 nm (PDI = 0.274) and 3.36 ± 0.68 mV, respectively. We believe that this phenomenon should be ascribed to the more compact condensation, as well as some extent of charge shielding induced by the large number of hydroxyl groups in sugar-rich polycations.

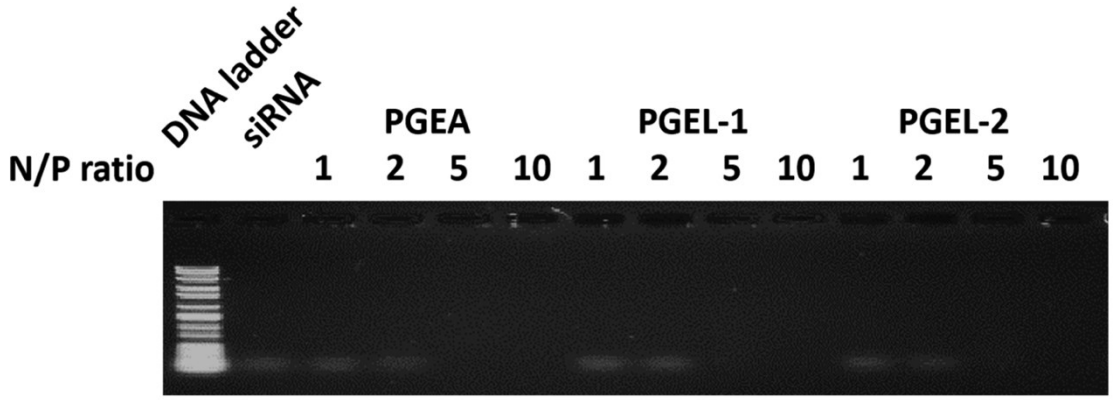

Figure 4-2. Electrophoretic mobility ofsiRNA polyplexes of the cationic PGEA and PGEL polymers with different sugar compositions.

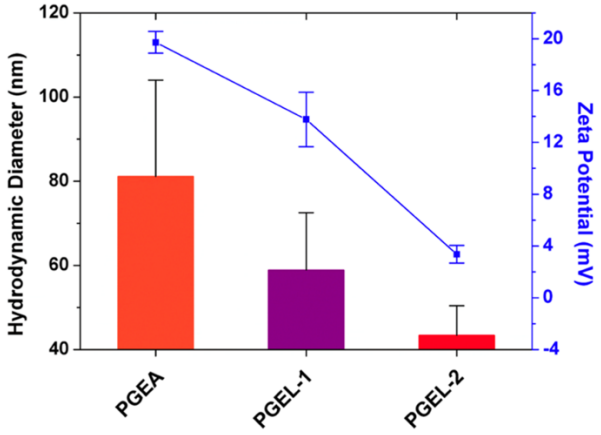

Figure 4-3. Hydrodynamic diameter and ζ-potential of the polycation/ siRNA complexes (0.16 μg of siRNA, N/P ratio = 40) measured at room temperature.

4.3.5. Cell Viability Assay. Glycopolymers, which can be obtained from natural sugar molecules, are usually considered as biocompatible materials.[45] The cytotoxicity of cationic glycopolymers, as shown in our previous studies, are highly related to polymer composition, architecture, molecular weight, and charge distribution.[21] In this study, we designed and synthesized PGMA-based cationic glycopolymers, which have different architecture and charge distribution manner with those reported previously in our and others' laboratories.[25,30] Therefore, MTT assay was carried out for PGEA and PGEL polymers in HeLa cells before conducting gene transfection studies. As shown in Figure 4S5, the three polycations exhibited concentration-dependent cytotoxicity after 48 h of incubation. Polymer with a higher sugar decoration degree (more hydroxyl groups) exhibited higher biocompatibility: PGEL-2 > PGEL-1 > PGEA. The IC_{50} values of the three polymers were determined to be 230.9, 48.04, and 18.42 μg/mL, respectively. The IC_{50} values based on residual amine concentration were then accordingly calculated to be 7.33×10^{-7}, 2.06×10^{-7}, and 9.07×10^{-8} mol/mL. The IC_{50} value of PGEL-2 was about 1 order of magnitude higher than that of PGEA, indicating significant enhancement of biocompatibility via conjugation of sugar molecules.

4.3.6. In Vitro Gene Transfection Efficiency and Cytotoxicity After Transfection. The charge and size of the polyplexes facilitate the permeation of the nanoparticles across the extracellular barriers, their uptake by cancer cells, and the suppression of cancer genes by

the encapsulated siRNA. After transfection, the cells expressing the target protein can be easily distinguished by evaluating the differences in protein expression by Western blot. The in vitro gene transfection efficiency of the polyplexes was assessed using EGFR protein quantification in HeLa cell line (Figure 4S6). Figure 4-4a shows the relative percentage of EGFR expression mediated by the PGMA-based vectors at an N/P ratio of 40 in the presence of 10% FBS. The N/P character of a polymer/ nucleic acid complex can influence many properties such as its net surface charge, size, and stability. At high N/P ratios, especially ones well above the point required to form charge- neutralized complexes with siRNA (in this case, N/P = 5), enhancement in in vitro gene expression is typically observed as a result of free cationic polymer, which enhances intracellular delivery, that is why we chose a higher N/P ratio of 40 for transfection experiments. We compared the gene expression of the cells transfected with our polyplexes to Lipofectamine 2000 at the w/w ratio of 1. Although Lipofectamine 2000 exhibited lower EGFR expression (∼32%) than PGMA-based polycation/siRNA complexes, the severe off-target silencing can be a serious problem for practical application. By contrast, PGEA showed similar EGFR expression level (∼34%) but with much less off-target silencing. The effective gene transfection capability of PGEA in this study was consistent with previous reports.[18,46] For the sugar-decorated polycations, PGEL-1 and PGEL-2, higher EGFR expression levels of ∼48% and ∼61% were observed, respectively. The less effective EGFR knockdown efficiency of polycation with higher sugar decoration degree could be induced by the lower surface charge as demonstrated above. Nevertheless, both PGEL-1 and PGEL-2 showed negligible off- target silencing. It is also worth mentioning here that the gene transfection experiments in this study were conducted using HeLa cell line, which may not show specificity to lactobionic acid residues in sugar-decorated polyplexes. Gene delivery to ASGPR-overexpressing HepG2 cell line by these sugar- decorated polycations will be conducted in the future and compared with the present work to investigate the importance of the specific cell−sugar recognition. Ideal gene delivery vectors should combine high gene expression/knockdown and excellent biocompatibility. The cytotoxicity after transfection is shown in Figure 4-4b. Lipofectamine 2000, similar to our previous studies,[28,40] showed high cytotoxicity to HeLa cells. In comparison, the hydroxyl-rich PGMA-based

polycations revealed a much better biocompatibility and polycations with higher number of hydroxyl groups revealed to be less toxic as shown by the polymer cytotoxicity data above. Therefore, considering both the biocompatibility and gene transfection efficiency observed, we believe that PGEL-1 can have great potential to serve as a safe and effective gene delivery vector to treat cervical carcinoma.

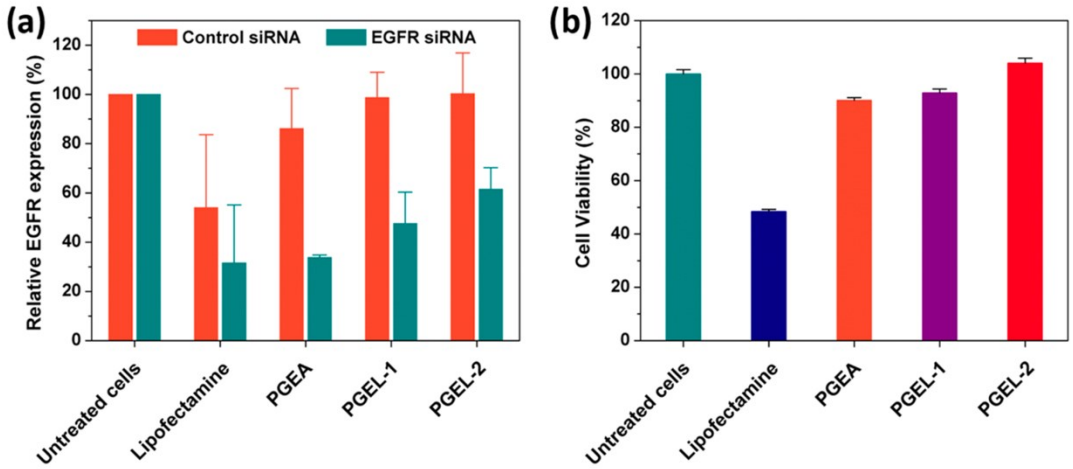

Figure 4-4. (a) Relative percentage ofEGFR expression as determined by Western blot analysis quantification with ImageJ. (b) Cell viability of HeLa cells after transfection.

4.3.7. Cellular Uptake of PGMA-Based Glycopolymer Polyplexes. The cellular uptake of hydroxyl-rich polycation/ siRNA complexes in HeLa cells was investigated using a confocal microscope. As shown in Figure 4-5, FITC-labeled siRNA was found in the cytoplasm for all these three polyplexes. We can also see that PGEA and PGEL-1 groups showed higher FITC fluorescent intensity than PGEL-2 group, which revealed higher cellular internalization of siRNA mediated by these polyplexes. This phenomenon is in accordance with the EGFR knockdown data discussed above, which should be mainly due to the lower surface net charge of PGEL-2/siRNA complex.

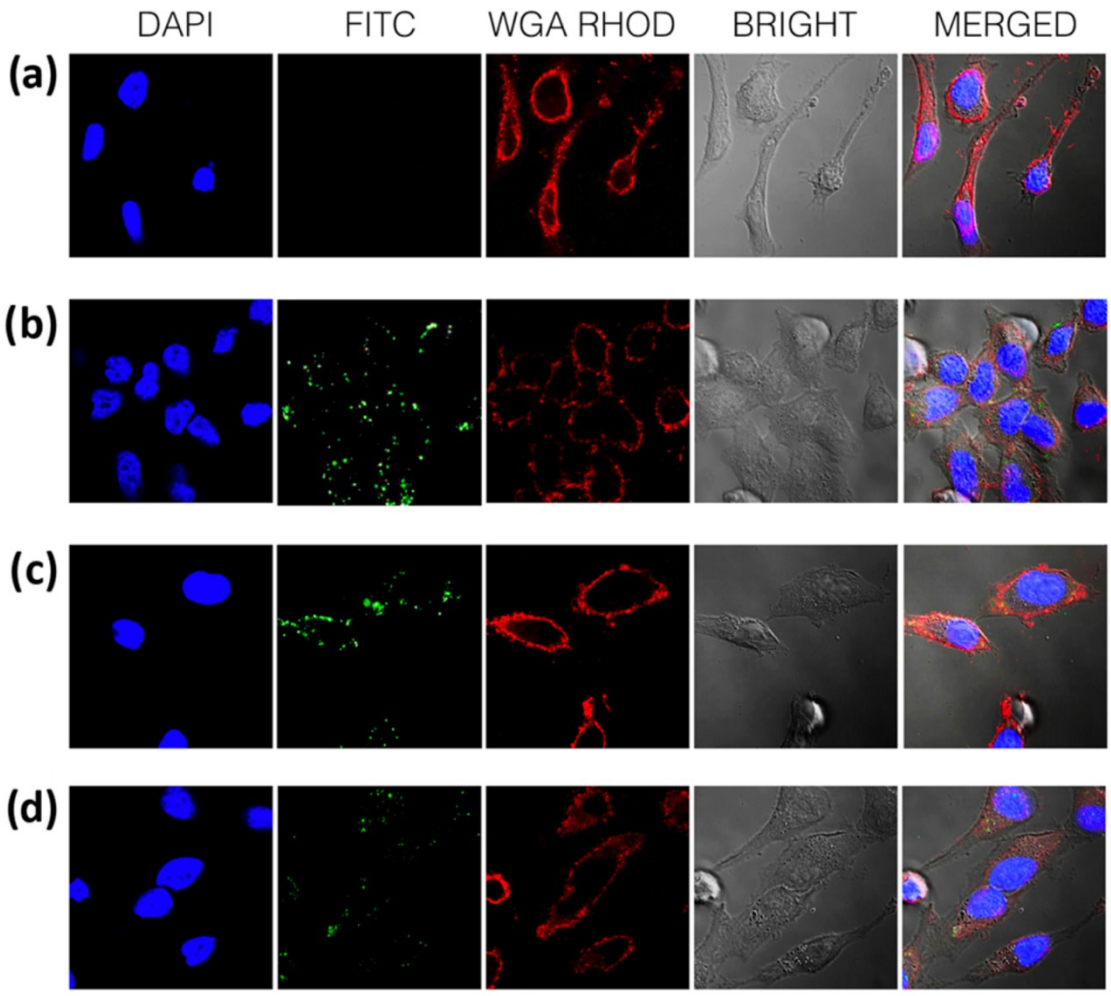

Figure 4-5. Confocal microscopy images in HeLa cells: (a) untreated cells, (b) PGEA, (c) PGEL-1, and (d) PGEL-2 after 6 h of incubation.

4.4 CONCLUSIONS

We have successfully introduced a novel approach to synthesize cationic glycopolymers based on ring-opening reaction of PGMA. The hydroxyl-rich cationic glycopolymers were explored for the use of intracellular EGFR-siRNA delivery. The biocompatibility of these glycopolymers was proved to be positively related to the sugar decoration degree. Despite the excellent capability to condense siRNA for all these polymers, the sugar decoration degree was found to be critically significant for gene knockdown efficiency. The cationic glycopolymer with the highest sugar composition (33%), however, was found to be less

effective in EGFR knockdown. Therefore, careful consideration of sugar deco- ration degree should be involved in the design of glycopolymers used as gene delivery vectors. We found that PGEL-1 with 9% sugar content should have satisfactory balance between the biocompatibility and gene transfection efficiency. Moreover, benefiting from the specific binding affinity of lactobionic acid to ASGPR, our novel PGMA-based cationic glycopolymers hold great potential for hepatocyte- selective targeting delivery of therapeutic genes in the future

4.5 REFERENCES

(1) Downward, J.; Yarden, Y.; Mayes, E.; Scrace, G.; Totty, N.; Stockwell, P.; Ullrich, A.; Schlessinger, J.; Waterfield, M. D. Close Similarity of Epidermal Growth Factor Receptor and v-erb-B Oncogene Protein Sequences. Nature **1984**, 307, 521−527.

(2) Wang, Z. ErbB Receptors and Cancer. ErbB Receptor Signaling; Springer: New York, **2017**; pp 3−35.

(3) Pagano, E.; Fontana, V.; Calvo, J. C. Expression of Erythroblastic Leukemia Viral Oncogene Homolog (erbBS) mRNAs and Possible Splice Variants in 3T3-L1 Preadipocytes. Mol. Med. Rep. **2011**, 4, 955−961.

(4) Hynes, N. E.; Lane, H. A. ERBB Receptors and Cancer: the Complexity of Targeted Inhibitors. Nat. Rev. Cancer **2005**, 5, 341− 354.

(5) Yun, U.-J.; Sung, J. Y.; Park, S.-Y.; Ye, S.-K.; Shim, J.; Lee, J.-S.; Hibi, M.; Bae, Y.-K.; Kim, Y.-N. Oncogenic Role of Rab Escort Protein 1 through EGFR and STAT3 Pathway. Cell Death Dis. **2017**, 8, No. e2621.

(6) Normanno, N.; De Luca, A.; Bianco, C.; Strizzi, L.; Mancino, M.; Maiello, M. R.; Carotenuto, A.; De Feo, G.; Caponigro, F.; Salomon, D. S. Epidermal Growth Factor Receptor (EGFR) Signaling in Cancer. Gene **2006**, 366,2−16.

(7) Lächelt, U.; Wagner, E. Nucleic Acid Therapeutics Using Polyplexes: A Journey of 50 Years (and Beyond). Chem. Rev. **2015**, 115, 11043−11078.

(8) Zaimy,M.A.; Saffarzadeh, N.;Mohammadi,A.;Pourghadamyari, H.; Izadi, P.; Sarli, A.; Moghaddam, L. K.; Paschepari, S. R.; Azizi, H.; Torkamandi, S.; Tavakkoly-Bazzaz, J. New Methods in the Diagnosis of Cancer and Gene Therapy of Cancer Based on Nanoparticles. Cancer Gene Ther. **2017**, 24, 233− 243

(9) Xu, F.-J. Versatile Types of Hydroxyl-Rich Polycationic Systems via O-Heterocyclic Ring-Opening Reactions: From Strategic Design to Nucleic Acid Delivery Applications. Prog. Polym. Sci. **2018**, 78,56− 91.

(10) Siegwart, D. J.; Whitehead, K. A.; Nuhn, L.; Sahay, G.; Cheng, H.; Jiang, S.; Ma, M.; Lytton-Jean, A.; Vegas, A.; Fenton, P.; Levins, C. G.; Love, K. T.; Lee, H.; Cortez, C.; Collins, S. P.; Li, Y. F.; Jang, J.; Querbes, W.; Zurenko, C.; Novobrantseva, T.; Langer, R.; Anderson, D. G. Combinatorial Synthesis of Chemically Diverse Core-Shell Nanoparticles for Intracellular Delivery. Proc. Natl. Acad. Sci. U.S.A. **2011**, 108, 12996.

(11) Wei, H.; Pahang, J. A.; Pun, S. H. Optimization of Brush-Like Cationic Copolymers for Nonviral Gene Delivery. Biomacromolecules **2013**, 14, 275−284.

(12) Li, Q. L.; Gu, W. X.; Gao, H.; Yang, Y. W. Self-Assembly and Applications of Poly(Glycidyl Methacrylate)s and Their Derivatives. Chem. Commun. **2014**, 50, 13201−13215.

(13) Han, X.; Chen, Q.; Lu, H.; Ma, J.; Gao, H. Probe Intracellular Trafficking of a Polymeric DNA Delivery Vehicle by Functionaliza- tion with an Aggregation-Induced Emissive Tetraphenylethene Derivative. ACS Appl. Mater. Interfaces **2015**, 7, 28494−28501.

(14) Blasco, E.; Sims, M. B.; Goldmann, A. S.; Sumerlin, B. S.; Barner-Kowollik, C. 50th Anniversary Perspective: Polymer Functionalization. Macromolecules **2017**, 50, 5215−5252.

(15) Cohen-Karni, D.; Kovaliov, M.; Li, S.; Jaffee, S.; Tomycz, N. D.; Averick, S. Fentanyl Initiated Polymers Prepared by ATRP for Targeted Delivery. Bioconjugate Chem. **2017**, 28, 1251−1259.

(16) Li, R. Q.; Wu, Y.; Zhi, Y.; Yang, X.; Li, Y.; Xua, F. J.; Du, J. PGMA-Based Star-Like Polycations with Plentiful Hydroxyl Groups Act as Highly Efficient miRNA Delivery Nanovectors for Effective Applications in Heart Diseases. Adv. Mater. **2016**, 28, 7204−7212.

(17) Hu, Y.; Li, Y.; Xu, F.-J. Versatile Functionalization of Polysaccharides via Polymer Grafts: From Design to Biomedical Applications. Acc. Chem. Res. **2017**, 50, 281−292.

(18) Sun, Y.; Hu, H.; Yu, B.; Xu, F. J. PGMA-Based Cationic Nanoparticles with Polyhydric Iodine Units for Advanced Gene Vectors. Bioconjugate Chem. **2016**, 27, 2744−2754.

(19) Sun, Y.; Hu, H.; Zhao, N.; Xia, T.; Yu, B.; Shen, C.; Xu, F. J. Multifunctional Polycationic Photosensitizer Conjugates with Rich Hydroxyl Groups for Versatile Water-Soluble Photodynamic Therapy Nanoplatforms. Biomaterials **2017**, 117,77−91.

(20) Hu, Y.; Wen, C.; Song, L.; Zhao, N.; Xu, F. J. Multifunctional Hetero-Nanostructures of Hydroxyl-Rich Polycation Wrapped Cellulose-Gold Hybrids for Combined Cancer Therapy. J. Controlled Release **2017**, 255, 154−163.

(21) Ahmed, M.; Narain, R. The Effect of Polymer Architecture, Composition, and Molecular Weight on the Properties of Glycopolymer-Based Non-Viral Gene Delivery Systems. Biomaterials **2011**, 32, 5279−5290.

(22) Ahmed, M.; Narain, R. The Effect of Molecular Weight, Compositions and Lectin Type on the Properties of Hyperbranched Glycopolymers as Non-Viral Gene Delivery Systems. Biomaterials **2012**, 33, 3990−4001.

(23) Ahmed, M.; Narain, R. Progress of RAFT Based Polymers in Gene Delivery. Prog. Polym. Sci. **2013**, 38, 767−790.

(24) Thapa, B.; Kumar, P.; Zeng, H.; Narain, R. Asialoglycoprotein Receptor-Mediated Gene Delivery to Hepatocytes Using Galactosy- lated Polymers. Biomacromolecules **2015**, 16, 3008−3020.

(25) Quan, S.; Kumar, P.; Narain, R. Cationic Galactose-Conjugated Copolymers for Epidermal Growth Factor (EGFR) Knockdown in Cervical Adenocarcinoma. ACS Biomater. Sci. Eng. **2016**, 2, 853−859.

(26) Diaz-Dussan, D.; Nakagawa, Y.; Peng, Y.-Y.; Ebara, M.; Kumar,P.; et al. Effective and Specific Gene Silencing of Epidermal Growth Factor Receptors Mediated by Conjugated Oxaborole and Galactose- Based Polymers. ACS Macro Lett. **2017**, 6, 768−774.

(27) Singhsa, P.; Diaz-Dussan, D.; Manuspiya, H.; Narain, R. Well- Defined Cationic N-[3-(Dimethylamino)propyl]methacrylamide Hy- drochloride-Based (Co)polymers for siRNA Delivery. Biomacromole- cules **2018**, 19, 209−221.

(28) Peng, Y.-Y.; Diaz-Dussan, D.; Kumar, P.; Narain, R. Acid Degradable Cationic Galactose-Based Hyperbranched Polymers as Nanotherapeutic Vehicles for Epidermal Growth Factor Receptor (EGFR) Knockdown in Cervical Carcinoma. Biomacromolecules **2018**, 19, 4052−4058.

(29) Sizovs, A.; Xue, L.; Tolstyka, Z. P.; Ingle, N. P.; Wu, Y.; Cortez, M.; Reineke, T. M. Poly(Trehalose): Sugar-Coated Nanocomplexes Promote Stabilization and Effective Polyplex-Mediated siRNA Delivery. J. Am. Chem. Soc. **2013**, 135, 15417−15424.

(30) Tolstyka, Z. P.; Phillips, H.; Cortez, M.; Wu, Y.; Ingle, N.; Bell, J. B.; Hackett, P. B.; Reineke, T. M. Trehalose-Based Block Copolycations Promote Polyplex Stabilization for Lyophilization and in Vivo pDNA Delivery. ACS Biomater. Sci. Eng. **2016**, 2,43−55.

(31) Tan, Z.; Dhande, Y. K.; Reineke, T. M. Cell Penetrating Polymers Containing Guanidinium Trigger Apoptosis in Human Hepatocellular Carcinoma Cells unless

Conjugated to a Targeting N- Acetyl-Galactosamine Block. Bioconjugate Chem. **2017**, 28, 2985− 2997.

(32) Williams, E. G. L.; Hutt, O. E.; Hinton, T. M.; Larnaudie, S. C.; Le, T.; MacDonald, J. M.; Gunatillake, P.; Thang, S. H.; Duggan, P. J. Glycosylated Reversible Addition-Fragmentation Chain Transfer Polymers with Varying Polyethylene Glycol Linkers Produce Different Short Interfering RNA Uptake, Gene Silencing, and Toxicity Profiles. Biomacromolecules **2017**, 18, 4099−4112.

(33) Zhao, L.; Li, Y.; Pei, D.; Huang, Q.; Zhang, H.; Yang, Z.; Li, F.; Shi, T. Glycopolymers/PEI Complexes as Serum-Tolerant Vectors for Enhanced Gene Delivery to Hepatocytes. Carbohydr. Polym. **2019**, 205, 167−175.

(34) Chen, Y.; Wang, W.; Wu, D.; Nagao, M.; Hall, D. G.; Thundat, T.; Narain, R. Injectable Self-Healing Zwitterionic Hydrogels Based on Dynamic Benzoxaborole−Sugar Interactions with Tunable Mechanical Properties. Biomacromolecules 2018, 19, 596−605. (35) Kotsuchibashi, Y.; Agustin, R. V. C.; Lu, J.-Y.; Hall, D. G.; Narain, R. Temperature, pH, and Glucose Responsive Gels via Simple Mixing of Boroxole- and Glyco-Based Polymers. ACS Macro Lett. **2013**, 2, 260−264.

(36) Guo, P.; Gu, W.; Chen, Q.; Lu, H.; Han, X.; Li, W.; Gao, H. Dual Functionalized Amino Poly(Glycerol Methacrylate) with Guanidine and Schiff-Base Linked Imidazole for Enhanced Gene Transfection and Minimized Cytotoxicity. J. Mater. Chem. B **2015**, 3, 6911−6918.

(37) Cerrada, M. L.; Sánchez-Chaves, M.; Ruiz, C.; Fernández- García, M. Recognition Abilities and Development of Heat-Induced Entangled Networks in Lactone-Derived Glycopolymers Obtained from Ethylene-vinyl Alcohol Copolymers. Biomacromolecules **2009**, 10, 1828−1837.

(38) Tian, M.; Han, B.; Tan, H.; You, C. Preparation and Characterization of Galactosylated Alginate-Chitosan Oligomer Microcapsule for Hepatocytes Microencapsulation. Carbohydr. Polym. **2014**, 112, 502−511.

(39) Narain, R.; Armes, S. P. Synthesis and Aqueous Solution Properties of Novel Sugar Methacrylate-Based Homopolymers and Block Copolymers. Biomacromolecules **2003**, 4, 1746−1758.

(40) Peng, Y.-Y.; Diaz-Dussan, D.; Kumar, P.; Narain, R. Tumor Microenvironment-Regulated Redox Responsive Cationic Galactose- Based Hyperbranched Polymers for siRNA Delivery. Bioconjugate Chem. **2019**, 30, 405−412.

(41) Adokoh, C. K.; Quan, S.; Hitt, M.; Darkwa, J.; Kumar, P.; Narain, R. Synthesis and Evaluation of Glycopolymeric Decorated Gold Nanoparticles Functionalized with Gold-Triphenyl Phosphine as Anti-Cancer Agents. Biomacromolecules **2014**, 15, 3802−3810.

(42) Quan, S.; Wang, Y.; Zhou, A.; Kumar, P.; Narain, R. Galactose- based Thermosensitive Nanogels for Targeted Drug Delivery of Iodoazomycin Arabinofuranoside (IAZA) for Theranostic Manage- ment of Hypoxic Hepatocellular Carcinoma. Biomacromolecules **2015**, 16, 1978−1986.

(43) Chen, Y.; Tan, Z.; Wang, W.; Peng, Y.-Y.; Narain, R. Injectable, Self-Healing, and Multi-Responsive Hydrogels via Dynamic Covalent Bond Formation between Benzoxaborole and Hydroxyl Groups. Biomacromolecules **2019**, 20, 1028−1035.

(44) Alonso,S. Exploiting the Bioengineering Versatility of Lactobionic Acid in Targeted Nanosystems and Biomaterials. J. Controlled Release **2018**, 287, 216−234.

(45) Ahmed, M.; Lai, B. F.; Kizhakkedathu, J. N.; Narain, R. Hyperbranched Glycopolymers for Blood Biocompatibility. Bioconju- gate Chem. **2012**, 23, 1050−1058.

(46) Xu, F. J.; Zhu, Y.; Chai, M. Y.; Liu, F. S. Comparison of Ethanolamine/Ethylenediamine-Functionalized Poly(Glycidyl Meth- acrylate) for Efficient Gene Delivery. Acta Biomater. **2011**, 7, 3131− 3140

CHAPTER 5. TREHALOSE-BASED POLYETHERS FOR CRYOPRESERVATION AND 3D CELL SCAFFOLDS.

The content of this chapter was published in

Journal of *Biomacromolecules*

5.1. INTRODUCTION

Anhydrobiotic organisms survive complete dehydration for several years and studies with these systems exposed to extreme environmental stresses, such as freezing and desiccation, have shown that trehalose accumulation is one of the responsible changes of this adaptative mechanism[1–4]. Trehalose, is a non-reducing disaccharide of glucose that can alter the physical properties of membrane phospholipids conserving its structural and functional integrities[5]. This sugars have been used for the bioprotection of cryopreserved samples[6–8]. Trehalose protection is related to its unique physicochemical properties, including its glass transition temperature and the interaction between the sugar and the plasma membrane, which can affect cellular osmotic responses[9]. Trehalose have shown to be an effective protein stabilizer, preventing aggregation and prolonging activity when exposed to stressors, including increased temperature, pH change, agitation, and desiccation[10]. Three mechanisms have been proposed by which trehalose guards proteins: 1) the direct interaction between trehalose molecules and proteins through hydrogen bonds (water replacement hypothesis)[11], 2) the trapping of water molecules close to protein surfaces (water-layer hypothesis)[12], and 3) the entrapment of protein conformations in high viscosity trehalose glasses (mechanical-entrapment hypothesis)[13,14]. Additionally, it also appears that trehalose is needed on both intra (permeating CPA) —and extracellular sides of the cell membrane (non-permeating CPA) to enable long-term preservation[15], but its high molecular weight limits its permeability properties. Multiple studies that confirm the effectiveness of trehalose in cryopreservation or drying of mammalian cells including, primary human hepatocyte cryopreservation[16], as well as preservation of red blood cells[9], hematopoietic cells and embryonic stem cells [17].

Use of cryoprotectants (CPA) such as dimethyl sulfoxide (DMSO)[18,19], glycerol[20] and ethylene glycol[21] has been employed over decades for the reliable long-term storage of biological samples, such as cells, tissues and organs. The cryogenic temperature —the temperature at which the biological samples are exposed— can inevitably induce ice formation and osmotic shock causing irreversible mechanical and physical damage to the cells[22]. The use of these CPAs aids in preventing cell injury, however some drawbacks are faced, such as their inherent toxicity. Adverse effects on patients after infusion of DMSO-

cryopreserved cells and induction of cell apoptosis and uncontrolled differentiation of stem cells have been reported[23–25]. Moreover, protocols for the addition and removal of CPAs can be time-consuming processes requiring several washes which can lead to elevated cell loss[26]. Synthetic polymers which mimic antifreeze proteins inspired by nature have been used as CPAs. These proteins and polysaccharides (macromolecular antifreezes) are known to restrain ice formation and growth by changing ice crystals morphologies and depressing the freezing point, the mechanisms, are still under exploration. Nonetheless, the faculty to tune and alter ice formation and growth has shown to protect cells during cryopreservation[27]. Huge advances in the synthetic polymer chemistry field, now facilitates the design of complex architectures enabling the development of manmade materials with protein-like functions. Compounds structured with poly(vinyl alcohol) (PVA)[28] and zwitterionic polymers, like 2-methacryloyloxyethyl phosphorylcholine (MPC)[29], have displayed macromolecular antifreeze properties by modulating ice formation and growth, and acting as ice recrystallization inhibiting (IRI)-polymers mimicking the complex function of antifreeze (glyco)proteins. Cell cryopreservation methods that utilize IRI agents are a promising technology since they eliminate or reduce the need for permeating cryoprotectants[30]. Moreover, organoid cultures based on 3D cell scaffolds are of great interest because they mimic living tissues[31]; in regenerative medicine, polymer scaffolds that promote cell and tissue associations and cell/scaffold integration are demanded. An integral component of the manufacture of potential artificial organs substitutes, is the cryopreservation of the whole construct. The cryopreservation of several layers of constructed cells poses a major difficulty as the models to described tissue responses to cryoinjury has not yet been elucidated, therefore designing a polymeric biocompatible scaffold like a hydrogel network, with high biocompatibility and tunable physicochemical properties, is a promising strategy to study tissue responses to freezing and thawing[23]. We previously reported the synthesis of a stimuli-responsive MPC-based hydrogel as a promising CPA and 3D cell scaffold[29]. Exceptional properties of trehalose, as mentioned earlier, shows the favorable use of this sugar for the synthesis of IRI-polymers. Trehalose glycopolymers have been investigated for their ability to stabilize proteins to heat and lyophilization stress[32] and offers a strong rationale to develop a trehalose-based hydrogel for cryopreservation and 3D cell scaffold applications, which is now described.

5.2 EXPERIMENTAL SECTION

5.2.1 Materials

Trehalose, epichlorhydrin and sodium hydroxide were purchased from Caledon Laboratories Ltd. (Georgetown, Canada) and thiazolyl blue tetrazolium bromide (MTT) was obtained from Sigma-Aldrich. Live/dead 488/570, R37601 assay was purchased from Thermo Fisher Scientific. All cell culture products, including DMEM medium, antibiotics (Streptomycin (10 mg mL^{-1}), penicillin (10 000 U mL^{-1})), fetal bovine serum (FBS), and trypsin with EDTA, were obtained from Gibco. All organic solvents, including methanol, ethyl acetate, tetrahydrofuran (THF), and dimethyl formamide (DMF), were obtained from Caledon Laboratories Ltd. (Canada).

5.2.2 Synthesis of Trehalose-epichlorohydrin (Tre-ECH) polymers.

Tre-ECH polymers were prepared as follow. In a typical procedure, 2 g of trehalose (5.84 mmol) and 0.7 g of NaOH (17.52 mmol) were dissolved in 5 ml of deionized water. The solutions were immersed in a warm water bath at 70 °C and stirred for 30 min until the solution was fully reacted (clear liquid). 1.62 g of epichlorohydrin (ECH) (17.52 mmol) was then added dropwise at the correct molar ratio (Scheme 5-1). This solution was left still for a period of time until the viscosity increased. After a minimum of 24 h, the reaction was neutralized with hydrochloric acid (HCl) and the solution was dialyzed for 48 h using a molecular membrane cut-off of 6000-8000. Once the impurities were removed, the solution was freeze dried to collect a dry powdered polymer, and the yield and properties were determined.

5.2.3 Gel permeation chromatography (GPC)

Average molecular weights and dispersity of the polymers were assessed by gel permeation chromatography (GPC) system using water columns (WAT011545) eluted at 1.0 mL/min using 0.5 M sodium acetate / 0.5 M acetic acid buffer as Eluent A. Monodisperse Pullulan standards (M_w = 5900−404 000 g mol^{-1}) were used for calibration.

5.2.4 Differential scanning calorimetry (DSC) tests. DSC analysis to assess ice formation was performed using polymer/water mixtures. 10 mg polymer samples were accurately weighted (± 0.01 mg) and transferred to a DSC-Q2000. Heat flow (W/g) was measured

and recorded against an empty pre-weighed 40 µL aluminum reference pan starting from −20 °C to 300 °C at a rate of 50 °C min^{-1}, with the presence of a large endothermic peak demonstrating ice melting.

5.2.5 Splat cooling assay for the ice recrystallization inhibition (IRI) activity.

The IRI activity of the polyethers was weighed by the splat cooling assay[33,34]. The sample (10 µL) suspended in PBS was released into an aluminum block chilled to approximately −80 °C with dry ice (2 m in height). Upon contact with the cooled block, the sample droplet instantaneously froze and created a wafer (1 cm in diameter and 20 µm thickness). The wafer was then moved to a cryo-stage maintained at −6.4 °C (Alpha Omega Instruments, Series 800 temperature controller). After annealing for 5 minutes at −6.4 °C, images of the wafer were taken between crossed-polarizing filters using a Nikon CoolPix 5000 digital camera through a microscope. The images were processed in ImageJ (imaging processing software) and ice crystals areas were calculated. The data was arranged into as has been previously described[29]. A curve was generated and the half-maximal inhibition concentration (IC_{50}) was computed using GraphPad Software, by fitting to a two-parameter sigmoidal curve.

5.2.6 Cell culture

The cell lines evaluated were PC-3 (prostate cancer), FaDu (head and neck cancer,) HeLa (cervical cancer) and skin fibroblasts (normal cell line). DMEM medium was used to grow the cells supplemented with 10% fetal bovine serum (FBS) and 1× antibiotic-antimycotic (100 units of penicillin, 100 µg streptomycin) in a humidified atmosphere at 37 °C and 5% CO_2. At about 80% confluency, the cells were sub-cultured by dissociating with 0.25% trypsin twice per week.

5.2.7 Metabolic Activity (MTT) assay

The HeLa cells (1×10^5 cells per well) were allowed to adhere overnight in 96-well tissue culture plates. After 24 h incubation the media was replaced by fresh media with assorted polymer concentrations in triplicate. The cells were grown for 24 h in the presence of the polyethers. The untreated cells were used as positive control and media alone was used as blank. The plate was incubated for 4 h after MTT solution addition (100 µL per well 1 g/L in sterilized PBS), followed by the addition of DMSO: 2-propanol lysis buffer. A

spectrophotometer was used to read the plate at 570 nm and the percent of metabolic activity was calculated by the following formula:

Eq. 5.1. Metabolic activity (%) = 100 × (treated cells – negative control) / (positive control – negative control)

5.2.8 Cryopreservation studies using the ultrarapid freezing method.

Polyether solutions from 0.5 to 10 wt % of the Tre-ECH polymers suspended in DMEM with 10% FBS for HeLa cells and 5 and 10 wt % for skin fibroblasts were evaluated. A solution of 1×10^6 cells/mL was mixed in 1 mL of each polymer solution and divided into each microtube (per 100 μL) and plunged directly into liquid nitrogen (~ −220 ˚C/min cooling rate) and stored in the freezer at −80 °C. After 24 h, the microtubes were immediately thawed by gentle shaking in a temperature controlled water bath equilibrated to 37 °C (thawing rate ~ 45 ˚C/min[35]). The cells were then mixed in a 1:1 ratio of cell suspension:trypan blue and counted using a hemocytometer. The ratio of membrane-compromised cells to the total number was determined to calculate the membrane integrity. All the experiments were done in triplicates.

The membrane integrity was estimated by the following formula:

Eq. 5.2. Membrane Integrity (%) = 100 × (number of intact cells) / (number of intact cells + number of damaged cells)

The cells were counted pre- and post-thawing to calculate the percentage of cell recovery after thawing. For this assay, as mentioned above, PC3 cells were cryopreserved by the ultra-rapid freezing method at 5 and 10 wt% polymer solutions. Post-thaw cell recovery and Platting efficiency post-thawing after 24 h of incubation were computed by the following formulas:

Eq. 5.3. Post-thawing cell recovery (%) = 100 × (post-thaw cell count)/ (pre-thaw cell count)

Eq. 5.4. Platting efficiency (%) = 100 × (cell count after 24 h of incubation)/ (post-thaw cell count)

5.2.9 Cryopreservation studies using temperature controlled freezing method.

Cryopreservation studies using the temperature controlled freezing method were done as previously described[29]. A solution of 3 wt% of poly(Tre-ECH) polymers **S1, S2** and **S3** and 1 × 10^6 cells/mL suspension (PC3) in freezing medium (DMEM + 10% DMSO)/0.5 M trehalose and DMEM + 3 wt% polymer solution in the absence or presence of 0.5 M trehalose (room temperature incubation) were slowly added to the freezing medium. A precooled (−12 °C) electronic controlled-rate freezer (VIA Freeze™ Research, GE Healthcare Life Sciences) was used and the samples were held in this freezer for 15 min before they were touch by pre-cooled forceps to induce ice nucleation. This technique ensured controlled nucleation at the same temperature (−12 °C) in each vial. All cryotubes were maintained at −12 °C for 15 min before cooling to −80 °C at a rate of 1 °C/min, and then transferred and stored in the freezer at −80 °C overnight. For thawing, the cryovials were rapidly thawed in a water bath at 37 °C (thawing rate ~ 45 ˚C/min[35]). Pre-warmed DMEM + 10% FBS was used to resuspend the cells and they were collected by centrifugation (200 × g for 5 min). The supernatant was then removed, and the cells were resuspended in warm DMEM + 10% FBS media. The proliferation rate and metabolic activity was evaluated after the cells were cultured for 24 h in the conditions described above.

5.2.10 Cellular Uptake of the Trehalose based polymers.

The polymers were labeled fluorescently with FITC by activating hydroxyl groups on carbohydrate moieties. In brief, the polyethers were dispersed in 4% $NaHCO_3$ in deionized water and calibrated to pH 8.5 to make 5 mg/mL solution. FITC was dissolved in DMSO to make 1 mg/mL solution. FITC-DMSO was added to the aqueous polyethers solution dropwise and stirred for 5 days under dark conditions. The FITC-labeled polyether solution was dialyzed to remove free FITC. The fluorescent polymers were freeze-dried and obtained as a yellow (FITC) powder[36]. For the cellular uptake procedure HeLa cells were seeded (1 × 10^6 cells/plate) were seeded onto a glass coverslip in tissue culture plates and allowed to adhere overnight. The media was then removed and replaced with 1 mg/mL of FITC-labeled polymer in DMEM with 10% FBS media and the cells were exposed to -80 °C overnight according to the rapid cryopreservation method described above. Following thawing of the cells, the plates were rapidly thawed in a water bath at 37 °C,

followed by three washes with PBS and fixed with 4% paraformaldehyde for 15 min at 37 °C. The cells were stained with 4',6-diamidino-2-phenylindole (DAPI) for cell nucleus, wheat germ agglutinin (WGA) Rhodamine for cellular membrane and were imaged using Zeiss AxioObserver (inverted) Confocal Microscope.

5.2.11 3D Cell Scaffold evaluation

The polyethers were dissolved in DMEM media containing antibiotics and glutamine. The hydrogels were created at a 15 w/w% concentration by resuspending PC3 cells ($1x10^5$ cells/mL) in a Poly(Tre-ECH) solution at 37 °C. The cell/hydrogel constructs were incubated for 24 h, in a humidified atmosphere incubator containing 5% CO_2. Membrane integrity was assessed using a commercial Live/Dead assay. The live cell component emits green fluorescence in live cells and the cells with compromised membranes (dead cells) emit a red fluorescence. Exposure of cells to 70% ethanol was used as a dead control and the untreated cells were used as a live control. The cells were incubated for 15 min at room temperature (22 °C) with 2x stock solution of LIVE/DEAD® Cell Imaging Kit 488/570, ThermoFisher R37601 (300 μL). Cells were imaged by confocal microscopy. Imaris Image Analysis software was used for quantification and imaging processing.

5.2.12 Stadistics. All statistical analysis was performed using GraphPad Prism 7 software. All experiments were performed in triplicates. *P* values were calculated using 1-way ANOVA, t-TEST. $*P < 0.05$ was considered significant, and $***P < 0.0001$ was considered highly significant.

5.3 RESULTS AND DISCUSSION

5.3.1 Synthesis of Trehalose-based hydrogels.

The trehalose-epichlorhydrin polymers (Tre-ECH) were synthesized as per the protocol for the synthesis of Ficoll[37], a sucrose-epichlorhydrin polyether, with some modifications (Scheme 5-1). In order to achieve water soluble, highly branched polyethers, a preliminary study was initially carried out with different ratios of ECH and NaOH to trehalose. Once the most appropriate conditions were identified, three different Tre-ECH polymers were synthesized as shown in Table 5-1. The molecular weights of the Poly(Tre-ECH) were determined by gel permeation chromatography. The polymers were labelled as **S1**, **S2** and

S3. **S1** had the highest molecular weight (M_n = 14,900 Da, M_w/M_n = 7.33) and high dispersity due to its highly branched nature, **S2** had the lowest molecular weight (M_n = 5,900 Da, M_w/M_n = 1.48), and **S3** had similar M_n as **S1** (M_n = 14,600 Da, M_w/M_n = 3.06) but slightly lower dispersity.

Table 5-1. Characterization of the Poly(Tre-ECH) polymers.

Sample	mol Ech/Tre	mol NaOH/Tre	M_w (g/mol)	M_n (g/mol)	M_w/M_n
S1	3	3.5	109,200	14,900	7.33
S2	3	4.5	8,700	5,900	1.48
S3	3	3	44,700	14,600	3.06

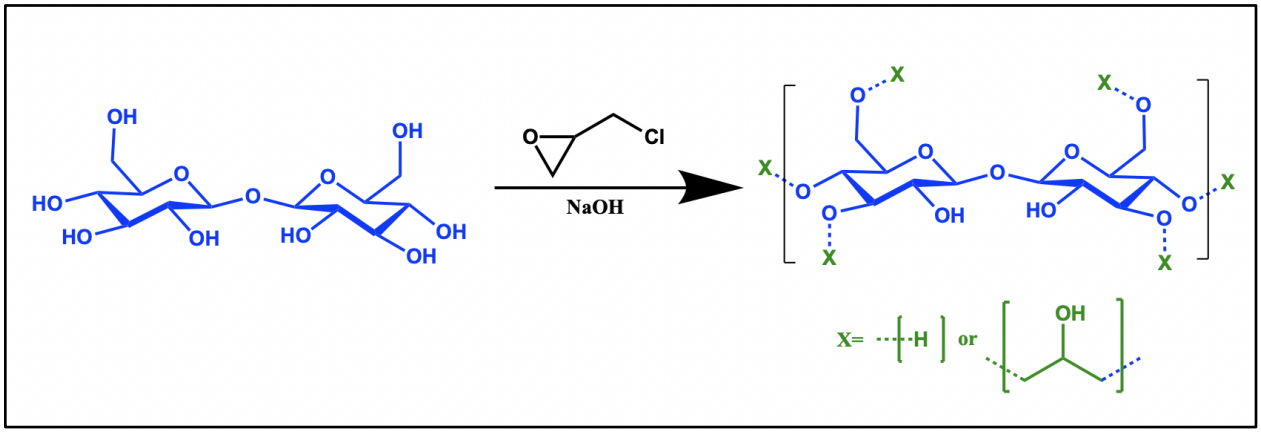

Scheme 5-1. Synthesis of the trehalose-based polymers. Poly (Tre-ECH).

5.3.2 DSC Analysis

Hydrophilicity of the trehalose-based hydrogels and its influence on ice formation was studied using DSC and compared with pure trehalose samples as shown in Figure 5S1. All the samples showed an endothermic peak due to the melting of the solute-water system. Among the three samples, **S1** (Figure 5S1a) showed the smallest melting peak in comparison to the other two polymers (Figure 5S1b-c) and comparable to the pure trehalose sample (Figure 5S1d). This indicates the strongest inhibition of **S1** to water crystallization[23].

5.3.3 Ice recrystallization inhibition (IRI) activity.

The IRI activity of the trehalose-based polymers was calculated using the splat cooling assay with PBS as a control for ice recrystallization[34]. The splat cooling IRI assay is widely used to probe recrystallization, which involves the formation of a polynucleated ice wafer by dropping a buffered solution containing the inhibitor onto a pre-cooled surface[27]. The ice crystals are then annealed at a sub-zero temperature, above the eutectic phase transition, and the growth of the ice crystals monitored. As demonstrated in Figure 5-1, the IC_{50} of the polymer **S1** was the highest (17 mg/mL) while both **S2** and **S3** showed an IC_{50} of 14 mg/mL. These results confirmed that these Poly(Tre-ECH) polymers are active IRIs.

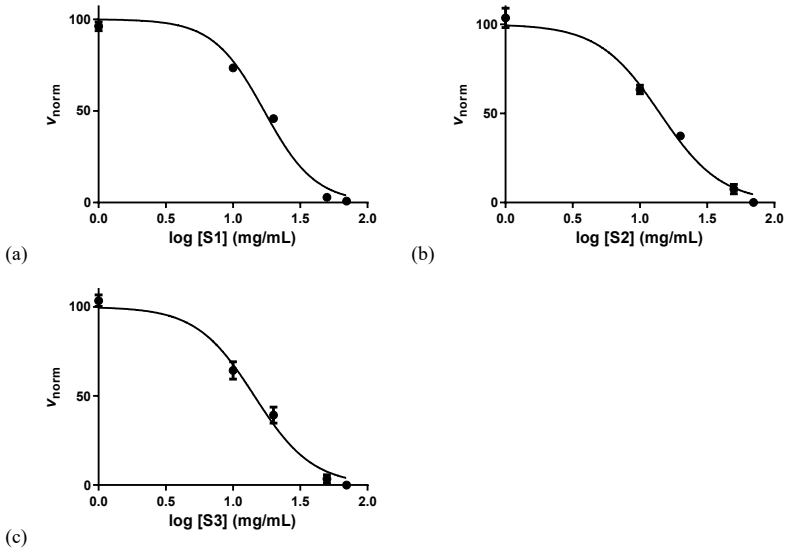

Figure 5-1. Dose-response curves for the IRI activity of (a) **S1** (IC_{50} = 17 mg/mL, R^2= 0.99)**,** (b) **S2** (IC_{50} = 14 mg/mL, R_2 = 0.99), and (c) **S3** (IC_{50} = 14 mg/mL, R_2 = 0.99).

5.3.4 Cell viability studies

The toxicity of current CPAs like DMSO presents a major challenge for its use in biomedical applications. Some cell damage has been seen on the cell membrane, enzymes and mitochondrial function, as well as cell development and proliferation[38]. Metabolic analysis of the cells to evaluate the biocompatibility of Poly(Tre-ECH) polymers was done by a MTT assay using HeLa cells (Figure 5S2). The cells were incubated for 24 h at 37 °C

in a polymer solution up to 100 mg/mL (Figure 5S2). The metabolic activities were close to 60% of the controls at the highest concentration (100 mg/mL) indicating partial maintenance of normal metabolic pathways even at high concentrations suggesting favorable biocompatibility of these trehalose-based polymers.

5.3.5 Cryopreservation studies

Cryoprotective efficacy of Poly(Tre-ECH) polymers was evaluated in HeLa cervical cancer, PC3 prostate cancer and skin fibroblast (normal cell line). To confirm that Poly(Tre-ECH) could afford rapid crioprotection, we compared the post-thaw membrane integrity of the Poly(Tre-ECH) polymers, DMSO (10 wt% + pure trehalose (10 wt%) and conventional cryopreservation conditions ~10 wt% DMSO in cell media with the ultra-rapid freezing protocol (Fig. 5-2). Trehalose (10 wt%) + DMSO (10 wt%) was selected as the control because without pretreatment trehalose is impermeable to the cell membrane and its cryoprotective effect is known to be strongly dependent on the incubation time[39]. As expected, samples with trehalose (10 wt%) + DMSO 10 wt% exhibited much lower membrane integrities as compared with the Tre-ECH polymer samples.

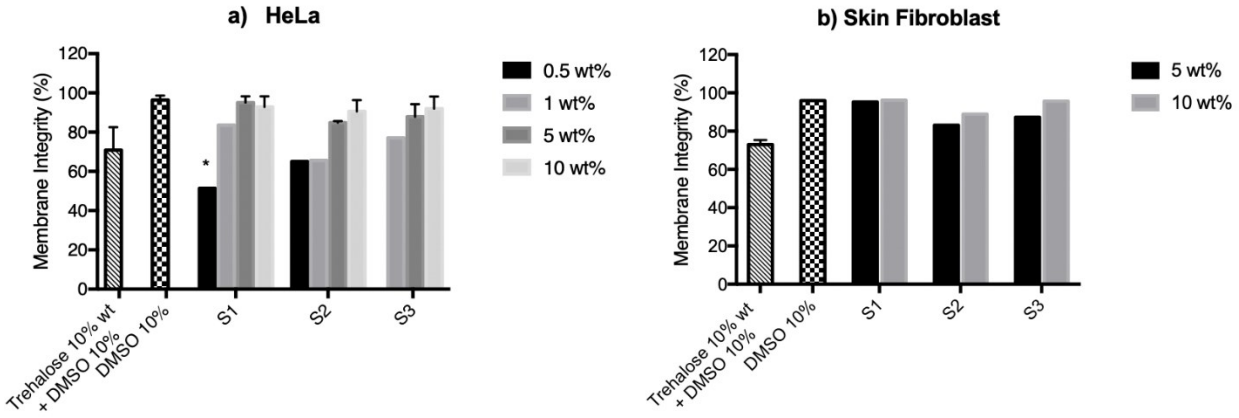

Figure 5-2. Rapid cryoprotection of Poly(Tre-ECH) Polymers. (a) Post-thaw membrane integrity of HeLa cells after incubation in media containing different polymer concentrations (0.5%, 1%, 5% and 10 wt%). Post-thaw survival efficiency of (b) Skin fibroblast cells with different polymer concentrations in media containing 5% and 10 wt%. Trehalose (10 wt%) + 10% DMSO and only 10% DMSO were used as controls with the

ultra-rapid freezing protocol. Value = mean ± standard deviation, n = 3, *P < 0.05 (One-way ANOVA).

5.3.6 Effect of trehalose-based polymers on freeze-thawing skin fibroblast cells with the controlled-freezing method.

To demonstrate the use of trehalose polyethers as CPAs, we tested the survival and function of skin fibroblasts treated with 5 wt% and 10 wt% Poly(Tre-ECH). Subsequently, cells were consigned on the controlled-rate freezer and incubated for 15 min at −12 °C before ice nucleation, and then further cooled to −80°C. Ice seeding (ice nucleation and growth) at a high subzero temperature during cooling can release the free energy that drives ice recrystallization (IR) during warming, which prevents the IR-induced cell injury[26]. Cells were thawed and counted after 24 h storage at −80 °C. High post-thaw cell recovery (Fig. 5-3a), as well as high post-thaw cell membrane integrities (Fig. 5-3b) were observed with the higher molecular weight polymers **S1** and **S3**.

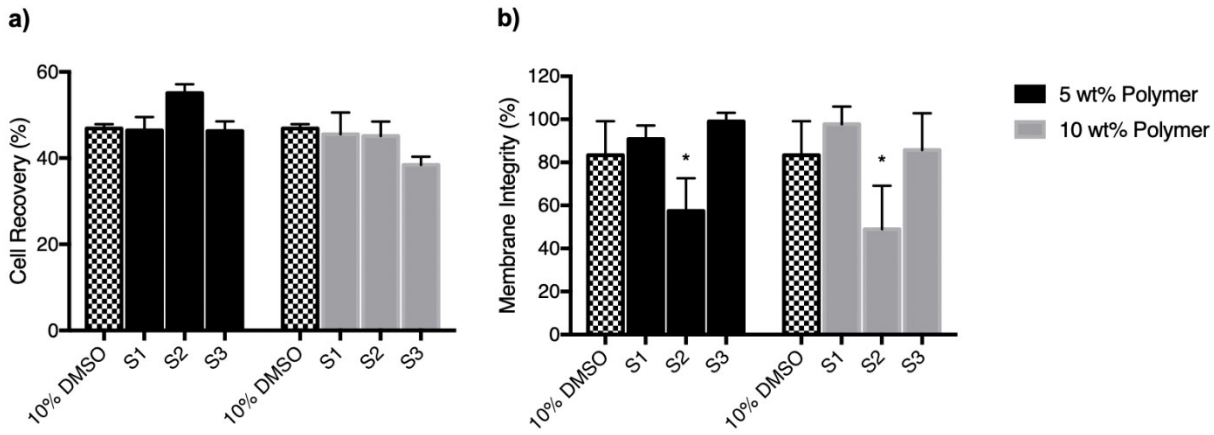

Figure 5-3. Cell recovery and membrane integrity test of Skin Fibroblast after controlled-freezing cryopreservation. (a) Post-thaw cell recovery of cryopreserved fibroblast for 24 h in **S1**, **S2** and **S3** polymer solutions at 5 wt% and 10 wt% and a solution of DMEM+10% DMSO+10% FBS as control. (b) Post-thaw cell membrane integrity of cryopreserved fibroblast for 24 h in **S1**, **S2** and **S3** polymer solutions at 5 wt% and 10 wt% and a solution of DMEM+10% DMSO+10% FBS as control. Value = mean ± standard deviation, n = 3, *P < 0.05 (One-way ANOVA).

5.3.7 Effect of trehalose predehydration and trehalose polyethers on freeze-thawing PC3 cells with the controlled-freezing method.

We wanted to explore the effects of delayed onset cryoinjury, typically observed within 6 to 24 h after thawing, and the effect of the addition of 0.5 M trehalose to the cryopreservation protocol. Predehydration of cells by extracellular trehalose at a nonfreezing temperature to their minimal volume with minimized osmotically active water can protect the cells from being injured by osmotic shock and intracellular ice formation (IIF) during ice seeding[26]. Due to the cells being slowly frozen (using a gradient of 1 °C /min) this eliminates critical supercooling due to cell dehydration making intracellular freezing not the main source of cryoinjury. As cryoprotectants affect the volume of ice crystals, they influence the direct damage of cell membranes and the viability of the frozen/ thawed cells. The trehalose-based polymers have exhibited macromolecular antifreeze properties by acting as ice recrystallization inhibiting (IRI)-polymers mimicking the function of antifreeze (glyco)proteins, without necessarily mimicking their chemical structure. The results from these experiments confirmed that Poly(Tre-ECH) **S1** and **S3** polymers, as well as DMSO offered the best cryoprotectant capabilities in combination with 0.5 M trehalose. Previous studies have shown that compounds like dimethyl sulfoxide and trehalose affect the thermodynamics of the freezing process. Crystal sizes in frozen 10% (w/w) DMSO solution (with or without trehalose) have exhibit ten times smaller sizes than ice in frozen water. Trehalose, on the other hand due to its high inter-molecular interaction potential can easily form cluster structures which can contain also glass phase and impact neighbouring water molecules, supporting the aggregation of crystals in the frozen samples. Thus, it has been stated that trehalose probably acts as a natural osmolyte (osmoprotectant), which then stabilizes phospholipid membranes and the tertiary structure of proteins[39]. We showed (DSC) that the presence of the trehalose polymers in the solution leads to changes in freezing process. In all studied polymer solutions, the melting/ freezing points were shifted to lower values (compared to deionized (pure) water/ice). These results correlate with the cryopreserved cell viability in PC3 cells where high post-thaw membrane integrity (over 70%) with the S3 + 0.5 M trehalose polymer was seen, similar to the DMSO + 0.5 M trehalose control (Fig. 5-4a). Higher cell recovery was also observed with more than 60% recovery both in the absence and presence of trehalose (Fig. 5-4b). After 24 h of

incubation, the membrane integrity of the cells cryopreserved with S3 + 0.5 M trehalose was close to 70% as seen with the DMSO + 0.5 M trehalose control (Fig. 5-5a). Perhaps the two most important criteria for cell cryopreservation are; cryosurvival and retention of normal cell processes. The latter is thought to be particularly important for both research and therapeutic applications [40]. Here, the degree of cell division after 24 h of incubation was also evaluated from the remaining viable cells and the results demonstrated that the trehalose-based polymers are equally potent at lower concentrations (3 wt%) and do not exhibit any cell cycle inhibition (Fig. 5-5b).

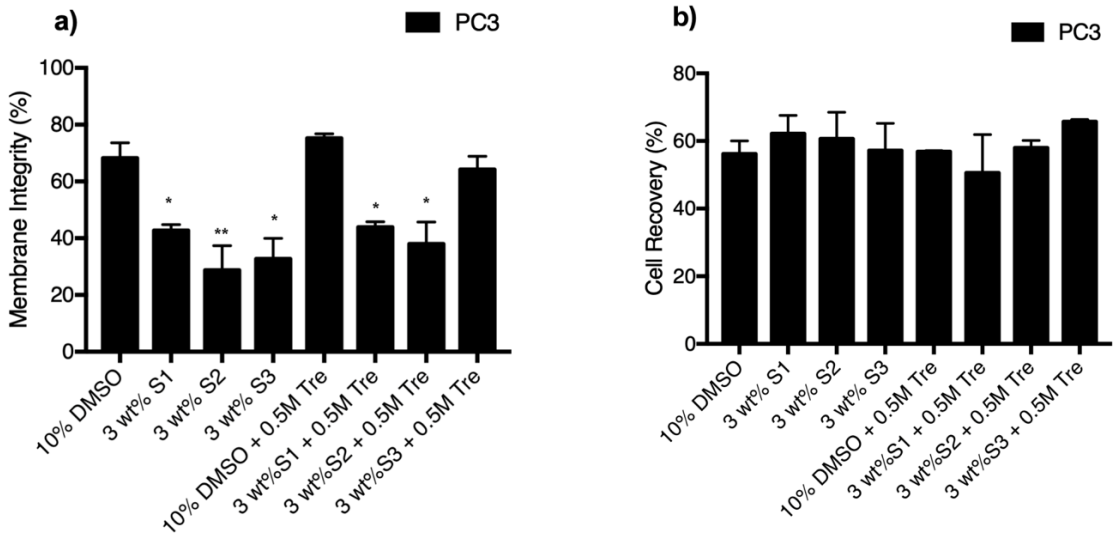

Figure 5-4. Post-Thaw membrane integrity and cell recovery after 24 h of cryopreservation at −80 °C a) Membrane integrity and b) Cell recovery percent of PC3 cell line after 24 h of controlled temperature cryopreservation in **S1, S2** and **S3** (3 wt%) polymer solution +/- 0.5M Trehalose and 10% DMSO / 10% FBS. Value = mean ±SD, n = 3. *P < 0.05, **P < 0.01 (One-way ANOVA).

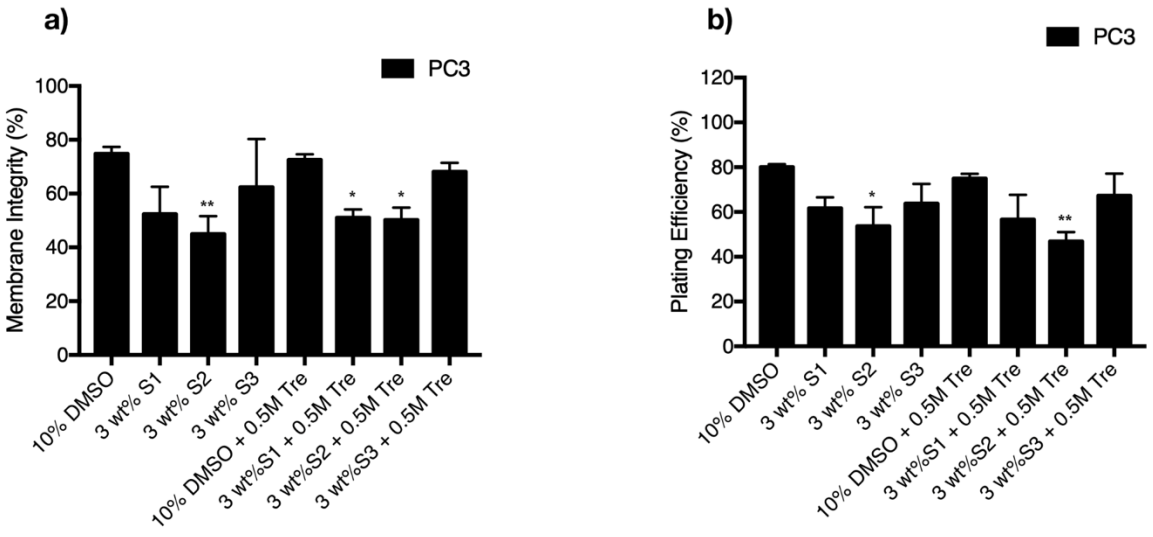

Figure 5-5. Post-Thaw membrane integrity and proliferation after 24h of incubation a) Membrane integrity and b) Platting efficiency of PC3 cell line after 24 h of controlled cryopreservation in **S1, S2** and **S3** (3 wt%) polymer solution +/- 0.5M Trehalose, 10% DMSO / 10% FBS. Value = mean ±SD, n = 3. *P < 0.05, **P < 0.01 (One-way ANOVA).

Mazur developed the two-factor hypothesis of freezing injury to explain the survival of cells when subjected to cryogenic temperatures; very fast cooling rates supercool the intracellular environment, typically causing intracellular freezing. While cooling cells slower than the optimal rate in the presence of ice results in the osmotic dehydration of cells and solute toxicity[4]. These osmotic stresses alone may be severe enough to cause lethal injury changes such as stated by Meryman in his "minimal critical volume" hypothesis[22]. Moreover, mechanical action of the extracellular ice is likely to "seed" nucleation within cells and to directly injure cell membranes by compressing cells together (unfrozen fraction hypothesis)[41]. During optimal cooling, cells experience a hypertonic environment and have time to sufficiently dehydrate before irreversible injury appears. Difficulties in designing cryopreservation protocols may arise from the complex interactions of these variables; thus, cooling rates that are low enough to avoid intracellular ice formation (IIF) may be slow and induce damage from solution effects. Many of the successes of cryobiology derive from manipulating these variables, using controlled freezing and rewarming protocols, along with cryoprotective agents (CPAs)[35,42].

Successful cryopreservation depends largely on the permeability of cells to water and CPAs, and on their tolerance concentration limits[43]. A more recent approach for cryopreservation involves the use of low concentrations of intracellular sugars to stabilize cells. The accumulation of internal sugars or mixtures of sugars, such as trehalose, sucrose, and raffinose is one of the complex physiological adaptations that allows some organisms to survive drying stress[5,14,17,42]. These sugars are believed to play a major role in the stabilization of membranes, proteins, and other key cellular structures. One of the major advantages is their high glass transition temperature (T_g) compared with conventional CPAs, such as DMSO, ethylene glycol (EG), and 1,2-propanediol (PROH). Sugars also deliver their protection by stabilizing lipid membranes through hydrogen bonding (water replacement hypothesis); by preventing aggregations of intracellular proteins and by acting as osmolytes against osmotic stresses[44]. In addition, to its non-toxic nature, sugars-based CPAs have the potential to infuse freeze-thawed cells directly into patients without the requirement of further steps involved in the removal of traditional CPAs[23]. Until recently, sugars have been used as extracellular additives due to impermeability of the cell membranes but in recent years, several groups overcame this barrier by using different approaches such as thermotropic lipid phase transition[7], reversible poration[21], transfection[45] and microinjection[46]. In this study we proposed the use of a trehalose-based polyether in combination with extracellular trehalose as CPAs. The non-permeating cryoprotectant trehalose may provide adequate cryoprotection however, to provide maximum protection to the cells, the trehalose should be present on both sides of the cell membrane. Endocytosis has previously been found to play an important role in the delivery of hydrophilic species into cells using related polymers such as PP-75[40]. In Figure 5-6 we observed the fluorescence microscopy images of HeLa cells after incubation with FITC-labeled polyethers at -80 °C overnight and we have concluded that polyethers are capable of delivering hydrophilic species, such as trehalose, into cells. Permeating CPAs like DMSO and our polyethers will protect cells by increasing intracellular and extracellular osmolality, depressing the freezing temperature which reduces the amount of ice formed and therefore the damaging effects of ice and solute concentration at a given temperature, reducing the extent of cell shrinkage, and raising the vitrification temperature. The non-permeating CPA, trehalose will protect the cells by increasing extracellular osmolality,

causing cells to dehydrate which reduces the likelihood of intracellular ice formation during cooling[47,48]. A combination of the polyethers and trehalose will allow the cell dehydration at higher temperatures while the water permeability of the cell is still high due to the high T_g of the solution. It is also known that the viscosity of trehalose solutions rapidly increases during cooling, posing another advantage, considering that increased viscosity may reduce crystal growth and thus potential damage[49].

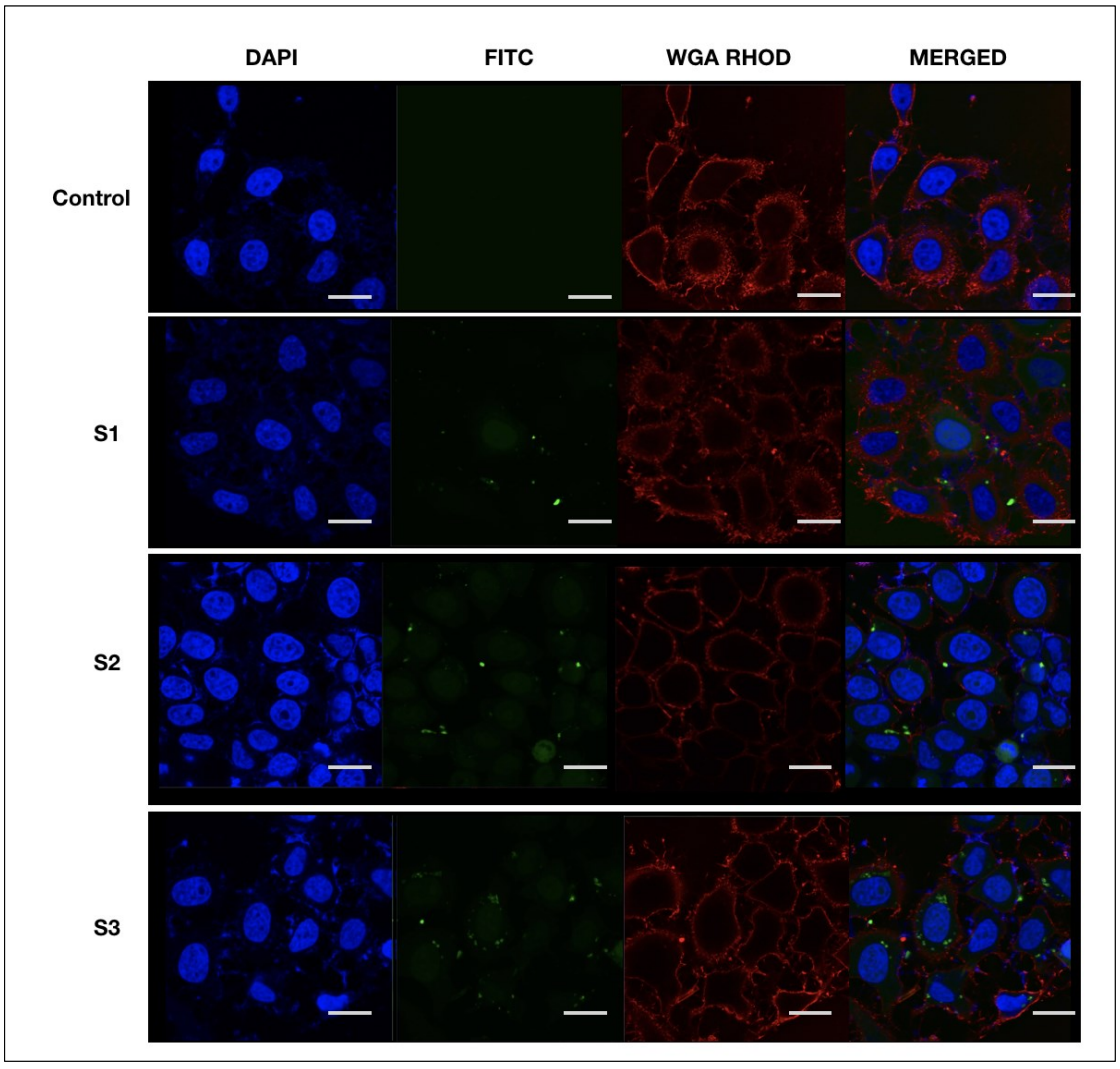

Figure 5-6. Representative fluorescence microscopy images of HeLa cells after cryopreservation with the fluorescently-labeled (FITC) polymers **S1**, **S2**, **S3** and DMEM + 10% FBS media fixed with 4% PFA. The cells were subsequently stained with DAPI and WGA Rhodamine following three washes with PBS. The scale bars represent 20 μm.

The trehalose-based polymers formed hydrogel networks at a concentration of 15 wt%. The 3D cytotoxicity evaluation of the hydrogel was performed using a membrane integrity assay. Unfrozen untreated (live) cells were used as positive control incubated with DMEM/10% FBS media, and cells exposed to 70% ethanol for 30 min as a positive dead control. Live cells are notable green fluorescent due to the alteration of calcein AM. Cells with compromised membranes are bright red fluorescence by the binding of propidium iodide (an impermeant dye) to DNA[50]. Images by confocal microscopy were acquired after 24 h of incubation (Fig. 5-7) and analysed using Imaris Imaging Software to quantify the membrane integrities (Figure 5-8). The results demonstrate that the polyether hydrogel scaffolds composed of the three trehalose polymers **S1**, **S2** and **S3** were favorably biocompatible exhibiting more than 95% viability and that can be custom to promote cell integration and growth.

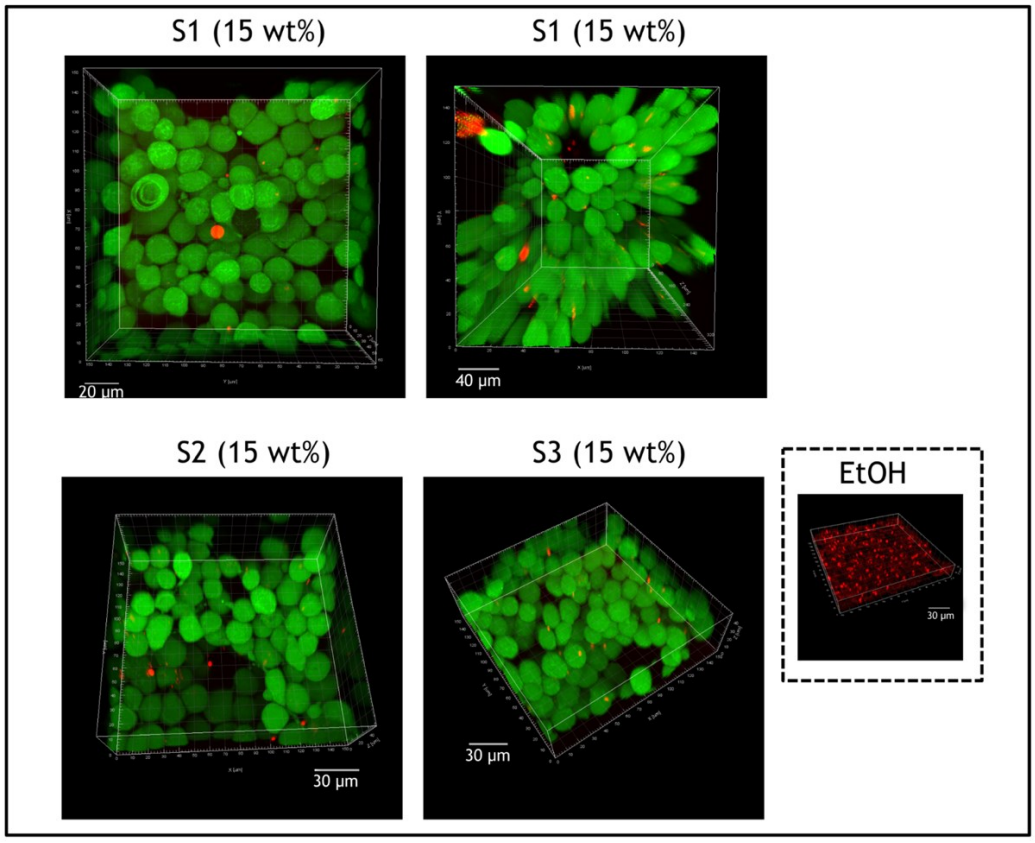

Figure 5-7. Confocal images of the 3D Cell culture constructs evaluated following 24 h incubation in trehalose-based hydrogels; most cells stained Calcein positive, indicating the

compatibility of the polymer scaffolds. ~1 x10^5 PC3 cells were seeded and grown in a polyether solution of 15 wt%. After 24 h of incubation, the cells were stained with Calcein AM and PI (LIVE/DEAD® Cell Imaging Kit 488/570, ThermoFisher R37601). Confocal microscopy (40X oil lens) through two fluorescent channels (FITC and Texas red) was used to capture the images. 70% ethanol (EtOH) treated cells served as positive control for dead cells. Scale bars represent 20-40 μm.

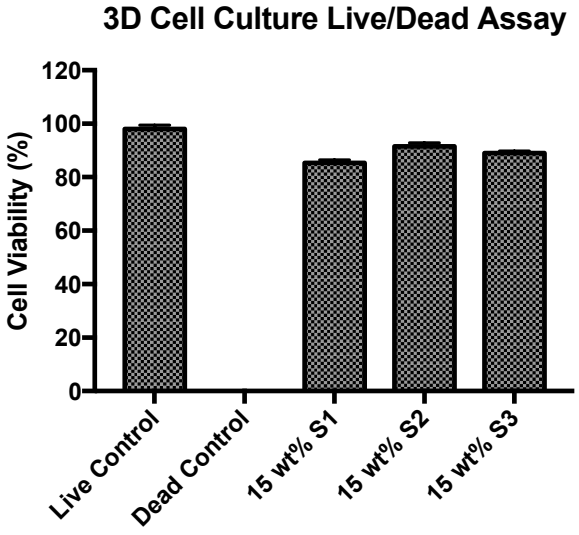

Figure 5-8. 3D cell culture Viability following 24 h incubation. Cell viability of PC3 (prostate cancer cell line) was measured using LIVE/DEAD® Cell Imaging Kit 488/570, ThermoFisher R37601. PC3 cells were grown in 15 wt% trehalose-based hydrogels. Value = mean ± standard deviation, n = 5. Imaris Imaging Software was used to estimate viability.

5.4 CONCLUSIONS

The present study evaluated the design and characterization of trehalose-based polymers for the cryopreservation and 3D cell culture of mammalian cells. The survival mechanisms of the anhydrobiotic organisms have inspired the development of these polymers due to the remarkable properties exhibited by the accumulation of trehalose. The presence of this sugar have shown to inhibit ice crystal growth, which reduces the possibility of damage to the cell membrane from recrystallizing, growing and enlarging ice crystals[51]. All of the resulting polymers were evaluated for their IRI activity and their cytotoxicity in HeLa cells

up to 100 mg/ml, showing low cell toxicity. Their ability as CPAs was determined by two freezing methods, ultra-rapid and controlled rate-freezing. In the ultra-rapid method, cells were rapidly frozen at −80 °C and the results showed more than 90% cell survival at polymer concentrations of 5 and 10 wt%. For the controlled-rate freezing, the polymers were tested at 5 and 10 wt% and 3 wt% in the presence and absence of trehalose and confirmed high membrane integrities (more than 70%) and higher cell recovery (more than 60%) as seen with the control DMSO+/- trehalose. Additionally, the cell encapsulation efficiency was evaluated by growing the cells inside a hydrogel with 15 wt% and the live/dead assay was performed to assess the hydrogel biocompatibility showing noticeable results (more than 95% viability). Our research has demonstrated that trehalose-based polymers act as cryoprotective agents that can significantly influence the ice crystal formation and growth which, in turn, can play a meaningful role in mitigating physical cellular damages during freezing and thawing by acting as antifreeze protein mimetics improving cryopreservation outcomes. Furthermore, these polymers have the additional ability to form 3D cellular scaffold, which may be useful in the development of organoids and ex vivo cell models for use in tissue engineering and biomedical applications. The bio-inspired polymers, which we have tested for mammalian cell storage and encapsulation, have provided a new platform to improve the cryopreservation procedures employed today. Future research could potentially investigate their used in cell dessication techniques to enable long-term higher temperature storage[52].

5.5 REFERENCES

(1) Yoshiyama, Y.; Tanaka, K.; Yoshiyama, K.; Hibi, M.; Ogawa, J.; Shima, J. Trehalose Accumulation Enhances Tolerance of Saccharomyces Cerevisiae to Acetic Acid. *J. Biosci. Bioeng.* **2015**, *119* (2), 172–175. https://doi.org/10.1016/j.jbiosc.2014.06.021.

(2) Benaroudj, N.; Lee, D. H.; Goldberg, A. L. Trehalose Accumulation during Cellular Stress Protects Cells and Cellular Proteins from Damage by Oxygen Radicals. *J. Biol. Chem.* **2001**, *276* (26), 24261–24267. https://doi.org/10.1074/jbc.M101487200.

(3) Hengherr, S.; Heyer, A. G.; Köhler, H.-R.; Schill, R. O. Trehalose and Anhydrobiosis in Tardigrades - Evidence for Divergence in Responses to Dehydration. *FEBS J.* **2008**, *275* (2), 281–288. https://doi.org/10.1111/j.1742-4658.2007.06198.x.

(4) Fuller, B. J.; Lane, N.; Benson, E. E. *Life in the Frozen State*; Boca Raton, Fla: CRC Press, 2004.

(5) Crowe, J. H.; Crowe, L. M.; Chapman, D. Preservation of Membranes in Anhydrobiotic Organisms: The Role of Trehalose. *Science (80-.).* **1984**, *223* (4637), 701–703. https://doi.org/10.1126/science.223.4637.701.

(6) Motta, J. P. R.; Paraguassú-Braga, F. H.; Bouzas, L. F.; Porto, L. C. Evaluation of Intracellular and Extracellular Trehalose as a Cryoprotectant of Stem Cells Obtained from Umbilical Cord Blood. *Cryobiology* **2014**, *68* (3), 343–348. https://doi.org/10.1016/j.cryobiol.2014.04.007.

(7) Beattie, G. M.; Crowe, J. H.; Lopez, A. D.; Cirulli, V.; Ricordi, C.; Hayek, A. Trehalose: A Cryoprotectant That Enhances Recovery and Preserves Function of Human Pancreatic Islets after Long-Term Storage. *Diabetes* **1997**, *46* (3), 519–523. https://doi.org/10.2337/diab.46.3.519.

(8) Chen, F.; Zhang, W.; Wu, W.; Jin, Y.; Cen, L.; Kretlow, J. D.; Gao, W.; Dai, Z.; Wang, J.; Zhou, G.; Liu, W.; Cui, L.; Cao, Y. Cryopreservation of Tissue-Engineered Epithelial Sheets in Trehalose. *Biomaterials* **2011**, *32* (33), 8426–8435. https://doi.org/10.1016/j.biomaterials.2011.07.008.

(9) Holovati, J. L.; Gyongyossy-Issa, M. I. C.; Acker, J. P. Effects of Trehalose-Loaded Liposomes on Red Blood Cell Response to Freezing and Post-Thaw Membrane Quality. *Cryobiology* **2009**, *58* (1), 75–83. https://doi.org/10.1016/j.cryobiol.2008.11.002.

(10) Messina, M. S.; Ko, J. H.; Yang, Z.; Strouse, M. J.; Houk, K. N.; Maynard, H. D. Effect of Trehalose Polymer Regioisomers on Protein Stabilization. *Polym. Chem.* **2017**, *8* (33), 4781–4788. https://doi.org/10.1039/c7py00700k.

(11) Clegg, J. S. The Physical Properties and Metabolic Status of Artemia Cysts at Low Water Contents: The Water Replacement Hypothesis. *Membr. Metab. dry Org.* **1986**, 169–187.

(12) Warner, D. T. Some Possible Relationships of Carbohydrates and Other Biological Components with the Water Structure at 37°. *Nature* **1962**, *196* (4859), 1055–1058. https://doi.org/10.1038/1961055a0.

(13) Lins, R. D.; Pereira, C. S.; Hünenberger, P. H. Trehalose-Protein Interaction in Aqueous Solution. *Proteins Struct. Funct. Bioinforma.* **2004**, *55* (1), 177–186. https://doi.org/10.1002/prot.10632.

(14) Sola-Penna, M.; Meyer-Fernandes, J. R. Stabilization against Thermal Inactivation Promoted by Sugars on Enzyme Structure and Function: Why Is Trehalose More Effective than Other Sugars? *Arch. Biochem. Biophys.* **1998**, *360* (1), 10–14. https://doi.org/10.1006/abbi.1998.0906.

(15) Tunnacliffe, A. Anhydrobiotic Engineering of Bacterial and Mammalian Cells: Is Intracellular Trehalose Sufficient? *Cryobiology* **2001**, *43* (2), 124–132. https://doi.org/10.1006/cryo.2001.2356.

(16) Katenz, E.; Vondran, F. W. R.; Schwartlander, R.; Pless, G.; Gong, X.; Cheng, X.; Neuhaus, P.; Sauer, I. M. Cryopreservation of Primary Human Hepatocytes: The Benefit of Trehalose as an Additional Cryoprotective Agent. *Liver Transplant.* **2007**, *13* (1), 38–45. https://doi.org/10.1002/lt.20921.

(17) Buchanan, S. S.; Gross, S. A.; Acker, J. P.; Toner, M.; Carpenter, J. F.; Pyatt, D. W. Cryopreservation of Stem Cells Using Trehalose: Evaluation of the Method Using a Human Hematopoietic Cell Line. *Stem Cells Dev.* **2004**, *13* (3), 295–305. https://doi.org/10.1089/154732804323099226.

(18) Notman, R.; Noro, M.; O'Malley, B.; Anwar, J. Molecular Basis for Dimethylsulfoxide (DMSO) Action on Lipid Membranes. *J. Am. Chem. Soc.* **2006**, *128* (43), 13982–13983. https://doi.org/10.1021/ja063363t.

(19) Hubel, A.; Skubitz, A. P. N. Principles of Cryopreservation. In *Biobanking of Human Biospecimens*; Springer International Publishing: Cham, 2017; pp 1–21. https://doi.org/10.1007/978-3-319-55120-3_1.

(20) Hubálek, Z. Protectants Used in the Cryopreservation of Microorganisms. *Cryobiology* **2003**, *46* (3), 205–229. https://doi.org/10.1016/S0011-2240(03)00046-4.

(21) Eroglu, A.; Russo, M. J.; Bieganski, R.; Fowler, A.; Cheley, S.; Bayley, H.; Toner, M. Intracellular Trehalose Improves the Survival of Cryopreserved Mammalian Cells. *Nat. Biotechnol.* **2000**, *18* (2), 163–167. https://doi.org/10.1038/72608.

(22) Meryman, H. T. T. Osmotic Stress as a Mechanism of Freezing Injury. *Cryobiology* **1971**, *8* (5), 489–500. https://doi.org/10.1016/0011-2240(71)90040-X.

(23) Yang, J.; Cai, N.; Zhai, H.; Zhang, J.; Zhu, Y.; Zhang, L. Natural Zwitterionic Betaine Enables Cells to Survive Ultrarapid Cryopreservation. *Sci. Rep.* **2016**, *6* (October), 1–9. https://doi.org/10.1038/srep37458.

(24) Shu, Z.; Heimfeld, S.; Gao, D. Hematopoietic SCT with Cryopreserved Grafts: Adverse Reactions after Transplantation and Cryoprotectant Removal before Infusion. *Bone Marrow Transplant.* **2014**, *49* (4), 469–476. https://doi.org/10.1038/bmt.2013.152.

(25) Davis, J. M.; Rowley, S. D.; Braine, H. G.; Piantadosi, S.; Santos, G. W. Clinical Toxicity of Cryopreserved Bone Marrow Graft Infusion. *Blood* **1990**, *75* (3), 781–786. https://doi.org/10.1182/blood.v75.3.781.bloodjournal753781.

(26) Huang, H.; Zhao, G.; Zhang, Y.; Xu, J.; Toth, T. L.; He, X. Predehydration and Ice Seeding in the Presence of Trehalose Enable Cell Cryopreservation. *ACS Biomater. Sci. Eng.* **2017**, *3* (8), 1758–1768. https://doi.org/10.1021/acsbiomaterials.7b00201.

(27) Biggs, C. I.; Bailey, T. L.; Ben Graham; Stubbs, C.; Fayter, A.; Gibson, M. I. Polymer Mimics of Biomacromolecular Antifreezes. *Nat. Commun.* **2017**, *8* (1), 1–11. https://doi.org/10.1038/s41467-017-01421-7.

(28) Vail, N. S.; Stubbs, C.; Biggs, C. I.; Gibson, M. I. Ultralow Dispersity Poly(Vinyl Alcohol) Reveals Significant Dispersity Effects on Ice Recrystallization Inhibition Activity. *ACS Macro Lett.* **2017**, *6* (9), 1001–1004. https://doi.org/10.1021/acsmacrolett.7b00595.

(29) Nagao, M.; Sengupta, J.; Diaz-Dussan, D.; Adam, M.; Wu, M.; Acker, J.; Ben, R.; Ishihara, K.; Zeng, H.; Miura, Y.; Narain, R. Synthesis of Highly Biocompatible and Temperature-Responsive Physical Gels for Cryopreservation and 3D Cell Culture. *ACS Appl. Bio Mater.* **2018**, *1* (2), 356–366. https://doi.org/10.1021/acsabm.8b00096.

(30) Yuan, Y.; Yang, Y.; Tian, Y.; Park, J.; Dai, A.; Roberts, R. M.; Liu, Y.; Han, X. Efficient Long-Term Cryopreservation of Pluripotent Stem Cells at-80 °c. *Sci. Rep.* **2016**, *6* (September), 1–13. https://doi.org/10.1038/srep34476.

(31) Rupf, T.; Ebert, S.; Lorenz, K.; Salvetter, J.; Bader, A. Cryopreservation of Organotypical Cultures Based on 3D Scaffolds. *Cryo-Letters* **2010**, *31* (2), 157–168.

(32) Lee, J.; Lin, E. W.; Lau, U. Y.; Hedrick, J. L.; Bat, E.; Maynard, H. D. Trehalose Glycopolymers as Excipients for Protein Stabilization. *Biomacromolecules* **2013**, *14* (8), 2561–2569. https://doi.org/10.1021/bm4003046.

(33) Knight, C. A.; Hallett, J.; DeVries, A. L. Solute Effects on Ice Recrystallization: An Assessment Technique. *Cryobiology* **1988**, *25* (1), 55–60. https://doi.org/10.1016/0011-2240(88)90020-X.

(34) Abraham, S.; Keillor, K.; Capicciotti, C. J.; Perley-Robertson, G. E.; Keillor, J. W.; Ben, R. N. Quantitative Analysis of the Efficacy and Potency of Novel Small Molecule Ice Recrystallization Inhibitors. *Cryst. Growth Des.* **2015**, *15* (10), 5034–5039. https://doi.org/10.1021/acs.cgd.5b00995.

(35) Baboo, J.; Kilbride, P.; Delahaye, M.; Milne, S.; Fonseca, F.; Blanco, M.; Meneghel, J.; Nancekievill, A.; Gaddum, N.; Morris, G. J. The Impact of Varying Cooling and Thawing Rates on the Quality of Cryopreserved Human Peripheral Blood T Cells. *Sci. Rep.* **2019**, *9* (1), 1–13. https://doi.org/10.1038/s41598-019-39957-x.

(36) Quan, S.; Wang, Y.; Zhou, A.; Kumar, P.; Narain, R. Galactose-Based Thermosensitive Nanogels for Targeted Drug Delivery of Iodoazomycin Arabinofuranoside (IAZA) for Theranostic Management of Hypoxic Hepatocellular Carcinoma. *Biomacromolecules* **2015**, *16* (7), 1978–1986. https://doi.org/10.1021/acs.biomac.5b00576.

(37) Flodin, G. M. P.; Perstorp; Ingelman, G. A. B. Sucrose Ether Copolymerizates. US Patent 3,300,474, 1967.

(38) Yuan, C.; Gao, J.; Guo, J.; Bai, L.; Marshall, C.; Cai, Z.; Wang, L.; Xiao, M. Dimethyl Sulfoxide Damages Mitochondrial Integrity and Membrane Potential in Cultured Astrocytes. *PLoS One* **2014**, *9* (9), e107447. https://doi.org/10.1371/journal.pone.0107447.

(39) Kratochvílová, I.; Golan, M.; Pomeisl, K.; Richter, J.; Sedláková, S.; Šebera, J.; Mičová, J.; Falk, M.; Falková, I.; Řeha, D.; Elliott, K. W.; Varga, K.; Follett, S. E.; Šimek, D. Theoretical and Experimental Study of the Antifreeze Protein AFP752, Trehalose and Dimethyl Sulfoxide Cryoprotection Mechanism: Correlation with Cryopreserved Cell Viability. *RSC Adv.* **2017**, *7* (1), 352–360. https://doi.org/10.1039/C6RA25095E.

(40) Sharp, D. M. C. C.; Picken, A.; Morris, T. J.; Hewitt, C. J.; Coopman, K.; Slater, N. K. H. H. Amphipathic Polymer-Mediated Uptake of Trehalose for Dimethyl Sulfoxide-Free Human Cell Cryopreservation. *Cryobiology* **2013**, *67* (3), 305–311. https://doi.org/10.1016/j.cryobiol.2013.09.002.

(41) Mazur, P.; Cole, K. W. Influence of Cell Concentration on the Contribution of Unfrozen Fraction and Salt Concentration to the Survival of Slowly Frozen Human Erythrocytes. *Cryobiology* **1985**, *22* (6), 509–536. https://doi.org/10.1016/0011-2240(85)90029-X.

(42) Chen, G.; Yue, A.; Ruan, Z.; Yin, Y.; Wang, R.; Ren, Y.; Zhu, L. Comparison of the Effects of Different Cryoprotectants on Stem Cells from Umbilical Cord Blood. *Stem Cells Int.* **2016**, *2016*, 1–7. https://doi.org/10.1155/2016/1396783.

(43) Kashuba Benson, C. M.; Benson, J. D.; Critser, J. K. An Improved Cryopreservation Method for a Mouse Embryonic Stem Cell Line. *Cryobiology* **2008**, *56* (2), 120–130. https://doi.org/10.1016/j.cryobiol.2007.12.002.

(44) Eroglu, A. Cryopreservation of Mammalian Oocytes by Using Sugars: Intra- and Extracellular Raffinose with Small Amounts of Dimethylsulfoxide Yields High Cryosurvival, Fertilization, and Development Rates. *Cryobiology* **2010**, *60* (706), 1–14. https://doi.org/10.1016/j.cryobiol.2009.07.001.Cryopreservation.

(45) Guo, N.; Puhlev, I.; Brown, D. R.; Mansbridge, J.; Levine, F. Trehalose Expression Confers Desiccation Tolerance on Human Cells. *Nat. Biotechnol.* **2000**, *18* (2), 168–171. https://doi.org/10.1038/72616.

(46) Eroglu, A.; Toner, M.; Toth, T. L. Beneficial Effect of Microinjected Trehalose on the Cryosurvival of Human Oocytes. *Fertil. Steril.* **2002**, *77* (1), 152–158. https://doi.org/10.1016/S0015-0282(01)02959-4.

(47) Mazur, P.; Koshimoto, C. Is Intracellular Ice Formation the Cause of Death of Mouse Sperm Frozen at High Cooling Rates?1. *Biol. Reprod.* **2005**, *66* (5), 1485–1490. https://doi.org/10.1095/biolreprod66.5.1485.

(48) Mazur, P.; Seki, S.; Pinn, I. L.; Kleinhans, F. W.; Edashige, K. Extra- and Intracellular Ice Formation in Mouse Oocytes. *Cryobiology* **2005**, *51* (1), 29–53. https://doi.org/10.1016/j.cryobiol.2005.04.008.

(49) Uchida, T.; Nagayama, M.; Gohara, K. Trehalose Solution Viscosity at Low Temperatures Measured by Dynamic Light Scattering Method: Trehalose Depresses Molecular Transportation for Ice Crystal Growth. *J. Cryst. Growth* **2009**, *311* (23–24), 4747–4752. https://doi.org/10.1016/j.jcrysgro.2009.09.023.

(50) Posimo, J. M.; Unnithan, A. S.; Gleixner, A. M.; Choi, H. J.; Jiang, Y.; Pulugulla, S. H.; Leak, R. K. Viability Assays for Cells in Culture. *J. Vis. Exp.* **2014**, *Jan20* (83), e50645. https://doi.org/10.3791/50645.

(51) Solocinski, J.; Osgood, Q.; Wang, M.; Connolly, A.; Menze, M. A.; Chakraborty,

N. Effect of Trehalose as an Additive to Dimethyl Sulfoxide Solutions on Ice Formation, Cellular Viability, and Metabolism. *Cryobiology* **2017**, *75*, 134–143. https://doi.org/10.1016/j.cryobiol.2017.01.001.

(52) Drake, A. C.; Lee, Y.; Burgess, E. M.; Karlsson, J. O. M.; Eroglu, A.; Higgins, A. Z. Effect of Water Content on the Glass Transition Temperature of Mixtures of Sugars, Polymers, and Penetrating Cryoprotectants in Physiological Buffer. *PLoS One* **2018**, *13* (1), 1–15. https://doi.org/10.1371/journal.pone.0190713.

CHAPTER 6. HYPOXIA-ACTIVATED CARBOHYDRATE-BASED *NANOTHERANOSTIC* TO MANAGE HYPOXIC CANCEROUS TUMOURS.

6.1 INTRODUCTION

Sub-optimal oxygen levels in cells, termed *hypoxia*, is present in tumours with abnormal vasculature that are found in all types of cancers. These hypoxic regions have been confirmed in several malignancies, including breast[1], cervix[2], head and neck [3], rectum[4], pancreas[5] and prostate cancers[6]. This trait is considered a negative prognostic marker for patients and a predictive factor to promote invasion[7–10], tumour progression and recurrence (metastasis) [9] through genetic and transcriptional alterations that lead to resistance to radiotherapy, chemotherapy (due to impaired drug delivery)[10,11], altered metabolism and genomic instability[12]. Hypoxia-associated therapies face significant challenges due to impaired drug delivery and metabolic degradation of existing drugs before reaching the target; escalating drug doses to deliver therapeutically effective doses inside tumours has resulted in associated neurotoxicity of the drugs[13–16]. From a clinical standpoint, targeting hypoxia is crucial for cancer remission, given the fact that it has a significant role in promoting tumour progression and therapy resistance. Therefore, delivering a hypoxia-activated theranostic (i.e. same molecule possessing both therapeutic and diagnostic properties) using nanotechnology to supply therapeutically effective drug doses within hypoxic cancer cells and precise therapeutic planning based on the level of hypoxia and diagnostic outcome is the legitimate strategy to provide an 'individualized' and effective management of therapy-resistant hypoxic cancerous tumours.

Hypoxia-activated prodrugs (HAPs) —bioreductive prodrugs activated by selective enzymatic reduction processes that are upregulated in hypoxic cells— offers a molecular approach to manage and target therapy-resistant hypoxic solid tumours. Radiolabeled 2-nitroimidazoles (2-NIs)[17] have shown proven clinical success as hypoxia selective radiotracers, and some widely used radiopharmaceuticals for hypoxia imaging include ^{18}F-fluoromisonidazole (^{18}F-FMISO)[13,17,18], ^{18}F- fluoroazomycin arabinoside (^{18}F-FAZA)[19–22] and ^{123}I-labeled iodoazomycin arabinoside (^{123}I-IAZA)[22–25]. In clinical settings, ^{123}I-IAZA has accurately detected hypoxia in a variety of cancer patients[19,20] and promises excellent therapeutic potential, either as a radiosensitizer (non-radioactive IAZA also termed as

"cold" IAZA; ^{127}IAZA) to enhance therapeutic effects of external X-ray beam (radiotherapy) or for delivering *in situ* molecular radiotherapy (MRT) when IAZA is labelled with a therapeutic radionuclide (^{131}I), i.e., by a simple change of the iodine isotope; the same IAZA molecule can deliver hypoxia (cancer) imaging as well as treatment. Peripheral neurotoxicity, a limitation seen with previous 2-NIs clinical trials[13], has not been reported with IAZA[22], which provides a valid rationale that hypoxic reduction of IAZA, combined with its proven hypoxia-selective properties, could offer a multi-fold theranostic value.

The complexity of the biological system offers significant impediments to the site-specific delivery of therapeutic drugs. Hypoxia in tumours augments the challenge due to poor angiogenesis, dense matrix structures and elevated levels of interstitial fluid pressure in tumour tissues resulting in low bioavailability of the pharmaceuticals[26,27]. Nanotechnology comes in hand to develop "smart delivery" vehicles to facilitate drugs reach target-specific cells and improve their intracellular localization[28]. Systemic administration of chemotherapeutics is limited by low solubility, pharmacokinetic factors and off-target toxicity[29] as they generally target rapidly dividing cells, which is not the case with hypoxic cancer cells. The use of nanoparticles has shown potential in overcoming these problems[30–32], but challenges, such as stable systemic circulation and tumour extravasation, are still faced by these nanocarriers. The enhanced permeation and retention effect (EPR) states that under pathological states like inflammation, infarcts and tumours, the endothelial lining tends to become more permeable leading to 'gaps' in the lining[33]. Nanoparticles with smaller hydrodynamic sizes can extravasate through these gaps to enter tumour space and localize there due to poor lymphatic drainage of the tumours[34]. Our group has successfully developed glycopolymer-based nanoparticles with passive and active targeting capabilities demonstrating significant cellular uptake, drug delivery and gene expression[35–38]. The development of stimuli-responsive carbohydrate-based nanogels (NGs) with N,N′-methylene bisacrylamide (MBAm) crosslinker have conferred high hydrating capacity proven to encapsulate a significant amount of drug within their polymer matrix increasing the drug stability and reducing drug elimination. NGs are defined as an aqueous dispersion of hydrogel nanoparticles, formed by physical and/or chemical cross-linking and hydrophobic polymer networks of nanoscale size[39]. These NGs can be considered as

"smart" delivery systems; loading biological agents to these vehicles is usually achieved spontaneously through electrostatic, van der Waals and/or hydrophobic interactions with the loading-agent. There are thermoresponsive materials, becoming hydrophobic above a specific lower critical solution temperature (LCST). Thermo-responsive NGs with an LCST at ~35-37 ºC have been developed such that at body temperature, the nanogels collapse and become hydrophobic, releasing the encapsulated agent slowly in a controlled manner. These thermal changes in the physicochemical behaviour of the NGs are responsible for enhanced physical targeted delivery of nanoHAP and thermoresponsive release of HAP in tumour cells therein, increasing the drug bioavailability, offering higher permeability and absorption and low pre-target metabolic degradation[40].

Cancer therapeutics is undergoing a new post-genomics targeted era. New anti-cancer drugs that target specific tumour cells and are non-toxic to normal healthy cells are beginning to change cancer treatment. The creation of hybrid systems at the nanoscale that combines pharmaceuticals and mimics biological entities provides the possibility of overcoming the complex challenges of enhancing detection sensitivity and improving drug efficacy. Passive delivery of a drug payload to cancer cells is mediated via the EPR effect, but in some cases, active targeting is used to mediate ligand-receptor specific interactions. Every cell's surface contains carbohydrates in the form of polysaccharides, glycoproteins, glycolipids, and/or other glycoconjugates. These naturally occurring glycoconjugates play essential roles as recognition sites that are involved in biological functions[41]. Coupling of ligands to the nanoparticle's surface for active targeting of nano-based drugs is a biomimetic approach with similar or even superior functions to those of natural glycoconjugates. Complex carbohydrates and carbohydrate-based polymers require sugar ligands to be anchored on the nanoparticle's external surface by chemical modification to effectuate their binding to the cell surface lectins. Nonetheless, understanding glycopolymers' role in molecular mimicry and the complex interactions between these polymers and the lectin receptors are still relatively poorly defined.

Our study pursued a translational approach of using *nano*IAZA, i.e., IAZA encapsulated in glyco-nanogels for theranostic management of hypoxic cancerous tumours. Oxygen-mimicking cytotoxic activation and iodine's unique existence in several isotopic forms confers IAZA with an unparalleled potential to bestow both cancer imaging and

multimodal therapy —as a hypoxia-selective chemotoxic agent, a radiosensitizer[42] and as an MRT agent[24]. The glyco-nanogel used here developed as a nanocarrier is composed of LAEMA (2-lactobionamidoethyl methacrylamide) decorated with an outer shell of thermoresponsive DEGMA (di(ethylene glycol) methyl ethyl methacrylate) and crosslinked inner core of MBAm (N, N'-methylenebis(acrylamide)). This amphipathic polymer (LAEMA)-*b*-(DEGMA-*st*-MBAm) has a cross-linked segment that can encapsulate different types of compounds. Due to the thermosensitive properties of DEGMA, the core is modulated by changes in temperature to encapsulate or release the drugs; as the temperature rises above the polymer LCST, the nanogel core collapses and shrinks, becoming hydrophobic. The LAEMA motif, a hydrophilic component, is reported to increase the solubility and stability of the nanogels. Galactose-based nanoparticles have displayed high uptake by HepG2 cells (liver cancer) due to the presence of the asialoglycoprotein receptor (ASPGR)[35,37,43]. Likewise, galactose moieties are known to interact with carbohydrate receptors found on the cell membrane like lectins and glucose transport proteins (GLUTs) that enhance its cellular uptake due to the "cluster glycoside effect" [44]. Many tumours display high rates of sugar uptake[45]. GLUT transporters overexpression has been observed in many human cancers and correlated with alterations in different signalling pathways like ras or src oncogenes[46–48]. Furthermore, Galectin family of galactose-binding proteins are associated with the ability of many tumour cell types to metastasize[49].

Herein, we have designed and optimized a galactose-based nanogel[35] by varying the hydrodynamic size, core composition, hydrophobicity, surface/core charge and crosslinker percentage, that improved IAZA-loading capacity (≅ 80-88%) and offered a time-controlled slow release of IAZA (over 50 h at 5 mM IAZA loading). *In vitro* studies have confirmed that *nano*IAZA (1 mM) encapsulated in a functionally-modified nanogel (**NG1)** improved the drug-bioavailability in hypoxic cancer cells and enhanced hypoxia-selective chemotoxicity and sensitivity to external-beam radiotherapy (EBRT) in comparison to IAZA itself. Higher sensitizer enhancement ratio (SER) for *nano*IAZA in comparison to the parent drug (IAZA) at 100 μM (1.58 vs. 1.4 for IAZA alone in PC3 cell line and 1.41 vs 1.09 for IAZA in FaDu cells), with a little or no effects under normoxia, has been observed. A dose-escalated toxicity evaluation on both the nanogel (**NG1**) and IAZA in

NSG mice at a dose of 615/600 mg/kg body weight, respectively, administered via the intraperitoneal route (i.p.), confirmed no histopathological toxicity indicating the safety of both **NG1** and IAZA at these doses for in vivo experiments. An evaluation of the chemotoxic therapy potential of IAZA and *nano*IAZA in a FaDu tumour-bearing NU/NU mouse model, when administered via i.p. at a single dose (400 mg/kg IAZA/*nano*IAZA; 308 mg/kg **NG1**), showed an improvement in the median survival of the animals injected with *nano*IAZA (16 days survival in comparison to 12.5 days for the control DMSO). The studies described here provide proof of principle evidence for using an *engineered nanoformulation* to deliver IAZA to oxygen-deprived cancer cells and enhance the therapeutic effects of IAZA. Further, based on the (radio)iodine incorporated, *nano*IAZA demonstrates the potential to offer *both* imaging and 2-way killing of cancerous tumours and also delivers the promise to release the drug inside cancer cells over a period of 50 h (at 5 mM concentration), potentially leading to the build-up of IAZA doses in hypoxic cells over a longer time, thus bestowing enhanced therapeutic effects in comparison to the parent drug. The intricate design of multifunctional NG carriers has shown a promising approach to manage therapy-resistant hypoxic tumours. In this case, the aim is to shift from conventional hypoxic cancer therapeutic and diagnostic approaches to a *combined theranostic* strategy.

6.2 EXPERIMENTAL SECTION

6.2.1 Development of *nano*IAZA. The synthesis of 'cold' IAZA and its radioiodinated analog has been previously established[24]. Radioiodinated IAZA can be prepared directly from 'cold' IAZA by radioiodine 'exchange' labelling or nucleophilic substitution of a reactive leaving group as described for the novel patented precursors[50]. Synthesis of the NGs complexes cross-linked with di(ethylene glycol)methyl ethyl methacrylate (DEGMA) was materialized using reversible addition−fragmentation chain transfer (RAFT) polymerization (Scheme 6-1). NGs with an outer shell of LAEMA (2-lactobionamidoethyl methacrylamide), and thermoresponsive inner core of DEGMA (di(ethylene glycol) methyl ethyl methacrylate) crosslinked with MBAm (N, N'-methylenebis(acrylamide)) were synthesized. Synthesis of P(LAEMA) Macro-CTA carrying a neutral charge and the NGs was carried out according to our previous protocol[35,51]. Synthesis of the NGs' complexes

with di(ethylene glycol)methyl ethyl methacrylate (DEGMA) was done by employing 4,4′-azobis(4-cyanopentanoic acid) (ACVA) as the initiator and P(LAEMA) as macro-CTA. Three factors were considered to synthesize the NGs: 1) molecular weight and surface charge; 2) hydrodynamic size; 3) degree of cross-linking within the core[35].

6.2.2 Nanogels (NGs) characterization. Dynamic light scattering (DLS) and Zeta potential analysis. Hydrodynamic diameter and surface charges were determined at 15 ºC and 37 ºC in DI water using a Brookhaven DLS and Zeta potential instrument (Table 6-1). Further characterization of the NGs was done, as reported in our previous study[35].

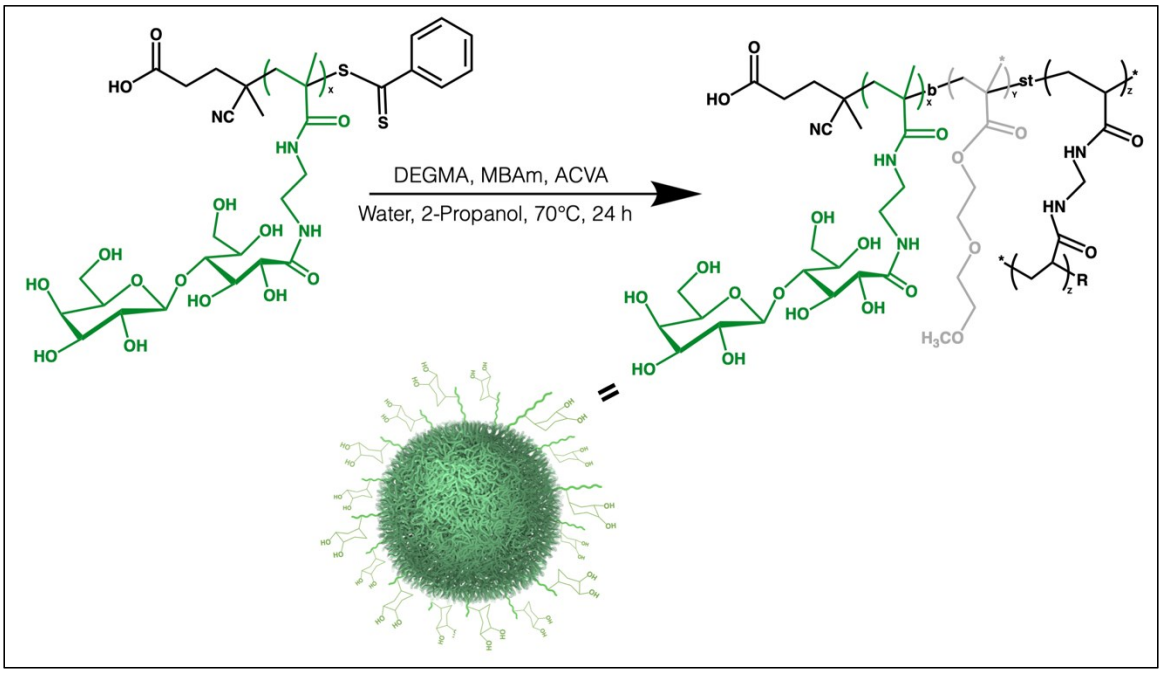

Scheme 6-1. Synthesis of thermoresponsive nanogel. Design of the stimuli-responsive NG with a thermoresponsive core composed of DEGMA (di(ethylene glycol) methyl ethyl methacrylate) cross-linked MBAm (N, N'-methylenebis(acrylamide)) with a carbohydrate shell composed of LAEMA(2-lactobionamidoethyl methacrylamide). The thermoresponsive nature of the NG allows controlled encapsulation and release of IAZA by undergoing a phase transition from a swollen state to a shrunken state at 37 ºC. Loading of biological agents is usually achieved spontaneously through electrostatic, van der Waals and/or hydrophobic interactions between the drug and the polymer matrix.

6.2.3 Determination of IAZA encapsulation in the NGs and release profiles. IAZA was loaded in the NGs by an incubation method —a solution of NGs was mixed with different amounts of IAZA (1, 2 and 5 mM) with a 10:1 feed ratio in excess NGs and then incubated for 24 h. The samples were centrifuged at 40 ºC, 14,000 rpm for 30 min. The amount of IAZA encapsulated in the NG was determined by sampling the supernatant using UV-visible spectroscopy at 320 nm (UVmax for IAZA). Release profile of IAZA from the NGs complex was established by re-suspending the NG complex in preheated phosphate-buffered saline (PBS). The sample was centrifuged, precipitating the 'unbound' NGs. The supernatant was removed, and the total drug content in the supernatant (released drug) was determined using a Jasco V-630 UV−visible spectrometer at 320 nm, as previously 'stated in our protocol[35]. The dissolving media was replaced with the same amount taken for sampling the supernatant to ensure 'sink' conditions.

6.2.4 In vitro hypoxia-selective evaluations of *nano*IAZA. Four key evaluations were done - **1)** cytotoxicity of the NGs, to prevent possible chemical toxicity to the delivery system; **2)** cytotoxicity of *nano*IAZA under normoxic and hypoxic conditions to evaluate its chemotherapeutic potential; **3)** radiosensitization potential of *nano*IAZA under hypoxic and normoxic conditions at various radiation doses; **4)** cellular uptake of the NGs and *nano*IAZA analog azidoazomycin arabinofuranoside (N_3-AZA) (ACN).

*6.2.4.1 Determination of cytotoxicity of the NGs and nano*IAZA. Proliferation 3-(4,5 Dimethylthiazol-2-Yl)-2,5-Diphenyltetrazolium Bromide (MTT) assay was performed to determine the inherent toxicity of the NGs in HeLa (cervical), PC3 (prostate) and FaDu (head & neck) cancer cell lines. Cells were seeded in 96 well plates at the density of 2,000 cells per well and incubated for 72 h in DMEM with 10% FBS and 1% antibiotic in a humidified atmosphere containing 5% CO_2 at 37 °C. The media was replaced with varying concentrations of NGs (up to 10 mg/ml) dissolved in fresh medium. The formazan crystals formed were dissolved in 100 µL of dimethylsulfoxide: isopropanol (1:1), and absorbance was measured at 570 nm using a Tecan Microplate reader. Untreated cells were used as a positive control, and the percentage of change in optical density (OD) was calculated in comparison to the control. For *nano*IAZA/IAZA, cells were exposed to increasing doses of IAZA or *nano*IAZA over a period of 72 h at 20% O_2 and <0.1% O_2 (in N_2 medical-grade gases) followed by staining with dimethyl thiazol dyes for metabolically viable cells.

Hypoxia was achieved using an in-house de-gassing system. Percent of OD values were calculated, and dose-response curves of *nano*IAZA and IAZA alone were generated to identify their effective chemo-toxic doses for hypoxic cells. For the colony formation assays, FaDu (a head & neck tumour cell line) and PC3 (prostate-specific membrane antigen-negative [PSMA-ve] cells) were seeded on 60-mm glass dishes (in triplicates) at densities ranging from 300 to 1,500 cells per plate. Cells were allowed to attach for 24 hours, followed by treatment with 0.1 mM concentration of IAZA and *nano*IAZA for 24 hours under normoxia (20% O_2) or hypoxia (<0.1% O_2) conditions. Cells were irradiated with 5 Gy of radiation and allowed to grow and form colonies for 14 days. Colonies were stained with crystal violet, counted and plotted as a percentage of the controls.

6.2.4.2 Determination of radiosensitization potential. Colony formation assays[52] were completed to determine radiosensitization potential. Briefly, cells were incubated with 0.1 mM IAZA or *nano*IAZA for 3 hours under normoxia (20% O_2) and hypoxia (<0.1% O_2) conditions, followed by irradiation (0, 4, 8, 12 and 20 Gy) and after 1 h cells were reoxygenated. Colonies were allowed to grow for up to 2 weeks, stained with crystal violet and then counted to evaluate the radiosensitization effect. Sensitivity enhancement ratio (SER) was calculated according to the following formula:

Equation 6-1.

$$\boldsymbol{SER} = \frac{D_{0\ Radiation\ Group\ Alone}}{D_{0\ Radiation\ Group\ with\ Drug\ under\ Hypoxia}}$$

6.2.4.3 Cellular uptake of nanogel (NG). Cells (1,000 cells/plate) were seeded onto sterilized 18 cm x 18 cm glass coverslips in 35 mm tissue culture plates and allowed to adhere overnight. The media was removed and replaced with 1 mg/mL of fluorescein isothiocyanate (FITC)-labelled NG/ACN according to our previous protocol[35]. The cells were incubated for 3 h, followed by three washes with PBS and fixed with 4% paraformaldehyde (PFA) for 15 min at 37 °C. Cells were stained with 4',6-diamidino-2-phenylindole (DAPI) for the cell nucleus, and with wheat germ agglutinin (WGA) Rhodamine for the cellular membrane. The slides were imaged using a Zeiss AxioObserver (inverted) Confocal Microscope. For flow cytometry, cells were grown in DMEM media supplemented with 10% FBS and 1% antibiotics. The cells were seeded at a density of $1x10^6$ cells per plate and were treated for 3 h hours with FITC-labelled-NGs. Fluorescence

intensity of the cells was analyzed using a BD FACS dual laser (488 and 635 nm) calibre flow.

6.2.4.4 In vitro validation of inverse oxygen-dependent entrapment of Azido-conjugated nitroimidazole (ACN). FaDu cells were trypsinized, and approximately $3x10^5$ cells were seeded in 35 mm tissue culture plates containing sterilized 18 cm x 18 cm glass coverslips. Cells were allowed to grow overnight and treated with two concentrations (1 μM and 10 μM) of ACN/*nano*ACN (**NG1**-encapsulated ACN) under normoxia (20% O_2) or hypoxia (<1% O_2) for up to 6 hours. For the time course evaluation, the cells were incubated with 100 μM *nano*ACN for 1, 2, 4 and 6 hours under normoxia and hypoxia (<0.1% O_2). Post-treatment, all steps were done at room temperature (22 °C). Cells were washed three to five times with 1X PBS, fixed in 2% paraformaldehyde (PFA) for 20 minutes, and washed again three times with 1X PBS. The fixed cells were then blocked and permeabilized with 1% BSA in 1X PBS containing 0.1% Triton-100 for 20 minutes, followed by incubation with a click cocktail containing Alexafluor 594 conjugated alkyne for 30 minutes. Subsequently, cells were washed and stained with Hoechst 33342 (1:10000 dilution in PBS, Life Technologies) for 5 minutes before mounting them on glass slides (Fluoroshield Mounting Medium, abcam). The prepared slides were kept at 4° C until imaged. Images were obtained using a Plan-Apochromat 40X/1.3 Oil DIC lens on a Zeiss 710 confocal microscope using Zen 2011 software.

6.2.4.5 Click chemistry reaction.

The Click-IT reaction cocktail (Molecular Probes) was made up according to the manufacturer's directions using a 1:5000 dilution of the 2 mg/ml Alexafluor 594 conjugated alkyne stock (Molecular Probes). The reaction cocktail was used within 15 minutes of preparation. All reactions were done at room temperature in dark conditions.

6.2.5 In vivo Acute Toxicity evaluation of a single dose of the nanogel (NG) polymer and IAZA in an immunocompromised mouse model. All animals used in this research project were housed and cared for as per the recommendations of the Canadian Council on Animal Care (CCAC) and any applicable federal or provincial legislation according the Cross Cancer Institute Vivarium regulations; male NSG and NU/NU mice weighing about 25–30 g were used for these studies.

6.2.5.1 In vivo Acute Toxicity. The 'single-dose' toxicity of the NG polymer in a healthy NSG mouse model was determined at three (3) different doses (308, 462 and 615 mg/kg of nanogel per mouse; via intraperitoneal injection (i.p.) For this study, 10 NSG mice were used: three (3) animals each for two groups that were evaluated at doses of 615 and 462 mg/kg **NG1**, respectively, and two (2) animals each for the lowest dose of 308 mg/kg of **NG1** and the control group (saline). The tested amount of **NG1** is based on delivering chemically safe doses of IAZA (200, 400 and 600 mg/kg) and to validate the slow release and safe use in future therapy studies. The animals were administered with 300 μL volume of the NG solutions/control (saline) i.p. and monitored daily for up to 8 days as per the CCAC guidelines.

For the toxicity evaluation of IAZA, three (3) doses were tested: 200, 400 and 600 mg/kg using i.p administration. The study used eight (8) animals for each dose, plus four (4) control animals. Three (3) animals from each group plus two (2) animals from the control group were euthanized after 8 days to evaluate internal organ pathology, blood chemistry and clotting factors. The remaining five (5) animals per group and two (2) animals from the control group were euthanized after 14 days to assess internal organ pathology and blood chemistry. Observations that included respiration, eating, locomotion, behaviour, appearance and weight were recorded on a monitoring chart. After 8 or 14 days of the injection, the animals were sacrificed and the organs including liver, kidneys, spleen, heart, lungs, brain, stomach, intestine and cecum were excised, collected and sent for pathology studies to the veterinarian pathologist Dr. Nick Nation to evaluate organ toxicity/abnormalities. Similarly, blood was collected immediately after euthanizing the mice by heart puncture, and the blood was analyzed by IDEXX laboratory for a liver panel testing that included the following enzymes: Alkaline phosphatase, ALT (SGPT), AST (SGOT), bilirubin (total), GGT, sorbitol dehydrogenase (SDH).

*6.2.5.2 Nano*IAZA *in vivo Chemotoxic assessment in a FaDu tumour mouse model.* A FaDu tumour model was used to determine the chemotoxicity of IAZA and *nano*IAZA. The tumours were grown by a subcutaneous injection of ~5-6 x 10^6 FaDu cells (in 0.1 ml serum-free media) in the mice's upper right flank. Tumour growth was monitored daily; a rotational ellipsoid formula determined tumour volume: $(\pi/6)ab^2$, where a is the longest and b is the perpendicular shorter tumour axis. An initial tumour volume range of 200-300

mm^3 was proposed to minimize the hypoxia heterogeneity within tumours. Once the tumour reached the desired volume, tumour-bearing animals were administered i.p. with a single dose of 400 mg/Kg of IAZA/*nano*IAZA; 308 mg/Kg NG; or 15% DMSO. Two (2) hours prior to sacrifice, all animals were administered, i.p. with ACN using a 60 mg/Kg dose. Once the tumour reached a volume of 1,500 mm^3, the animals were sacrificed. Eight (8) NU/NU mice per group were used in the IAZA/*nano*IAZA/NG groups, and six (6) mice were used for the 15% DMSO control group. An extra set of four (4) mice was used to evaluate the initial tumour hypoxia when the tumour size was between ~150-350 mm^3 range. For these animals, 60 mg/Kg ACN was injected i.p. two (2) hours prior to sacrifice. The tumours were frozen in optimal cutting temperature (OCT) compound solution and sliced axially, four (4) different tumour sections were taken, and two (2) sections were stained with the click cocktail staining protocol described above with DAPI and CD31 antibody (Figure 6-7b). For the hypoxic quantification MATLAB and Image Processing Toolbox Release 2018b, The MathWorks, Inc. was used. A manual threshold, determined from the negative control, was applied for the ACN stained slides. Edges were excluded from the quantification. The Otsu threshold was chosen for the Blue DAPI stained slides. Images were converted to binary according to their respective threshold, and the hypoxic fraction was calculated as:

Equation 2:

$$\textbf{Hypoxic fraction (HF)} = \frac{Area\ of\ pixels\ stained\ with\ ACN}{Area\ of\ pixels\ stained\ with\ Blue\ DAPI} * 100$$

6.3 RESULTS & DISCUSSION

6.3.1 Encapsulation efficiency and release profiles of *nano*IAZA. In a previous study conducted by our group, (poly[(LAEMA$_{21}$)-*b*-(DEGMA-*st*-MBAm)$_{300}$] was synthesized by the RAFT method with 7% crosslinker and 82 nm size at 37 ºC that showed 60% encapsulation efficiency for IAZA[35]. In this study, optimization of the NGs was achieved by modifying their hydrodynamic size, the composition of the core, hydrophobicity, surface/core charge and crosslinker percentage, as shown in Table 6-1. The NGs exhibited a neutral to slightly negative surface charge and small hydrodynamic sizes down to 55.1

nm at 37 °C for **NG1**. In some cases, possible aggregation was seen reaching a size up to 262.5 nm at 37 °C (**NG7**) (Figure 6S2).

Table 6-1. Analysis and characterization of the composition, hydrodynamic size, surface charge, and polydispersity of synthesized NGs.

Nanogel	Composition	Cross-linker %	Hydrodynamic size (nm)		Zeta Potential (mV)		PDI
			15 ºC	37 ºC	15 ºC	37 ºC	
NG1	Poly[(LAEMA$_{19}$)-*b*-(DEGMA-*st*-MBAm)$_{110}$]	9	70.9 ± 1.3	55.1 ± 0.6	-8.45 ± 1.19	-6.9 ±0.7	0.197
NG2	Poly[(LAEMA$_{22}$)-*b*-(DEGMA-*st*-MBAm)$_{100}$]	10	194.3 ± 8.2	81.3 ± 1.0	-0.18 ± 0.24	19.2 ± 1.09	0.223
NG3	Poly[(LAEMA$_{20}$)-*b*-(DEGMA-*st*-MBAm)$_{100}$]	10	287.7 ± 6.8	142.6 ± 7.5	0.04 ± 0.23	-8.28 ± 3.11	0.324
NG4	Poly[(LAEMA$_{20}$)-*b*-(DEGMA-*st*-MBAm)$_{300}$]	7	127.6 ± 1.3	96.5 ± 0.6	-0.04 ± 0.26	0.00 ± 0.3	0.321
NG5	Poly[(LAEMA$_{22}$)-*b*-(DEGMA-*st*-MBAm)$_{100}$]	7	79.8 ± 2.2	57.8 ± 2.0	-0.25 ± 0.29	-0.03 ± 0.25	0.262
NG6	Poly[(LAEMA$_{22}$)-*b*-(DEGMA-*st*-MBAm)$_{100}$]* *Different solvent ratio than NG5	7	287.6 ± 8.8	215.6 ± 11	-2.51 ± 2.46	-0.09 ± 0.09	0.223
NG7	Poly[(LAEMA$_{20}$)-*b*-(DEGMA-*st*-MBAm)$_{100}$]	7	288.1 ± 11.5	262.5 ± 4.2	-0.04 ± 0.14	-9.39 ± 3.64	0.193

The thermoresponsive nature of the NGs plays a critical role in the encapsulation and release of the drugs within the core as a function of temperature. At low temperatures (4 °C), the NGs core is hydrophilic. It swells in an aqueous solution (encapsulation), while as the temperature rises above the lower critical solution temperature (LCST) between ~34-35°C (Figure 6S1) , the polymer precipitates out of solution due to hydrophobic interactions with the aqueous solution causing the core to collapse, allowing the slow controlled release of the drug at physiological body temperature.

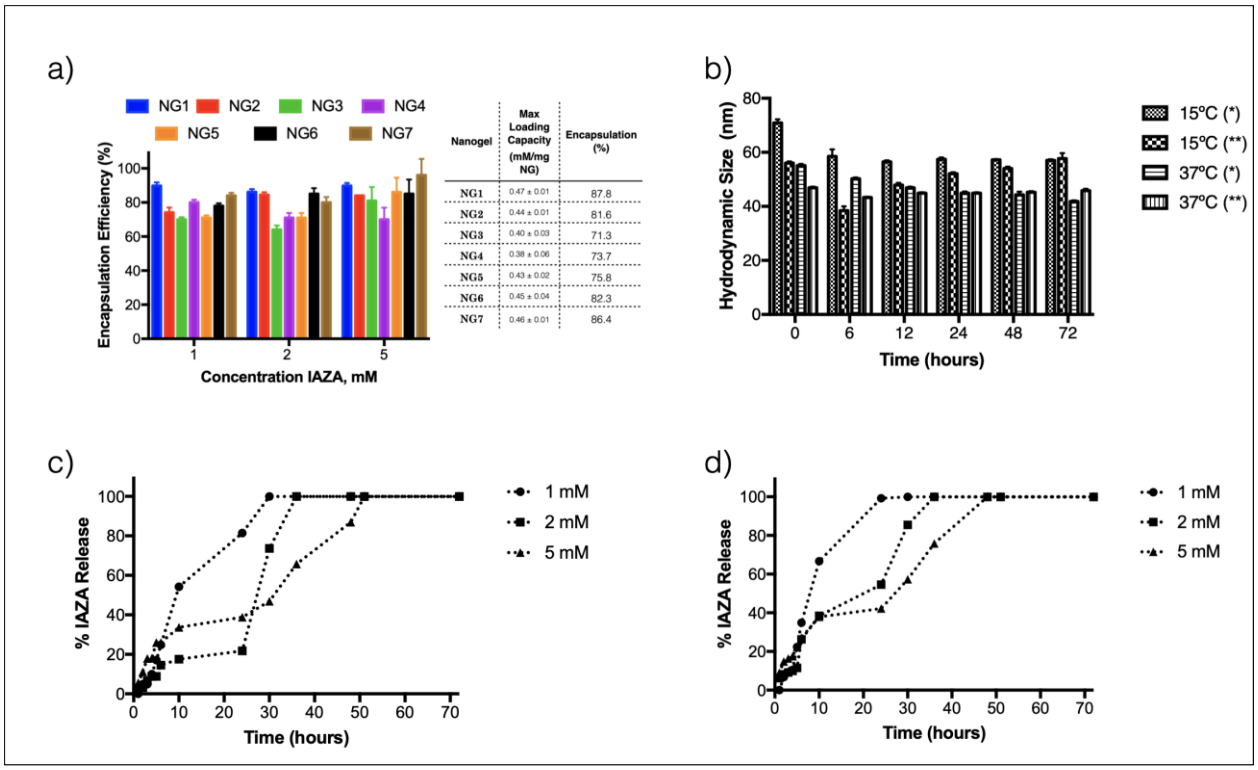

Figure 6-1. a) Encapsulation efficiency of 1, 2 and 5 mM of IAZA within NGs core and maximum loading capacity. IAZA has been loaded in the NGs by an incubation method - a solution of the NG was mixed with different amounts of IAZA (1, 2 and 5 mM) with a 10:1 feed ratio in excess NG and then incubated for 24 h. The amount of IAZA encapsulated in the NG was determined by sampling the supernatant using UV-visible spectroscopy at 320 nm (UVmax for IAZA). Value = mean ± standard deviation, n = 3. The table shows the calculation of the maximum loading capacity of the synthesized NGs. The amount of encapsulated IAZA was estimated by calculating the difference between the total amount of IAZA added in solution and the amount of free IAZA in the aqueous supernatant after the NG is precipitated. b) **NG1** stability up to 72 h. The nanogel stability was determined by measuring the change in the hydrodynamic size of the nanogel in the presence (*) and absence (**) of serum proteins up to 72 h at 15 and 37 ºC. Release profile of IAZA encapsulated in **NG1** at 1, 2 and 5 mM at (c) 37 ºC and (d) 39 ºC. Release profile of IAZA from the NGs complex has been established by re-suspending the NG complex in preheated phosphate-buffered saline (PBS). The sample was centrifuged, precipitating the

'unbound' NGs. The supernatant was removed, and the total drug content in the supernatant (released drug) was determined by Jasco V-630 UV−visible spectrometer at 320 nm.

Two factors have played important roles in enhancing the encapsulation capacity of the NGs for IAZA; 1) the degree of cross-linking in the core with MBAm, and 2) the hydrodynamic size of the NGs[35]. At higher concentration (5 mM), **NG4** showed lower encapsulation efficiency (~ 73.7%) due to its smaller size (127.6 ± 1.3 nm and 96.5 ± 0.6 at 15 ºC and 37 ºC, respectively) in comparison to **NG7,** which showed higher encapsulation efficiency (~86.4%) with a size of 288.1±11.5 and 262.5±4.2 nm at 15 ºC, 37 ºC. The most hydrophobic core **NG4** (DP:300) showed less encapsulation capacity (~73.7%) compared to **NG7** (DP:100) (~86.4%). At lower concentrations (1-2 mM), **NG1** showed the highest encapsulation efficiency (87.8%) (Figure 6-1a). The smallest size and crosslinker density within the core (9%) favoured the encapsulation of IAZA in a more compact and stable structure, protecting the hydrophobic core from collapsing and burst-releasing IAZA. The maximum encapsulation loading capacity within the core was **NG1** with 0.47 mM IAZA per milligram of NG (Figure 6-1a).

Above the lower critical solution temperature (LCST), the polymer precipitates out of solution due to hydrophobic interactions with the aqueous solution, which triggers a phase transition from a swollen hydrated state (hydrophilic) to a shrunken dehydrated state (hydrophobic), allowing the encapsulated (macro)molecules to be released (Figure 6S1). **NG1** and **NG5** were the smallest NGs (70.9 ± 1.3 and 55.1 ± 0.6 nm / 79.8 ± 2.2 and 57.8 ± 2.0 nm at 15 ºC, 37 ºC respectively) and exhibited the slowest release profiles at 1, 2 mM and 5 mM. It was also evident that at higher concentrations (5 mM), lower percentage (%) of the crosslinker displayed a slower release (**NG2** (10%) crosslinker than **NG5** (7%) and **NG3** (10%) crosslinker than **NG7** (7%); **NG2** and **NG3** have faster release) (Figure 6S3)**. NG3** has a higher cross-linker % (10%) in comparison to **NG4** (7%), thus **NG3** may have a longer length of polymer than **NG4** resulting in a larger size (287.7 ± 6.8 nm vs. 127.6 ± 1.3 at 15 ºC respectively) .

The gradual release of 5 mM IAZA at 37 ºC and 39 ºC over a period of 50 h (Figure 6-1c-d) demonstrated the potential of **NG1** to deliver IAZA in therapeutically effective doses in

a controlled manner securing higher bioavailability of the drug. **NG1** was selected for further experiments due to its smaller size (70.9±1.3 and 55.1±0.6 nm at 15 ºC, 37 ºC), highest encapsulation efficiency (87.8%), slowest release (50 h) at 37 ºC and 39 ºC and high stability up to 72 h (Figure 6-1b); attributes that could potentially grant an optimal cellular delivery of IAZA.

6.3.2 Cellular uptake of *nano*IAZA. FITC-labeled-**NG1** was used to evaluate the cellular internalization of the NGs. The release profile of the FITC-labeled **NG1** was evaluated for encapsulated IAZA and Azido Conjugated Nitroimidazole (ACN) (IAZA analog) up to 10 h (Figure 6S4) showing a similar percentage of release at 5 mM (~65%) than the unlabelled **NG1**. Studies after 3 h of incubation by flow cytometry in FaDu, HeLa and PC3 cell lines (Figure 6-2) showed higher fluorescence intensities of the FITC-labeled **NG1** in all the cell lines compared to the untreated cells validating the cellular uptake of **NG1** and unveiling its promising ability as delivery vectors.

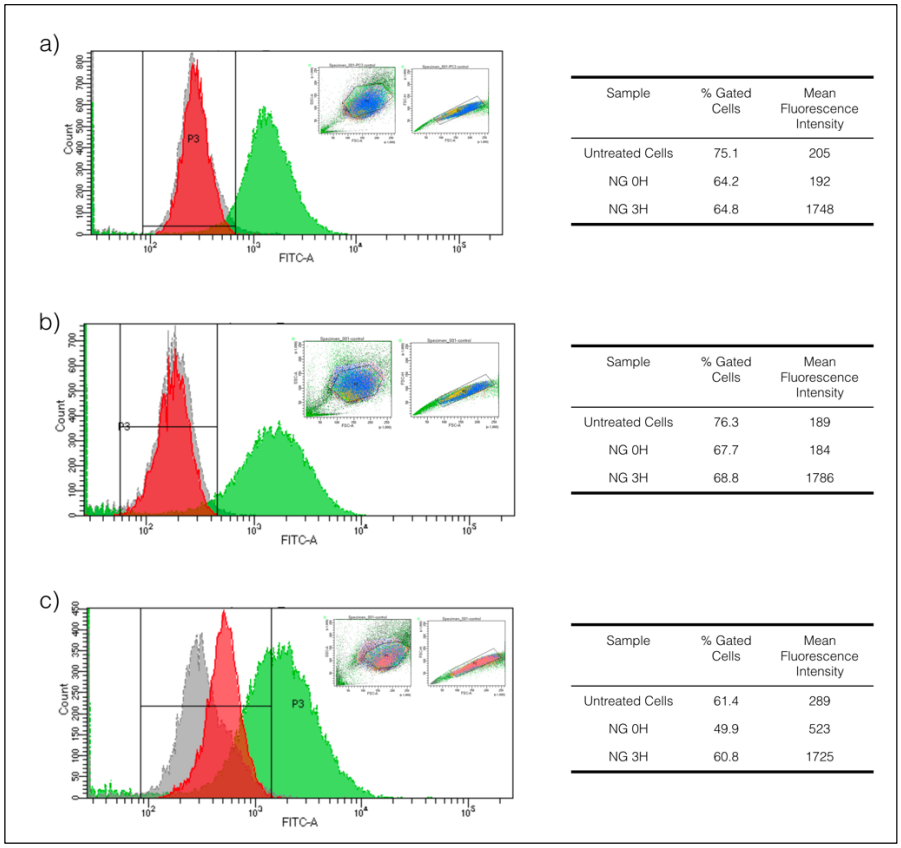

Sample	% Gated Cells	Mean Fluorescence Intensity
Untreated Cells	75.1	205
NG 0H	64.2	192
NG 3H	64.8	1748

Sample	% Gated Cells	Mean Fluorescence Intensity
Untreated Cells	76.3	189
NG 0H	67.7	184
NG 3H	68.8	1786

Sample	% Gated Cells	Mean Fluorescence Intensity
Untreated Cells	61.4	289
NG 0H	49.9	523
NG 3H	60.8	1725

Figure 6-2. Flow cytometry analysis of cellular uptake of FITC-labelled-**NG1,** as compared to untreated cells (gray colour); negative control; cells incubated with FITC-labeled-**NG1** but washed immediately after addition (red) and cells incubated for 3 h with FITC-labeled-**NG1** (green) in a) HeLa b) FaDu c) PC3 cell lines. Cells were grown in DMEM media supplemented with 10% FBS and 1% antibiotics. The cells were seeded at a density of $1x10^6$ per plate and were treated for 3 h hours with FITC-labelled-**NG1**. Cells were analyzed using a BD FACS dual laser (488 and 635 nm) calibre flow.

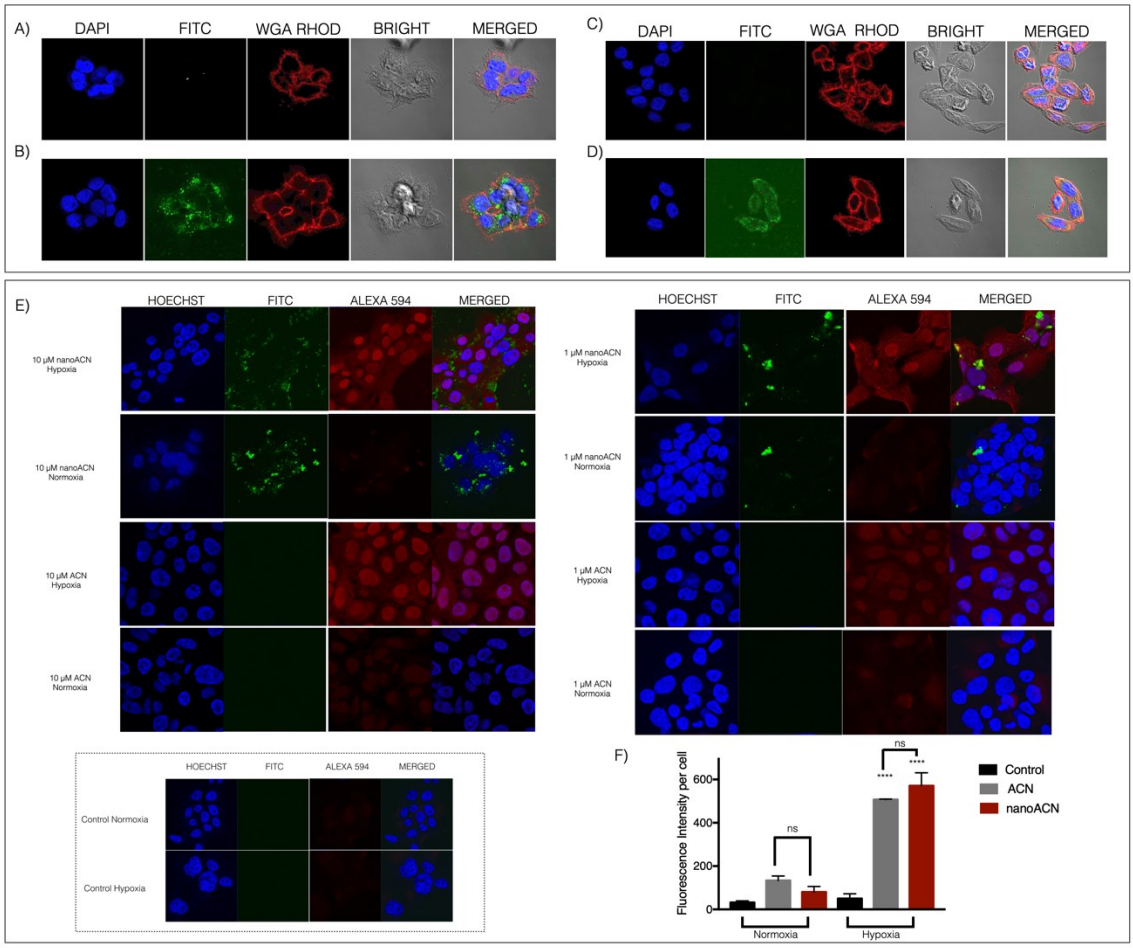

Figure 6-3. Cellular uptake of FITC-labeled **NG1** in FaDu and PC3 cell lines A) Control (FaDu) B) FITC-labeled-**NG1** (FaDu) C) Control (PC3) D) FITC-labeled-**NG1** (PC3) after 3 h of incubation. Cells (1000 cells/plate) were seeded onto glass coverslips in 60 mm tissue culture plates and allowed to adhere overnight. The media was removed and replaced

with 1 mg/mL of FITC-labeled **NG1** in DMEM media and incubated for 3 h, followed by three washes with PBS and fixed with 4% paraformaldehyde (PFA) for 15 min at 37 °C. Cells were stained with 4',6-diamidino-2-phenylindole (DAPI) for cell nucleus, wheat germ agglutinin (WGA) Rhodamine for cellular membrane and were imaged using a Zeiss AxioObserver (inverted) Confocal Microscope. E) ACN encapsulated in FITC-labeled **NG1** (*nano*ACN) after 6 h of incubation. ~0.5 million FaDu cells were seeded on 18 mm x 18 mm coverslips and were allowed to attach for 24 h. Cells were incubated with 10 μM and 1 μM ACN encapsulated in **NG1** (*nano*ACN) and ACN for 6 h under normoxia and hypoxia (<0.1% O_2). Cells were fixed with 2% PFA. Click chemistry was performed using an Alexa 594 conjugated alkyne followed by nuclear staining with Hoechst. Normoxic treated cells displayed minimal background signal. F) Fluorescent intensity quantification per cell. Images were processed with IMARIS software (Bitplane, Zürich, Switzerland) to quantify average channel intensity per cell. No statistical significance was found in the fluorescence levels between ACN and nanoACN both under normoxia and hypoxia.

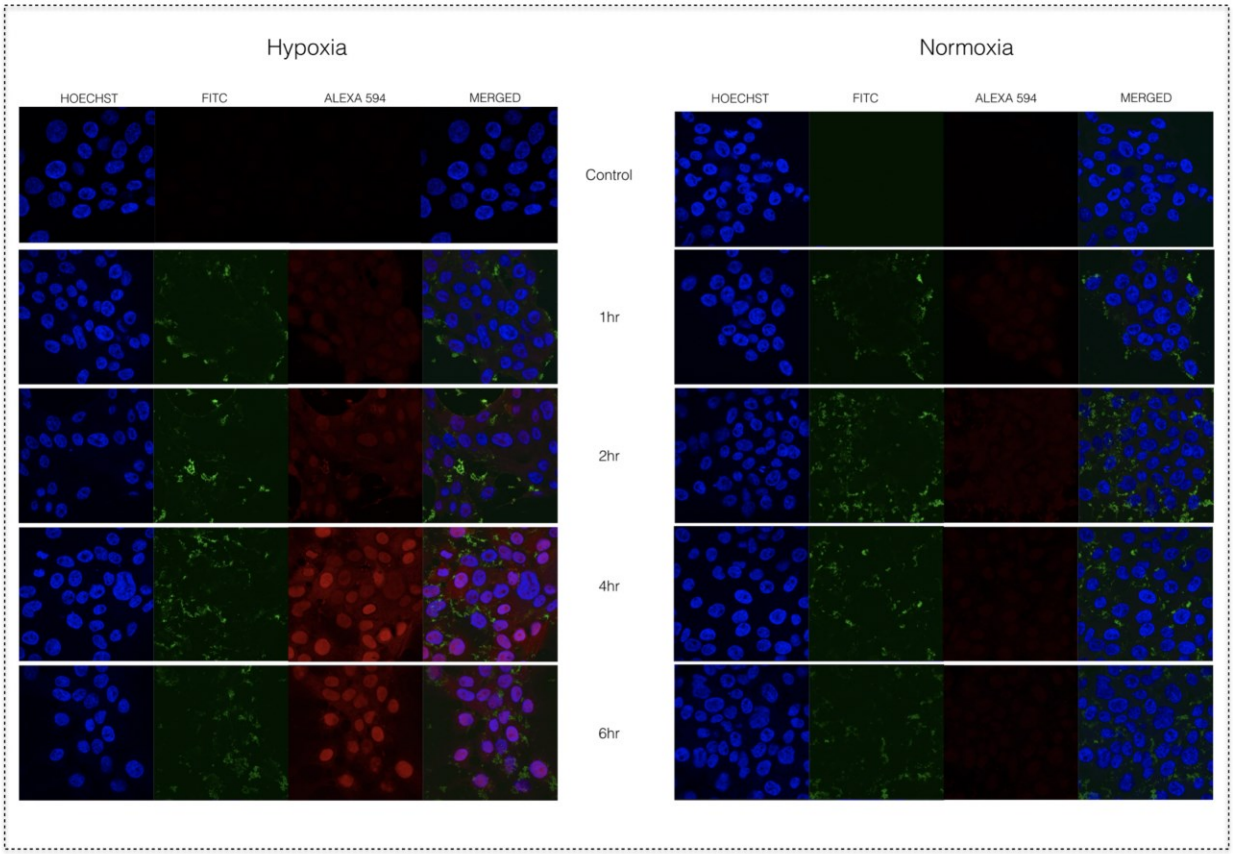

Figure 6-4. Time course release of ACN encapsulated in FITC-labeled **NG1** (nanoACN). ~0.5 million FaDu cells were seeded on 18 mm x 18 mm coverslips and were allowed to attach for 24 h. Cells were incubated with 100 μM *nano*ACN for 1, 2 ,4 and 6 h under normoxia and hypoxia (<0.1% O_2). Cells were fixed with 2% PFA after the previously mentioned intervals of incubation. Click chemistry was performed using an Alexa 594 conjugated alkyne followed by nuclear staining with Hoechst.

The delivery of drugs to targeted regions by evading phagocytic uptake, enzymatic degradation by nucleases, triggering of the immune response, and the hydrophobic plasma membrane barrier pose significant challenges to the internalization of small molecule therapeutics[53]. IAZA is prone to deiodination and non-specific interactions with blood proteins under biological conditions[25,54] that can be overcome by encapsulating IAZA in thermoresponsive NGs, such as **NG1** that forms a stable and compact complex, i.e., *nano*IAZA, which will assure prolonged stability in the physiological environment and transport to the intracellular side as seen in Figure 6-3. Localization of FITC-labeled **NG1** within the cytoplasm (Figure 6-3A-B; C-D) corroborates this vector's successful use to deliver IAZA and upholds its mechanistic selective bioreduction in hypoxic cells. A confocal microscopy simulation video of the cellular uptake of the FITC-labeled **NG1** in a FaDu cell is included as supporting information.

Rashed *et al.* have developed a click chemistry-based approach using an azido (N_3)-conjugated derivative of IAZA, the parent compound; (Azido Conjugated Nitroimidazole, ACN). ACN is a structural analogue of IAZA; it contains an azido (N_3) group instead of iodine at *C5* of the arabinose sugar. In the presence of a copper (I)-catalyst, the N_3 group of ACN reacts with an alkyne at room temperature, forming regioselective cycloadditions. Using a fluorescent alkyne molecule, the drug can be imaged. The same cellular uptake experiment was conducted with ACN and FITC-labelled **NG1** (*nano*ACN) to observe the co-localization of **NG1** and the release of the IAZA analog. Encapsulation of ACN in FITC-labeled **NG1** validated the internalization and selective activation of ACN in the hypoxic environment (Figure 6-3E). FaDu cells entrapped ACN in an inverse oxygen-dependent manner. Normoxic cells showed minimal to almost no entrapment of *nano*ACN. A time-course incubation with *nano*ACN (Figure 6-4) showed that ACN was released from the **NG1** after 2 h of incubation and was bio-reduced (hypoxic selective activation) in a

hypoxic environment as compared to the lower fluorescence signal observed under normoxia.

Additionally, the fluorescence of *nano*ACN was still present after 6 h of incubation. These results conferred *nano*ACN with great hypoxia-specific imaging capabilities and improved reagent characteristics for assessing hypoxia in cells and tumour sections. The click chemistry design offers the advantage of a single-step detection of hypoxia over traditional immunostaining. The click chemistry between the azide moiety of ACN and the fluorophore-conjugated alkyne permitted mapping of the selective hypoxia entrapment of the IAZA analog using fluorescence microscopy, thus allowing us to trace the release of ACN from the NGs, which is demonstrated by enhanced signal than the corresponding non-encapsulated ACN.

6.3.3 Cytotoxicity of NGs and *nano*IAZA. The cells' metabolic activity in the presence of the nanogels was determined by MTT assay showing high metabolic activity up to a concentration of 500 μg/ml. IC_{50} values for **NG1** were determined for PC3, HeLa (376.1 and 304.8 mg/L respectively) and FaDu cells (170.9 mg/L), indicating **NG1** to be slightly more toxic to FaDu cells (Figure 6-5a,b,c). The inherent toxicity of IAZA was determined under normoxia (20% O_2), and hypoxia conditions (<1% O_2) conditions; cells were exposed to increasing doses of IAZA up to 1 mM. For the MTT assay, FaDu, HeLa and PC3 cells were incubated for 72 h (Figure 6S5). For the colony formation assays, FaDu and PC3 cells were incubated for 24 h under normoxia and hypoxia conditions followed by 14 days of normoxic incubation to form the colonies. IAZA was found to be relatively non-toxic under normoxia at concentrations up to 1 mM, and about 50% killing was observed under hypoxic conditions for head & neck (FaDu) and prostate (PC3) cancer cell line at relatively high concentrations (>0.5 and 1 mM respectively). (Figure 6S6). *Nano*IAZA was evaluated as a chemosensitizer at a concentration of 1 mM according to the previous drug screening. The chemotoxic potential of *nano*IAZA and IAZA alone was determined at 20% O_2 (normoxia) and <0.1% O_2 (hypoxia). A dose of 1 mM IAZA alone/*nano*IAZA was added to cells and exposed for 72 hours, followed by MTT staining. Under normoxia, the *nano*IAZA complex showed similar toxicity as IAZA alone for PC3 cell line and lower toxicity in FaDu and HeLa. Overall, IAZA exhibited more cytotoxicity

under hypoxic conditions in the encapsulated form except for HeLa, which was comparable to the non-encapsulated form (Figure 6-5d).

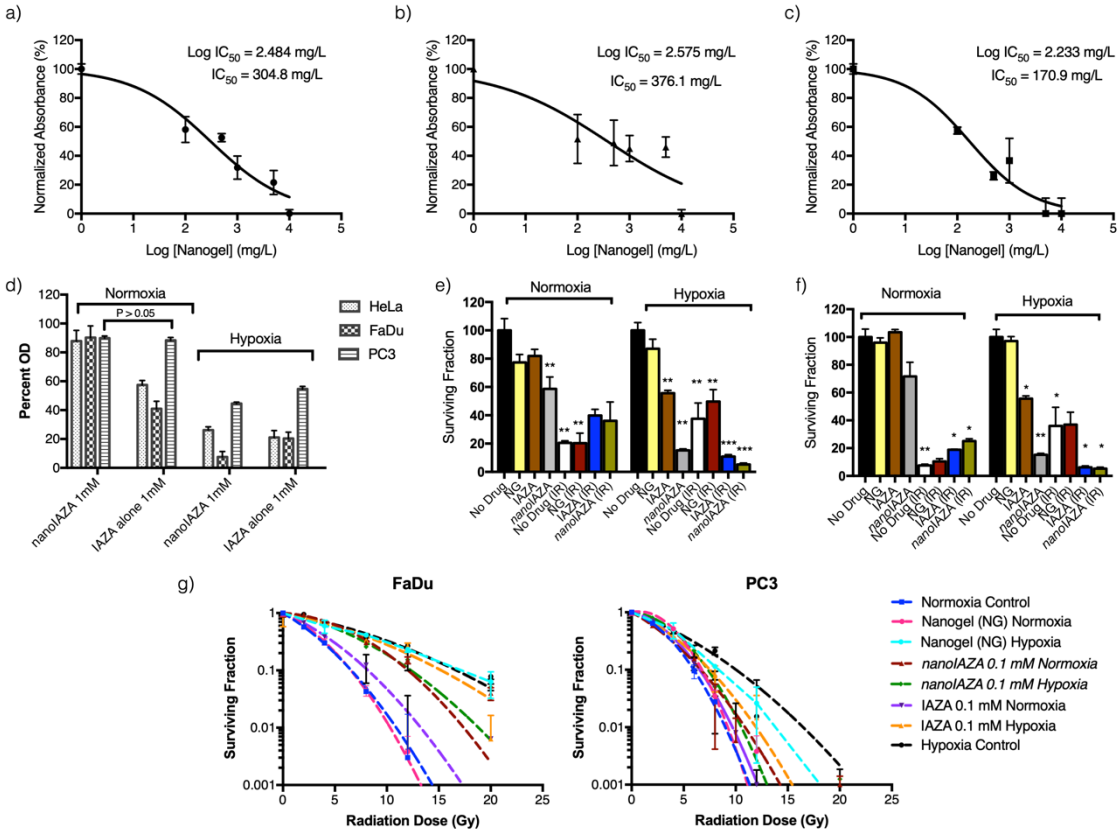

Figure 6-5. Cytotoxicity evaluation of **NG1** in (a) HeLa (cervical), (b) PC3 (prostate) and (c) FaDu (head & neck) cell lines. Proliferation MTT assay was performed to determine the inherent toxicity of the NG1 in the proposed cell lines. IC_{50} values were calculated, showing low toxicity and high biocompatibility up to a concentration of ~300 mg/L for HeLa and PC3 and 170 mg/L for FaDu. d) Cytotoxicity evaluation of *nano*IAZA (2.13 mg **NG1** + 1mM IAZA) complex and 1 mM IAZA alone under normoxia and hypoxia for HeLa, FaDu, and PC3 cell lines. Cells were treated with 1mM IAZA or *nano*IAZA for 72 h at 20% O_2 (normoxia) and <0.1% O_2 (hypoxia), followed by staining with dimethyl thiazol dyes for metabolically viable cells. Untreated cells were used as a positive control, and the percentage of OD was calculated. All experiments were performed in triplicates. *P* values were calculated using 1-way ANOVA, t-TEST. $P > 0.05$ was considered not statistically significant. Colony Formation Assay of e) FaDu cell line f) PC3 cell line with

0.1 mM IAZA/*nano*IAZA or 0.21 mg **NG1** after irradiating with 5 Gy. Colony formation assays were performed to determine the radiosensitization potential. Cells were incubated with 0.1 mM IAZA/*nano*IAZA or 0.21 mg NG for 24 hours under normoxic (20% O_2) and hypoxic (<0.1% O_2) conditions, followed by irradiation with 5 Gy. Colonies were allowed to grow for up to 2 weeks, stained with crystal violet and then counted to evaluate the radiosensitization effect. Value = mean ±SD, n = 3. *P < 0.05, **P < 0.01, ***P < 0.001 (One-way ANOVA). g) *In vitro* radiosensitization of FaDu and PC3 cells by IAZA alone, nanogel (NG) and *nano*IAZA complex under normoxia (20% O_2) and hypoxia (<0.1% O_2) conditions. Clonogenic survival assays were done to evaluate the radiosensitization potential of *nano*IAZA. The cells were incubated with IAZA/*nano*IAZA/NG for 3 h under hypoxic and normoxic conditions, followed by exposure to ^{60}Co X-ray radiation (0, 4, 8, 12 and 20 Gy) and hypoxic cells were reoxygenated after 1h incubation.

6.3.4 *Nano*IAZA is selectively more toxic to hypoxic cells, acting as a radiosensitizer and also provides radioprotection to normoxic cells. Radiosensitizers are defined as chemical or pharmacologic agents that *mimic* oxygen to enhance hypoxic tumour cells' sensitivity to external-beam radiation therapy's killing effects. Radiation-resistant cells might arise from differences in the distributions of the initial ionization events, leading to variances in spatial clustering of damage from the free radicals that are the ultimate cause of cell death[55]. Three main biological factors that have been shown to affect the outcome of radiotherapy are 1) hypoxia, 2) the ability of the surviving cells to repopulate after treatment, and 3) intrinsic radio-resistance of the tumour cells[56]. Similarly, radiosensitivity might be caused by differences in proteins' levels or activity involved in DNA repair mechanisms or signalling proteins. Hence chemo-radiosensitizers can be categorized into agents that react with short-lived free radicals or those that target DNA repair enzymes or cell signalling proteins that affect radiation damage more indirectly. IAZA undergoes an intracellular single-electron reduction of the nitro group to form a radical anion at -390 mV. The reduction ($^1E_7$) step is reversible in the presence of O_2[57] while under hypoxic conditions, radical anions are generated that bind to cellular molecules to form trapped covalent adducts. The degree of binding relies on the O_2 concentration[58] and cell viability with no accrual of bioreductive species observed in necrotic cells and little accumulation and low toxicity in normal cells. In a colony formation assay, hypoxia selective cytotoxicity

was seen in IAZA- and *nano*IAZA-treated cells (Figure 6-5e-f). For colony formation, FaDu and PC3 cells were seeded at densities ranging from 300 to 1,500 cells per plate, followed by treatment with 0.1 mM IAZA/*nano*IAZA for 24 h under normoxia (20% O_2) or hypoxia (<0.1% O_2). Cells were irradiated with 5 Gy single radiation dose and allowed to grow and form colonies for 14 days. According to the observed results in Figure 6-5e-f, both IAZA and *nano*IAZA act as radiosensitizers, with the latter (*nano*IAZA) showing relatively higher cytotoxicity to hypoxic cells than IAZA alone. Under normoxic conditions, both acted as radioprotectants.

6.3.5 In vitro evaluation of radiosensitization potential of *nano*IAZA. Clonogenic survival assays were done to evaluate the radiosensitization potential of *nano*IAZA. The cells were incubated with IAZA and *nano*IAZA for 3 h under hypoxic and normoxic conditions, followed by exposure to escalating single doses of ^{60}Co X-ray radiation. Cells situated beyond the diffusion distance of oxygen (70 μm)[59] within tumours (hypoxic cells) exhibited a clonogenic and radioresistant phenotype. Aberrant tumour vasculature and rapid growth of solid tumours facilitate the creation of regions with low oxygen tensions. Hypoxia is recognized to change neoplastic cell metabolism and contributes to therapy resistance by inducing cell quiescence and stimulating complex cell signalling networks, including the HIF, PI3K, MAPK, RAS, mTOR and NFκB pathways involved in tumour blood vessel formation, metastasis, and development of resistance to chemo/radio therapy[60]. Hypoxic cells typically require two to three times (2-3X) higher radiation doses to potentiate a killing effect in comparison to well-oxygenated cells. Radiosensitizers are intended to enhance tumour cell killing while having fewer effects on normal tissues since they do not get bioreduced in the presence of oxygen[55]. Fixation of radiation-induced DNA damage usually requires high levels of toxic compounds that would affect normal cells; an efficient hypoxic radiosensitizer is the one that can mimic the effects of oxygen without harming normal cells in a significant manner[61]. A way to modulate the tumour microenvironment to improved radiotherapy is by targeting hypoxia using hypoxia-activated prodrugs (HAPs) that selectively activate under bioreductive conditions to induce tumour-specific toxicity. Hypoxia-selective cytotoxicity requires one-electron reduction of a HAP to a radical more toxic than superoxide. Radiosensitizers, such as nitroimidazoles

that radiosensitize hypoxic cells with radiation-induced free radicals, has been studied since the 1960s.

The most popular nitroimidazole-based compound is Misonidazole; however, it was found to cause dose-limiting neuropathies in Phase I clinical trials[62]. Pimonidazole is another drug that showed enhanced efficacy in vitro and good tumoral uptake, but despite these features is was not found useful in clinical trials as a radiosensitizer and was later used as a radiotracer for hypoxia imaging[63]. Nimorazole, a 5-nitroimidazole derivative, has been effective in several clinical trials and has been used to treat head and neck cancers in Denmark[64]. Nonetheless, poor performance as *in vivo* radiosensitizers, when used in conjunction with X-ray treatment, has been attributed to their inability to achieve radiosensitizing concentrations at dose-limiting neurotoxicities[65]. Several positron emission tomography (PET) tracers, including fluorine18-labelled fluoromisonidazole ([^{18}F]FMISO,)[66], fluorine18-labelled fluoroazomycin arabinoside ([^{18} F]FAZA)[67,68], and the single-photon emission computed tomography (SPECT) agent iodine-123-labelled iodoazomycin arabinoside ([^{123}I]IAZA)[18,54] have found extensive clinical use in diagnostic imaging of a variety of hypoxic tumors[69]. Here we confirmed the potential therapeutic effects of *nano*IAZA as a radiosensitizer. To find a useful application in the clinic, a radiosensitizer must show a therapeutic improvement for tumours with non- to minimal damage to healthy tissues, which is facilitated by hypoxia-selective uptake, differential absorption rate, or extent of the biological half-life. The radiosensitizers must be effective at systemically non-toxic dosages (minimal side effects), and their effectiveness is measured in terms of the sensitization enhancement ratio (SER)[70]. The SER ratio for IAZA/*nano*IAZA was calculated as the radiation dose needed for radiation alone divided by the dose needed for 1mM IAZA/*nano*IAZA plus radiation at a survival fraction of 0.1%. The SER value for *nano*IAZA was ~1.41 compared to 1.09 for IAZA alone in FaDu cells, and 1.58 vs 1.40 for PC3 cells (Figure 6-5g) for a 99.9% cell kill. This shows significant radiation sensitivity enhancement in both cell lines with the encapsulated compound. Additional *in vivo* studies are required to corroborate the radiosensitization effects seen with *nano*IAZA *in vitro* and to extend the potential use of this drug-delivery system as a hypoxic radiosensitizer.

6.3.6 Determination of a single dose toxicity of the nanogel (NG) polymer used for delivering IAZA. Nanogels (NGs) and their unique stimuli-responsive features, loading capacity, high stability, cationic/anionic functionalization, and responsiveness to environmental factors (ionic strength, pH, and temperature sensitivity) have proven to be a promising material for delivering IAZA *in vitro*. Our proof-of-principle studies confirmed that the encapsulated form of IAZA (*nano*IAZA) in functionally-modified NGs improved the drug-bioavailability in hypoxic cancer cells *in vitro,* which enhanced their radiosensitization potential. The first phase in the animal studies was the determination of the biocompatibility of the NG. The NG used is composed of LAEMA (2-lactobionamidoethyl methacrylamide) decorated with an outer shell of thermoresponsive DEGMA (di(ethylene glycol) methyl ethyl methacrylate) and crosslinker inner core of MBAm (N, N'-methylenebis(acrylamide)), which have shown low cytotoxicity (more than 70% cell viability) up to 10 mg/ml. Polyacrylamide (PAAm) polymers have been widely used in biological and biomedical research for gel electrophoresis, preparation of soft contact lenses, tissue implants, and as carriers for drugs in animal models[71]. These polymers are thought not to elicit a biological response because of their size and the absence of any reactive groups or double bonds by which they can undergo chemical reactions. Glycopolymers composed of galactose-based LAEMA are designed as biological mimetics of complex saccharides that allow the bioconjugation to cell receptors enhancing the affinity of the nanogels to these ligands. Loading IAZA to the NGs is achieved spontaneously through electrostatic, van der Waals and hydrophobic interactions between IAZA and the polymer matrix. IAZA experiences some deiodination and non-specific interactions with blood proteins that can be overcome by the NG encapsulation, thus improving the bioavailability of IAZA in the tumour sites. The thermal changes in the physicochemical behaviour of the NGs are responsible for enhanced drug delivery, increased half-life and maximized passive targeting to tumour cells, offering higher tumoral uptake and reducing the pre-target metabolic degradation. A 'single-dose' toxicity of our NG polymer in an immunocompromised NSG mouse model at 3 different doses (615, 462 and 308 mg of nanogel per Kg of mice) was determined via; intraperitoneal (i.p) mode of administration. The loading capacity of **NG1** is 1.3 mg of IAZA per mg of NG; the proposed single doses ensure the administration of 400-800 mg/Kg of IAZA. The tested

amount of nanogel is based on delivering chemically safe doses of IAZA to each animal during the chemotoxicity studies and validating the slow release of IAZA and safe use of *nano*IAZA in future therapy studies. The animals were monitored for up to 7 days as per the Canadian Council of Animal Care (CCAC) guidelines, and the observations were recorded on monitoring charts. No abnormalities were observed in the animals. The necropsy studies were performed to evaluate the polymer's toxic effects on various tissues without showing any signs of adverse effects (Figure 6-6).

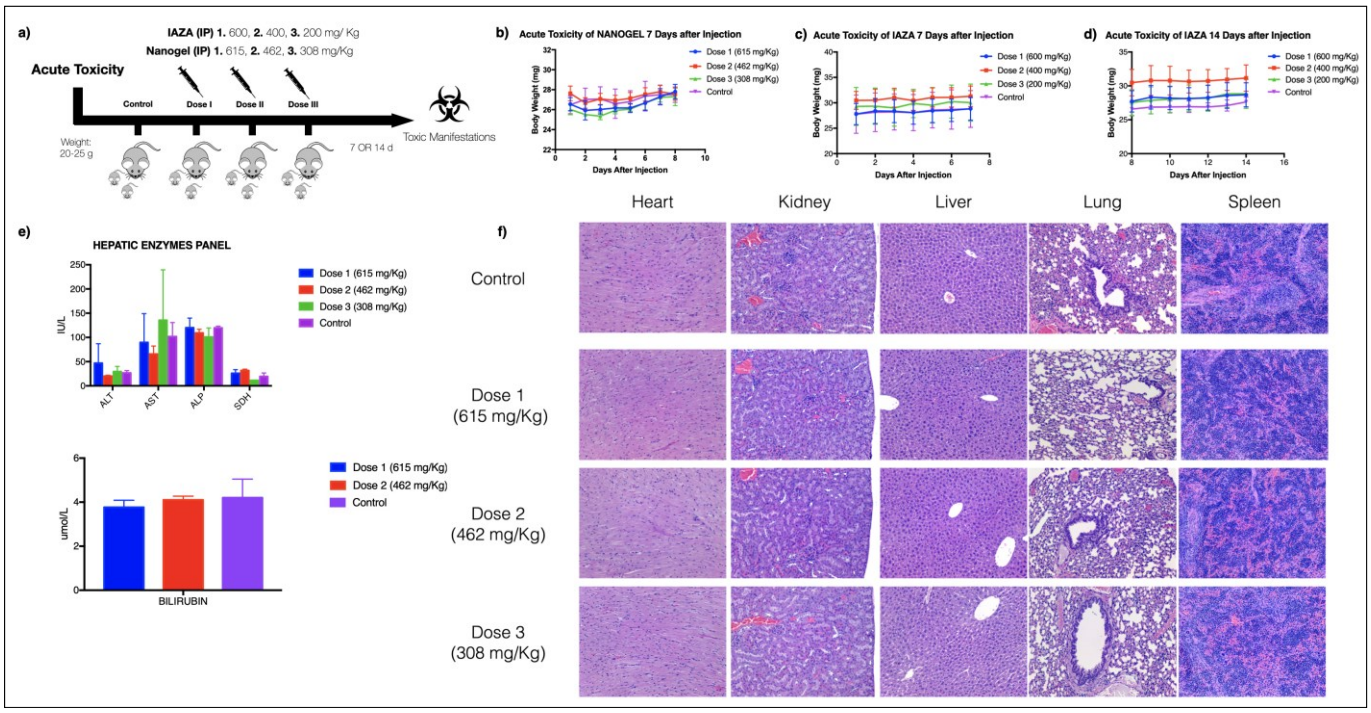

Figure 6-6. In vivo Acute Toxicity Evaluation. **a)** Acute toxicity evaluation 7 days or 14 days after administering IAZA/Nanogel at three different doses. **b)** Mice body weight monitoring after 7 days of Nanogel administration. **c)** Mice body weight monitoring after 7 days of IAZA administration, and **d)** after 14 days of IAZA administration. **e)** Hepatic enzyme panel and Bilirubin values were taken from blood samples after mice were euthanized 7 days post-NG injection. **(f)** Tissue and organ pathology evaluation of the NG acute toxicity.

6.3.7 Determination of a single dose chemotoxicity of *nano*IAZA in a hypoxic FaDu tumour model. Tissue hypoxia can mature in the solid tumour microenvironment and

induce transcriptional and translational cellular adaptations, including up-regulation of drug resistance transporters and carbohydrate metabolism, modulation of apoptotic processes and induction of gene expression that promote metastases and compromise therapy outcomes[10,72,73]. This strongly supports the necessity to identify tumours with high hypoxic fractions and treat such tumours with hypoxia directed therapeutics to maximize treatment efficacy. Tumour hypoxia can be diagnosed and detected with various molecular probes, especially with radiotracers. Iodoazomycin Arabinoside (IAZA), an O_2-mimicking nucleoside-based compound, was developed as a hypoxia selective diagnostic agent at the University of Alberta[23,74]. IAZA is a 2-nitroimidazole derivative that undergoes bioreductive activation under low O_2, which leads to its selective entrapment inside hypoxic cells. Successful clinical trials at the Cross Cancer Institute had validated its potency as a hypoxia selective SPECT imaging agent[19,75,76].

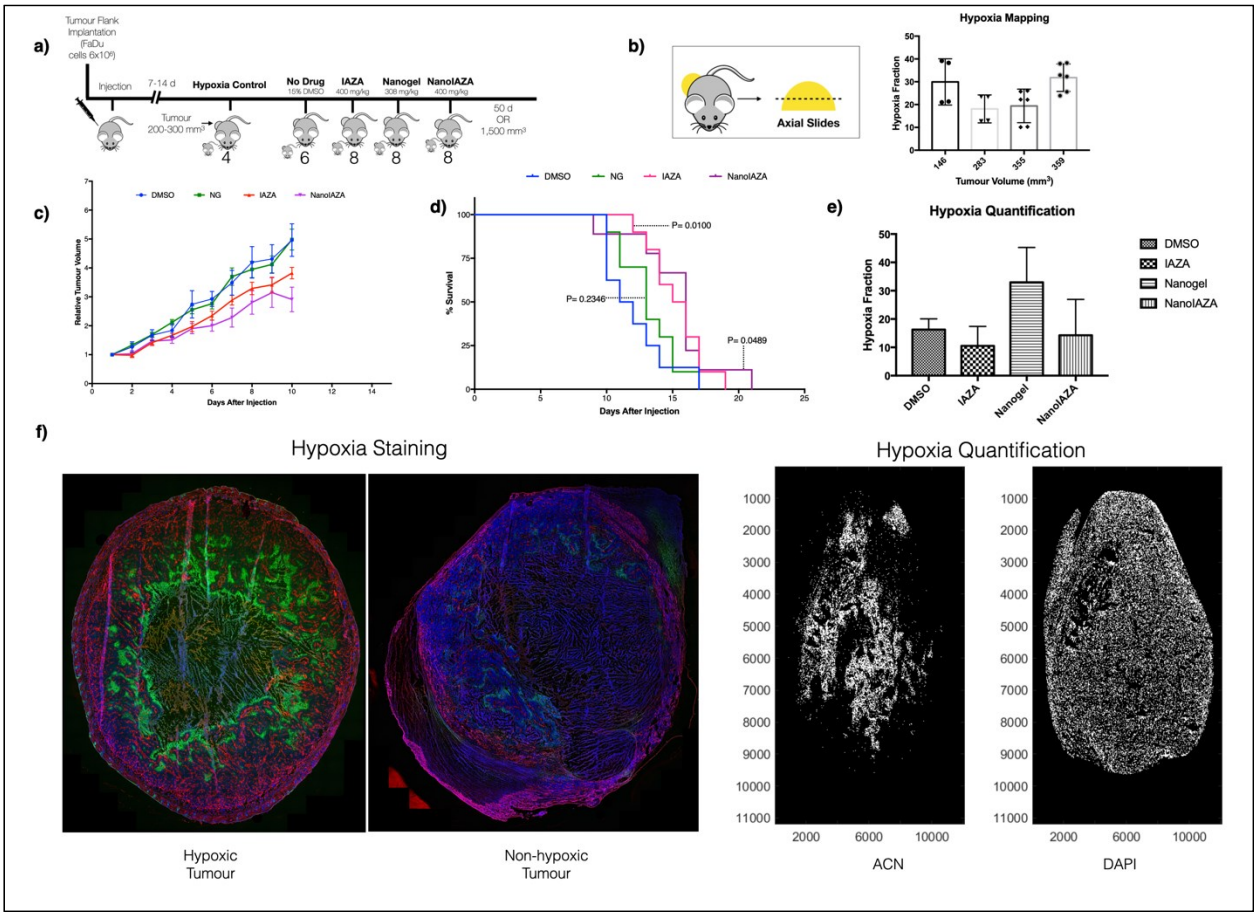

Figure 6-7. In vivo chemotoxicity of IAZA and nanoIAZA. **(a)** The proposed protocol evaluated the chemotherapeutic potential of IAZA and *nano*IAZA (IAZA encapsulated in a galactose-based nanogel **NG1**) in FaDu tumour-bearing NU/NU mice. A group of 36 mice was distributed in five (5) sub-groups, as stated here: 1. Control DMSO (n=6), 2. IAZA only (n=8), 3. *nano*IAZA only (n=8), 4. Nanogel only (n=8), and 5. Hypoxia mapping (n=4). (Total = 34 mice). Nu/Nu tumour-bearing mice received a single i.p. administration of 400 mg/Kg of IAZA and *nano*IAZA/ 308 mg/Kg, NG / 15% DMSO when the tumour reached between 200-300 mm^3. The mice were monitored daily and administered i.p. with ACN at 60 mg/Kg, 2 h before sacrifice when the tumour reached a volume of 1,500 mm^3. **(b)** For hypoxia mapping, one group of four (4) mice was sacrificed once the tumours reached between ~150-350 mm^3. ACN staining was correlated with hypoxic regions and quantify using MATLAB. The tumours were frozen in optimal cutting temperature (OCT) compound solution and sliced axially, four (4) different tumour sections were taken, and two (2) sections were stained and quantified. **(c)** Relative tumour volume of the different groups was evaluated. Data are shown as mean ± SD (n = 6-8). **(d)** Kaplan-Meier curve for the different treatment groups. **(f)** Tumour staining with ACN, DAPI and CD31 antibody; green fluorescence corresponds to hypoxic regions (ACN), red fluorescence to the blood vessels (CD31) and blue to the cell nuclei (DAPI). Example of the hypoxia quantification performed with MATLAB.

This study pursues a translational approach to the theranostic management of hypoxic cancerous tumours and explores the potential of *nano*IAZA in a therapeutic setting as a hypoxic chemosensitizer. Encapsulation of the drug should improve its bioavailability and tumour uptake and slow down the drug's metabolic degradation. Kumar and Weinfeld have developed a non-invasive 'click chemistry' approach using Azido Conjugated Nitroimidazole (ACN, an azido analogue of IAZA) to detect hypoxic fractions in cell culture and on tumour sections. This technique was used in the present study to assess initial and final tumour hypoxia fractions to ensure the proper tumour hypoxia stratification and minimize the tumour heterogeneity in tissue oxygenation. A hypoxic tumour model based in FaDu tumour cells —an established human hypopharyngeal squamous cell

carcinoma— was used according to the study reported by Vaupel *et. al*[77]. In this study, it was concluded that the oxygenation status of FaDu tumours is heterogeneous and depends on the tumour volume. According to Maftei *et al.* .[78], for a tumour of approximately 200 mm^3, the observed total hypoxia is between 40-50% in the central tumour sections. To corroborate this result, one group of four (4) mice were sacrificed once the tumours reached ~150-350 mm^3. Histology and hypoxia mapping [with i.p. injection of ACN two (2) hours before sacrifice] was done to quantify tumour hypoxia. According to our results there is no clear relationship between tumour volume and hypoxic fraction as stated before. This corroborates the tumour hypoxia heterogeneity in this murine model (Figure 6-7b). The chemotoxicity evaluation of IAZA and *nano*IAZA was assessed in 4–6 weeks old male NU/NU mice bearing FaDu tumours. We have chosen the NU/NU strain of mice because (i) it is a well-characterized immune-deficient strain for engraftment of human tumour cell lines, (ii) the hairless phenotype enables more accessible assessment of tumour growth, (iii) it does not show the radiation hypersensitive phenotype displayed by NSG immunocompromised mice for future radiosensitization studies. The mice were divided into four (4) groups: 15% DMSO as the no drug control group, 400 mg/Kg IAZA/*nano*IAZA and 308 mg/Kg NG. All the groups were administered i.p. with appropriate agents when the tumour volume reached 200-300 mm^3. The animals were sacrificed once the tumour volume reached 1,500 mm^3 and were injected with ACN for hypoxia mapping two (2) h prior to sacrifice. Both the DMSO control and NG groups exhibited similar survival curves and relative tumour volume growth. The animals injected with IAZA or *nano*IAZA showed longer survival rates and decreased tumour growth than the controls. For *nano*IAZA, a median survival of 16 days was observed compared to 12.5 days for the DMSO group (Figure 6-7d). It is worth mentioning that this study only pursued a single injection of IAZA/*nano*IAZA, which demonstrates significant results. Future work should evaluate multiple doses and combination with radiation therapy.

6.4 CONCLUSIONS

Clinical efficacy of ^{123}I-labelled IAZA in imaging and diagnosing hypoxic tumours[18] and its unique structural traits confer IAZA with a potential for a multimodal theranostic intervention and benefits for managing solid hypoxic tumours. Encapsulation of IAZA in

galactose-based NGs will potentially overcome significant biological barriers, including pre-target metabolism and clearance of IAZA, improving its bioavailability in hypoxic cancer cells, which are required for effective therapeutic intervention and reduced toxicity to healthy cells. The hypoxic microenvironment in tumours initiates bioreductive activation of IAZA that generates cytotoxic intermediates to facilitate hypoxia-specific chemotherapeutic effects. *In vitro* radiosensitization and cytotoxicity of *nano*IAZA have shown promising results, and *in vivo,* NG toxicity evaluation validated the safety of **NG1** as a delivery vehicle. The successful single-dose chemotoxicity study with *nano*IAZA may lead to an innovative opportunity for nanocarriers in treating solid hypoxic tumours by optimizing drug target delivery, which in summary, could lead to improved patient care, reduction in mortality, and reduced health care costs associated with the management of hypoxic cancers[79].

6.5 REFERENCES

(1) Vaupel, P.; Briest, S.; Höckel, M. Hypoxia in Breast Cancer: Pathogenesis, Characterization and Biological/Therapeutic Implications. *Wiener Medizinische Wochenschrift* **2002**, *152* (13–14), 334–342. https://doi.org/10.1046/j.1563-258X.2002.02032.x.

(2) Kim, B. W.; Cho, H.; Chung, J.-Y.; Conway, C.; Ylaya, K.; Kim, J.-H.; Hewitt, S. M. Prognostic Assessment of Hypoxia and Metabolic Markers in Cervical Cancer Using Automated Digital Image Analysis of Immunohistochemistry. *J. Transl. Med.* **2013**, *11* (1), 185. https://doi.org/10.1186/1479-5876-11-185.

(3) Brizel, D. M.; Sibley, G. S.; Prosnitz, L. R.; Scher, R. L.; Dewhirst, M. W. Tumor Hypoxia Adversely Affects the Prognosis of Carcinoma of the Head and Neck. *Int. J. Radiat. Oncol. Biol. Phys.* **1997**, *38* (2), 285–289. https://doi.org/10.1016/S0360-3016(97)00101-6.

(4) Kuwai, T.; Kitadai, Y.; Tanaka, S.; Onogawa, S.; Matsutani, N.; Kaio, E.; Ito, M.;

Chayama, K. Expression of Hypoxia-Inducible Factor-1alpha Is Associated with Tumor Vascularization in Human Colorectal Carcinoma. *Int. J. Cancer* **2003**, *105* (2), 176–181. https://doi.org/10.1002/ijc.11068.

(5) Duffy, J. P.; Eibl, G.; Reber, H. A.; Hines, O. J. Influence of Hypoxia and Neoangiogenesis on the Growth of Pancreatic Cancer. *Mol. Cancer* **2003**, *2* (2), 12. https://doi.org/10.1097/01.mpa.0000229010.62538.f2.

(6) Stewart, G. D.; Ross, J. A.; McLaren, D. B.; Parker, C. C.; Habib, F. K.; Riddick, A. C. P. The Relevance of a Hypoxic Tumour Microenvironment in Prostate Cancer. *BJU Int.* **2010**, *105* (1), 8–13. https://doi.org/10.1111/j.1464-410X.2009.08921.x.

(7) Vaupel, P.; Mayer, A. Hypoxia in Cancer: Significance and Impact on Clinical Outcome. *Cancer Metastasis Rev.* **2007**, *26* (2), 225–239. https://doi.org/10.1007/s10555-007-9055-1.

(8) Bennewith, K. L.; Dedhar, S. Targeting Hypoxic Tumour Cells to Overcome Metastasis. *BMC Cancer* **2011**, *11*, 504. https://doi.org/10.1186/1471-2407-11-504.

(9) Brown, J. M.; Wilson, W. R. Exploiting Tumour Hypoxia in Cancer Treatment. *Nat. Rev. Cancer* **2004**, *4* (6), 437–447. https://doi.org/10.1038/nrc1367.

(10) Walsh, J. C.; Lebedev, A.; Aten, E.; Madsen, K.; Marciano, L.; Kolb, H. C. The Clinical Importance of Assessing Tumor Hypoxia: Relationship of Tumor Hypoxia to Prognosis and Therapeutic Opportunities. *Antioxid. Redox Signal.* **2014**, *21* (10), 1516–1554. https://doi.org/10.1089/ars.2013.5378.

(11) Rockwell, S.; Dobrucki, I. T.; Kim, E. Y.; Marrison, S. T.; Vu, V. T. Hypoxia and Radiation Therapy: Past History, Ongoing Research, and Future Promise. *Curr. Mol. Med.* **2009**, *9* (4), 442–458. https://doi.org/10.2174/156652409788167087.

(12) Wilson, W. R.; Hay, M. P. Targeting Hypoxia in Cancer Therapy. *Nat. Rev. Cancer* **2011**, *11* (6), 393–410. https://doi.org/10.1038/nrc3064.

(13) Workman, P. The Neurotoxicity of Misonidazole: Potential Modifying Role of Dexamethasone. *Br. J. Radiol.* **1980**, *53* (631), 736–736. https://doi.org/10.1259/0007-1285-53-631-736.

(14) Reck, M.; von Pawel, J.; Nimmermann, C.; Groth, G.; Gatzemeier, U. Phase II-Trial of Tirapazamine in Combination with Cisplatin and Gemcitabine in Patients with Advanced Non-Small-Cell-Lung-Cancer (NSCLC). *Pneumologie* **2004**, *58* (12), 845–849. https://doi.org/10.1055/s-2004-830056.

(15) Rischin, D.; Peters, L. J.; O'Sullivan, B.; Giralt, J.; Fisher, R.; Yuen, K.; Trotti, A.; Bernier, J.; Bourhis, J.; Ringash, J.; Henke, M.; Kenny, L. Tirapazamine, Cisplatin, and Radiation versus Cisplatin and Radiation for Advanced Squamous Cell Carcinoma of the Head and Neck (TROG 02.02, HeadSTART): A Phase III Trial of the Trans-Tasman Radiation Oncology Group. *J. Clin. Oncol.* **2010**, *28* (18), 2989–2995. https://doi.org/10.1200/JCO.2009.27.4449.

(16) Hicks, K.; Siim, B.; Pruijn, F.; Wilson, W. Oxygen Dependence of the Metabolic Activation and Cytotoxicity of Tirapazamine: Implications for Extravascular Transport and Activity in Tumors. *Radiat Res* **2004**, *161* (6), 656–666. https://doi.org/10.1667/RR3178.

(17) Sorger D, Patt M, Kumar P, Wiebe L, Barthel H, Seese A, Dannenberg C, Tannapfel A, Kluge R, S. S.; Sorger, D.; Patt, M.; Kumar, P.; Wiebe, L. I.; Barthel, H.; Seese, A.; Dannenberg, C.; Tannapfel, A.; Kluge, R.; Sabri, O. Fluoroazomycinarabinofuranoside (18FAZA) and [18F]Fluoromisonidazole

(18FMISO): A Comparative Study of Their Selective Uptake in Hypoxic Cells and PET Imaging in Experimental Rat Tumors. *Nucl. Med. Biol.* **2003**, *30* (3), 317–326. https://doi.org/10.1016/S0969-8051(02)00442-0.

(18) Reischl, G.; Dorow, D. S.; Cullinane, C.; Katsifis, A.; Roselt, P.; Binns, D.; Hicks, R. J. Imaging of Tumor Hypoxia with [124I]IAZA in Comparison with [18F]FMISO and [18F]FAZA–First Small Animal PET Results. *J Pharm Pharm Sci Publ Can Soc Pharm Sci Société Can Des Sci Pharm* **2007**, *10* (2), 203–211.

(19) Urtasun, R. C.; Parliament, M. B.; McEwan, A. J.; Mercer, J. R.; Mannan, R. H.; Wiebe, L. I.; Morin, C.; Chapman, J. D. Measurement of Hypoxia in Human Tumours by Non-Invasive Spect Imaging of Iodoazomycin Arabinoside. *Br. J. Cancer. Suppl.* **1996**, *27*, S209-12.

(20) Parliament M, Chapman J, Urtasun R, McEwan A, Golberg L, Mercer J, Mannan R, W. L. Non-Invasive Assessment of Human Tumour Hypoxia with - Iodoazomycinarabinoside: Preliminary Report of a Clinical Study. *Br. J. Cancer* **1992**, *65* (1), 90–95.

(21) Rezaul H. Mannan, Vijayalakashmi V. Somayaji, Jane Lee, John R. Mercer, J. Donald Chapman, and L. I. W. Radioiodinated 1-(5-Iodo-5-Deoxy-@3-D-Arabinofuranosyl)-2-Thtroimidazole (Lodoazomycin Arabinoside: IAZA): A Novel Marker of Tissue Hypoxia. *J. Nucl. Med.* **1991**, *32* (9).

(22) Kumar, P.; McQuarrie, S. A.; Zhou, A.; McEwan, A. J. B.; Wiebe, L. I. [131I]Iodoazomycin Arabinoside for Low-Dose-Rate Isotope Radiotherapy: Radiolabeling, Stability, Long-Term Whole-Body Clearance and Radiation Dosimetry Estimates in Mice. *Nucl. Med. Biol.* **2005**, *32* (6), 647–653.

https://doi.org/10.1016/j.nucmedbio.2005.04.019.

(23) Mercer, J. R.; Urtasun, R. C.; McEwan, A. J.; Parliament, M. B.; Chapman, J. D.; Goldberg, L.; Mannan, R. H.; Wiebe, L. I. 123IAZA: Iodomyzin Arabinoside. Synthesis, Purification and Clinical Evaluation in Cancer Patients. *Clin. Nucl. Med.* **1991**, *16* (10), 796. https://doi.org/10.1097/00003072-199110000-00046.

(24) Mercer, J. R.; McEwan, A. J.; Wiebe, L. I.; J.R., M.; A.J., M.; L.I., W.; Mercer, J. R.; McEwan, A. J.; Wiebe, L. I. [131I]IAZA as a Molecular Radiotherapeutic (MRT) Drug: Wash-out with Cold IAZA Accelerates Clearance in a Murine Tumor Model. *Curr. Radiopharm.* **2013**, *6* (2), 87–91. https://doi.org/10.2174/1874471011306020004.

(25) Jans H-S, D Stypinski, P Kumar, JR Mercer, LI Liebe, A. M. Dosimetry Comparison of the Hypoxia Agent Iodoazomycin Arabinoside (IAZA) Labeled with the Radioisotopes I-123/124/131. *Med. Phys.* **2014**, *41* (6), 385.

(26) Boucher, Y.; Baxter, L. T.; Jain, R. K. Interstitial Pressure Gradients in Tissue-Isolated and Subcutaneous Tumors: Implications for Therapy. *Cancer Res.* **1990**, *50* (15), 4478–4484.

(27) Jain, R. K. Delivery of Molecular Medicine to Solid Tumors: Lessons from in Vivo Imaging of Gene Expression and Function. In *Journal of Controlled Release*; 2001; Vol. 74, pp 7–25. https://doi.org/10.1016/S0168-3659(01)00306-6.

(28) Parveen, S.; Misra, R.; Sahoo, S. K. Nanoparticles: A Boon to Drug Delivery, Therapeutics, Diagnostics and Imaging. *Nanomedicine Nanotechnology, Biol. Med.* **2012**, *8* (2), 147–166. https://doi.org/10.1016/j.nano.2011.05.016.

(29) Sriraman, S. K.; Aryasomayajula, B.; Torchilin, V. P. Barriers to Drug Delivery in

Solid Tumors. *Tissue Barriers* **2014**, *2* (3), e29528. https://doi.org/10.4161/tisb.29528.

(30) Onaca-Fischer, O.; Liu, J.; Inglin, M.; Palivan, C. G. Polymeric Nanocarriers and Nanoreactors: A Survey of Possible Therapeutic Applications. *Curr. Pharm. Des.* **2012**, *18* (18), 2622–2643.

(31) Singh, R.; Lillard, J. W. Nanoparticle-Based Targeted Drug Delivery. *Exp. Mol. Pathol.* **2009**, *86* (3), 215–223. https://doi.org/10.1016/j.yexmp.2008.12.004.

(32) Loh, X. J.; Lee, T.-C.; Dou, Q.; Deen, G. R. Utilising Inorganic Nanocarriers for Gene Delivery. *Biomater. Sci.* **2016**, *4* (1), 70–86. https://doi.org/10.1039/C5BM00277J.

(33) Maeda, H.; Wu, J.; Sawa, T.; Matsumura, Y.; Hori, K. Tumor Vascular Permeability and the EPR Effect in Macromolecular Therapeutics: A Review. *Journal of Controlled Release*. 2000, pp 271–284. https://doi.org/10.1016/S0168-3659(99)00248-5.

(34) Matsumura, Y.; Maeda, H. A New Concept for Macromolecular Therapeutics in Cancer Chemotherapy: Mechanism of Tumoritropic Accumulation of Proteins and the Antitumor Agent Smancs. *Cancer Res.* **1986**, *46* (8), 6387–6392. https://doi.org/10.1021/bc100070g.

(35) Quan, S.; Wang, Y.; Zhou, A.; Kumar, P.; Narain, R. Galactose-Based Thermosensitive Nanogels for Targeted Drug Delivery of Iodoazomycin Arabinofuranoside (IAZA) for Theranostic Management of Hypoxic Hepatocellular Carcinoma. *Biomacromolecules* **2015**, *16* (7), 1978–1986. https://doi.org/10.1021/acs.biomac.5b00576.

(36) Kotsuchibashi, Y.; Agustin, R. V. C.; Lu, J.-Y. Y.; Hall, D. G.; Narain, R. Temperature, PH, and Glucose Responsive Gels via Simple Mixing of Boroxole- and Glyco-Based Polymers. *ACS Macro Lett.* **2013**, *2* (3), 260–264. https://doi.org/10.1021/mz400076p.

(37) Ahmed, M.; Narain, R. Carbohydrate-Based Materials for Targeted Delivery of Drugs and Genes to the Liver. *Nanomedicine (Lond)* **2015**, *10* (14), 2263–2288. https://doi.org/10.2217/nnm.15.58.

(38) Ahmed, M.; Pan, D. W.; Davis, M. E. Lack of in Vivo Antibody Dependent Cellular Cytotoxicity with Antibody Containing Gold Nanoparticles. *Bioconjug. Chem.* **2015**, *26* (5), 812–816. https://doi.org/10.1021/acs.bioconjchem.5b00139.

(39) Kabanov, A. V.; Vinogradov, S. V. Nanogels as Pharmaceutical Carriers:Finite Networks of Infinite Capabilities. *Angew. Chemie - Int. Ed.* **2009**, *48* (30), 5418–5429. https://doi.org/10.1002/anie.200900441.Nanogels.

(40) Abulateefeh, S. R.; Spain, S. G.; Aylott, J. W.; Chan, W. C.; Garnett, M. C.; Alexander, C. Thermoresponsive Polymer Colloids for Drug Delivery and Cancer Therapy. *Macromol. Biosci.* **2011**, *11* (12), 1722–1734. https://doi.org/10.1002/mabi.201100252.

(41) Ahmed M. Eissa; Cameron, N. R. Glycopolymer Conjugates. In *Advances in Polymer Science*; 2013; Vol. 253, pp 71–114. https://doi.org/10.1007/12_2012_177.

(42) Wiebe, L. I.; McEwan, A. J. B. Scintigraphic Imaging of Focal Hypoxic Tissue: Development and Clinical Applications of 123I-IAZA. *Braz. arch. biol. technol.* **2002**, *45* (September), 69–81. https://doi.org/10.1590/S1516-89132002000500010.

(43) Thapa, B.; Kumar, P.; Zeng, H.; Narain, R. Asialoglycoprotein Receptor-Mediated

Gene Delivery to Hepatocytes Using Galactosylated Polymers. *Biomacromolecules* **2015**, *16* (9), 3008–3020. https://doi.org/10.1021/acs.biomac.5b00906.

(44) Lu, M.; Khine, Y. Y.; Chen, F.; Cao, C.; Garvey, C. J.; Lu, H.; Stenzel, M. H. Sugar Concentration and Arrangement on the Surface of Glycopolymer Micelles Affect the Interaction with Cancer Cells. *Biomacromolecules* **2019**, *20* (1), 273–284. https://doi.org/10.1021/acs.biomac.8b01406.

(45) Zambrano, A.; Molt, M.; Uribe, E.; Salas, M. Glut 1 in Cancer Cells and the Inhibitory Action of Resveratrol as a Potential Therapeutic Strategy. *Int. J. Mol. Sci.* **2019**, *20* (13), 1–20. https://doi.org/10.3390/ijms20133374.

(46) Aparicio, L. A.; Calvo, M. B.; Figueroa, A.; Pulido, E. G.; Campelo, R. G. Potential Role of Sugar Transporters in Cancer and Their Relationship with Anticancer Therapy. *Int. J. Endocrinol.* **2010**, *2010*. https://doi.org/10.1155/2010/205357.

(47) Hamanaka, R. B.; Chandel, N. S. Targeting Glucose Metabolism for Cancer Therapy: Figure 1. *J. Exp. Med.* **2012**, *209* (2), 211–215. https://doi.org/10.1084/jem.20120162.

(48) Kuo, M. H.; Chang, W. W.; Yeh, B. W.; Chu, Y. S.; Lee, Y. C.; Lee, H. Te. Glucose Transporter 3 Is Essential for the Survival of Breast Cancer Cells in the Brain. *Cells* **2019**, *8* (12). https://doi.org/10.3390/cells8121568.

(49) Häuselmann, I.; Borsig, L. Altered Tumor-Cell Glycosylation Promotes Metastasis. *Front. Oncol.* **2014**, *4 MAR* (February), 1–15. https://doi.org/10.3389/fonc.2014.00028.

(50) Kumar, P.; Wiebe, L.; Mcewan, A. Compounds Useful in Imaging and Therapy. Patent. No.: US 2013/0211066A1, 2013.

(51) Deng, Z.; Ahmed, M.; Narain, R. Novel Well-Defined Glycopolymers Synthesized via the Reversible Addition Fragmentation Chain Transfer Process in Aqueous Media. *J. Polym. Sci. Part A Polym. Chem.* **2009**, *47* (2), 614–627. https://doi.org/10.1002/pola.23187.

(52) Munshi, A.; Hobbs, M.; Meyn, R. E. Clonogenic Cell Survival Assay. *Chemosensitivity* **2005**, *110*, 021–028. https://doi.org/10.1385/1-59259-869-2:021.

(53) Diaz-Dussan, D.; Nakagawa, Y.; Peng, Y.-Y. Y.; Sanchez, L. V.; Ebara, M.; Kumar, P.; Narain, R.; C, L. V. S.; Ebara, M.; Kumar, P.; Narain, R. Effective and Specific Gene Silencing of Epidermal Growth Factor Receptors Mediated by Conjugated Oxaborole and Galactose-Based Polymers. *ACS Macro Lett.* **2017**, *6* (7), 768–774. https://doi.org/10.1021/acsmacrolett.7b00388.

(54) Stypinski, D.; McQuarrie, S. A.; Wiebe, L. I.; Tam, Y. K.; Mercer, J. R.; McEwan, A. J. Dosimetry Estimations for 123I-IAZA in Healthy Volunteers. *J. Nucl. Med.* **2001**, *42* (9), 1418–1423.

(55) Wardman, P. Chemical Radiosensitizers for Use in Radiotherapy. *Clin. Oncol.* **2007**, *19* (6), 397–417. https://doi.org/10.1016/j.clon.2007.03.010.

(56) Begg, A. C.; Stewart, F. A.; Vens, C. Strategies to Improve Radiotherapy with Targeted Drugs. *Nat. Rev. Cancer* **2011**, *11* (4), 239–253. https://doi.org/10.1038/nrc3007.

(57) Adams, G. E.; Flockhart, I. R.; Smithen, C. E.; Stratford, I. J.; Wardman, P.; Watts, M. E. Electron-Affinic Sensitization: VII. A Correlation between Structures, One-Electron Reduction Potentials, and Efficiencies of Nitroimidazoles as Hypoxic Cell Radiosensitizers. *Radiat. Res.* **1976**. https://doi.org/10.2307/3574491.

(58) Bischoff, P.; Altmeyer, A.; Dumont, F. Radiosensitising Agents for the Radiotherapy of Cancer: Advances in Traditional and Hypoxia Targeted Radiosensitisers. *Expert Opinion on Therapeutic Patents*. 2009. https://doi.org/10.1517/13543770902824172.

(59) Zeman, E. M. *Biologic Basis of Radiation Oncology*, Thrid Edit.; Elsevier Inc., 2011. https://doi.org/10.1016/B978-1-4377-1637-5.00001-8.

(60) Muz, B.; de la Puente, P.; Azab, F.; Luderer, M.; Azab, A. K. The Role of Hypoxia and Exploitation of the Hypoxic Environment in Hematologic Malignancies. *Mol. Cancer Res.* **2014**, *12* (10).

(61) De Ridder, M.; Verellen, D.; Verovski, V.; Storme, G. Hypoxic Tumor Cell Radiosensitization through Nitric Oxide. *Nitric Oxide - Biology and Chemistry*. 2008. https://doi.org/10.1016/j.niox.2008.04.015.

(62) Chapman, J Donald; Lee, Jane; Meeker, B. E. Keynote Address: Cellular Reduction of Nitroimidazole Drugs: Potential for Selective Chemotherapy and Diagnosis of Hypoxic Cells. *Int. J. Radiat. Oncol. Biol. Phys.* **1989**, *16* (4), 911–917. https://doi.org/10.1016/0360-3016(89)90886-9.

(63) Watts, M. E.; Dennis, M. F.; Roberts, I. J.; Wattst, M. E. International Journal of Radiation Biology Radiosensitization by Misonidazole, Pimonidazole and Azomycin and Intracellular Uptake in Human Tumour Cell Lines Radiosensitization by Misonidazole, Pimonidazole and Azomycin and Intracellular Uptake in Human Tu. *Int. J. Radiat. Biol. INT . J . RADIAT . BIOL* **1990**, *57* (3), 361–372. https://doi.org/10.1080/09553009014552461.

(64) Overgaard, J.; Hansen, H. S.; Overgaard, M.; Bastholt, L.; Berthelsen, A.; Specht,

L.; Lindeløv, B.; Jørgensen, K. A Randomized Double-Blind Phase III Study of Nimorazole as a Hypoxic Radiosensitizer of Primary Radiotherapy in Supraglottic Larynx and Pharynx Carcinoma. Results of the Danish Head and Neck Cancer Study (DAHANCA) Protocol 5-85. *Radiother. Oncol.* **1998**, *46* (2), 135–146. https://doi.org/10.1016/S0167-8140(97)00220-X.

(65) Dische, S. Chemical Sensitizers for Hypoxic Cells: A Decade of Experience in Clinical Radiotherapy. *Radiother. Oncol.* **1985**, *3* (2), 97–115. https://doi.org/10.1016/S0167-8140(85)80015-3.

(66) Lawrentschuk, N.; Poon, A. M. T.; Foo, S. S.; Putra, L. G. J.; Murone, C.; Davis, I. D.; Bolton, D. M.; Scott, A. M. Assessing Regional Hypoxia in Human Renal Tumours Using 18F-Fluoromisonidazole Positron Emission Tomography. *BJU Int.* **2005**, *96* (4), 540–546. https://doi.org/10.1111/j.1464-410X.2005.05681.x.

(67) Kumar, P.; Stypinski, D.; Xia, H.; McEwan, A. J. B.; Machulla, H.-J. J.; Wiebe, L. I. Fluoroazomycin Arabinoside (FAZA): Synthesis, 2H and 3H-Labelling and Preliminary Biological Evaluation of a Novel 2-Nitroimidazole Marker of Tissue Hypoxia. *J. Label. Compd. Radiopharm.* **1999**, *42* (1), 3–16. https://doi.org/10.1002/(SICI)1099-1344(199901)42:1<3::AID-JLCR160>3.0.CO;2-H.

(68) Wiebe, L. I. PET Radiopharmaceuticals for Metabolic Imaging in Oncology. *Int. Congr. Ser.* **2004**, *1264*, 53–76. https://doi.org/10.1016/j.ics.2003.12.102.

(69) Kumar, P.; Elsaidi, H. R. H.; Zorniak, B.; Laurens, E.; Yang, J.; Bacchu, V.; Wang, M.; Wiebe, L. I. Synthesis and Biological Evaluation of Iodoglucoazomycin (I-GAZ), an Azomycin–Glucose Adduct with Putative Applications in Diagnostic

Imaging and Radiotherapy of Hypoxic Tumors. *ChemMedChem* **2016**, 1638–1645. https://doi.org/10.1002/cmdc.201600213.

(70) Murshed, H.; Murshed, H. Radiation Biology. *Fundam. Radiat. Oncol.* **2019**, 57–87. https://doi.org/10.1016/B978-0-12-814128-1.00003-9.

(71) Smith, E. A.; Oehme, F. W. Acrylamide and Polyacrylamide: A Review of Production, Use, Environmental Fate and Neurotoxicity. *Rev. Environ. Health* **1991**, *9* (4), 215–228. https://doi.org/10.1515/REVEH.1991.9.4.215.

(72) Brown, J. M. The Hypoxic Cell: A Target for Selective Cancer Therapy - Eighteenth Bruce F. Cain Memorial Award Lecture. *Cancer Res.* **1999**, *59* (23), 5863–5870.

(73) Bristow, R. G.; Hill, R. P. Hypoxia and Metabolism. Hypoxia, DNA Repair and Genetic Instability. *Nat. Rev. Cancer* **2008**, *8* (3), 180–192. https://doi.org/10.1038/nrc2344.

(74) Wiebe, L.; McEwan, A. J. B.; Kumar, P. Novel Compounds Fro Hypoxic Cell Therapy and Imaging. Patent. No.: US 2006/0270610 A1, 2006.

(75) Parliament, M. B.; Chapman, J. D.; Urtasun, R. C.; McEwan, a J.; Golberg, L.; Mercer, J. R.; Mannan, R. H.; Wiebe, L. I. Non-Invasive Assessment of Human Tumour Hypoxia with 123I-Iodoazomycin Arabinoside: Preliminary Report of a Clinical Study. *Br. J. Cancer* **1992**, *65* (1), 90–95.

(76) Wiebe, L. I.; Mannan, R. H.; Mercer, J. R.; Chapman, J. D.; Miller, G.; Moore, R.; Lee, J. Iaza: Iodoazomycin Arabinoside. the Development of a Marker for Hypoxic Tissue. *Clin. Nucl. Med.* **1991**, *16* (10), 796. https://doi.org/10.1097/00003072-199110000-00046.

(77) Vaupel, P.; Hockel, M.; Mayer, A. Detection and Characterization of Tumor

Hypoxia Using PO2 Histography. *Antioxid Redox Signal* **2007**, *9* (8), 1221–1235. https://doi.org/10.1089/ars.2007.1628.

(78) Maftei, C. A.; Bayer, C.; Shi, K.; Vaupel, P. Intra-and Intertumor Heterogeneities in Total, Chronic, and Acute Hypoxia in Xenografted Squamous Cell Carcinomas : Detection and Quantification Using (Immuno-)Fluorescence Techniques. *Strahlentherapie und Onkol.* **2012**, *188* (7), 606–615. https://doi.org/10.1007/s00066-012-0105-4.

(79) Young, S. W. S.; Stenzel, M.; Jia-Lin, Y. Nanoparticle-SiRNA: A Potential Cancer Therapy? *Crit. Rev. Oncol. Hematol.* **2016**, *98*, 159–169. https://doi.org/10.1016/j.critrevonc.2015.10.015.

CHAPTER 7. CONCLUSIONS, DISCUSSION AND FUTURE DIRECTIONS

7.1 SUMMARY OF KEY FINDINGS

Cancer therapeutics are undergoing a new post-genomics target era. New anti-cancer drugs that target specific tumour cells and leave normal healthy cells behind are beginning to change the face of cancer treatment. Knowledge of the regulation of cell growth and biochemical changes that lead to malignancy has created many opportunities for designing molecularly targeted anti-cancer drugs. Clinical use of chemotherapeutic agents against malignant tumours is successful in many cases but suffers from significant drawbacks - one being the lack of selectivity which leads to severe side effects and limited efficacy, and the other is the emergence/selection of drug resistance. Despite these limitations, many oncologists believe that traditional agents will continue to be used for at least a decade[1]. The emergence of nanotechnology has, however, provided a strategic approach to overcome these problems. Advances in colloidal science have made enormous contributions in the fields of biology, biomedicine and biotechnology, specifically in the development of novel drug/gene delivery vehicles and cell therapies. Recent years have witnessed remarkable advances in the synthesis of innovative structures such as liposomes, nanocapsules, polymeric nanoparticles, micelles, and other bioconjugates, that have proved to be attractive for tumour imaging, gene and pharmaceutical delivery[2–4]. Nonetheless, various challenges must be overcome for these carriers, such as efficient therapeutic loading capacity, targeted delivery and controlled release, among other physiological barriers to improve selective uptake[5]. The complex design of multifunctional polymeric carriers, including the emergence of novel stimuli-responsive[6] glycoconjugates[7–9], has demonstrated an outstanding approach to introduce carbohydrate targeting moieties to trigger target drug/gene delivery and release. Glycoproteins and glycolipids are involved in vital processes, like cell recognition, activation and development. The complexity of glycans from their highly branched nature is still very challenging to be mimicked by synthetic polymers, but novel and more efficient synthesis techniques have created well-

defined and complex polysaccharides[10]. State-of-the-art research in functionally modified glycopolymers and glycoconjugates has shown many advantages for their use as drug/gene delivery vehicles and cell therapies[10–12]. Bioengineered carbohydrate-based nanoparticles showing specific-gene regulation have proved to be a precise rational design for delivering therapeutic genes to multiple cancer cells lines *in vitro* by fulfilling three functions: 1) stimuli-responsive modulation allowing endosomal cleavage following cellular uptake, promoting membrane fusion and cytoplasm payload delivery, 2) zwitterionic charge to reduce immune responses and prolong circulation time, and 3) mimic of naturally existing glycans showing effective cellular uptake due to lectin interactions. The hydrophilicity. biodegradability, unique biomimicking structure, and easy modification confer these molecules' essential advantages for the design of novel delivery systems. Narain's group has developed unique synthesis approaches that have allowed the design of new polymeric architectures in high precision with improved binding affinity. Well-defined glycopolymers with varying molecular weights, compositions and architectures have been synthesized to evaluate their potential as gene/drug delivery vectors and cell scaffolds, allowing facile tailoring with pendant biocompatible moieties with complex structure-activity relationships. As a result, the importance of recent advancements in glycopolymer synthesis to manipulate lectin–carbohydrate recognition has been linked directly to discovering new therapeutic targets and creating biocompatible and biodegradable carbohydrate functionalized polymers as potent gene/drug delivery vectors and cellular therapeutic platforms *in vitro*.

This thesis has explored the design of suitable and functional glycopolymers to facilitate improved therapeutic approaches. Different chemistries and architectures were developed for drug and gene delivery and cryopreservation cell therapies based on biological and chemical perspectives. In **chapters 2, 3 and 4,** we explored the synthesis of novel benzoxaborole polymers and the effect of sugar decoration in different glycopolymers design and synthesized to optimize therapeutic genes' delivery. Gene therapy encompasses the delivery of nucleic acids such as plasmid DNA (pDNA), messenger RNA (mRNA), short interfering or silencing RNA (siRNA), microRNA (miRNA), short-hairpin RNA (shRNA), antisense oligonucleotides (antisense ODNs) and DNAzymes into the cell. These nucleic acids introduce genes that encode a functional protein or block the translation of

specific mRNAs for gene and protein expression[13]. Administration of naked DNA/RNA, without any carrier, into local tissues or into the systemic circulation, is perhaps the easiest and safest physical approach. Nonetheless, due to their rapid degradation by nucleases and fast clearance by the immune system, efficiency of this transfection method is reduced[14]. Consequently, attention has turned to the development of better strategies and improved carriers for effective DNA/RNA transfection. Non-viral delivery vehicles mainly have a cationic charge that electrostatically interacts with the negative charge of the oligonucleotides. Hydrogen-bonding between polycations and nucleic acids enhances the interaction and contributes to the stabilization of the polyplexes[15]. To ensure the delivery of a transgene into the targeted cell nucleus or cytoplasm, the delivery system needs to circumvent the vascular endothelial cells and blood components, avoid uptake by the reticuloendothelial system, and it must be small enough to extravasate into the cell membrane and reach the cytoplasm or the nucleus[16]. The development of versatile and advanced siRNA nanocarriers that can successfully and safely deliver and release siRNA inside the targeted cells is the main objective of this research. Most siRNA carriers are developed from cationic polymers as these materials spontaneously bind to siRNA via electrostatic interactions and form stable polyplexes, resulting in siRNA protection against degradation and extension of blood circulation time. This improves the cellular uptake of the polyplexes, however the vector or carrier used should not induce any antagonistic effects on normal cells. Previous studies have shown that the viability of normal cells can be significantly compromised with these cationic vectors. The use of natural polysaccharides for gene delivery has reduced the need for an excess cationic charge, hence decreasing the system's toxicity, as carbohydrates condensed the oligonucleotides via hydrogen bonding. These carbohydrate units also interact with specific cell receptors (glycans) and serve as targeting agents without a need for further modifications[17]. In **chapters 2 and 3,** we explored the dynamic bond between sugar diols and benzoxaborole to develop novel gene delivery vehicles to knockdown cancer-causing genes in cervical carcinomas. Oxaborole-based glycopolymers are stimuli-responsive materials that can reversibly interact with diols at pH values higher than their pKa. The strong binding of the oxaborole with cis-hydroxyl groups allows the rapid cross-linking of the polymer chains. **Chapter 2** exploited this phenomenon to develop a unique delivery system for the

complexation, protection, and delivery of epidermal growth factor receptors (EGFR) siRNA. Galactose and oxaborole polymers were first synthesized by the reversible addition−fragmentation chain transfer (RAFT) process. They were found to show a robust interaction with each other via the oxaborole-diol effect, which allowed the formation of stable polyplexes with siRNA. Although complexes were successfully formed between the neutral galactose and oxaborole-based polymers, these complexes were ineffective in protecting the siRNA. Therefore, cationic glycopolymers and oxaborole polymers were investigated, showing superior complexation with siRNA and exhibiting effective gene silencing in HeLa (cervical) cancer cells while offering lower toxicities. Gene silencing of up to 60% was achieved with these new complexes in the presence and absence of serum proteins. Excellent stability of the complexes under physiological conditions and the observed low cytotoxicity 48 h post-transfection demonstrated high potential for this new system in gene silencing therapy application *in vivo*.

Chapter 3 aimed to design a glycopolymer vector with an omega-end modified oxaborole group via thiol-ene click chemistry that responds to the acidic tumour microenvironment to provide physical targeting capabilities. Two kinds of RAFT-made, biocompatible, and cationic polymers composed of AEMA and 2-methacryloyloxyethyl phosphorylcholine (MPC) or 2-hydroxyethyl methacrylate (HEMA) were synthesized to modify the genetic profile of cervical cancer cells by silencing the expression of the EGFR receptor. These polymeric vectors had a dual capability – a cationic segment to complex with the siRNA and an oxaborole group complexed via thiol-ene click chemistry that responds to the acidic environment. This structural innovation enables this macromolecule to interact with multiple polyplexes and release the siRNA at a mildly acidic environment, like the one exhibited by tumour cells; a targeting strategy that has shown enhanced gene silencing (~70% knockdown of EGFR) without elevating the system's cytotoxicity, as determined by western blot analysis. The use of oxaborole-glycopolymer nanocomplexes to deliver siRNA to knockdown EGFR receptor genes has further demonstrated that these nanoformulations are effective carriers of cancer therapeutics. Success of this approach has created further interest in utilizing boron-carbohydrate interaction in the development of non-viral vectors.

We have also studied in **chapter 4** the biocompatibility and the impact of sugar decoration in novel hydroxyl-rich poly(glycidyl methacrylate) (PGMA)-based cationic glycopolymers; designed for intracellular delivery of siRNA to silence the ErbB family of proteins. The cationic polymers with different sugar decoration degrees (0, 9, and 33%) were synthesized by ring-opening reaction of PGMA with ethanolamine and a lactobionic acid-derived aminosaccharide (Lac-NH2). ErbB family is structurally related to the EGFR receptor, and is found to be overexpressed in many cancers such as gliomas, lung and cervical carcinomas. In this research work, specific EGFR knockdown of the protein tyrosine kinase ErbB-overexpressed in HeLa cells (cervical cancer) was achieved using these hydroxyl-rich polycation/siRNA complexes. Higher sugar content improved the biocompatibility of the polymers, though it also seemed to decrease the EGFR knockdown capability which was thought to be mainly related to the polyplexes' surface charge. The cationic glycopolymer with the highest sugar composition (33%) was found to be less effective in knocking down EGFR. Therefore, careful consideration of sugar decoration degree should be taken into account in designing glycopolymers as gene delivery vectors. An optimum balance was observed with PGEL-1 (9% sugar content) formulation, achieving ∼52% knockdown efficiency as well as high cell viability. Some systems rely on interaction with proteins to permit their uptake by target cells, such as the selective uptake of galactose-conjugated polyplexes through the asialoglycoprotein receptors[18–20]; considering this specific recognition, these novel PGMA-based cationic glycopolymers could be further explored to serve as a safe targeting gene delivery vectors to hepatocellular carcinomas.

In **chapter 5,** a novel sugar polycondensate was investigated as a cryoprotective agent for cell therapy applications. Cryopreservation has become an integral part of many cellular therapies. Immune cell-based cancer therapies rely on the infusion of highly viable post-thaw cells that effectively recognize and destroy the target tumour. Autologous and allogeneic stem cell therapies are known for substantially extending the lives of patients who have devastating diseases like cancer[21,22]. Cryopreservation plays a crucial role in the success of these therapeutics. The capability to slow ice growth and recrystallization is compulsory in the cryopreservation of cells and tissues to avoid injuries associated with the physical and chemical responses of freezing and thawing. Cryoprotective agents (CPAs) have been added to the cell suspension to mitigate cryoinjury and increase cell survival.

Still, some of these compounds pose greater risks for the clinical application of cryopreserved cells due to the inherent toxicity. Trehalose is known for its unique physicochemical properties, and its interaction with the phospholipids of the plasma membrane can reduce cell osmotic stress and stabilize the cryopreserved cells. Nonetheless, there has been a shortage of relevant studies on the synthesis of trehalose-based CPAs. We reported in **chapter 5** the synthesis and evaluation of a trehalose-based polymer and hydrogel and its use as a cryoprotectant and 3D cell scaffold for cell encapsulation and organoid production. *In vitro* cytotoxicity studies with the trehalose-based polymers (poly(Tre-ECH)) demonstrated biocompatibility up to 100 mg/mL. High post-thaw cell membrane integrity and post-thaw cell plating efficiencies were achieved after 24 h of incubation with skin fibroblast, HeLa (cervical) and PC3 (prostate) cancer cell lines under both ultra-rapid and controlled-rate freezing protocols. Differential scanning calorimetry (DSC) and a splat cooling assay for the determination of ice recrystallization inhibition (IRI) activity corroborated these trehalose-based polyethers' unique properties as cryoprotectants. Furthermore, the ability to form hydrogels as 3D cell scaffolds encourages the use of these novel polymers to develop cell organoids and cryopreservation platforms.

The fundamental role of nanotechnology in the biomedical field is to improve the drug therapeutic index by increasing efficacy and/or reducing toxicities associated with the drug, ensuring the targeted delivery of the drugs in a tissue-, cell- or organelle- in a specific manner. In **chapter 6,** a galactose-based nanogel was designed and synthesized for the delivery of a hypoxia-activated prodrug (HAP). Enhancement of the pharmaceutical properties (stability, solubility, circulating half-life and tumour accumulation) of the therapeutic molecules and a sustained and stimulus-triggered release are key features that have provided this physically-targeted nanogel unique characteristics and potential to be used as a cancer nanomedicine. In the later years, special attention has been given to the co-delivery of multiple drugs to improve therapeutic efficacy, overcome drug resistance and visualization of drug delivery sites by combining therapeutic agents with imaging modalities. These tactics have provided more precise control of each drug's bioavailability, the delivery of an appropriate drug ratio to the targeted sites, and/or real-time feedback on a therapeutic agent's *in vivo* efficacy, providing new approaches for the development of novel theranostics (therapy+diagnostics)[23]. Iodoazomycin Arabinoside (IAZA), an O_2-

mimicking nucleoside-based imaging agent that accumulates selectively in hypoxic tumours, has been used successfully to diagnose hypoxic tumours in a variety of cancer patients and has demonstrated its safety in healthy volunteers at a low chemical dose with no side effects. Structural features of IAZA, such as a bioreductive moiety liable for the selective activation and accrual in hypoxic tissue, a sugar conjugate facilitating its cellular intake and blood clearance and the iodine moiety allowing substitution with radioactive Iodine for imaging ($^{124/131}$I) and radiotherapy (^{131}I)— contribute to theranostic potential of this drug[24].

Significant progress in the synthesis of innovative colloidal bioconjugates, involved in various biomedical applications as delivery vehicles for tumour imaging and pharmaceutical delivery, especially in cancer treatment, has been seen in recent years. Current challenges that must be overcome by these colloidal systems to act as competitive carriers include efficient therapeutic loading capacity, targeted and specific delivery and controlled release profiles. Some of these issues have been met by this novel stimuli-responsive carbohydrate-based nanogel, where hydrodynamic size and composition play a key role in the encapsulation and target release efficiency of this versatile vehicle. IAZA has shown a promising theranostic (therapy and diagnostic) value for managing therapy-resistant hypoxic cancer cells[18], however poor solubility and deiodination under physiological conditions need to be addressed to enhance therapeutic efficacy of this drug. One of the leading causes of poor prognosis and high cancer mortality is the prevalence of therapy-resistant hypoxic tumour cells that promote metastases and increase conventional therapy resistance. The use of traditional therapeutic methods (radiotherapy and chemotherapy) is no longer effective to halt the progression of hypoxic cancer cells[25]. The emergence of novel mutations that confer more heterogeneity, allow tumour cells to avoid immune surveillance and exploit the immune system to continue local tumour growth and metastasis has increased the complexity of hypoxic cancer therapies[26]. Hypoxic tumours have poorly vascularized structures, which impairs drug delivery and oxygen supply to the cells. As a result, several genetic and translational processes start that promote tumour progression, invasion, metastasis, and make tumour resistant to conventional chemo-/radiotherapy.

A hypoxia directed nanotheranostic transformation of a hypoxia-activated prodrug (HAP) that facilitates delivery and accrual selectively in hypoxic cancer cells was developed by encapsulating IAZA in a functionally modified carbohydrate-based nanogel (*nano*IAZA) that demonstrate hypoxia-selective activation and accumulation in hypoxic tumour cells. In **chapter 6**, the therapeutic potential of *nano*IAZA was evaluated in different hypoxic cell lines *in vitro* [FaDu (head & neck) and PC3 (prostate) cancer cells] and subsequently *in vivo* chemotoxic potential of *nano*IAZA in a head & neck cancer tumour mouse xenograft was investigated. The nanogels were composed of a dense galactose outer shell and a crosslinked thermoresponsive DEGMA (di(ethylene glycol) methyl ethyl methacrylate) core. Optimization of the nanogels has led to high IAZA-loading capacity (≅ 80-88%) and a time-controlled release over 50 h. The synthesis procedure yielded favourable size and physical characteristics, high stability in physiological environment, and negligible toxicity of the nanogels *in vitro* and *in vivo*. The nanogels also exhibited no burst-release and high encapsulation efficiency, which would potentially improve the pharmacokinetic distribution of IAZA. Furthermore, *nano*IAZA (encapsulated IAZA) displayed superior *in vitro* hypoxia-selective cytotoxicity and radiosensitization therapeutic effects in comparison to IAZA itself in head and neck (FaDu) and prostate (PC3) cancer cell lines. The acute systemic toxicity profile of the nanogel was studied in immunocompromised mice, indicating no acute toxicity. Additionally, animal studies in hypoxic FaDu tumour-bearing mouse models have been used to evaluate the chemotoxicity of *nano*IAZA and the results showed that this nanoformulation offers a significant improvement in survival and tumour regression compared to the control group. To our advantage, iodine exists in several isotopic forms useful for both imaging and therapy, which make *nano*IAZA unique for multimodal theranosis of hypoxic tumours, either as a radiosensitizer or for *in-situ* molecular radionuclide therapy (MRT). Understanding the molecular phenotype induced by this drug and elucidating the observed *in vivo* chemosensitization mechanism and possible radiosensitization potential is still under investigation.

7.2 WHAT ARE THE CHALLENGES, LOOPHOLES AND HOW TO OVERCOME THEM?

The bottleneck in glycopolymers' application is understanding the molecular recognition and the multivalency interaction of saccharides. Living polymerization techniques have made it possible to control the preparation of multivalent glycoclusters, allowing the design of complex carbohydrate constructs applied in nanomedicines. However, elucidation of the molecular interaction between the constructs and the cell ligands is necessary to develop effective therapeutics. Pharmacokinetics of nanomedicine-based therapies and host immune system interactions could potentially affect drug tolerability and efficacy. Tumour stratification and selection, combination and multimodal therapies for synergistic effects, including immunotherapy, need to be considered when exploring new glyco-nanomedicines[27].

The potential toxicity of nanocarriers is a factor that limits their clinical use. Some carriers have complex chemical ligands or moieties to prevent their degradation by nucleases, immune system evasion, specificity and binding affinity for targets to enhance cellular uptake, the related effects are unknown in the human body[28]. Some of the biomaterials used for nanocarriers' development have been employed to synthesize macromolecules used in the clinic. However, their nano size confers unique material characteristics and possible effects that are still unspecified in the long term. In these studies, we designed novel glycopolymers with innovative architectures that reduced the cationic charge minimizing the *in vitro* cytotoxicity exhibited by these carriers. Nevertheless, the *in vivo* toxicity evaluation of the oxaborole-based and PGMA-based glycopolymers is required to demonstrate its safety in advanced studies. Likewise, siRNA dose scalability *in vivo* models with these vectors to ensure low cytotoxicity, cost and minimize off-target effects are factors that will need to be studied prior to the clinical translation of these glycopolymers siRNA-based systems.

Cancer drugs have notoriously been difficult to translate to standard care therapies successfully. Tumour hypoxia is prevalent in the microenvironment of solid tumours. Hypoxia induces transcriptional and translational cellular adaptations, including up-regulation of drug resistance transporters and energy metabolism, modulation of apoptotic

processes and induction of gene expression that promote metastases and compromise therapy outcomes. In oncology, tumour hypoxia is particularly associated with poor response to radiation and chemotherapy. This strongly supports the need to identify tumours with high hypoxic fractions and treat them with hypoxia directed therapeutics, which requires optimized treatment to assess the efficacy. When designing the animal experiments, the heterogeneity in the hypoxic fractions presented in the tumour mouse xenografts presented a complexity. A hypoxic tumour model based on FaDu tumour cells, an established human hypopharyngeal squamous cell carcinoma, was used to ensure proper stratification and minimize tumour heterogeneity in tissue oxygenation. According to Maftei *et al.* [29], the tumour oxygenation status is related to the tumour volume. For a tumour of approximately 200 mm^3, the observed total hypoxia is between 40-50% in the central tumour sections. When planning our animal studies, one group of six (6) mice was used as a hypoxia mapping group to corroborate this result however it was found that tumout hypoxia was heterogenic between the different tumours and it was not correlated with the tumour volume. The mice were sacrificed once the tumours reached 200-300 mm^3. Histology and hypoxia mapping using i.p. injection of ACN 2 hours prior to sacrifice were performed to quantify tumour hypoxia. Tumour cell implantation proved crucial for developing homogeneous tumours. Measuring the initial hypoxic fraction (prior to starting drug treatment) is recommended for better stratification of future studies. Proper dose escalation study in the animal studies design is also necessary to determine precise doses for the radiosensitization therapy potential of IAZA/*nano*IAZA. An *in vivo* radiosensitization study was conducted with IAZA and *nano*IAZA, where the survival of the mice injected with a single dose of 400 mg/Kg of IAZA/*nano*IAZA + IR was not significantly different from the results observed in the DMSO + IR control group. We conclude that possibly a single dose could not be enough to provide a therapeutic effect compared to a multi-dose course treatment, which is a common clinical practice. Biodistribution profiles, scalable dosage and possible treatment modalities concomitant with radiotherapy and chemotherapeutic drugs needs to be explored. If these considerations proved to be successful, advances to clinical trials could be a reality with the *in vivo* results observed with our carbohydrate-based nanogels for drug delivery applications.

7.3 NOVEL THERAPEUTIC SYSTEMS.

An alternative for the transient delivery of nucleic acids (siRNA) to cells is to make permanent changes into the genome. Genome editing allows the targeted alteration of genomic sequences in cells and organisms by inducing a DNA double-stranded break (DSB) by a nuclease at a targeted site. Clustered regularly interspaced short palindromic repeat (CRISPR)/Cas) system is an RNA-guided nuclease that has revolutionized the way that genome editing is performed. It was derived from bacteria's adaptable immune mechanisms to protect themselves from foreign nucleic acids, such as viruses or plasmids[30]. The potential to facilitate the *in vivo* delivery of CRISPR/Cas genome-editing systems have used viral vectors, including adenoviral, adeno-associated viral (AAV), and lentiviral vectors; but the emerging field of nanotechnology provides the use of nanosized carriers. This may have diverse potentials in targeted delivery of these editing systems to specific sites by particle surface modifications or tuning of physicochemical properties. A polymer-based Cas9 protein delivery has been reported, in which the Cas9–sgRNA complex was loaded into DNA-based self-assembled nanoparticles called 'DNA nanoclews' coated with the cationic polymer PEI[31]. Another study used non-viral nanoparticles that are synthesized by mixing C15 epoxide-terminated lipids to low-molecular-weight (MW= 600) PEI, C14 PEG2000 and sgRNAs[32]. Although *in vivo* applications of the system are still in infancy, currently, no glycopolymer-based vector has been reported for CRISPR/Cas9 editing applications. The challenge remains to design effective delivery systems with targeting capabilities that will improve the CRISPR/Cas9 system's performance *in vivo*.

Combinational immunotherapy is another novel approach employed in the gene therapy field. Engineering the delivery of the immunotherapeutics, focusing on target tissues to control the timing in terms of the duration of the active immune stimuli in tumours and location of the immunomodulation could prove to be effective in successful implementation of these therapeutics in the clinic while minimizing adverse effects[33]. Still, lack of insight into the nanomaterial–tissue interactions in the human body, from traversing biological barriers to clearance, the possible alternative nanoparticle uptake mechanisms, and the heterogeneity of the enhanced permeation and retention effect (EPR) effect in solid tumours do this translation into the clinic challenging.

Translation of nanomedicines into the clinic has been an intricate task due to the EPR effect's different characteristics. Nanomedicines have been tested in clinical trials mostly in advanced stages of cancers where metastasis and the development of multidrug resistance are observed. These tumours metastases habitually have fewer inflammatory cells and seem to have a weaker EPR effect than the primary tumour sites. EPR is associated with being more effective in smaller tumours; thus, nanomedicines' therapeutic potential could be more significant when treating the primary tumour site rather than the metastatic disease. Nevertheless, advanced imaging techniques and nanotheranostic compounds could explain the tumour microenvironment and the differences between the primary and metastatic sites. Additionally, the EPR effect has shown to be heterogeneous among tumour types and patients are influenced by properties such as particle size (< 1 mm to > 10 cm), tumour location, blood pressure, and vascular density[34]. Limited animal tumours models have been used to elucidate these changes, however these tumour models cannot accurately represent human tumours in terms of histological characteristics, metastatic pathways, post-treatment responses and pharmacokinetic properties of various nanostructures[35]. Xenografts models embody a straightforward model to study the pharmacokinetics, tumour accumulation, and biodistribution of nanomedicines, yet tumour characteristics vary considerably with different cell lines and sizes. The density and vascularization of similar size tumours can differ significantly, so establishing a standard cell line and tumour size for xenografts could substantially enhance the success of preclinical trials of the delivery system[36]. Recently Chan and colleagues studied the mechanisms mediating nanoparticle uptake into solid tumours[37]. They found that the frequency of gaps in the endothelial lining (EPR effect) is too low to account for the accumulation of nanoparticles using a combination of TEM, 3D imaging, the Zombie experiment and computational analysis. Interestingly, the evidence reinforced the conclusion that nanoparticles enter the tumour from blood vessels predominantly due to active trans-endothelial mechanisms (the process of transcytosis), not through passive targeting through the EPR effect. Controversy and debate have argued that the study only evaluated Gold nanoparticles and that further understanding of the molecular mechanisms that drive nanoparticles' trafficking into solid tumours is required. Nevertheless, challenging the EPR paradigm could provide a clue for the poor efficacy of nanomedicines

in the clinic. Approaches like the use of tumour penetrating peptides and cationic polymer conjugates[38] that enhance the delivery efficacy by harnessing the active transcytosis process could be the future in the design of cancer nanomedicines[39].

Biological cell culture models have hampered the discovery and therapeutic assessment of nanomedicines. Traditional 2D models constrained cells to non-physiological conditions; as a consequence, these cells have excessive nutrition and oxygenation, as well as active immortalization processes through multiple passages that result in cancer selection of rapidly proliferating cells which are known to be specifically susceptible to therapies, misrepresenting the whole tumour cell population. Metastatic cells are not easily cultured in classical culture dishes due to their poor adhesion, which has limited their screening process. Therefore, it is essential to develop higher complexity models that are reproducible and have the capacity of cellular imaging, like 3D multicellular spheroids. This can contain multiple cell phenotypes like quiescent and hypoxic cells within their hollow cores exhibiting more anti-cancer drug resistance than monolayer cultures representing the actual tumour. It has been shown that during spheroids growth, a gradient of oxygen is also established. this is explained by the oxygen availability and diffusion from the medium as the spheroid grows. As a consequence of the hypoxic environment found in spheroids, cells display the hypoxia genotypic profile exhibited in solid tumours, like the upregulation of hypoxia-inducible factors and vascular endothelial growth factors, linked with the hypoxic-resistant phenotype[40]. Still, limitations in the interactions with the tumour microenvironment, are faced but designing the appropriate 3D model can help in identifying cancer cells plasticity and the factors involved in tumour regulation such as cell-matrix, cell-cell interactions, cell growth factor receptors and multidrug resistance mechanisms (like the expression of efflux transporters, DNA repair and apoptosis signalling)[41].

In summary, the versatility of therapeutic strategies of glycopolymers-based nanomedicine shows the potential of its use in implementing personalized, targeted therapies. Further studies need to focus on the nanocarriers' molecular interaction mechanisms and innovative cell culture models to elucidate the role of surface ligand proteins and their interaction with tumour endothelial cells to enhance the cellular uptake and the role of different nanoparticle

sizes, shapes and surface chemistries in the extravasation of trans-endothelial pathways. Lastly, we need to understand the role of immune cells in the tumour microenvironment to hopefully work together with our body's defense mechanism to transfer glyco-nanomedicines from the bench to the clinic successfully.

7.4 REFERENCES

(1) Schultz, R. M. *Advances in Targeted Cancer Therapy (Progress in Drug Research)*; Herrling, P. L., Matter, A., Schultz, R. M., Eds.; Birkhäuser Basel: Basel, 2005. https://doi.org/10.1007/3-7643-7414-4.

(2) Tanner, P.; Baumann, P.; Enea, R.; Onaca, O.; Palivan, C.; Meier, W. Polymeric Vesicles: From Drug Carriers to Nanoreactors and Artificial Organelles. *Acc. Chem. Res.* **2011**, *44* (10), 1039–1049. https://doi.org/10.1021/ar200036k.

(3) Beija, M.; Salvayre, R.; Viguerie, N.; Marty, J.-D. D.; Lauth-de Viguerie, N.; Marty, J.-D. D.; Viguerie, N.; Marty, J.-D. D. Colloidal Systems for Drug Delivery: From Design to Therapy. *Trends Biotechnol.* **2012**, *30* (9), 485–496. https://doi.org/10.1016/j.tibtech.2012.04.008.

(4) Manjila, S. B.; Baby, J. N.; Bijin, E. N.; Constantine, I.; Pramod, K.; Valsalakumari, J. Novel Gene Delivery Systems. *Int. J. Pharm. Investig.* **2013**, *3* (1), 1–7. https://doi.org/10.4103/2230-973X.108958.

(5) McCrudden, C.; McCarthy, H. *Cancer Gene Therapy–Key Biological Concepts in the Design of Multifunctional Non-Viral Delivery Systems*; 2013.

(6) Abulateefeh, S. R.; Spain, S. G.; Aylott, J. W.; Chan, W. C.; Garnett, M. C.; Alexander, C. Thermoresponsive Polymer Colloids for Drug Delivery and Cancer Therapy. *Macromol. Biosci.* **2011**, *11* (12), 1722–1734. https://doi.org/10.1002/mabi.201100252.

(7) Ahmed, M.; Wattanaarsakit, P.; Narain, R. Cationic Glyco-Nanogels for Epidermal Growth Factor Receptor (EGFR) Specific SiRNA Delivery in Ovarian Cancer Cells. *Polym. Chem.* **2013**, *4* (13), 3829–3836. https://doi.org/10.1039/c3py00425b.

(8) Kabanov, A. V.; Vinogradov, S. V. Nanogels as Pharmaceutical Carriers:Finite Networks of Infinite Capabilities. *Angew. Chemie - Int. Ed.* **2009**, *48* (30), 5418–5429. https://doi.org/10.1002/anie.200900441.Nanogels.

(9) Sunasee, R.; Wattanaarsakit, P.; Ahmed, M.; Lollmahomed, F. B.; Narain, R. Biodegradable and Nontoxic Nanogels as Nonviral Gene Delivery Systems. *Bioconjug. Chem.* **2012**, *23* (9), 1925–1933. https://doi.org/10.1021/bc300314u.

(10) Yilmaz, G.; Becer, C. R. Glycopolymer Code: Programming Synthetic Macromolecules for Biological Targeting. *Macromol. Chem. Phys.* **2020**, *221* (7), 1–3. https://doi.org/10.1002/macp.202000006.

(11) Van Bruggen, C.; Hexum, J. K.; Tan, Z.; Dalal, R. J.; Reineke, T. M. Nonviral Gene Delivery with Cationic Glycopolymers. *Acc. Chem. Res.* **2019**. https://doi.org/10.1021/acs.accounts.8b00665.

(12) Roche, A. C.; Fajac, I.; Grosse, S.; Frison, N.; Rondanino, C.; Mayer, R.; Monsigny, M. Glycofection: Facilitated Gene Transfer by Cationic Glycopolymers. *Cell. Mol. Life Sci.* **2003**, *60* (2), 288–297. https://doi.org/10.1007/s000180300024.

(13) Wong, J. K. L.; Mohseni, R.; Hamidieh, A. A.; MacLaren, R. E.; Habib, N.; Seifalian, A. M. Will Nanotechnology Bring New Hope for Gene Delivery? *Trends Biotechnol.* **2017**, *35* (5), 434–451. https://doi.org/10.1016/j.tibtech.2016.12.009.

(14) Mehier-Humbert, S.; Guy, R. H. Physical Methods for Gene Transfer: Improving the Kinetics of Gene Delivery into Cells. *Adv. Drug Deliv. Rev.* **2005**, *57* (5), 733–753. https://doi.org/10.1016/j.addr.2004.12.007.

(15) Thapa, B.; Narain, R. *Mechanism, Current Challenges and New Approaches for Non Viral Gene Delivery*; Elsevier Ltd., 2016. https://doi.org/10.1016/B978-0-08-100520-0.00001-1.

(16) Ibraheem, D.; Elaissari, A.; Fessi, H. Gene Therapy and DNA Delivery Systems. *Int. J. Pharm.* **2014**, *459* (1–2), 70–83. https://doi.org/10.1016/j.ijpharm.2013.11.041.

(17) Ahmed, M.; Narain, R. The Effect of Polymer Architecture, Composition, and

Molecular Weight on the Properties of Glycopolymer-Based Non-Viral Gene Delivery Systems. *Biomaterials* **2011**, *32* (22), 5279–5290. https://doi.org/10.1016/j.biomaterials.2011.03.082.

(18) Quan, S.; Wang, Y.; Zhou, A.; Kumar, P.; Narain, R. Galactose-Based Thermosensitive Nanogels for Targeted Drug Delivery of Iodoazomycin Arabinofuranoside (IAZA) for Theranostic Management of Hypoxic Hepatocellular Carcinoma. *Biomacromolecules* **2015**, *16* (7), 1978–1986. https://doi.org/10.1021/acs.biomac.5b00576.

(19) Quan, S.; Kumar, P.; Narain, R. Cationic Galactose-Conjugated Copolymers for Epidermal Growth Factor (EGFR) Knockdown in Cervical Adenocarcinoma. *ACS Biomater. Sci. Eng.* **2016**, *2* (5), 853–859. https://doi.org/10.1021/acsbiomaterials.6b00085.

(20) Thapa, B.; Kumar, P.; Zeng, H.; Narain, R. Asialoglycoprotein Receptor-Mediated Gene Delivery to Hepatocytes Using Galactosylated Polymers. *Biomacromolecules* **2015**, *16* (9), 3008–3020. https://doi.org/10.1021/acs.biomac.5b00906.

(21) Pattabiraman, D. R.; Weinberg, R. A. Tackling the Cancer Stem Cells - What Challenges Do They Pose? *Nat. Rev. Drug Discov.* **2014**, *13* (7), 497–512. https://doi.org/10.1038/nrd4253.

(22) Sioud, M. Engineering Better Immunotherapies via RNA Interference. *Hum. Vaccines Immunother.* **2014**, *10* (11), 3165–3174. https://doi.org/10.4161/hv.29754.

(23) Shi, J.; Kantoff, P. W.; Wooster, R.; Farokhzad, O. C. Cancer Nanomedicine: Progress, Challenges and Opportunities. *Nat. Rev. Cancer* **2017**, *17* (1), 20–37. https://doi.org/10.1038/nrc.2016.108.Cancer.

(24) Kumar. Iodoazomycin Arabinoside for Low-Dose-Rate Isotope Radiotherapy: Radiolabeling, Stability, Long-Term Whole-Body Clearance and Radiation Dosimetry Estimates in Mice. *Nucl. Med. Biol.* **2005**, *32* (6), 647–653. https://doi.org/10.1016/j.nucmedbio.2005.04.019.

(25) Mattia, G.; Puglisi, R.; Ascione, B.; Malorni, W.; Carè, A.; Matarrese, P. Cell Death-

Based Treatments of Melanoma:Conventional Treatments and New Therapeutic Strategies Review-Article. *Cell Death Dis.* **2018**, *9* (2). https://doi.org/10.1038/s41419-017-0059-7.

(26) Velpurisiva, P.; Gad, A.; Piel, B.; Jadia, R.; Rai, P. Nanoparticle Design Strategies for Effective Cancer Immunotherapy. *J. Biomed.* **2017**, *2* (2), 64–77. https://doi.org/10.7150/jbm.18877.Nanoparticle.

(27) Gabizon, A. A.; de Rosales, R. T. M.; La-Beck, N. M. Translational Considerations in Nanomedicine: The Oncology Perspective. *Adv. Drug Deliv. Rev.* **2020**. https://doi.org/10.1016/j.addr.2020.05.012.

(28) Jin, J. O.; Kim, G.; Hwang, J.; Han, K. H.; Kwak, M.; Lee, P. C. W. Nucleic Acid Nanotechnology for Cancer Treatment. *Biochim. Biophys. Acta - Rev. Cancer* **2020**, *1874* (1), 188377. https://doi.org/10.1016/j.bbcan.2020.188377.

(29) Maftei, C. A.; Bayer, C.; Shi, K.; Vaupel, P. Intra-and Intertumor Heterogeneities in Total, Chronic, and Acute Hypoxia in Xenografted Squamous Cell Carcinomas : Detection and Quantification Using (Immuno-)Fluorescence Techniques. *Strahlentherapie und Onkol.* **2012**, *188* (7), 606–615. https://doi.org/10.1007/s00066-012-0105-4.

(30) Ran, F. A.; Hsu, P. D.; Wright, J.; Agarwala, V.; Scott, D. A.; Zhang, F. Genome Engineering Using the CRISPR-Cas9 System. *Nat. Protoc.* **2013**, *8* (11), 2281–2308. https://doi.org/10.1038/nprot.2013.143.

(31) Sun, W.; Ji, W.; Hall, J. M.; Hu, Q.; Wang, C.; Beisel, C. L.; Gu, Z. Self-Assembled DNA Nanoclews for the Efficient Delivery of CRISPR-Cas9 for Genome Editing. *Angew. Chemie - Int. Ed.* **2015**. https://doi.org/10.1002/anie.201506030.

(32) Platt, R. J.; Chen, S.; Zhou, Y.; Yim, M. J.; Swiech, L.; Kempton, H. R.; Dahlman, J. E.; Parnas, O.; Eisenhaure, T. M.; Jovanovic, M.; Graham, D. B.; Jhunjhunwala, S.; Heidenreich, M.; Xavier, R. J.; Langer, R.; Anderson, D. G.; Hacohen, N.; Regev, A.; Feng, G.; Sharp, P. A.; Zhang, F. CRISPR-Cas9 Knockin Mice for Genome Editing and Cancer Modeling. *Cell* **2014**. https://doi.org/10.1016/j.cell.2014.09.014.

(33) Irvine, D. J.; Dane, E. L. Enhancing Cancer Immunotherapy with Nanomedicine. *Nat. Rev. Immunol.* **2020**, *20* (5), 321–334. https://doi.org/10.1038/s41577-019-0269-6.

(34) Maeda, H.; Wu, J.; Sawa, T.; Matsumura, Y.; Hori, K. Tumor Vascular Permeability and the EPR Effect in Macromolecular Therapeutics: A Review. *J. Control. Release* **2000**, *65* (1–2), 271–284. https://doi.org/10.1016/S0168-3659(99)00248-5.

(35) He, Q.; Chen, J.; Yan, J.; Cai, S.; Xiong, H.; Liu, Y.; Peng, D.; Liu, Z.; Mo, M. Tumor Microenvironment Responsive Drug Delivery Systems. *Asian J. Pharm. Sci.* **2019**, *15* (4), 416–448. https://doi.org/10.1016/j.ajps.2019.08.003.

(36) El-Readi, M. Z.; Althubiti, M. A. Cancer Nanomedicine: A New Era of Successful Targeted Therapy. *J. Nanomater.* **2019**, *2019*. https://doi.org/10.1155/2019/4927312.

(37) Sindhwani, S.; Syed, A. M.; Ngai, J.; Kingston, B. R.; Maiorino, L.; Rothschild, J.; MacMillan, P.; Zhang, Y.; Rajesh, N. U.; Hoang, T.; Wu, J. L. Y.; Wilhelm, S.; Zilman, A.; Gadde, S.; Sulaiman, A.; Ouyang, B.; Lin, Z.; Wang, L.; Egeblad, M.; Chan, W. C. W. The Entry of Nanoparticles into Solid Tumours. *Nat. Mater.* **2020**, *19* (5), 566–575. https://doi.org/10.1038/s41563-019-0566-2.

(38) Zhou, Q.; Shao, S.; Wang, J.; Xu, C.; Xiang, J.; Piao, Y.; Zhou, Z.; Yu, Q.; Tang, J.; Liu, X.; Gan, Z.; Mo, R.; Gu, Z.; Shen, Y. Enzyme-Activatable Polymer–Drug Conjugate Augments Tumour Penetration and Treatment Efficacy. *Nat. Nanotechnol.* **2019**, *14* (8), 799–809. https://doi.org/10.1038/s41565-019-0485-z.

(39) Challenging Paradigms in Tumour Drug Delivery. *Nat. Mater.* **2020**, *19* (5), 477. https://doi.org/10.1038/s41563-020-0676-x.

(40) Nunes, A. S.; Barros, A. S.; Costa, E. C.; Moreira, A. F.; Correia, I. J. 3D Tumor Spheroids as in Vitro Models to Mimic in Vivo Human Solid Tumors Resistance to Therapeutic Drugs. *Biotechnol. Bioeng.* **2019**, *116* (1), 206–226. https://doi.org/10.1002/bit.26845.

(41) Alemany-Ribes, M.; Semino, C. E. Bioengineering 3D Environments for Cancer

Models. *Adv. Drug Deliv. Rev.* **2014**, *79*, 40–49. https://doi.org/10.1016/j.addr.2014.06.004.

BIBLIOGRAPHY

Abdellatif, A. A. H.; Abdelhafez, W. A.; Sarhan, H. A. Somatostatin Decorated Quantum Dots for Targeting of Somatostatin Receptors. *Iran. J. Pharm. Res.* **2018**, *17* (2), 513–524. https://doi.org/10.22037/ijpr.2018.2189.

Abdul Karim, A.; Dou, Q.; Li, Z.; Loh, X. J. Emerging Supramolecular Therapeutic Carriers Based on Host-Guest Interactions. *Chem. - An Asian J.* **2016**, *00*, 0–0. https://doi.org/10.1002/asia.201501434.

Abraham, S.; Keillor, K.; Capicciotti, C. J.; Perley-Robertson, G. E.; Keillor, J. W.; Ben, R. N. Quantitative Analysis of the Efficacy and Potency of Novel Small Molecule Ice Recrystallization Inhibitors. *Cryst. Growth Des.* **2015**, *15* (10), 5034–5039. https://doi.org/10.1021/acs.cgd.5b00995.

Abulateefeh, S. R.; Spain, S. G.; Aylott, J. W.; Chan, W. C.; Garnett, M. C.; Alexander, C. Thermoresponsive Polymer Colloids for Drug Delivery and Cancer Therapy. *Macromol. Biosci.* **2011**, *11* (12), 1722–1734. https://doi.org/10.1002/mabi.201100252.

Adams, G. E.; Flockhart, I. R.; Smithen, C. E.; Stratford, I. J.; Wardman, P.; Watts, M. E. Electron-Affinic Sensitization: VII. A Correlation between Structures, One-Electron Reduction Potentials, and Efficiencies of Nitroimidazoles as Hypoxic Cell Radiosensitizers. *Radiat. Res.* **1976**. https://doi.org/10.2307/3574491.

Adjei, I. M.; Sharma, B.; Labhasetwar, V. Nanoparticles: Cellular Uptake and Cytotoxicity. In *Nanomaterial, Advances in Experimental Medicine and Biology*; Chen, Y., Capco, D. G., Eds.; **2014**; Vol. 811. https://doi.org/10.1007/978-94-017-8739-0.

Adokoh, C. K.; Quan, S.; Hitt, M.; Darkwa, J.; Kumar, P.; Narain, R. Synthesis and Evaluation of Glycopolymeric Decorated Gold Nanoparticles Functionalized with Gold-Triphenyl Phosphine as Anti-Cancer Agents. *Biomacromolecules* **2014**, *15* (10), 3802–3810. https://doi.org/10.1021/bm5010977.

Ahmed M. Eissa; Cameron, N. R. Glycopolymer Conjugates. In *Advances in Polymer Science*; **2013**; Vol. 253, pp 71–114. https://doi.org/10.1007/12_2012_177.

Ahmed, M.; Deng, Z.; Liu, S.; Lafrenie, R.; Kumar, A.; Narain, R. Cationic glyconanoparticles: Their complexation with DNA, cellular uptake, and transfection efficiencies. *Bioconjug. Chem.* **2009**, *20* (11), 2169–2176 DOI: 10.1021/bc900350c.

Ahmed, M.; Deng, Z.; Narain, R. Study of transfection efficiencies of cationic glyconanoparticles of different sizes in human cell line. *ACS Appl. Mater. Interfaces* **2009**, *1* (9), 1980–1987 DOI: 10.1021/am900357x.

Ahmed, M.; Ishihara, K.; Narain, R. Calcium mediated formation of phosphorylcholine-based polyplexes for efficient knockdown of epidermal growth factor receptors (EGFR) in HeLa cells. *Chem. Commun.* **2014**, *50* (22), 2943 DOI: 10.1039/c4cc00181h.

Ahmed, M.; Lai, B. F.; Kizhakkedathu, J. N.; Narain, R. Hyperbranched Glycopolymers for Blood Biocompatibility. Bioconju- gate Chem. **2012**, 23, 1050−1058. (46) Xu, F. J.; Zhu, Y.; Chai, M. Y.; Liu, F. S. Comparison of Ethanolamine/Ethylenediamine-Functionalized Poly(Glycidyl Meth- acrylate) for Efficient Gene Delivery. Acta Biomater. 2011, 7, 3131− 3140

Ahmed, M.; Narain, R. Carbohydrate-Based Materials for Targeted Delivery of Drugs and Genes to the Liver. *Nanomedicine (Lond)* **2015**, *10* (14), 2263–2288. https://doi.org/10.2217/nnm.15.58.

Ahmed, M.; Narain, R. Glycopolymer Bioconjugates. In *Engineered Carbohydrate-Based Materials for Biomedical Applications: Polymers, Surfaces, Dendrimers, Nanoparticles, and Hydrogels*; **2011**; pp 167–188.

Ahmed, M.; Narain, R. Progress of RAFT Based Polymers in Gene Delivery. *Prog. Polym. Sci.* **2013**, *38* (5), 767–790. https://doi.org/10.1016/j.progpolymsci.2012.09.008.

Ahmed, M.; Narain, R. *Synthetic Cationic Glycopolymers for Gene Delivery*; Elsevier Ltd., **2016**. https://doi.org/10.1016/B978-0-08-100520-0.00004-7.

Ahmed, M.; Narain, R. The Effect of Molecular Weight, Compositions and Lectin Type on the Properties of Hyperbranched Glycopolymers as Non-Viral Gene Delivery Systems. Biomaterials **2012**, 33, 3990−4001.

Ahmed, M.; Narain, R. The Effect of Polymer Architecture, Composition, and Molecular Weight on the Properties of Glycopolymer-Based Non-Viral Gene Delivery Systems. *Biomaterials* **2011**, *32* (22), 5279–5290. https://doi.org/10.1016/j.biomaterials.2011.03.082.

Ahmed, M.; Pan, D. W.; Davis, M. E. Lack of in Vivo Antibody Dependent Cellular Cytotoxicity with Antibody Containing Gold Nanoparticles. *Bioconjug. Chem.* **2015**, *26* (5), 812–816. https://doi.org/10.1021/acs.bioconjchem.5b00139.

Ahmed, M.; Wattanaarsakit, P.; Narain, R. Cationic glyco-nanogels for epidermal growth factor receptor (EGFR) specific siRNA delivery in ovarian cancer cells. *Polym Chem* **2013**, *4* (13), 3829–3836 DOI: 10.1039/C3PY00425B.

Aleku, M.; Schulz, P.; Keil, O.; Santel, A.; Schaeper, U.; Dieckhoff, B.; Janke, O.; Endruschat, J.; Durieux, B.; Roder, N.; et al. Atu027, a Liposomal Small Interfering RNA Formulation Targeting Protein Kinase N3, Inhibits Cancer Progression. *Cancer Res.* **2008**, *68* (23), 9788–9798 DOI: 10.1158/0008-5472.CAN-08-2428.

Alemany-Ribes, M.; Semino, C. E. Bioengineering 3D Environments for Cancer Models. *Adv. Drug Deliv. Rev.* **2014**, *79*, 40–49. https://doi.org/10.1016/j.addr.2014.06.004.

Alexis, F.; Pridgen, E.; Molnar, L. K.; Farokhzad, O. C. Factors Affecting the Clearance and Biodistribution of Polymeric Nanoparticles. In *Molecular Pharmaceutics*; **2008**. https://doi.org/10.1021/mp800051m.

Alfayez, M.; Kantarjian, H.; Kadia, T.; Ravandi-Kashani, F.; Daver, N. CPX-351 (Vyxeos) in AML. *Leuk. Lymphoma* **2020**, *61* (2), 288–297. https://doi.org/10.1080/10428194.2019.1660970.

Ali, F., Huang, J., & Hongbo, Z. Properties and Characterization of Biomaterials. In *Chemistry of Bioconjugates*; Narain, R., Ed.; Jon Wiley & Sons, **2013**; pp 427–428. https://doi.org/doi:10.1142/9789812700858_0005.

Alonso,S. Exploiting the Bioengineering Versatility of Lactobionic Acid in Targeted Nanosystems and Biomaterials. J. Controlled Release **2018**, 287, 216−234.

Anguela, X. M.; High, K. A. Entering the Modern Era of Gene Therapy. *Annu. Rev. Med.* **2019**, *70* (1), 273–288. https://doi.org/10.1146/annurev-med-012017-043332.

Anselmo, A. C.; Mitragotri, S. Nanoparticles in the Clinic: An Update. *Bioeng. Transl. Med.* **2019**, *4* (3), 1–16. https://doi.org/10.1002/btm2.10143.

Anselmo, A. C.; Mitragotri, S. Nanoparticles in the Clinic. *Bioeng. Transl. Med.* **2016**, *1* (1), 10–29. https://doi.org/10.1002/btm2.10003.

Aparicio, L. A.; Calvo, M. B.; Figueroa, A.; Pulido, E. G.; Campelo, R. G. Potential Role of Sugar Transporters in Cancer and Their Relationship with Anticancer Therapy. *Int. J. Endocrinol.* **2010**, *2010*. https://doi.org/10.1155/2010/205357.

Arruebo, M.; Vilaboa, N.; Sáez-Gutierrez, B.; Lambea, J.; Tres, A.; Valladares, M.; González-Fernández, Á. Assessment of the Evolution of Cancer Treatment Therapies. *Cancers (Basel).* **2011**, *3* (3), 3279–3330. https://doi.org/10.3390/cancers3033279.

Baboo, J.; Kilbride, P.; Delahaye, M.; Milne, S.; Fonseca, F.; Blanco, M.; Meneghel, J.; Nancekievill, A.; Gaddum, N.; Morris, G. J. The Impact of Varying Cooling and Thawing Rates on the Quality of Cryopreserved Human Peripheral Blood T Cells. *Sci. Rep.* **2019**, *9* (1), 1–13. https://doi.org/10.1038/s41598-019-39957-x.

Balcerzak, A. K.; Capicciotti, C. J.; Briard, J. G.; Ben, R. N. Designing Ice Recrystallization Inhibitors: From Antifreeze (Glyco)Proteins to Small Molecules. *RSC Adv.* **2014**, *4* (80), 42682–42696. https://doi.org/10.1039/c4ra06893a.

Barenholz, Y. Doxil® - The First FDA-Approved Nano-Drug: Lessons Learned. *J. Control. Release* **2012**, *160* (2), 117–134. https://doi.org/10.1016/j.jconrel.2012.03.020.

Barui, A. *Synthetic Polymeric Gel*; Elsevier Ltd, **2018**. https://doi.org/10.1016/b978-0-08-102179-8.00003-x.

Beattie, G. M.; Crowe, J. H.; Lopez, A. D.; Cirulli, V.; Ricordi, C.; Hayek, A. Trehalose: A Cryoprotectant That Enhances Recovery and Preserves Function of Human Pancreatic Islets after Long-Term Storage. *Diabetes* **1997**, *46* (3), 519–523. https://doi.org/10.2337/diab.46.3.519.

Begg, A. C.; Stewart, F. A.; Vens, C. Strategies to Improve Radiotherapy with Targeted Drugs. *Nat. Rev. Cancer* **2011**, *11* (4), 239–253. https://doi.org/10.1038/nrc3007.

Behzadi, S.; Serpooshan, V.; Tao, W.; Hamaly, M. A.; Alkawareek, M. Y.; Dreaden, E. C.; Brown, D.; Alkilany, A. M.; Farokhzad, O. C.; Mahmoudi, M. Cellular Uptake of Nanoparticles: Journey inside the Cell. *Chem. Soc. Rev.* **2017**, *46* (14), 4218–4244. https://doi.org/10.1039/c6cs00636a.

Beija, M.; Salvayre, R.; Viguerie, N.; Marty, J.-D. D.; Lauth-de Viguerie, N.; Marty, J.-D. D.; Viguerie, N.; Marty, J.-D. D. Colloidal Systems for Drug Delivery: From Design to Therapy. *Trends Biotechnol.* **2012**, *30* (9), 485–496. https://doi.org/10.1016/j.tibtech.2012.04.008.

Benaroudj, N.; Lee, D. H.; Goldberg, A. L. Trehalose Accumulation during Cellular Stress Protects Cells and Cellular Proteins from Damage by Oxygen Radicals. *J. Biol. Chem.* **2001**, *276* (26), 24261–24267. https://doi.org/10.1074/jbc.M101487200.

Bennewith, K. L.; Dedhar, S. Targeting Hypoxic Tumour Cells to Overcome Metastasis. *BMC Cancer* **2011**, *11*, 504. https://doi.org/10.1186/1471-2407-11-504.

Biggs, C. I.; Bailey, T. L.; Ben Graham; Stubbs, C.; Fayter, A.; Gibson, M. I. Polymer Mimics of Biomacromolecular Antifreezes. *Nat. Commun.* **2017**, *8* (1), 1–11. https://doi.org/10.1038/s41467-017-01421-7.

Bischoff, P.; Altmeyer, A.; Dumont, F. Radiosensitising Agents for the Radiotherapy of Cancer: Advances in Traditional and Hypoxia Targeted Radiosensitisers. *Expert Opinion on Therapeutic Patents*. **2009**. https://doi.org/10.1517/13543770902824172.

Blanco, E.; Shen, H.; Ferrari, M. Principles of nanoparticle design for overcoming biological barriers to drug delivery. *Nat. Biotechnol.* **2015**, *33* (9), 941–951 DOI: 10.1038/nbt.3330.

Blasco, E.; Sims, M. B.; Goldmann, A. S.; Sumerlin, B. S.; Barner-Kowollik, C. 50th Anniversary Perspective: Polymer Functionalization. *Macromolecules* **2017**, *50* (14), 5215–5252. https://doi.org/10.1021/acs.macromol.7b00465.

Boldt, J. Current Results with Slow Freezing and Vitrification of the Human Oocyte. *Reprod. Biomed. Online* **2011**, *23* (3), 314–322. https://doi.org/10.1016/j.rbmo.2010.11.019.

Bono, N.; Ponti, F.; Mantovani, D.; Candiani, G. Non-Viral in Vitro Gene Delivery: It Is Now Time to Set the Bar! *Pharmaceutics* **2020**, *12* (2). https://doi.org/10.3390/pharmaceutics12020183.

Boucher, Y.; Baxter, L. T.; Jain, R. K. Interstitial Pressure Gradients in Tissue-Isolated and Subcutaneous Tumors: Implications for Therapy. *Cancer Res.* **1990**, *50* (15), 4478–4484.

Brenner, D. R.; Weir, H. K.; Demers, A. A.; Ellison, L. F.; Mhsc, C. L.; Shaw, A.; Turner, D.; Woods, R. R.; Smith, L. M. Projected Estimates of Cancer in Canada in 2020. **2020**, *192* (9), 199–205. https://doi.org/10.1503/cmaj.191292.

Bristow, R. G.; Hill, R. P. Hypoxia and Metabolism. Hypoxia, DNA Repair and Genetic Instability. *Nat. Rev. Cancer* **2008**, *8* (3), 180–192. https://doi.org/10.1038/nrc2344.

Brizel, D. M.; Sibley, G. S.; Prosnitz, L. R.; Scher, R. L.; Dewhirst, M. W. Tumor Hypoxia Adversely Affects the Prognosis of Carcinoma of the Head and Neck. *Int. J. Radiat. Oncol. Biol. Phys.* **1997**, *38* (2), 285–289. https://doi.org/10.1016/S0360-3016(97)00101-6.

Brown, J. M.; Wilson, W. R. Exploiting Tumour Hypoxia in Cancer Treatment. *Nat. Rev. Cancer* **2004**, *4* (6), 437–447. https://doi.org/10.1038/nrc1367.

Buchanan, S. S.; Gross, S. A.; Acker, J. P.; Toner, M.; Carpenter, J. F.; Pyatt, D. W. Cryopreservation of Stem Cells Using Trehalose: Evaluation of the Method Using a Human Hematopoietic Cell Line. *Stem Cells Dev.* **2004**, *13* (3), 295–305. https://doi.org/10.1089/154732804323099226.

Cai, H.; Xiang, Y.; Zeng, Y.; Li, Z.; Zheng, X.; Luo, Q.; Zhu, H.; Gong, Q.; Gu, Z.; Liu, Y.; Zhang, H.; Luo, K. Cathepsin B-Responsive and Gadolinium-Labeled Branched Glycopolymer-PTX Conjugate-Derived Nanotheranostics for Cancer Treatment. *Acta Pharm. Sin. B* **2020**. https://doi.org/10.1016/j.apsb.2020.07.023.

Cardarelli, F.; Digiacomo, L.; Marchini, C.; Amici, A.; Salomone, F.; Fiume, G.; Rossetta, A.; Gratton, E.; Pozzi, D.; Caracciolo, G. The intracellular trafficking mechanism of Lipofectamine-based transfection reagents and its implication for gene delivery. *Sci. Rep.* **2016**, *6* (1), 25879 DOI: 10.1038/srep25879.

Cerrada, M. L.; Sánchez-Chaves, M.; Ruiz, C.; Fernández- García, M. Recognition Abilities and Development of Heat-Induced Entangled Networks in Lactone-Derived Glycopolymers Obtained from Ethylene-vinyl Alcohol Copolymers. Biomacromolecules **2009**, 10, 1828−1837.

Challenging Paradigms in Tumour Drug Delivery. *Nat. Mater.* **2020**, *19* (5), 477. https://doi.org/10.1038/s41563-020-0676-x.

Chapman, J Donald; Lee, Jane; Meeker, B. E. Keynote Address: Cellular Reduction of Nitroimidazole Drugs: Potential for Selective Chemotherapy and Diagnosis of Hypoxic Cells. *Int. J. Radiat. Oncol. Biol. Phys.* **1989**, *16* (4), 911–917. https://doi.org/10.1016/0360-3016(89)90886-9.

Chaytor, J. L.; Ben, R. N. Assessing the Ability of a Short Fluorinated Antifreeze Glycopeptide and a Fluorinated Carbohydrate Derivative to Inhibit Ice Recrystallization. *Bioorg. Med. Chem. Lett.* **2010**, *20* (17), 5251–5254. https://doi.org/10.1016/J.BMCL.2010.06.148.

Chen, F.; Zhang, W.; Wu, W.; Jin, Y.; Cen, L.; Kretlow, J. D.; Gao, W.; Dai, Z.; Wang, J.; Zhou, G.; Liu, W.; Cui, L.; Cao, Y. Cryopreservation of Tissue-Engineered Epithelial Sheets in Trehalose. *Biomaterials* **2011**, *32* (33), 8426–8435. https://doi.org/10.1016/j.biomaterials.2011.07.008.

Chen, G.; Yue, A.; Ruan, Z.; Yin, Y.; Wang, R.; Ren, Y.; Zhu, L. Comparison of the Effects of Different Cryoprotectants on Stem Cells from Umbilical Cord Blood. *Stem Cells Int.* **2016**, *2016*, 1–7. https://doi.org/10.1155/2016/1396783.

Chen, S.; Sun, B.; Miao, H.; Wang, G.; Sun, P.; Li, J.; Wang, W.; Fan, Q.; Huang, W. NIR-II Dye-Based Multifunctional Telechelic Glycopolymers for NIR-IIa Fluorescence Imaging-Guided Stimuli-Responsive Chemo-Photothermal Combination Therapy. *ACS Mater. Lett.* **2020**, *2* (2), 174–183. https://doi.org/10.1021/acsmaterialslett.9b00480.

Chen, Y.; Diaz-Dussan, D.; Peng, Y.-Y. Y.; Narain, R. Hydroxyl-Rich PGMA-Based Cationic Glycopolymers for Intracellular SiRNA Delivery: Biocompatibility and Effect of Sugar Decoration Degree. *Biomacromolecules* **2019**, *20* (5), 2068–2074. https://doi.org/10.1021/acs.biomac.9b00274.

Chen, Y.; Tan, Z.; Wang, W.; Peng, Y.-Y.; Narain, R. Injectable, Self-Healing, and Multi-Responsive Hydrogels via Dynamic Covalent Bond Formation between Benzoxaborole and Hydroxyl Groups. Biomacromolecules **2019**, 20, 1028−1035.

Chen, Y.; Wang, W.; Wu, D.; Nagao, M.; Hall, D. G.; Thundat, T.; Narain, R. Injectable Self-Healing Zwitterionic Hydrogels Based on Dynamic Benzoxaborole−Sugar Interactions with Tunable Mechanical Properties. Biomacromolecules **2018**, 19, 596−605.

Ciardiello, F.; De Vita, F. Epidermal Growth Factor Receptor (EGFR) Inhibitors in Cancer Therapy. In *Advances in Targeted Cancer Therapy*; Birkhäuser Basel: Basel, **2005**; pp 93–115. https://doi.org/10.1007/3-7643-7414-4_5.

Cleary, J.; Gelband, H.; Wagner, J. Cancer: Disease Control Priorities. *Dis. Control Priorities 3rd Ed.* **2015**, 1–363. https://doi.org/10.1017/CBO9781107415324.004.

Clegg, J. S. The Physical Properties and Metabolic Status of Artemia Cysts at Low Water Contents: The Water Replacement Hypothesis. *Membr. Metab. dry Org.* **1986**, 169–187.

Cohen-Karni, D.; Kovaliov, M.; Li, S.; Jaffee, S.; Tomycz, N. D.; Averick, S. Fentanyl Initiated Polymers Prepared by ATRP for Targeted Delivery. Bioconjugate Chem. **2017**, 28, 1251−1259.

Crowe, J. H.; Crowe, L. M.; Chapman, D. Preservation of Membranes in Anhydrobiotic Organisms: The Role of Trehalose. *Science (80-.).* **1984**, *223* (4637), 701–703. https://doi.org/10.1126/science.223.4637.701.

Cyprian, F. S.; Akhtar, S.; Gatalica, Z.; Vranic, S. Targeted Immunotherapy with a Checkpoint Inhibitor in Combination with Chemotherapy: A New Clinical Paradigm in the Treatment of Triple-Negative Breast Cancer. *Bosn. J. basic Med. Sci.* **2019**, *19* (3), 227–233. https://doi.org/10.17305/bjbms.2019.4204.

Dalby, B.; Cates, S.; Harris, A.; Ohki, E. C.; Tilkins, M. L.; Price, P. J.; Ciccarone, V. C. Advanced Transfection with Lipofectamine 2000 Reagent: Primary Neurons, SiRNA, and High-Throughput Applications. *Methods* **2004**, *33* (2), 95–103. https://doi.org/10.1016/j.ymeth.2003.11.023.

Dang, C. V.; Reddy, E. P.; Shokat, K. M.; Soucek, L. Drugging the "undruggable" Cancer Targets. *Nat. Rev. Cancer* **2017**, *17* (8), 502–508. https://doi.org/10.1038/nrc.2017.36.

Davidson, B. L.; McCray, P. B. Current Prospects for RNA Interference-Based Therapies. *Nat. Rev. Genet.* **2011**, *12* (5), 329–340. https://doi.org/10.1038/nrg2968.

Davis, J. M.; Rowley, S. D.; Braine, H. G.; Piantadosi, S.; Santos, G. W. Clinical Toxicity of Cryopreserved Bone Marrow Graft Infusion. *Blood* **1990**, *75* (3), 781–786. https://doi.org/10.1182/blood.v75.3.781.bloodjournal753781.

Davis, M. E.; Zuckerman, J. E.; Choi, C. H. J.; Seligson, D.; Tolcher, A.; Alabi, C. A.; Yen, Y.; Heidel, J. D.; Ribas, A. Evidence of RNAi in Humans from Systemically Administered SiRNA via Targeted Nanoparticles. *Nature* **2010**, *464* (7291), 1067–1070. https://doi.org/10.1038/nature08956.

de Fougerolles, A.; Vornlocher, H.-P.; Maraganore, J.; Lieberman, J. Interfering with disease: a progress report on siRNA-based therapeutics. *Nat. Rev. Drug Discov.* **2007**, *6* (6), 443–453 DOI: 10.1038/nrd2310.

De Ridder, M.; Verellen, D.; Verovski, V.; Storme, G. Hypoxic Tumor Cell Radiosensitization through Nitric Oxide. *Nitric Oxide - Biology and Chemistry*. **2008**. https://doi.org/10.1016/j.niox.2008.04.015.

Deng, W.; Chen, W.; Clement, S.; Guller, A.; Zhao, Z.; Engel, A.; Goldys, E. M. Controlled Gene and Drug Release from a Liposomal Delivery Platform Triggered by X-Ray Radiation. *Nat. Commun.* **2018**, *9* (1), 1–11. https://doi.org/10.1038/s41467-018-05118-3.

Deng, Z.; Ahmed, M.; Narain, R. Novel well-defined glycopolymers synthesized via the reversible addition fragmentation Chain transfer process in aqueous media. *J. Polym. Sci. Part A Polym. Chem.* **2009**, *47* (2), 614–627 DOI: 10.1002/pola.23187.

Devi, G. R. SiRNA-Based Approaches in Cancer Therapy. *Cancer Gene Ther.* **2006**, *13* (9), 819–829. https://doi.org/10.1038/sj.cgt.7700931.

Diaz-Dussan, D.; Nakagawa, Y.; Peng, Y.-Y. Y.; Sanchez, L. V.; Ebara, M.; Kumar, P.; Narain, R.; C, L. V. S.; Ebara, M.; Kumar, P.; Narain, R. Effective and Specific

Gene Silencing of Epidermal Growth Factor Receptors Mediated by Conjugated Oxaborole and Galactose-Based Polymers. *ACS Macro Lett.* **2017**, *6* (7), 768–774. https://doi.org/10.1021/acsmacrolett.7b00388.

Dickerson, E. B.; Blackburn, W. H.; Smith, M. H.; Kapa, L. B.; Lyon, L. A.; McDonald, J. F. Chemosensitization of cancer cells by siRNA using targeted nanogel delivery. *BMC Cancer* **2010**, *10* (1), 10 DOI: 10.1186/1471-2407-10-10.

Dische, S. Chemical Sensitizers for Hypoxic Cells: A Decade of Experience in Clinical Radiotherapy. *Radiother. Oncol.* **1985**, *3* (2), 97–115. https://doi.org/10.1016/S0167-8140(85)80015-3.

Downward, J.; Yarden, Y.; Mayes, E.; Scrace, G.; Totty, N.; Stockwell, P.; Ullrich, A.; Schlessinger, J.; Waterfield, M. D. Close Similarity of Epidermal Growth Factor Receptor and v-erb-B Oncogene Protein Sequences. Nature **1984**, 307, 521−527.

Drake, A. C.; Lee, Y.; Burgess, E. M.; Karlsson, J. O. M.; Eroglu, A.; Higgins, A. Z. Effect of Water Content on the Glass Transition Temperature of Mixtures of Sugars, Polymers, and Penetrating Cryoprotectants in Physiological Buffer. *PLoS One* **2018**, *13* (1), 1–15. https://doi.org/10.1371/journal.pone.0190713.

Duffy, J. P.; Eibl, G.; Reber, H. A.; Hines, O. J. Influence of Hypoxia and Neoangiogenesis on the Growth of Pancreatic Cancer. *Mol. Cancer* **2003**, *2* (2), 12. https://doi.org/10.1097/01.mpa.0000229010.62538.f2.

El-Readi, M. Z.; Althubiti, M. A. Cancer Nanomedicine: A New Era of Successful Targeted Therapy. *J. Nanomater.* **2019**, *2019*. https://doi.org/10.1155/2019/4927312.

Emdad, L.; Sarkar, D.; Fisher, P. B. Gene Therapies for Cancer: Strategies, Challenges and Successes. *HHS Public Access* **2016**, *230* (2), 259–271. https://doi.org/10.1002/jcp.24791.Gene.

Eroglu, A. Cryopreservation of Mammalian Oocytes by Using Sugars: Intra- and Extracellular Raffinose with Small Amounts of Dimethylsulfoxide Yields High Cryosurvival, Fertilization, and Development Rates. *Cryobiology* **2010**, *60* (706), 1–14. https://doi.org/10.1016/j.cryobiol.2009.07.001.Cryopreservation.

Eroglu, A.; Russo, M. J.; Bieganski, R.; Fowler, A.; Cheley, S.; Bayley, H.; Toner, M. Intracellular Trehalose Improves the Survival of Cryopreserved Mammalian Cells. *Nat. Biotechnol.* **2000**, *18* (2), 163–167. https://doi.org/10.1038/72608.

Eroglu, A.; Toner, M.; Toth, T. L. Beneficial Effect of Microinjected Trehalose on the Cryosurvival of Human Oocytes. *Fertil. Steril.* **2002**, *77* (1), 152–158. https://doi.org/10.1016/S0015-0282(01)02959-4.

Fihurka, O.; Sanchez-Ramos, J.; Sava, V. Optimizing Nanoparticle Design for Gene Therapy: Protection of Oligonucleotides from Degradation Without Impeding Release of Cargo. *Nanomed Nanosci Res* **2018**, *2* (6), 139–148. https://doi.org/10.29011/2577-1477.100055.

Filipová, M.; Bojarová, P.; Rodrigues Tavares, M.; Bumba, L.; Elling, L.; Chytil, P.; Gunár, K.; Křen, V.; Etrych, T.; Janoušková, O. Glycopolymers for Efficient Inhibition of Galectin-3: In Vitro Proof of Efficacy Using Suppression of T Lymphocyte Apoptosis and Tumor Cell Migration. *Biomacromolecules* **2020**. https://doi.org/10.1021/acs.biomac.0c00515.

Fire, A.; Xu, S.; Montgomery, M. K.; Kostas, S. A.; Driver, S. E.; Mello, C. C. Potent and Specific Genetic Interference by Double-Stranded RNA in Caenorhabditis Elegans. *Nature* **1998**, *391* (6669), 806–811. https://doi.org/10.1038/35888.

Fisher, D. A.; Lakshmanan, J. Metabolism and Effects of Epidermal Growth Factor and Related Growth Factors in Mammals. *Endocr. Rev.* **1990**. https://doi.org/10.1210/edrv-11-3-418.

Flodin, G. M. P.; Perstorp; Ingelman, G. A. B. Sucrose Ether Copolymerizates. US Patent 3,300,474, **1967**.

Foroozandeh, P.; Aziz, A. A. Insight into Cellular Uptake and Intracellular Trafficking of Nanoparticles. *Nanoscale Res. Lett.* **2018**, *13*. https://doi.org/10.1186/s11671-018-2728-6.

Fuller, B. J.; Lane, N.; Benson, E. E. *Life in the Frozen State*; Boca Raton, Fla: CRC Press, **2004**.

Gabizon, A. A.; de Rosales, R. T. M.; La-Beck, N. M. Translational Considerations in Nanomedicine: The Oncology Perspective. *Adv. Drug Deliv. Rev.* **2020**. https://doi.org/10.1016/j.addr.2020.05.012.

Gary, D. J.; Min, J. Bin; Kim, Y.; Park, K.; You-Yeon, W. The Effect of N/P Ratio on the In Vitro and In Vivo Interaction Properties of PEGylated Poly(2-(Dimethylamino)Ethyl Methacrylate)-Based SiRNA Complexes. *Macromol. Biosci.* **2014**, *71* (11), 3831–3840. https://doi.org/10.1158/0008-5472.CAN-10-4002.BONE.

Gavrilov, K.; Saltzman, W. M. Therapeutic siRNA: Principles, challenges, and strategies. *Yale J. Biol. Med.* **2012**, *85* (2), 187–200.

Germain, M.; Caputo, F.; Metcalfe, S.; Tosi, G.; Spring, K.; Åslund, A. K. O.; Pottier, A.; Schiffelers, R.; Ceccaldi, A.; Schmid, R. Delivering the Power of Nanomedicine to Patients Today. *J. Control. Release* **2020**, *326* (July), 164–171. https://doi.org/10.1016/j.jconrel.2020.07.007.

Gonzalez-Cao, M.; Karachaliou, N.; Santarpia, M.; Viteri, S.; Meyerhans, A.; Rosell, R. Activation of Viral Defense Signaling in Cancer. *Ther. Adv. Med. Oncol.* **2018**, *10*, 175883591879310. https://doi.org/10.1177/1758835918793105.

Goodwin, E. C.; DiMaio, D. Repression of Human Papillomavirus Oncogenes in HeLa Cervical Carcinoma Cells Causes the Orderly Reactivation of Dormant Tumor Suppressor Pathways. *Proc. Natl. Acad. Sci. U. S. A.* **2000**, *97* (23), 12513–12518. https://doi.org/10.1073/pnas.97.23.12513.

Gotwals, P.; Cameron, S.; Cipolletta, D.; Cremasco, V.; Crystal, A.; Hewes, B.; Mueller, B.; Quaratino, S.; Sabatos-Peyton, C.; Petruzzelli, L.; Engelman, J. A.; Dranoff, G. Prospects for Combining Targeted and Conventional Cancer Therapy with Immunotherapy. *Nat. Rev. Cancer* **2017**, *17* (5), 286–301. https://doi.org/10.1038/nrc.2017.17.

Graham, B.; Fayter, A. E. R.; Houston, J. E.; Evans, R. C.; Gibson, M. I. Facially Amphipathic Glycopolymers Inhibit Ice Recrystallization. *J. Am. Chem. Soc.* **2018**, *140* (17), 5682–5685. https://doi.org/10.1021/jacs.8b02066.

Guo, N.; Puhlev, I.; Brown, D. R.; Mansbridge, J.; Levine, F. Trehalose Expression Confers Desiccation Tolerance on Human Cells. *Nat. Biotechnol.* **2000**, *18* (2), 168–171. https://doi.org/10.1038/72616.

Guo, P.; Gu, W.; Chen, Q.; Lu, H.; Han, X.; Li, W.; Gao, H. Dual Functionalized Amino Poly(Glycerol Methacrylate) with Guanidine and Schiff-Base Linked Imidazole

for Enhanced Gene Transfection and Minimized Cytotoxicity. J. Mater. Chem. B **2015**, 3, 6911−6918.

Gupta, S.; Gupta, M. K. Possible Role of Nanocarriers in Drug Delivery against Cervical Cancer. *Nano Rev. Exp.* **2017**, *8* (1), 1335567. https://doi.org/10.1080/20022727.2017.1335567.

Hamilton, A. J.; Baulcombe, D. C. A Species of Small Antisense RNA in Posttranscriptional Gene Silencing in Plants. *Science (80-.).* **1999**, *286* (5441), 950-2. https://doi.org/10.1126/science.286.5441.950.

Han, X.; Chen, Q.; Lu, H.; Ma, J.; Gao, H. Probe Intracellular Trafficking of a Polymeric DNA Delivery Vehicle by Functionaliza- tion with an Aggregation-Induced Emissive Tetraphenylethene Derivative. ACS Appl. Mater. Interfaces **2015**, 7, 28494−28501.

Hanahan, D.; Weinberg, R. A.; Pan, K. H.; Shay, J. W.; Cohen, S. N.; Taylor, M. B.; Clarke, N. W.; Jayson, G. C.; Eshleman, J. R.; Nowak, M. A.; al., et. Hallmarks of Cancer: The Next Generation. *Cell* **2011**, *144* (5), 646–674. https://doi.org/10.1016/j.cell.2011.02.013.

Hashida, M.; Hirabayashi, H.; Nishikawa, M.; Takakura, Y. Targeted Delivery of Drugs and Proteins to the Liver via Receptor-Mediated Endocytosis. *J. Control. Release* **1997**, *46* (1–2), 129–137. https://doi.org/10.1016/S0168-3659(96)01577-5.

Häuselmann, I.; Borsig, L. Altered Tumor-Cell Glycosylation Promotes Metastasis. *Front. Oncol.* **2014**, *4 MAR* (February), 1–15. https://doi.org/10.3389/fonc.2014.00028.

He, Q.; Chen, J.; Yan, J.; Cai, S.; Xiong, H.; Liu, Y.; Peng, D.; Liu, Z.; Mo, M. Tumor Microenvironment Responsive Drug Delivery Systems. *Asian J. Pharm. Sci.* **2019**, *15* (4), 416–448. https://doi.org/10.1016/j.ajps.2019.08.003.

Heidenreich, O. Targeting Oncogenes with siRNAs. In *Methods in Molecular Biology, siRNA and miRNA Gene Silencing*; **2009**; Vol. 487, pp 221–242.

Hengherr, S.; Heyer, A. G.; Köhler, H.-R.; Schill, R. O. Trehalose and Anhydrobiosis in Tardigrades - Evidence for Divergence in Responses to Dehydration. *FEBS J.* **2008**, *275* (2), 281–288. https://doi.org/10.1111/j.1742-4658.2007.06198.x.

Hicks, K.; Siim, B.; Pruijn, F.; Wilson, W. Oxygen Dependence of the Metabolic Activation and Cytotoxicity of Tirapazamine: Implications for Extravascular Transport and Activity in Tumors. *Radiat Res* **2004**, *161* (6), 656–666. https://doi.org/10.1667/RR3178.

Higashiyama, S.; Abraham, J.; Miller, J.; Fiddes, J.; Klagsbrun, M. A Heparin-Binding Growth Factor Secreted by Macrophage-like Cells That Is Related to EGF. *Science (80-.).* **1991**. https://doi.org/10.1126/science.1840698.

Holban, A. M.; Grumezescu, A. M.; Frère, A.; Evrard, B.; Mottet, D.; Piel, G. Polymeric Nanoparticles as SiRNA Drug Delivery System for Cancer Therapy: The Long Road to Therapeutic Efficiency. In *Nanoarchitectonics for Smart Delivery and Drug Targeting*; **2016**; pp 503–540. https://doi.org/10.1016/B978-0-323-47347-7.00018-5.

Holovati, J. L.; Gyongyossy-Issa, M. I. C.; Acker, J. P. Effects of Trehalose-Loaded Liposomes on Red Blood Cell Response to Freezing and Post-Thaw Membrane Quality. *Cryobiology* **2009**, *58* (1), 75–83. https://doi.org/10.1016/j.cryobiol.2008.11.002.

Hu, Y.; Li, Y.; Xu, F.-J. Versatile Functionalization of Polysaccharides via Polymer Grafts: From Design to Biomedical Applications. Acc. Chem. Res. **2017**, 50, 281−292.

Hu, Y.; Wen, C.; Song, L.; Zhao, N.; Xu, F. J. Multifunctional Hetero-Nanostructures of Hydroxyl-Rich Polycation Wrapped Cellulose-Gold Hybrids for Combined Cancer Therapy. J. Controlled Release **2017**, 255, 154−163.

Huang, H.; Zhao, G.; Zhang, Y.; Xu, J.; Toth, T. L.; He, X. Predehydration and Ice Seeding in the Presence of Trehalose Enable Cell Cryopreservation. *ACS Biomater. Sci. Eng.* **2017**, *3* (8), 1758–1768. https://doi.org/10.1021/acsbiomaterials.7b00201.

Huang, Y. Preclinical and Clinical Advances of GalNAc-Decorated Nucleic Acid Therapeutics. *Mol. Ther. - Nucleic Acids* **2017**, *6* (March), 116–132. https://doi.org/10.1016/j.omtn.2016.12.003.

Huang, Y.; Luo, Y.; Zheng, W.; Chen, T. Rational Design of Cancer-Targeted BSA Protein Nanoparticles as Radiosensitizer to Overcome Cancer Radioresistance.

ACS Appl. Mater. Interfaces **2014**, *6* (21), 19217–19228. https://doi.org/10.1021/am505246w.

Hubálek, Z. Protectants Used in the Cryopreservation of Microorganisms. *Cryobiology* **2003**, *46* (3), 205–229. https://doi.org/10.1016/S0011-2240(03)00046-4.

Hubel, A.; Skubitz, A. P. N. Principles of Cryopreservation. In *Biobanking of Human Biospecimens*; Springer International Publishing: Cham, **2017**; pp 1–21. https://doi.org/10.1007/978-3-319-55120-3_1.

Hynes, N. E.; Lane, H. A. ERBB Receptors and Cancer: the Complexity of Targeted Inhibitors. Nat. Rev. Cancer **2005**, 5, 341− 354.

Ibraheem, D.; Elaissari, A.; Fessi, H. Gene Therapy and DNA Delivery Systems. *Int. J. Pharm.* **2014**, *459* (1–2), 70–83. https://doi.org/10.1016/j.ijpharm.2013.11.041.

Irvine, D. J.; Dane, E. L. Enhancing Cancer Immunotherapy with Nanomedicine. *Nat. Rev. Immunol.* **2020**, *20* (5), 321–334. https://doi.org/10.1038/s41577-019-0269-6.

Jahrsdörfer, B.; Weiner, G. J. CpG Oligodeoxynucleotides as Immunotherapy in Cancer. *Update on Cancer Therapeutics*. **2008**, pp 27–32. https://doi.org/10.1016/j.uct.2007.11.003.

Jain, R. K. Delivery of Molecular Medicine to Solid Tumors: Lessons from in Vivo Imaging of Gene Expression and Function. In *Journal of Controlled Release*; **2001**; Vol. 74, pp 7–25. https://doi.org/10.1016/S0168-3659(01)00306-6.

Jans H-S, D Stypinski, P Kumar, JR Mercer, LI Liebe, A. M. Dosimetry Comparison of the Hypoxia Agent Iodoazomycin Arabinoside (IAZA) Labeled with the Radioisotopes I-123/124/131. *Med. Phys.* **2014**, *41* (6), 385.

Jiang, K.; Wang, Y.; Thakur, G.; Kotsuchibashi, Y.; Naicker, S.; Narain, R.; Thundat, T. Rapid and Highly Sensitive Detection of Dopamine Using Conjugated Oxaborole-Based Polymer and Glycopolymer Systems. *ACS Appl. Mater. Interfaces* **2017**, *9* (18), 15225–15231 DOI: 10.1021/acsami.7b04178.

Jiang, T.; Chen, X.; Zhou, W.; Fan, G.; Zhao, P.; Ren, S.; Zhou, C.; Zhang, J. Immunotherapy with Dendritic Cells Modified with Tumor-Associated Antigen Gene Demonstrates Enhanced Antitumor Effect Against Lung Cancer. *Transl. Oncol.* **2017**, *10* (2), 132–141. https://doi.org/10.1016/j.tranon.2016.12.002.

Jin, J. O.; Kim, G.; Hwang, J.; Han, K. H.; Kwak, M.; Lee, P. C. W. Nucleic Acid Nanotechnology for Cancer Treatment. *Biochim. Biophys. Acta - Rev. Cancer* **2020**, *1874* (1), 188377. https://doi.org/10.1016/j.bbcan.2020.188377.

Jin, X.; Zhang, X.; Wu, Z.; Teng, D.; Zhang, X.; Wang, Y.; Wang, Z.; Li, C. Amphiphilic Random Glycopolymer Based on Phenylboronic Acid: Synthesis, Characterization, and Potential as Glucose-Sensitive Matrix. *Biomacromolecules* **2009**. https://doi.org/10.1021/bm8010006.

Kabanov, A. V.; Vinogradov, S. V. Nanogels as Pharmaceutical Carriers:Finite Networks of Infinite Capabilities. *Angew. Chemie - Int. Ed.* **2009**, *48* (30), 5418–5429. https://doi.org/10.1002/anie.200900441.Nanogels.

Kadam, R. S.; Bourne, D. W. A.; Kompella, U. B. Nano-Advantage in Enhanced Drug Delivery with Biodegradable Nanoparticles: Contribution of Reduced Clearance. *Drug Metab. Dispos.* **2012**, *40* (7), 1380–1388. https://doi.org/10.1124/dmd.112.044925.

Kafil, V.; Omidi, Y. Cytotoxic Impacts of Linear and Branched Polyethylenimine Nanostructures in A431 Cells. *Bioimpacts* **2011**, *1* (1), 23–30. https://doi.org/10.5681/bi.2011.004.

Kanasty, R.; Dorkin, J. R.; Vegas, A.; Anderson, D. Delivery materials for siRNA therapeutics. *Nat. Mater.* **2013**, *12* (11), 967–977 DOI: 10.1038/nmat3765.

Kandil, R.; Merkel, O. M. Recent Progress of Polymeric Nanogels for Gene Delivery. *Curr. Opin. Colloid Interface Sci.* **2019**, *39*, 11–23. https://doi.org/10.1016/j.cocis.2019.01.005.

Kashuba Benson, C. M.; Benson, J. D.; Critser, J. K. An Improved Cryopreservation Method for a Mouse Embryonic Stem Cell Line. *Cryobiology* **2008**, *56* (2), 120–130. https://doi.org/10.1016/j.cryobiol.2007.12.002.

Kasper, B. The Challenge of Finding New Therapeutic Avenues in Soft Tissue Sarcomas. *Clin. Sarcoma Res.* **2019**, *9* (1), 1–5. https://doi.org/10.1186/s13569-019-0115-4.

Katenz, E.; Vondran, F. W. R.; Schwartlander, R.; Pless, G.; Gong, X.; Cheng, X.; Neuhaus, P.; Sauer, I. M. Cryopreservation of Primary Human Hepatocytes: The

Benefit of Trehalose as an Additional Cryoprotective Agent. *Liver Transplant.* **2007**, *13* (1), 38–45. https://doi.org/10.1002/lt.20921.

Kim, B. W.; Cho, H.; Chung, J.-Y.; Conway, C.; Ylaya, K.; Kim, J.-H.; Hewitt, S. M. Prognostic Assessment of Hypoxia and Metabolic Markers in Cervical Cancer Using Automated Digital Image Analysis of Immunohistochemistry. *J. Transl. Med.* **2013**, *11* (1), 185. https://doi.org/10.1186/1479-5876-11-185.

Kim, T. K.; Eberwine, J. H. Mammalian Cell Transfection: The Present and the Future. *Anal. Bioanal. Chem.* **2010**, *397* (8), 3173–3178. https://doi.org/10.1007/s00216-010-3821-6.

Kim, Y. T.; Park, S. W.; Kim, J. W. Correlation between Expression of EGFR and the Prognosis of Patients with Cervical Carcinoma. *Gynecol. Oncol.* **2002**, *87* (1), 84–89. https://doi.org/10.1006/gyno.2002.6803.

Knight, C. A.; Hallett, J.; DeVries, A. L. Solute Effects on Ice Recrystallization: An Assessment Technique. *Cryobiology* **1988**, *25* (1), 55–60. https://doi.org/10.1016/0011-2240(88)90020-X.

Knox, S. S. From "omics" to Complex Disease: A Systems Biology Approach to Gene-Environment Interactions in Cancer. *Cancer Cell Int.* **2010**, *10*, 1–13. https://doi.org/10.1186/1475-2867-10-11.

Koide, H.; Yoshimatsu, K.; Hoshino, Y.; Lee, S.-H.; Okajima, A.; Ariizumi, S.; Narita, Y.; Yonamine, Y.; Weisman, A. C.; Nishimura, Y.; Oku, N.; Miura, Y.; Shea, K. J. A Polymer Nanoparticle with Engineered Affinity for a Vascular Endothelial Growth Factor (VEGF165). *Nat. Chem.* **2017**, *9* (7), 715–722. https://doi.org/10.1038/nchem.2749.

Kotsuchibashi, Y.; Agustin, R. V. C.; Lu, J.-Y. Y.; Hall, D. G.; Narain, R. Temperature, PH, and Glucose Responsive Gels via Simple Mixing of Boroxole- and Glyco-Based Polymers. *ACS Macro Lett.* **2013**, *2* (3), 260–264. https://doi.org/10.1021/mz400076p.

Kranz, Lena M. Diken, M.; Haas, Heinrich. Kreiter, S. Systemic RNA Delivery to Dendritic Cells Exploits Antiviral Defence for Cancer Immunotherapy. *Nat* **2016**, *534*.

Kratochvílová, I.; Golan, M.; Pomeisl, K.; Richter, J.; Sedláková, S.; Šebera, J.; Mičová, J.; Falk, M.; Falková, I.; Řeha, D.; Elliott, K. W.; Varga, K.; Follett, S. E.; Šimek, D. Theoretical and Experimental Study of the Antifreeze Protein AFP752, Trehalose and Dimethyl Sulfoxide Cryoprotection Mechanism: Correlation with Cryopreserved Cell Viability. *RSC Adv.* **2017**, *7* (1), 352–360. https://doi.org/10.1039/C6RA25095E.

Krause, M.; Ostermann, G.; Petersen, C.; Yaromina, A.; Hessel, F.; Harstrick, A.; Van Der Kogel, A. J.; Thames, H. D.; Baumann, M. Decreased Repopulation as Well as Increased Reoxygenation Contribute to the Improvement in Local Control after Targeting of the EGFR by C225 during Fractionated Irradiation. In *Radiotherapy and Oncology*; **,**; Vol. 76, pp 162–167. https://doi.org/10.1016/j.radonc.2005.06.032.

Kumar, P.; Elsaidi, H. R. H.; Zorniak, B.; Laurens, E.; Yang, J.; Bacchu, V.; Wang, M.; Wiebe, L. I. Synthesis and Biological Evaluation of Iodoglucoazomycin (I-GAZ), an Azomycin–Glucose Adduct with Putative Applications in Diagnostic Imaging and Radiotherapy of Hypoxic Tumors. *ChemMedChem* **2016**, 1638–1645. https://doi.org/10.1002/cmdc.201600213.

Kumar, P.; McQuarrie, S. A.; Zhou, A.; McEwan, A. J. B.; Wiebe, L. I. [131I]Iodoazomycin Arabinoside for Low-Dose-Rate Isotope Radiotherapy: Radiolabeling, Stability, Long-Term Whole-Body Clearance and Radiation Dosimetry Estimates in Mice. *Nucl. Med. Biol.* **2005**, *32* (6), 647–653. https://doi.org/10.1016/j.nucmedbio.2005.04.019.

Kumar, P.; Stypinski, D.; Xia, H.; McEwan, A. J. B.; Machulla, H.-J. J.; Wiebe, L. I. Fluoroazomycin Arabinoside (FAZA): Synthesis, 2H and 3H-Labelling and Preliminary Biological Evaluation of a Novel 2-Nitroimidazole Marker of Tissue Hypoxia. *J. Label. Compd. Radiopharm.* **1999**, *42* (1), 3–16. https://doi.org/10.1002/(SICI)1099-1344(199901)42:1<3::AID-JLCR160>3.0.CO;2-H.

Kumar. Iodoazomycin Arabinoside for Low-Dose-Rate Isotope Radiotherapy: Radiolabeling, Stability, Long-Term Whole-Body Clearance and Radiation

Dosimetry Estimates in Mice. *Nucl. Med. Biol.* **2005**, *32* (6), 647–653. https://doi.org/10.1016/j.nucmedbio.2005.04.019.

Kumari, J.; Kumar, A. Development of Polymer Based Cryogel Matrix for Transportation and Storage of Mammalian Cells. *Sci. Rep.* **2017**, *7* (December 2016), 1–13. https://doi.org/10.1038/srep41551.

Kunath, K.; von Harpe, A.; Fischer, D.; Kissel, T. Galactose-PEI–DNA Complexes for Targeted Gene Delivery: Degree of Substitution Affects Complex Size and Transfection Efficiency. *J. Control. Release* **2003**, *88* (1), 159–172. https://doi.org/10.1016/S0168-3659(02)00458-3.

Kunz-Schughart, L. A.; Dubrovska, A.; Peitzsch, C.; Ewe, A.; Aigner, A.; Schellenburg, S.; Muders, M. H.; Hampel, S.; Cirillo, G.; Iemma, F.; Tietze, R.; Alexiou, C.; Stephan, H.; Zarschler, K.; Vittorio, O.; Kavallaris, M.; Parak, W. J.; Mädler, L.; Pokhrel, S. Nanoparticles for Radiooncology: Mission, Vision, Challenges. *Biomaterials* **2017**, *120*, 155–184. https://doi.org/10.1016/j.biomaterials.2016.12.010.

Kuwai, T.; Kitadai, Y.; Tanaka, S.; Onogawa, S.; Matsutani, N.; Kaio, E.; Ito, M.; Chayama, K. Expression of Hypoxia-Inducible Factor-1alpha Is Associated with Tumor Vascularization in Human Colorectal Carcinoma. *Int. J. Cancer* **2003**, *105* (2), 176–181. https://doi.org/10.1002/ijc.11068.

Lächelt, U.; Wagner, E. Nucleic Acid Therapeutics Using Polyplexes: A Journey of 50 Years (and Beyond). Chem. Rev. **2015**, 115, 11043−11078.

Ladmiral, V.; Semsarilar, M.; Canton, I.; Armes, S. P. Polymerization-Induced Self-Assembly of Galactose-Functionalized Biocompatible Diblock Copolymers for Intracellular Delivery. *J. Am. Chem. Soc.* **2013**. https://doi.org/10.1021/ja407033x.

Lam, J. K. W.; Chow, M. Y. T.; Zhang, Y.; Leung, S. W. S. siRNA Versus miRNA as Therapeutics for Gene Silencing. *Mol. Ther. Nucleic Acids* **2015**, *4* (9), e252 DOI: 10.1038/mtna.2015.23.

Lawrentschuk, N.; Poon, A. M. T.; Foo, S. S.; Putra, L. G. J.; Murone, C.; Davis, I. D.; Bolton, D. M.; Scott, A. M. Assessing Regional Hypoxia in Human Renal

Tumours Using 18F-Fluoromisonidazole Positron Emission Tomography. *BJU Int.* **2005**, *96* (4), 540–546. https://doi.org/10.1111/j.1464-410X.2005.05681.x.

Lee, J. Y.; Termsarasab, U.; Park, J. H.; Lee, S. Y.; Ko, S. H.; Shim, J. S.; Chung, S. J.; Cho, H. J.; Kim, D. D. Dual CD44 and Folate Receptor-Targeted Nanoparticles for Cancer Diagnosis and Anticancer Drug Delivery. *J. Control. Release* **2016**. https://doi.org/10.1016/j.jconrel.2016.06.021.

Lee, J.; Lin, E. W.; Lau, U. Y.; Hedrick, J. L.; Bat, E.; Maynard, H. D. Trehalose Glycopolymers as Excipients for Protein Stabilization. *Biomacromolecules* **2013**, *14* (8), 2561–2569. https://doi.org/10.1021/bm4003046.

Lee, S.-Y. Y.; Yang, C.-Y. Y.; Peng, C.-L. L.; Wei, M.-F. F.; Chen, K.-C. C.; Yao, C.-J. J.; Shieh, M.-J. J. A Theranostic Micelleplex Co-Delivering SN-38 and VEGF SiRNA for Colorectal Cancer Therapy. *Biomaterials* **2016**, *86*, 92–105. https://doi.org/10.1016/j.biomaterials.2016.01.068.

Lee, Y. A.; Kim, Y. H.; Kim, B. J.; Kim, B. G.; Kim, K. J.; Auh, J. H.; Schmidt, J. A.; Ryu, B. Y. Cryopreservation in Trehalose Preserves Functional Capacity of Murine Spermatogonial Stem Cells. *PLoS One* **2013**, *8* (1). https://doi.org/10.1371/journal.pone.0054889.

Lehrman, S. Virus Treatment Questioned after Gene Therapy Death. *Nature* **1999**. https://doi.org/10.1038/43977.

Li, J.; Zhang, Y.; Cai, C.; Rong, X.; Shao, M.; Li, J.; Yang, C.; Yu, G. Collaborative Assembly of Doxorubicin and Galactosyl Diblock Glycopolymers for Targeted Drug Delivery of Hepatocellular Carcinoma. *Biomater. Sci.* **2020**, *8* (1), 189–200. https://doi.org/10.1039/c9bm01604j.

Li, Q. L.; Gu, W. X.; Gao, H.; Yang, Y. W. Self-Assembly and Applications of Poly(Glycidyl Methacrylate)s and Their Derivatives. Chem. Commun. **2014**, 50, 13201−13215.

Li, R. Q.; Wu, Y.; Zhi, Y.; Yang, X.; Li, Y.; Xua, F. J.; Du, J. PGMA-Based Star-Like Polycations with Plentiful Hydroxyl Groups Act as Highly Efficient miRNA Delivery Nanovectors for Effective Applications in Heart Diseases. Adv. Mater. **2016**, 28, 7204−7212.

Li, R. Q.; Wu, Y.; Zhi, Y.; Yang, X.; Li, Y.; Xua, F. J.; Du, J. PGMA-Based Star-Like Polycations with Plentiful Hydroxyl Groups Act as Highly Efficient MiRNA Delivery Nanovectors for Effective Applications in Heart Diseases. *Adv. Mater.* **2016**. https://doi.org/10.1002/adma.201602319.

Li, Y.; Gao, J.; Zhang, C.; Cao, Z.; Cheng, D.; Liu, J.; Shuai, X. Stimuli-Responsive Polymeric Nanocarriers for Efficient Gene Delivery. *Top. Curr. Chem.* **2017**, *375* (2), 27. https://doi.org/10.1007/s41061-017-0119-6.

Li, Y.; Ma, T. Bioprocessing of Cryopreservation for Large-Scale Banking of Human Pluripotent Stem Cells. *Biores. Open Access* **2012**, *1* (5), 205–214. https://doi.org/10.1089/biores.2012.0224.

Lins, R. D.; Pereira, C. S.; Hünenberger, P. H. Trehalose-Protein Interaction in Aqueous Solution. *Proteins Struct. Funct. Bioinforma.* **2004**, *55* (1), 177–186. https://doi.org/10.1002/prot.10632.

Liu, L. I.; Zhang, J.; Wenhui, L. V.; Luo, Y. A. N.; Wang, X. Well-Defined pH-Sensitive Block Glycopolymers via Reversible Addition-Fragmentation Chain Transfer Radical Polymerization: Synthesis, Characterization, and Recognition with Lectin. *J. Polym. Sci. Part A Polym. Chem.* **2010**. https://doi.org/10.1002/pola.24119.

Loh, X. J.; Lee, T.-C.; Dou, Q.; Deen, G. R. Utilising Inorganic Nanocarriers for Gene Delivery. *Biomater. Sci.* **2016**, *4* (1), 70–86. https://doi.org/10.1039/C5BM00277J.

Lord, C. J.; Ashworth, A. The DNA Damage Response and Cancer Therapy. *Nature* **2012**, *481* (7381), 287–294. https://doi.org/10.1038/nature10760.

Lowe, A. B.; Sumerlin, B. S.; McCormick, C. L. The Direct Polymerization of 2-Methacryloxyethyl Glucoside via Aqueous Reversible Addition-Fragmentation Chain Transfer (RAFT) Polymerization. *Polymer (Guildf).* **2003**. https://doi.org/10.1016/j.polymer.2003.08.039.

Lu, J.; Zhang, W.; Yuan, L.; Ma, W.; Li, X.; Lu, W.; Zhao, Y.; Chen, G. One-Pot Synthesis of Glycopolymer-Porphyrin Conjugate as Photosensitizer for Targeted Cancer Imaging and Photodynamic Therapy. *Macromol. Biosci.* **2014**, *14* (3), 340–346. https://doi.org/10.1002/mabi.201300451.

Lu, M.; Khine, Y. Y.; Chen, F.; Cao, C.; Garvey, C. J.; Lu, H.; Stenzel, M. H. Sugar Concentration and Arrangement on the Surface of Glycopolymer Micelles Affect the Interaction with Cancer Cells. *Biomacromolecules* **2019**, *20* (1), 273–284. https://doi.org/10.1021/acs.biomac.8b01406.

Luk, B. T.; Zhang, L. Current Advances in Polymer-Based Nanotheranostics for Cancer Treatment and Diagnosis. *ACS Appl. Mater. Interfaces* **2014**, *6* (24), 21859–21873. https://doi.org/10.1021/am5036225.

Luo, M.; Samandi, L. Z.; Wang, Z.; Chen, Z. J.; Gao, J. Synthetic Nanovaccines for Immunotherapy. *J. Control. Release* **2017**. https://doi.org/10.1016/j.jconrel.2017.03.033.

Ma, Z.; Liu, H.; Peng, Z.; Xuan, Y.; Rivera, E.; Zhu, X. X. Star-Shaped Glycopolymers with a Porphyrin Core: Synthesis, Singlet Oxygen Generation, and Photodynamic Therapy. *ACS Appl. Polym. Mater.* **2020**, *2* (6), 2477–2484. https://doi.org/10.1021/acsapm.0c00451.

Maeda, H.; Wu, J.; Sawa, T.; Matsumura, Y.; Hori, K. Tumor Vascular Permeability and the EPR Effect in Macromolecular Therapeutics: A Review. *J. Control. Release* **2000**, *65* (1–2), 271–284. https://doi.org/10.1016/S0168-3659(99)00248-5.

Maftei, C. A.; Bayer, C.; Shi, K.; Vaupel, P. Intra-and Intertumor Heterogeneities in Total, Chronic, and Acute Hypoxia in Xenografted Squamous Cell Carcinomas : Detection and Quantification Using (Immuno-)Fluorescence Techniques. *Strahlentherapie und Onkol.* **2012**, *188* (7), 606–615. https://doi.org/10.1007/s00066-012-0105-4.

Manjila, S. B.; Baby, J. N.; Bijin, E. N.; Constantine, I.; Pramod, K.; Valsalakumari, J. Novel Gene Delivery Systems. *Int. J. Pharm. Investig.* **2013**, *3* (1), 1–7. https://doi.org/10.4103/2230-973X.108958.

Mannan, R. H.; Somayaji, V. V; Lee, J.; Mercer, J. R. 1-(5-Iodo-5-Deoxy-b-D-Arabinofuranosyl)-2-Nitroimidazole (Iodoazomycin Arabinoside:IAZA), a Novel Marker of Tissue Hypoxia. *Nucl. Med. Biol.* **1991**, *32*, 1764–1770.

Mastrobattista, E.; Hennink, W. E. Polymers for Gene Delivery: Charged for Success. *Nat. Mater.* **2011**. https://doi.org/10.1038/nmat3209.

Matsumura, Y.; Maeda, H. A New Concept for Macromolecular Therapeutics in Cancer Chemotherapy: Mechanism of Tumoritropic Accumulation of Proteins and the Antitumor Agent Smancs. *Cancer Res.* **1986**, *46* (8), 6387–6392. https://doi.org/10.1021/bc100070g.

Mattia, G.; Puglisi, R.; Ascione, B.; Malorni, W.; Carè, A.; Matarrese, P. Cell Death-Based Treatments of Melanoma:Conventional Treatments and New Therapeutic Strategies Review-Article. *Cell Death Dis.* **2018**, *9* (2). https://doi.org/10.1038/s41419-017-0059-7.

Mazur, P. Equilibrium, Quasi-Equilibrium, and Nonequilibrium Freezing of Mammalian Embryos. *Cell Biophys.* **1990**, *17* (1), 53–92. https://doi.org/10.1007/BF02989804.

Mazur, P.; Cole, K. W. Influence of Cell Concentration on the Contribution of Unfrozen Fraction and Salt Concentration to the Survival of Slowly Frozen Human Erythrocytes. *Cryobiology* **1985**, *22* (6), 509–536. https://doi.org/10.1016/0011-2240(85)90029-X.

Mazur, P.; Koshimoto, C. Is Intracellular Ice Formation the Cause of Death of Mouse Sperm Frozen at High Cooling Rates?1. *Biol. Reprod.* **2005**, *66* (5), 1485–1490. https://doi.org/10.1095/biolreprod66.5.1485.

Mazur, P.; Rigopoulos, N. Contributions of Unfrozen Fraction and of Salt Concentration to the Survival of Slowly Frozen Human Erythrocytes: Influence of Warming Rate. *Cryobiology* **1983**, *20* (3), 274–289. https://doi.org/10.1016/0011-2240(83)90016-0.

Mazur, P.; Seki, S.; Pinn, I. L.; Kleinhans, F. W.; Edashige, K. Extra- and Intracellular Ice Formation in Mouse Oocytes. *Cryobiology* **2005**, *51* (1), 29–53. https://doi.org/10.1016/j.cryobiol.2005.04.008.

McCain, J. The Future of Human Gene Therapy. *Biotechnol. Healthc.* **2005**, *22* (3), 113–142. https://doi.org/10.1016/S0098-2997(01)00004-8.

McCrudden, C.; McCarthy, H. *Cancer Gene Therapy–Key Biological Concepts in the Design of Multifunctional Non-Viral Delivery Systems*; **2013**.

Meenu Vasudevan, S.; Ashwanikumar, N.; Vinod Kumar, G. S. Peptide Decorated Glycolipid Nanomicelles for Drug Delivery across the Blood-Brain Barrier

(BBB). *Biomater. Sci.* **2019**, *7* (10), 4017–4021. https://doi.org/10.1039/c9bm00955h.

Mehier-Humbert, S.; Guy, R. H. Physical Methods for Gene Transfer: Improving the Kinetics of Gene Delivery into Cells. *Adv. Drug Deliv. Rev.* **2005**, *57* (5), 733–753. https://doi.org/10.1016/j.addr.2004.12.007.

Mercer, J. R.; McEwan, A. J.; Wiebe, L. I.; J.R., M.; A.J., M.; L.I., W.; Mercer, J. R.; McEwan, A. J.; Wiebe, L. I. [131I]IAZA as a Molecular Radiotherapeutic (MRT) Drug: Wash-out with Cold IAZA Accelerates Clearance in a Murine Tumor Model. *Curr. Radiopharm.* **2013**, *6* (2), 87–91. https://doi.org/10.2174/1874471011306020004.

Mercer, J. R.; Urtasun, R. C.; McEwan, A. J.; Parliament, M. B.; Chapman, J. D.; Goldberg, L.; Mannan, R. H.; Wiebe, L. I. 123IAZA: Iodomyzin Arabinoside. Synthesis, Purification and Clinical Evaluation in Cancer Patients. *Clin. Nucl. Med.* **1991**, *16* (10), 796. https://doi.org/10.1097/00003072-199110000-00046.

Meryman, H. T. T. Osmotic Stress as a Mechanism of Freezing Injury. *Cryobiology* **1971**, *8* (5), 489–500. https://doi.org/10.1016/0011-2240(71)90040-X.

Messina, M. S.; Ko, J. H.; Yang, Z.; Strouse, M. J.; Houk, K. N.; Maynard, H. D. Effect of Trehalose Polymer Regioisomers on Protein Stabilization. *Polym. Chem.* **2017**, *8* (33), 4781–4788. https://doi.org/10.1039/c7py00700k.

Mi, Y.; Shao, Z.; Vang, J.; Kaidar-Person, O.; Wang, A. Z. Application of Nanotechnology to Cancer Radiotherapy. *Cancer Nanotechnol.* **2016**, *7* (1), 11. https://doi.org/10.1186/s12645-016-0024-7.

Longmire, M.; Choyke, P.; and Kobayashi, H. Clearance Properties of Nano-Sized Particles and Molecules as Imagin Agents: Consideration and Caveats. **2012**, *3* (5), 703–717. https://doi.org/10.2217/17435889.3.5.703.

Miconnet, I.; Koenig, S.; Speiser, D.; Krieg, A.; Guillaume, P.; Cerottini, J.-C.; Romero, P. CpG Are Efficient Adjuvants for Specific CTL Induction Against Tumor Antigen-Derived Peptide. *J. Immunol.* **2002**, *168* (3), 1212–1218. https://doi.org/10.4049/jimmunol.168.3.1212.

Miele, E. E.; Spinelli, G. P.; Miele, E. E.; Tomao, F.; Tomao, S. Albumin-Bound Formulation of Paclitaxel (Abraxane® ABI-007) in the Treatment of Breast

Cancer. *Int. J. Nanomedicine* **2009**, *4* (1), 99–105. https://doi.org/10.2147/ijn.s3061.

Milas, L.; Hunter, N.; Mason, K. a; Milross, C.; Peters, L. J. Tumor Reoxygenation as a Mechanism of Taxol-Induced Enhancement of Tumor Radioresponse. *Acta Oncol.* **1995**, *34* (3), 409–412. https://doi.org/10.3109/02841869509093999.

Miura, Y. Design and Synthesis of Well-Defined Glycopolymers for the Control of Biological Functionalities. *Polym. J.* **2012**, *44* (7), 679–689. https://doi.org/10.1038/pj.2012.4.

Miura, Y.; Hoshino, Y.; Seto, H. Glycopolymer Nanobiotechnology. *Chem. Rev.* **2016**, *116* (4), 1673–1692. https://doi.org/10.1021/acs.chemrev.5b00247.

Moad, G.; Chong, Y. K.; Postma, A.; Rizzardo, E.; Thang, S. H. Advances in RAFT polymerization: The synthesis of polymers with defined end-groups. *Polymer (Guildf).* **2005**, *46* (19 SPEC. ISS.), 8458–8468 DOI: 10.1016/j.polymer.2004.12.061.

Moad, G.; Rizzardo, E.; Thang, S. H. RAFT Polymerization and Some of Its Applications. *Chem. - An Asian J.* **2013**, *8* (8), 1634–1644. https://doi.org/10.1002/asia.201300262.

Monaco, A.; Beyer, V. P.; Napier, R.; Becer, C. R. Multi-Arm Star Shaped Glycopolymers with Precisely Controlled Core Size and Arm Length. *Biomacromolecules* **2020**. https://doi.org/10.1021/acs.biomac.0c00838.

Moselhy, J.; Srinivasan, S.; Ankem, M. K.; Damodaran, C. Natural Products That Target Cancer Stem Cells. *Anticancer Res.* **2015**, *35* (11), 5773–5788.

Motta, J. P. R.; Paraguassú-Braga, F. H.; Bouzas, L. F.; Porto, L. C. Evaluation of Intracellular and Extracellular Trehalose as a Cryoprotectant of Stem Cells Obtained from Umbilical Cord Blood. *Cryobiology* **2014**, *68* (3), 343–348. https://doi.org/10.1016/j.cryobiol.2014.04.007.

Muñoz-Bonilla, A.; Fernández-García, M. Glycopolymeric Materials for Advanced Applications. *Materials (Basel).* **2015**, *8* (5), 2276–2296. https://doi.org/10.3390/ma8052276.

Munshi, A.; Hobbs, M.; Meyn, R. E. Clonogenic Cell Survival Assay. *Chemosensitivity* **2005**, *110*, 021–028. https://doi.org/10.1385/1-59259-869-2:021.

Mura, S.; Nicolas, J.; Couvreur, P. Stimuli-Responsive Nanocarriers for Drug Delivery. *Nat. Mater.* **2013**, *12* (11), 991–1003. https://doi.org/10.1038/nmat3776.

Murshed, H.; Murshed, H. Radiation Biology. *Fundam. Radiat. Oncol.* **2019**, 57–87. https://doi.org/10.1016/B978-0-12-814128-1.00003-9.

Muz, B.; de la Puente, P.; Azab, F.; Azab, A. K. The Role of Hypoxia in Cancer Progression, Angiogenesis, Metastasis, and Resistance to Therapy. *Hypoxia* **2015**, *3*, 83. https://doi.org/10.2147/HP.S93413.

Muz, B.; de la Puente, P.; Azab, F.; Luderer, M.; Azab, A. K. The Role of Hypoxia and Exploitation of the Hypoxic Environment in Hematologic Malignancies. *Mol. Cancer Res.* **2014**, *12* (10).

Nagao, M.; Sengupta, J.; Diaz-Dussan, D.; Adam, M.; Wu, M.; Acker, J.; Ben, R.; Ishihara, K.; Zeng, H.; Miura, Y.; Narain, R. Synthesis of Highly Biocompatible and Temperature-Responsive Physical Gels for Cryopreservation and 3D Cell Culture. *ACS Appl. Bio Mater.* **2018**, *1* (2), 356–366. https://doi.org/10.1021/acsabm.8b00096.

Nair, J. K.; Willoughby, J. L. S.; Chan, A.; Charisse, K.; Alam, M. R.; Wang, Q.; Hoekstra, M.; Kandasamy, P.; Kelin, A. V.; Milstein, S.; Taneja, N.; Oshea, J.; Shaikh, S.; Zhang, L.; Van Der Sluis, R. J.; Jung, M. E.; Akinc, A.; Hutabarat, R.; Kuchimanchi, S.; Fitzgerald, K.; Zimmermann, T.; Van Berkel, T. J. C.; Maier, M. A.; Rajeev, K. G.; Manoharan, M. Multivalent N -Acetylgalactosamine-Conjugated SiRNA Localizes in Hepatocytes and Elicits Robust RNAi-Mediated Gene Silencing. *J. Am. Chem. Soc.* **2014**, *136* (49), 16958–16961. https://doi.org/10.1021/ja505986a.

Nakamura, Y.; Mochida, A.; Choyke, P. L.; Kobayashi, H. Nanodrug Delivery: Is the Enhanced Permeability and Retention Effect Sufficient for Curing Cancer? *Bioconjug. Chem.* **2016**, *27* (10), 2225–2238. https://doi.org/10.1021/acs.bioconjchem.6b00437.

Naldini, L. Gene Therapy Returns to Centre Stage. *Nature* **2015**, *526* (7573), 351–360. https://doi.org/10.1038/nature15818.

Narain, R.; Armes, S. P. Synthesis and Aqueous Solution Properties of Novel Sugar Methacrylate-Based Homopolymers and Block Copolymers. Biomacromolecules **2003**, 4, 1746−1758.

Narain, R.; Wang, Y.; Ahmed, M.; Lai, B. F. L.; Kizhakkedathu, J. N. Blood Components Interactions to Ionic and Nonionic Glyconanogels. *Biomacromolecules* **2015**, *16* (9), 2990–2997. https://doi.org/10.1021/acs.biomac.5b00890.

Naves, L. B.; Dhand, C.; Venugopal, J. R.; Rajamani, L.; Ramakrishna, S.; Almeida, L. Nanotechnology for the Treatment of Melanoma Skin Cancer. *Prog. Biomater.* **2017**, *6* (1–2), 13–26. https://doi.org/10.1007/s40204-017-0064-z.

Nicholson, R. .; Gee, J. M. .; Harper, M. . EGFR and cancer prognosis. *Eur. J. Cancer* **2001**, *37*, 9–15 DOI: 10.1016/S0959-8049(01)00231-3.

Nicholson, R. .; Gee, J. M. .; Harper, M. . EGFR and Cancer Prognosis. *Eur. J. Cancer* **2001**, *37*, 9–15. https://doi.org/10.1016/S0959-8049(01)00231-3.

Noordhuis, M. G.; Eijsink, J. J. H.; Hoor, K. A. Expression of Epidermal Growth Factor Receptor (EGFR) and Activated EGFR Predict Poor Response to (Chemo) radiation and Survival in Cervical Cancer Expression of Epidermal Growth Factor Receptor (EGFR) and and Survival in Cervical Cancer. *Clin. Cancer Res.* **2009**, *15* (23), 7389–7397 DOI: 10.1158/1078-0432.CCR-09-1149.

Normanno, N.; De Luca, A.; Bianco, C.; Strizzi, L.; Mancino, M.; Maiello, M. R.; Carotenuto, A.; De Feo, G.; Caponigro, F.; Salomon, D. S. Epidermal growth factor receptor (EGFR) signaling in cancer. *Gene* **2006**, *366* (1), 2–16 DOI: 10.1016/j.gene.2005.10.018.

Notman, R.; Noro, M.; O'Malley, B.; Anwar, J. Molecular Basis for Dimethylsulfoxide (DMSO) Action on Lipid Membranes. *J. Am. Chem. Soc.* **2006**, *128* (43), 13982–13983. https://doi.org/10.1021/ja063363t.

Nunes, A. S.; Barros, A. S.; Costa, E. C.; Moreira, A. F.; Correia, I. J. 3D Tumor Spheroids as in Vitro Models to Mimic in Vivo Human Solid Tumors Resistance to Therapeutic Drugs. *Biotechnol. Bioeng.* **2019**, *116* (1), 206–226. https://doi.org/10.1002/bit.26845.

Ohno, K.; Tsujii, Y.; Miyamoto, T.; Fukuda, T.; Goto, M.; Kobayashi, K.; Akaike, T. Synthesis of a Well-Defined Glycopolymer by Nitroxide-Controlled Free Radical Polymerization. *Macromolecules* **1998**. https://doi.org/10.1021/ma971329g.

Oishi, M.; Nagasaki, Y.; Nishiyama, N.; Itaka, K.; Takagi, M.; Shimamoto, A.; Furuichi, Y.; Kataoka, K. Enhanced Growth Inhibition of Hepatic Multicellular Tumor Spheroids by Lactosylated Poly(Ethylene Glycol)-SiRNA Conjugate Formulated in PEGylated Polyplexes. *ChemMedChem* **2007**. https://doi.org/10.1002/cmdc.200700076.

Omurtag Ozgen, P. S.; Atasoy, S.; Zengin Kurt, B.; Durmus, Z.; Yigit, G.; Dag, A. Glycopolymer Decorated Multiwalled Carbon Nanotubes for Dual Targeted Breast Cancer Therapy. *J. Mater. Chem. B* **2020**, *8* (15), 3123–3137. https://doi.org/10.1039/c9tb02711d.

Onaca-Fischer, O.; Liu, J.; Inglin, M.; Palivan, C. G. Polymeric Nanocarriers and Nanoreactors: A Survey of Possible Therapeutic Applications. *Curr. Pharm. Des.* **2012**, *18* (18), 2622–2643.

Overgaard, J.; Hansen, H. S.; Overgaard, M.; Bastholt, L.; Berthelsen, A.; Specht, L.; Lindeløv, B.; Jørgensen, K. A Randomized Double-Blind Phase III Study of Nimorazole as a Hypoxic Radiosensitizer of Primary Radiotherapy in Supraglottic Larynx and Pharynx Carcinoma. Results of the Danish Head and Neck Cancer Study (DAHANCA) Protocol 5-85. *Radiother. Oncol.* **1998**, *46* (2), 135–146. https://doi.org/10.1016/S0167-8140(97)00220-X.

Pacchiarotti, J.; Ramos, T.; Howerton, K.; Greilach, S.; Zaragoza, K.; Olmstead, M.; Izadyar, F. Developing a Clinical-Grade Cryopreservation Protocol for Human Testicular Tissue and Cells. *Biomed Res. Int.* **2013**, *2013*, 1–10. https://doi.org/10.1155/2013/930962.

Pagano, E.; Fontana, V.; Calvo, J. C. Expression of Erythroblastic Leukemia Viral Oncogene Homolog (erbBS) mRNAs and Possible Splice Variants in 3T3-L1 Preadipocytes. Mol. Med. Rep. **2011**, 4, 955−961.

Palucka, K.; Banchereau, J. Cancer Immunotherapy via Dendritic Cells. *Nat. Rev. Cancer* **2012**, *12* (4), 265–277. https://doi.org/10.1038/nrc3258.

Panariti, A.; Miserocchi, G.; Rivolta, I. The Effect of Nanoparticle Uptake on Cellular Behavior: Disrupting or Enabling Functions? *Nanotechnol. Sci. Appl.* **2012**, *5* (1), 87–100. https://doi.org/10.2147/NSA.S25515.

Park, H.; Walta, S.; Rosencrantz, R. R.; Körner, A.; Schulte, C.; Elling, L.; Richtering, W.; Böker, A. Micelles from Self-Assembled Double-Hydrophilic PHEMA-Glycopolymer-Diblock Copolymers as Multivalent Scaffolds for Lectin Binding. *Polym. Chem.* **2016**. https://doi.org/10.1039/c5py00797f.

Parliament, M. B.; Chapman, J. D.; Urtasun, R. C.; McEwan, a J.; Golberg, L.; Mercer, J. R.; Mannan, R. H.; Wiebe, L. I. Non-Invasive Assessment of Human Tumour Hypoxia with 123I-Iodoazomycin Arabinoside: Preliminary Report of a Clinical Study. *Br. J. Cancer* **1992**, *65* (1), 90–95.

Parveen, S.; Misra, R.; Sahoo, S. K. Nanoparticles: A Boon to Drug Delivery, Therapeutics, Diagnostics and Imaging. *Nanomedicine Nanotechnology, Biol. Med.* **2012**, *8* (2), 147–166. https://doi.org/10.1016/j.nano.2011.05.016.

Pattabiraman, D. R.; Weinberg, R. A. Tackling the Cancer Stem Cells - What Challenges Do They Pose? *Nat. Rev. Drug Discov.* **2014**, *13* (7), 497–512. https://doi.org/10.1038/nrd4253.

Pearson, S.; Allen, N.; Stenzel, M. H. Core-Shell Particles with Glycopolymer Shell and Polynucleoslde Core via RAFT: From Micelles to Rods. *J. Polym. Sci. Part A Polym. Chem.* **2009**. https://doi.org/10.1002/pola.23275.

Peer, D. Nanotechnology for the delivery of therapeutic nucleic acids. *Nanotechnol. Deliv. Ther. Nucleic Acids* **2013** DOI: 10.4032/9789814411059.

Peng, Y.-Y. Y.; Diaz-Dussan, D.; Kumar, P.; Narain, R. Tumor Microenvironment-Regulated Redox Responsive Cationic Galactose-Based Hyperbranched Polymers for SiRNA Delivery. *Bioconjug. Chem.* **2019**, *30* (2), 405–412. https://doi.org/10.1021/acs.bioconjchem.8b00785.

Peng, Y.-Y.; Diaz-Dussan, D.; Kumar, P.; Narain, R. Acid Degradable Cationic Galactose-Based Hyperbranched Polymers as Nanotherapeutic Vehicles for Epidermal Growth Factor Receptor (EGFR) Knockdown in Cervical Carcinoma. Biomacromolecules **2018**, 19, 4052−4058.

Peng, Y.-Y.; Diaz-Dussan, D.; Vani, J.; Hao, X.; Kumar, P.; Narain, R. Achieving Safe and Highly Efficient Epidermal Growth Factor Receptor Silencing in Cervical Carcinoma by Cationic Degradable Hyperbranched Polymers. *ACS Appl. Bio Mater.* **2018**, *1* (4), 961–966. https://doi.org/10.1021/acsabm.8b00371.

Perez, R.; Crombet, T.; Leon, J. de; Moreno, E. A View on EGFR-Targeted Therapies from the Oncogene-Addiction Perspective. *Front. Pharmacol.* **2013**, *4*, 53. https://doi.org/10.3389/fphar.2013.00053.

Pernin, V.; Mégnin-Chanet, F.; Pennaneach, V.; Fourquet, A.; Kirova, Y.; Hall, J. Inhibiteurs de PARP et Radiothérapie : Rationnel et Perspectives Pour Une Utilisation En Clinique. *Cancer/Radiothérapie* **2014**, *18* (8), 790–798. https://doi.org/10.1016/j.canrad.2014.05.012.

Petros, R. A.; DeSimone, J. M. Strategies in the design of nanoparticles for therapeutic applications. *Nat. Rev. Drug Discov.* **2010**, *9* (8), 615–627.

Platt, R. J.; Chen, S.; Zhou, Y.; Yim, M. J.; Swiech, L.; Kempton, H. R.; Dahlman, J. E.; Parnas, O.; Eisenhaure, T. M.; Jovanovic, M.; Graham, D. B.; Jhunjhunwala, S.; Heidenreich, M.; Xavier, R. J.; Langer, R.; Anderson, D. G.; Hacohen, N.; Regev, A.; Feng, G.; Sharp, P. A.; Zhang, F. CRISPR-Cas9 Knockin Mice for Genome Editing and Cancer Modeling. *Cell* **2014**. https://doi.org/10.1016/j.cell.2014.09.014.

Posimo, J. M.; Unnithan, A. S.; Gleixner, A. M.; Choi, H. J.; Jiang, Y.; Pulugulla, S. H.; Leak, R. K. Viability Assays for Cells in Culture. *J. Vis. Exp.* **2014**, *Jan20* (83), e50645. https://doi.org/10.3791/50645.

Qi, M.; Duan, S.; Yu, B.; Yao, H.; Tian, W.; Xu, F.-J. PGMA-Based Supramolecular Hyperbranched Polycations for Gene Delivery. *Polym. Chem.* **2016**, *7* (26), 4334–4341. https://doi.org/10.1039/C6PY00759G.

Quan, S.; Kumar, P.; Narain, R. Cationic Galactose-Conjugated Copolymers for Epidermal Growth Factor (EGFR) Knockdown in Cervical Adenocarcinoma. *ACS Biomater. Sci. Eng.* **2016**, *2* (5), 853–859 DOI: 10.1021/acsbiomaterials.6b00085.

Quan, S.; Wang, Y.; Zhou, A.; Kumar, P.; Narain, R. Galactose-Based Thermosensitive Nanogels for Targeted Drug Delivery of Iodoazomycin Arabinofuranoside

(IAZA) for Theranostic Management of Hypoxic Hepatocellular Carcinoma. *Biomacromolecules* **2015**, *16* (7), 1978–1986. https://doi.org/10.1021/acs.biomac.5b00576.

Ramamoorth, M.; Narvekar, A. Non Viral Vectors in Gene Therapy - An Overview. *J. Clin. Diagnostic Res.* **2015**, *9* (1), GE01–GE06. https://doi.org/10.7860/JCDR/2015/10443.5394.

Ran, F. A.; Hsu, P. D.; Wright, J.; Agarwala, V.; Scott, D. A.; Zhang, F. Genome Engineering Using the CRISPR-Cas9 System. *Nat. Protoc.* **2013**, *8* (11), 2281–2308. https://doi.org/10.1038/nprot.2013.143.

Reck, M.; von Pawel, J.; Nimmermann, C.; Groth, G.; Gatzemeier, U. Phase II-Trial of Tirapazamine in Combination with Cisplatin and Gemcitabine in Patients with Advanced Non-Small-Cell-Lung-Cancer (NSCLC). *Pneumologie* **2004**, *58* (12), 845–849. https://doi.org/10.1055/s-2004-830056.

Reineke, T. M. Poly(Glycoamidoamine)s: Cationic Glycopolymers for DNA Delivery. *J. Polym. Sci. Part A Polym. Chem.* **2006**, *44* (24), 6895–6908. https://doi.org/10.1002/pola.21697.

Reineke, T. M.; Davis, M. E. *Nucleic Acid Delivery via Polymer Vehicles*; Elsevier B.V., **2012**; Vol. 9. https://doi.org/10.1016/B978-0-444-53349-4.00239-9.

Reischl, G.; Dorow, D. S.; Cullinane, C.; Katsifis, A.; Roselt, P.; Binns, D.; Hicks, R. J. Imaging of Tumor Hypoxia with [124I]IAZA in Comparison with [18F]FMISO and [18F]FAZA–First Small Animal PET Results. *J Pharm Pharm Sci Publ Can Soc Pharm Sci Société Can Des Sci Pharm* **2007**, *10* (2), 203–211.

Rezaul H. Mannan, Vijayalakashmi V. Somayaji, Jane Lee, John R. Mercer, J. Donald Chapman, and L. I. W. Radioiodinated 1-(5-Iodo-5-Deoxy-@3-D-Arabinofuranosyl)-2-Thtroimidazole (Lodoazomycin Arabinoside: IAZA): A Novel Marker of Tissue Hypoxia. *J. Nucl. Med.* **1991**, *32* (9).

Rischin, D.; Peters, L. J.; O'Sullivan, B.; Giralt, J.; Fisher, R.; Yuen, K.; Trotti, A.; Bernier, J.; Bourhis, J.; Ringash, J.; Henke, M.; Kenny, L. Tirapazamine, Cisplatin, and Radiation versus Cisplatin and Radiation for Advanced Squamous Cell Carcinoma of the Head and Neck (TROG 02.02, HeadSTART): A Phase III

Trial of the Trans-Tasman Radiation Oncology Group. *J. Clin. Oncol.* **2010**, *28* (18), 2989–2995. https://doi.org/10.1200/JCO.2009.27.4449.

Roche, A. C.; Fajac, I.; Grosse, S.; Frison, N.; Rondanino, C.; Mayer, R.; Monsigny, M. Glycofection: Facilitated Gene Transfer by Cationic Glycopolymers. *Cell. Mol. Life Sci.* **2003**, *60* (2), 288–297. https://doi.org/10.1007/s000180300024.

Rockwell, S.; Dobrucki, I. T.; Kim, E. Y.; Marrison, S. T.; Vu, V. T. Hypoxia and Radiation Therapy: Past History, Ongoing Research, and Future Promise. *Curr. Mol. Med.* **2009**, *9* (4), 442–458. https://doi.org/10.2174/156652409788167087.

Roggenbuck, D.; Mytilinaiou, M. G.; Lapin, S. V.; Reinhold, D.; Conrad, K. Asialoglycoprotein Receptor (ASGPR): A Peculiar Target of Liver-Specific Autoimmunity. *Autoimmun. Highlights* **2012**, *3* (3), 119–125. https://doi.org/10.1007/s13317-012-0041-4.

Roy, R. Syntheses and Some Applications of Chemically Defined Multivalent Glycoconjugates. *Curr. Opin. Struct. Biol.* **1996**, *6* (5), 692–702. https://doi.org/10.1016/S0959-440X(96)80037-6.

Rupf, T.; Ebert, S.; Lorenz, K.; Salvetter, J.; Bader, A. Cryopreservation of Organotypical Cultures Based on 3D Scaffolds. *Cryo-Letters* **2010**, *31* (2), 157–168.

Sahay, G.; Alakhova, D. Y.; Kabanov, A. V. Endocytosis of nanomedicines. *J. Control. Release* **2010**, *145* (3), 182–195 DOI: 10.1016/j.jconrel.2010.01.036.

Sahay, G.; Querbes, W.; Alabi, C.; Eltoukhy, A.; Sarkar, S.; Zurenko, C.; Karagiannis, E.; Love, K.; Chen, D.; Zoncu, R.; et al. Efficiency of siRNA delivery by lipid nanoparticles is limited by endocytic recycling. *Nat Biotech* **2013**, *31* (7), 653–658.

Salatin, S.; Yari Khosroushahi, A. Overviews on the Cellular Uptake Mechanism of Polysaccharide Colloidal Nanoparticles. *J. Cell. Mol. Med.* **2017**, *21* (9), 1668–1686. https://doi.org/10.1111/jcmm.13110.

Sathiyajith, C. W. Nanovaccines for Cancer Immunotherapy. *Int. J. Vaccines Vaccin.* **2017**, *4* (4). https://doi.org/10.15406/ijvv.2017.04.00085.

Satpathy, M.; Mezencev, R.; Wang, L.; McDonald, J. F.; Sood, A. K. Targeted in vivo delivery of EGFR siRNA inhibits ovarian cancer growth and enhances drug sensitivity. *Sci. Rep.* **2016**, *6* (1), 36518 DOI: 10.1038/srep36518.

Schmidt, J. J.; Rowley, J.; Hyun, J. K. Hydrogels Used for Cell-Based Drug Delivery. *J. Biomed. Mater. Res. - Part A* **2008**, *87* (4), 1113–1122. https://doi.org/10.1002/jbm.a.32287.

Schrevel, M.; Gorter, A.; Kolkman-Uljee, S. M.; Trimbos, J. B. M. Z.; Fleuren, G. J.; Jordanova, E. S. Molecular Mechanisms of Epidermal Growth Factor Receptor Overexpression in Patients with Cervical Cancer. *Mod. Pathol.* **2011**, *24* (5), 720–728. https://doi.org/10.1038/modpathol.2010.239.

Schultz, R. M. *Advances in Targeted Cancer Therapy (Progress in Drug Research)*; Herrling, P. L., Matter, A., Schultz, R. M., Eds.; Birkhäuser Basel: Basel, **2005**. https://doi.org/10.1007/3-7643-7414-4.

Seiwert, T. Y.; Salama, J. K.; Vokes, E. E. The Concurrent Chemoradiation Paradigm—General Principles. *Nat. Clin. Pract. Oncol.* **2007**, *4* (2), 86–100. https://doi.org/10.1038/ncponc0714.

Senderowicz, A. M. Inhibitors of Cyclin-Dependent Kinase Modulators for Cancer Therapy. In *Advances in Targeted Cancer Therapy*; Birkhäuser-Verlag: Basel, **2005**; pp 183–206. https://doi.org/10.1007/3-7643-7414-4_8.

Sharp, D. M. C. C.; Picken, A.; Morris, T. J.; Hewitt, C. J.; Coopman, K.; Slater, N. K. H. H. Amphipathic Polymer-Mediated Uptake of Trehalose for Dimethyl Sulfoxide-Free Human Cell Cryopreservation. *Cryobiology* **2013**, *67* (3), 305–311. https://doi.org/10.1016/j.cryobiol.2013.09.002.

Shi, J.; Kantoff, P. W.; Wooster, R.; Farokhzad, O. C. Cancer Nanomedicine: Progress, Challenges and Opportunities. *Nat. Rev. Cancer* **2017**, *17* (1), 20–37. https://doi.org/10.1038/nrc.2016.108.Cancer.

Shi, Y.; van der Meel, R.; Chen, X.; Lammers, T. The EPR Effect and beyond: Strategies to Improve Tumor Targeting and Cancer Nanomedicine Treatment Efficacy. *Theranostics* **2020**, *10* (17), 7921–7924. https://doi.org/10.7150/thno.49577.

Shoyab, M.; Plowman, G. D.; McDonald, V. L.; Bradley, J. G.; Todaro, G. J. Structure and Function of Human Amphiregulin: A Member of the Epidermal Growth Factor Family. *Science (80-.).* **1989**. https://doi.org/10.1126/science.2466334.

Shu, Z.; Heimfeld, S.; Gao, D. Hematopoietic SCT with Cryopreserved Grafts: Adverse Reactions after Transplantation and Cryoprotectant Removal before Infusion. *Bone Marrow Transplant.* **2014**, *49* (4), 469–476. https://doi.org/10.1038/bmt.2013.152.

Siegwart, D. J.; Whitehead, K. A.; Nuhn, L.; Sahay, G.; Cheng, H.; Jiang, S.; Ma, M.; Lytton-Jean, A.; Vegas, A.; Fenton, P.; Levins, C. G.; Love, K. T.; Lee, H.; Cortez, C.; Collins, S. P.; Li, Y. F.; Jang, J.; Querbes, W.; Zurenko, C.; Novobrantseva, T.; Langer, R.; Anderson, D. G. Combinatorial Synthesis of Chemically Diverse Core-Shell Nanoparticles for Intracellular Delivery. Proc. Natl. Acad. Sci. U.S.A. **2011**, 108, 12996.

Siirilä, J.; Hietala, S.; Ekholm, F. S.; Tenhu, H. Glucose and Maltose Surface-Functionalized Thermoresponsive Poly(N-Vinylcaprolactam) Nanogels. *Biomacromolecules* **2020**, *21* (2), 955–965. https://doi.org/10.1021/acs.biomac.9b01596.

Silva, V. L.; Al-Jamal, T. Exploiting the Cancer Niche: Tumor-Associated Macrophages and Hypoxia as Promising Synergistic Targets for Nano-Based Therapy. *J. Control. Release* **2017**, *253*, 82–96. https://doi.org/10.1016/j.jconrel.2017.03.013.

Sindhwani, S.; Syed, A. M.; Ngai, J.; Kingston, B. R.; Maiorino, L.; Rothschild, J.; MacMillan, P.; Zhang, Y.; Rajesh, N. U.; Hoang, T.; Wu, J. L. Y.; Wilhelm, S.; Zilman, A.; Gadde, S.; Sulaiman, A.; Ouyang, B.; Lin, Z.; Wang, L.; Egeblad, M.; Chan, W. C. W. The Entry of Nanoparticles into Solid Tumours. *Nat. Mater.* **2020**, *19* (5), 566–575. https://doi.org/10.1038/s41563-019-0566-2.

Singh, R.; Lillard, J. W. Nanoparticle-Based Targeted Drug Delivery. *Exp. Mol. Pathol.* **2009**, *86* (3), 215–223. https://doi.org/10.1016/j.yexmp.2008.12.004.

Singhsa, P.; Diaz-Dussan, D.; Manuspiya, H.; Narain, R. Well- Defined Cationic N-[3-(Dimethylamino)propyl]methacrylamide Hy- drochloride-Based (Co)polymers for siRNA Delivery. Biomacromole- cules **2018**, 19, 209−221.

Sioud, M. Engineering Better Immunotherapies via RNA Interference. *Hum. Vaccines Immunother.* **2014**, *10* (11), 3165–3174. https://doi.org/10.4161/hv.29754.

Sizovs, A.; Xue, L.; Tolstyka, Z. P.; Ingle, N. P.; Wu, Y.; Cortez, M.; Reineke, T. M. Poly(Trehalose): Sugar-Coated Nanocomplexes Promote Stabilization and Effective Polyplex-Mediated siRNA Delivery. J. Am. Chem. Soc. **2013**, 135, 15417−15424.

Smith, A. E.; Sizovs, A.; Grandinetti, G.; Xue, L.; Reineke, T. M. Diblock Glycopolymers Promote Colloidal Stability of Polyplexes and Effective PDNA and SiRNA Delivery under Physiological Salt and Serum Conditions. *Biomacromolecules* **2011**, *12* (8), 3015–3022. https://doi.org/10.1021/bm200643c.

Smith, E. A.; Oehme, F. W. Acrylamide and Polyacrylamide: A Review of Production, Use, Environmental Fate and Neurotoxicity. *Rev. Environ. Health* **1991**, *9* (4), 215–228. https://doi.org/10.1515/REVEH.1991.9.4.215.

Sola-Penna, M.; Meyer-Fernandes, J. R. Stabilization against Thermal Inactivation Promoted by Sugars on Enzyme Structure and Function: Why Is Trehalose More Effective than Other Sugars? *Arch. Biochem. Biophys.* **1998**, *360* (1), 10–14. https://doi.org/10.1006/abbi.1998.0906.

Solocinski, J.; Osgood, Q.; Wang, M.; Connolly, A.; Menze, M. A.; Chakraborty, N. Effect of Trehalose as an Additive to Dimethyl Sulfoxide Solutions on Ice Formation, Cellular Viability, and Metabolism. *Cryobiology* **2017**, *75*, 134–143. https://doi.org/10.1016/j.cryobiol.2017.01.001.

Song, C.-Z. Gene Silencing Therapy Against Cancer. In *Gene Therapy for Cancer*; Humana Press: Totowa, NJ, **2007**; pp 185–196. https://doi.org/10.1007/978-1-59745-222-9_11.

Sorger D, Patt M, Kumar P, Wiebe L, Barthel H, Seese A, Dannenberg C, Tannapfel A, Kluge R, S. S.; Sorger, D.; Patt, M.; Kumar, P.; Wiebe, L. I.; Barthel, H.; Seese, A.; Dannenberg, C.; Tannapfel, A.; Kluge, R.; Sabri, O. Fluoroazomycinarabinofuranoside (18FAZA) and [18F]Fluoromisonidazole (18FMISO): A Comparative Study of Their Selective Uptake in Hypoxic Cells

and PET Imaging in Experimental Rat Tumors. *Nucl. Med. Biol.* **2003**, *30* (3), 317–326. https://doi.org/10.1016/S0969-8051(02)00442-0.

Spain, S. G.; Cameron, N. R. A Spoonful of Sugar: The Application of Glycopolymers in Therapeutics. *J. Mater. Chem. C* **2015**, *3*, 10715–10722. https://doi.org/10.1039/b000000x.

Springsteen, G.; Wang, B. Alizarin Red S. as a General Optical Reporter for Studying the Binding of Boronic Acids with Carbohydrates. *Chem. Commun.* **2001**. https://doi.org/10.1039/b104895n.

Sriraman, S. K.; Aryasomayajula, B.; Torchilin, V. P. Barriers to Drug Delivery in Solid Tumors. *Tissue Barriers* **2014**, *2* (3), e29528. https://doi.org/10.4161/tisb.29528.

Stewart, G. D.; Ross, J. A.; McLaren, D. B.; Parker, C. C.; Habib, F. K.; Riddick, A. C. P. The Relevance of a Hypoxic Tumour Microenvironment in Prostate Cancer. *BJU Int.* **2010**, *105* (1), 8–13. https://doi.org/10.1111/j.1464-410X.2009.08921.x.

Stypinski, D.; McQuarrie, S. A.; Wiebe, L. I.; Tam, Y. K.; Mercer, J. R.; McEwan, A. J. Dosimetry Estimations for 123I-IAZA in Healthy Volunteers. *J. Nucl. Med.* **2001**, *42* (9), 1418–1423.

Sultana, F.; Manirujjaman; Imran-Ul-Haque; Arafat, M.; Sharmin, S. An Overview of Nanogel Drug Delivery System. *J. Appl. Pharm. Sci.* **2013**. https://doi.org/10.7324/JAPS.2013.38.S15.

Sultani, A. B.; Marquez-Curtis, L. A.; Elliott, J. A. W.; McGann, L. E. Improved Cryopreservation of Human Umbilical Vein Endothelial Cells: A Systematic Approach. *Sci. Rep.* **2016**, *6* (September), 1–14. https://doi.org/10.1038/srep34393.

Sun, W.; Ji, W.; Hall, J. M.; Hu, Q.; Wang, C.; Beisel, C. L.; Gu, Z. Self-Assembled DNA Nanoclews for the Efficient Delivery of CRISPR-Cas9 for Genome Editing. *Angew. Chemie - Int. Ed.* **2015**. https://doi.org/10.1002/anie.201506030.

Sun, Y.; Hu, H.; Yu, B.; Xu, F. J. PGMA-Based Cationic Nanoparticles with Polyhydric Iodine Units for Advanced Gene Vectors. *Bioconjug. Chem.* **2016**. https://doi.org/10.1021/acs.bioconjchem.6b00509.

Sun, Y.; Hu, H.; Zhao, N.; Xia, T.; Yu, B.; Shen, C.; Xu., F. J. Multifunctional Polycationic Photosensitizer Conjugates with Rich Hydroxyl Groups for Versatile Water-Soluble Photodynamic Therapy Nanoplatforms. *Biomaterials* **2017**. https://doi.org/10.1016/j.biomaterials.2016.11.055.

Sunasee, R.; Wattanaarsakit, P.; Ahmed, M.; Lollmahomed, F. B.; Narain, R. Biodegradable and Nontoxic Nanogels as Nonviral Gene Delivery Systems. *Bioconjug. Chem.* **2012**, *23* (9), 1925–1933. https://doi.org/10.1021/bc300314u.

Talebpour Amiri, F.; Fadaei Fathabadi, F.; Mahmoudi Rad, M.; Piryae, A.; Ghasemi, A.; Khalilian, A.; Yeganeh, F.; Mosaffa, N. The Effects of Insulin-Like Growth Factor-1 Gene Therapy and Cell Transplantation on Rat Acute Wound Model. *Iran. Red Crescent Med. J.* **2014**, *16* (10), 1–7. https://doi.org/10.1177/0269881103017001687.

Tan, Z.; Dhande, Y. K.; Reineke, T. M. Cell Penetrating Polymers Containing Guanidinium Trigger Apoptosis in Human Hepatocellular Carcinoma Cells unless Conjugated to a Targeting N- Acetyl-Galactosamine Block. Bioconjugate Chem. **2017**, 28, 2985− 2997.

Tanaka, M.; Rosser, C. J.; Grossman, H. B. PTEN Gene Therapy Induces Growth Inhibition and Increases Efficacy of Chemotherapy in Prostate Cancer. *Cancer Detect. Prev.* **2005**. https://doi.org/10.1016/j.cdp.2004.07.006.

Tanner, P.; Baumann, P.; Enea, R.; Onaca, O.; Palivan, C.; Meier, W. Polymeric Vesicles: From Drug Carriers to Nanoreactors and Artificial Organelles. *Acc. Chem. Res.* **2011**, *44* (10), 1039–1049. https://doi.org/10.1021/ar200036k.

Thapa, B.; Kumar, P.; Zeng, H.; Narain, R. Asialoglycoprotein receptor-mediated gene delivery to hepatocytes using galactosylated polymers. *Biomacromolecules* **2015**, *16* (9), 3008–3020 DOI: 10.1021/acs.biomac.5b00906.

Thapa, B.; Narain, R. *Mechanism, Current Challenges and New Approaches for Non Viral Gene Delivery*; Elsevier Ltd., **2016**. https://doi.org/10.1016/B978-0-08-100520-0.00001-1.

The Two Directions of Cancer Nanomedicine. *Nat. Nanotechnol.* **2019**, *14* (12), 1083. https://doi.org/10.1038/s41565-019-0597-5.

Thomas Carroll. Introduction to Gene Therapy. *Eur. Soc. Cell Gene Ther.* **2011**, 1–7. https://doi.org/10.1007/978-3-0348-0402-8_1.

Tian, M.; Han, B.; Tan, H.; You, C. Preparation and Characterization of Galactosylated Alginate-Chitosan Oligomer Microcapsule for Hepatocytes Microencapsulation. Carbohydr. Polym. **2014**, 112, 502−511.

Tolstyka, Z. P.; Phillips, H.; Cortez, M.; Wu, Y.; Ingle, N.; Bell, J. B.; Hackett, P. B.; Reineke, T. M. Trehalose-Based Block Copolycations Promote Polyplex Stabilization for Lyophilization and in Vivo pDNA Delivery. ACS Biomater. Sci. Eng. **2016**, 2,43−55.

Tunnacliffe, A. Anhydrobiotic Engineering of Bacterial and Mammalian Cells: Is Intracellular Trehalose Sufficient? *Cryobiology* **2001**, *43* (2), 124–132. https://doi.org/10.1006/cryo.2001.2356.

Uchida, T.; Nagayama, M.; Gohara, K. Trehalose Solution Viscosity at Low Temperatures Measured by Dynamic Light Scattering Method: Trehalose Depresses Molecular Transportation for Ice Crystal Growth. *J. Cryst. Growth* **2009**, *311* (23–24), 4747–4752. https://doi.org/10.1016/j.jcrysgro.2009.09.023.

Urtasun, R. C.; Parliament, M. B.; McEwan, A. J.; Mercer, J. R.; Mannan, R. H.; Wiebe, L. I.; Morin, C.; Chapman, J. D. Measurement of Hypoxia in Human Tumours by Non-Invasive Spect Imaging of Iodoazomycin Arabinoside. *Br. J. Cancer. Suppl.* **1996**, *27*, S209-12.

Vail, N. S.; Stubbs, C.; Biggs, C. I.; Gibson, M. I. Ultralow Dispersity Poly(Vinyl Alcohol) Reveals Significant Dispersity Effects on Ice Recrystallization Inhibition Activity. *ACS Macro Lett.* **2017**, *6* (9), 1001–1004. https://doi.org/10.1021/acsmacrolett.7b00595.

Vales, T. P.; Jee, J. P.; Lee, W. Y.; Cho, S.; Lee, G. M.; Kim, H. J.; Kim, J. S. Development of Poly (2-Methacryloyloxyethyl Phosphorylcholine)-Functionalized Hydrogels for Reducing Protein and Bacterial Adsorption. *Materials (Basel).* **2020**, *13* (4). https://doi.org/10.3390/ma13040943.

Van Bruggen, C.; Hexum, J. K.; Tan, Z.; Dalal, R. J.; Reineke, T. M. Nonviral Gene Delivery with Cationic Glycopolymers. *Acc. Chem. Res.* **2019**. https://doi.org/10.1021/acs.accounts.8b00665.

van der Meel, R.; Sulheim, E.; Shi, Y.; Kiessling, F.; Mulder, W. J. M.; Lammers, T. Smart Cancer Nanomedicine. *Nat. Nanotechnol.* **2019**, *14* (11), 1007–1017. https://doi.org/10.1038/s41565-019-0567-y.

Vaupel, P.; Briest, S.; Höckel, M. Hypoxia in Breast Cancer: Pathogenesis, Characterization and Biological/Therapeutic Implications. *Wiener Medizinische Wochenschrift* **2002**, *152* (13–14), 334–342. https://doi.org/10.1046/j.1563-258X.2002.02032.x.

Vaupel, P.; Hockel, M.; Mayer, A. Detection and Characterization of Tumor Hypoxia Using PO2 Histography. *Antioxid Redox Signal* **2007**, *9* (8), 1221–1235. https://doi.org/10.1089/ars.2007.1628.

Vaupel, P.; Mayer, A. Hypoxia in Cancer: Significance and Impact on Clinical Outcome. *Cancer Metastasis Rev.* **2007**, *26* (2), 225–239. https://doi.org/10.1007/s10555-007-9055-1.

Velpurisiva, P.; Gad, A.; Piel, B.; Jadia, R.; Rai, P. Nanoparticle Design Strategies for Effective Cancer Immunotherapy. *J. Biomed.* **2017**, *2* (2), 64–77. https://doi.org/10.7150/jbm.18877.Nanoparticle.

Wadhwa*, M. S.; Rice*, K. G. Receptor Mediated Glycotargeting. *J. Drug Target.* **2003**, *11* (5), 255–268. https://doi.org/10.1080/10611860310001636557.

Walsh, J. C.; Lebedev, A.; Aten, E.; Madsen, K.; Marciano, L.; Kolb, H. C. The Clinical Importance of Assessing Tumor Hypoxia: Relationship of Tumor Hypoxia to Prognosis and Therapeutic Opportunities. *Antioxid. Redox Signal.* **2014**, *21* (10), 1516–1554. https://doi.org/10.1089/ars.2013.5378.

Wang, B.; Shao, P.; Wang, Y.; Li, J.; Zhang, Y. The Application of Thermosensitive Nanocarriers in Controlled Drug Delivery. *J. Nanomater.* **2011**, *2011*. https://doi.org/10.1155/2011/389640.

Wang, H.; Agarwal, P.; Zhao, S.; Xu, R. X.; Yu, J.; Lu, X.; He, X. Hyaluronic Acid-Decorated Dual Responsive Nanoparticles of Pluronic F127, PLGA, and Chitosan for Targeted Co-Delivery of Doxorubicin and Irinotecan to Eliminate Cancer Stem-like Cells. *Biomaterials* **2015**, *72*, 74–89. https://doi.org/10.1016/j.biomaterials.2015.08.048.

Wang, Y.; Zhang, X.; Yu, P.; Li, C. Glycopolymer Micelles with Reducible Ionic Cores for Hepatocytes-Targeting Delivery of DOX. *Int. J. Pharm.* **2013**. https://doi.org/10.1016/j.ijpharm.2012.12.001.

Wang, Z. ErbB Receptors and Cancer. ErbB Receptor Signaling; Springer: New York, **2017**; pp 3−35.

Wardman, P. Chemical Radiosensitizers for Use in Radiotherapy. *Clin. Oncol.* **2007**, *19* (6), 397–417. https://doi.org/10.1016/j.clon.2007.03.010.

Warner, D. T. Some Possible Relationships of Carbohydrates and Other Biological Components with the Water Structure at 37°. *Nature* **1962**, *196* (4859), 1055–1058. https://doi.org/10.1038/1961055a0.

Watts, M. E.; Dennis, M. F.; Roberts, I. J.; Wattst, M. E. International Journal of Radiation Biology Radiosensitization by Misonidazole, Pimonidazole and Azomycin and Intracellular Uptake in Human Tumour Cell Lines Radiosensitization by Misonidazole, Pimonidazole and Azomycin and Intracellular Uptake in Human Tu. *Int. J. Radiat. Biol. INT . J . RADIAT . BIOL* **1990**, *57* (3), 361–372. https://doi.org/10.1080/09553009014552461.

Wei, H.; Pahang, J. A.; Pun, S. H. Optimization of Brush-Like Cationic Copolymers for Nonviral Gene Delivery. Biomacromolecules **2013**, 14, 275−284.

Wiebe, L. I. PET Radiopharmaceuticals for Metabolic Imaging in Oncology. *Int. Congr. Ser.* **2004**, *1264*, 53–76. https://doi.org/10.1016/j.ics.2003.12.102.

Wiebe, L. I.; Mannan, R. H.; Mercer, J. R.; Chapman, J. D.; Miller, G.; Moore, R.; Lee, J. Iaza: Iodoazomycin Arabinoside. the Development of a Marker for Hypoxic Tissue. *Clin. Nucl. Med.* **1991**, *16* (10), 796. https://doi.org/10.1097/00003072-199110000-00046.

Wiebe, L. I.; McEwan, A. J. B. Scintigraphic Imaging of Focal Hypoxic Tissue: Development and Clinical Applications of 123I-IAZA. *Braz. arch. biol. technol.* **2002**, *45* (September), 69–81. https://doi.org/10.1590/S1516-89132002000500010.

Williams, E. G. L.; Hutt, O. E.; Hinton, T. M.; Larnaudie, S. C.;Le, T.; MacDonald, J. M.; Gunatillake, P.; Thang, S. H.; Duggan, P. J. Glycosylated Reversible Addition-Fragmentation Chain Transfer Polymers with Varying Polyethylene

Glycol Linkers Produce Different Short Interfering RNA Uptake, Gene Silencing, and Toxicity Profiles. Biomacromolecules **2017**, 18, 4099−4112.

Wilson, W. R.; Hay, M. P. Targeting Hypoxia in Cancer Therapy. *Nat. Rev. Cancer* **2011**, *11* (6), 393–410. https://doi.org/10.1038/nrc3064.

Wong, J. K. L.; Mohseni, R.; Hamidieh, A. A.; MacLaren, R. E.; Habib, N.; Seifalian, A. M. Will Nanotechnology Bring New Hope for Gene Delivery? *Trends Biotechnol.* **2017**, *35* (5), 434–451. https://doi.org/10.1016/j.tibtech.2016.12.009.

Workman, P. The Neurotoxicity of Misonidazole: Potential Modifying Role of Dexamethasone. *Br. J. Radiol.* **1980**, *53* (631), 736–736. https://doi.org/10.1259/0007-1285-53-631-736.

Wu, D.; Wang, W.; Diaz-Dussan, D.; Peng, Y.-Y.; Chen, Y.; Narain, R.; Hall, D. G. In Situ Forming, Dual-Crosslink Network, Self-Healing Hydrogel Enabled by a Bioorthogonal Nopoldiol–Benzoxaborolate Click Reaction with a Wide PH Range. *Chem. Mater.* **2019**, acs.chemmater.9b00769. https://doi.org/10.1021/acs.chemmater.9b00769.

Wu, J.; Yuan, J.; Ye, B.; Wu, Y.; Xu, Z.; Chen, J.; Chen, J. Dual-Responsive Core Crosslinking Glycopolymer-Drug Conjugates Nanoparticles for Precise Hepatocarcinoma Therapy. *Front. Pharmacol.* **2018**, *9* (JUL), 1–12. https://doi.org/10.3389/fphar.2018.00663.

Wuest, K. N. R.; Lu, H.; Thomas, D. S.; Goldmann, A. S.; Stenzel, M. H.; Barner-Kowollik, C. Fluorescent Glyco Single-Chain Nanoparticle-Decorated Nanodiamonds. *ACS Macro Lett.* **2017**. https://doi.org/10.1021/acsmacrolett.7b00659.

Xu, F.-J. Versatile Types of Hydroxyl-Rich Polycationic Systems via O-Heterocyclic Ring-Opening Reactions: From Strategic Design to Nucleic Acid Delivery Applications. Prog. Polym. Sci. **2018**, 78,56− 91.

Xu, H.; Ma, H.; Yang, P.; Zhang, X.; Wu, X.; Yin, W.; Wang, H.; Xu, D. Targeted polymer-drug conjugates: Current progress and future perspective. *Colloids Surfaces B Biointerfaces* **2015**, *136*, 729–734 DOI: 10.1016/j.colsurfb.2015.10.001.

Xu, X. C.; Abuduhadeer, X.; Zhang, W. B.; Li, T.; Gao, H.; Wang, Y. H. Knockdown of RAGE Inhibits Growth and Invasion of Gastric Cancer Cells. *Eur. J. Histochem.* **2013**, *57* (4), 36. https://doi.org/10.4081/ejh.2013.e36.

Xue, L.; Ingle, N. P.; Reineke, T. M. Highlighting the role of polymer length, carbohydrate size, and nucleic acid type in potency of glycopolycation agents for pDNA and siRNA delivery. *Biomacromolecules* **2013**, *14* (11), 3903–3915 DOI: 10.1021/bm401026n.

Yalcin, A.; Telang, S.; Clem, B.; Chesney, J. Regulation of Glucose Metabolism by 6-Phosphofructo-2-Kinase/Fructose-2,6-Bisphosphatases in Cancer. *Experimental and Molecular Pathology*. **2009**, pp 174–179. https://doi.org/10.1016/j.yexmp.2009.01.003.

Yang, J.; Cai, N.; Zhai, H.; Zhang, J.; Zhu, Y.; Zhang, L. Natural Zwitterionic Betaine Enables Cells to Survive Ultrarapid Cryopreservation. *Sci. Rep.* **2016**, *6* (October), 1–9. https://doi.org/10.1038/srep37458.

Yilmaz, G.; Becer, C. R. Glycopolymer Code Based on Well-Defined Glycopolymers or Glyconanomaterials and Their Biomolecular Recognition. *Front. Bioeng. Biotechnol.* **2014**, *2* (OCT), 1–18. https://doi.org/10.3389/fbioe.2014.00039.

Yilmaz, G.; Becer, C. R. Glycopolymer Code: Programming Synthetic Macromolecules for Biological Targeting. *Macromol. Chem. Phys.* **2020**, *221* (7), 1–3. https://doi.org/10.1002/macp.202000006.

Yoshida, G. J.; Saya, H. Therapeutic Strategies Targeting Cancer Stem Cells. *Cancer Sci.* **2016**, *107* (1), 5–11. https://doi.org/10.1111/cas.12817.

Yoshiyama, Y.; Tanaka, K.; Yoshiyama, K.; Hibi, M.; Ogawa, J.; Shima, J. Trehalose Accumulation Enhances Tolerance of Saccharomyces Cerevisiae to Acetic Acid. *J. Biosci. Bioeng.* **2015**, *119* (2), 172–175. https://doi.org/10.1016/j.jbiosc.2014.06.021.

Young, S. W. S.; Stenzel, M.; Jia-Lin, Y. Nanoparticle-siRNA: A potential cancer therapy? *Crit. Rev. Oncol. Hematol.* **2016**, *98*, 159–169 DOI: 10.1016/j.critrevonc.2015.10.015.

Yuan, C.; Gao, J.; Guo, J.; Bai, L.; Marshall, C.; Cai, Z.; Wang, L.; Xiao, M. Dimethyl Sulfoxide Damages Mitochondrial Integrity and Membrane Potential in Cultured

Astrocytes. *PLoS One* **2014**, *9* (9), e107447. https://doi.org/10.1371/journal.pone.0107447.

Yuan, Y.; Yang, Y.; Tian, Y.; Park, J.; Dai, A.; Roberts, R. M.; Liu, Y.; Han, X. Efficient Long-Term Cryopreservation of Pluripotent Stem Cells at-80 °c. *Sci. Rep.* **2016**, *6* (September), 1–13. https://doi.org/10.1038/srep34476.

Yun, U.-J.; Sung, J. Y.; Park, S.-Y.; Ye, S.-K.; Shim, J.; Lee, J.-S.; Hibi, M.; Bae, Y.-K.; Kim, Y.-N. Oncogenic role of rab escort protein 1 through EGFR and STAT3 pathway. *Cell Death Dis.* **2017**, *8* DOI: 10.1038/cddis.2017.50.

Zaimy,M.A.; Saffarzadeh, N.;Mohammadi,A.;Pourghadamyari, H.; Izadi, P.; Sarli, A.; Moghaddam, L. K.; Paschepari, S. R.; Azizi, H.; Torkamandi, S.; Tavakkoly-Bazzaz, J. New Methods in the Diagnosis of Cancer and Gene Therapy of Cancer Based on Nanoparticles. Cancer Gene Ther. **2017**, 24, 233− 243

Zelepukin, I. V.; Yaremenko, A. V.; Yuryev, M. V.; Mirkasymov, A. B.; Sokolov, I. L.; Deyev, S. M.; Nikitin, P. I.; Nikitin, M. P. Fast Processes of Nanoparticle Blood Clearance: Comprehensive Study. *J. Control. Release* **2020**, *326*, 181–191. https://doi.org/10.1016/J.JCONREL.2020.07.014.

Zeman, E. M. *Biologic Basis of Radiation Oncology*, Thrid Edit.; Elsevier Inc., **2011**. https://doi.org/10.1016/B978-1-4377-1637-5.00001-8.

Zhang, C. G.; Zhu, W. J.; Liu, Y.; Yuan, Z. Q.; Yang, S. Di; Chen, W. L.; Li, J. Z.; Zhou, X. F.; Liu, C.; Zhang, X. N. Novel Polymer Micelle Mediated Co-Delivery of Doxorubicin and P-Glycoprotein SiRNA for Reversal of Multidrug Resistance and Synergistic Tumor Therapy. *Sci. Rep.* **2016**, *6* (March), 1–12. https://doi.org/10.1038/srep23859.

Zhang, H. Onivyde for the Therapy of Multiple Solid Tumors. *Onco. Targets. Ther.* **2016**, *9*, 3001–3007. https://doi.org/10.2147/OTT.S105587.

Zhang, W.-W.; Li, L.; Li, D.; Liu, J.; Li, X.; Li, W.; Xu, X.; Zhang, M. J.; Chandler, L. A.; Lin, H.; Hu, A.; Xu, W.; Lam, D. M.-K. The First Approved Gene Therapy Product for Cancer Ad- *P53* (Gendicine): 12 Years in the Clinic. *Hum. Gene Ther.* **2018**. https://doi.org/10.1089/hum.2017.218.

Zhang, Y.; Wang, B.; Zhang, Y.; Zheng, Y.; Wen, X.; Bai, L.; Wu, Y. Hyperbranched Glycopolymers of 2-(α-D-Mannopyranose) Ethyl Methacrylate and N, N'-

Methylenebisacrylamide: Synthesis, Characterization and Multivalent Recognitions with Concanavalin A. *Polymers (Basel).* **2018**, *10* (2). https://doi.org/10.3390/polym10020171.

Zhao, L.; Li, Y.; Pei, D.; Huang, Q.; Zhang, H.; Yang, Z.; Li, F.; Shi, T. Glycopolymers/PEI Complexes as Serum-Tolerant Vectors for Enhanced Gene Delivery to Hepatocytes. Carbohydr. Polym. **2019**, 205, 167−175.

Zhong, Y.-Q.; Wei, J.; Fu, Y.-R.; Shao, J.; Liang, Y.-W.; Lin, Y.-H.; Liu, J.; Zhu, Z.-H. Toxicity of Cationic Liposome Lipofectamine 2000 in Human Pancreatic Cancer Capan-2 Cells. *Nan Fang Yi Ke Da Xue Xue Bao* **2008**, *28* (11), 1981–1984.

Zhou, Q.; Shao, S.; Wang, J.; Xu, C.; Xiang, J.; Piao, Y.; Zhou, Z.; Yu, Q.; Tang, J.; Liu, X.; Gan, Z.; Mo, R.; Gu, Z.; Shen, Y. Enzyme-Activatable Polymer–Drug Conjugate Augments Tumour Penetration and Treatment Efficacy. *Nat. Nanotechnol.* **2019**, *14* (8), 799–809. https://doi.org/10.1038/s41565-019-0485-z.

Zhu, G.; Mei, L.; Vishwasrao, H. D.; Jacobson, O.; Wang, Z.; Liu, Y.; Yung, B. C.; Fu, X.; Jin, A.; Niu, G.; Wang, Q.; Zhang, F.; Shroff, H.; Chen, X. Intertwining DNA-RNA Nanocapsules Loaded with Tumor Neoantigens as Synergistic Nanovaccines for Cancer Immunotherapy. *Nat. Commun.* **2017**, *8* (1). https://doi.org/10.1038/s41467-017-01386-7.

Zhu, G.; Zhang, F.; Ni, Q.; Niu, G.; Chen, X. Efficient Nanovaccine Delivery in Cancer Immunotherapy. *ACS Nano* **2017**, *11* (3), 2387–2392. https://doi.org/10.1021/acsnano.7b00978.

APPENDIX

CHAPTER 2

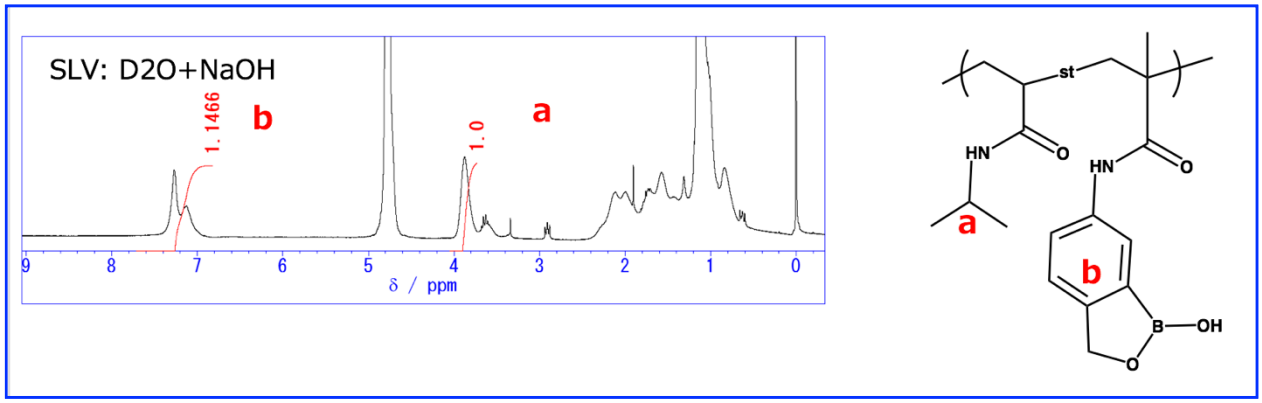

Figure 2S1. Characterization of MCTA by ^{1}H-NMR P(NIPAAm$_{32}$-*st*-MAAmBO$_{12}$).

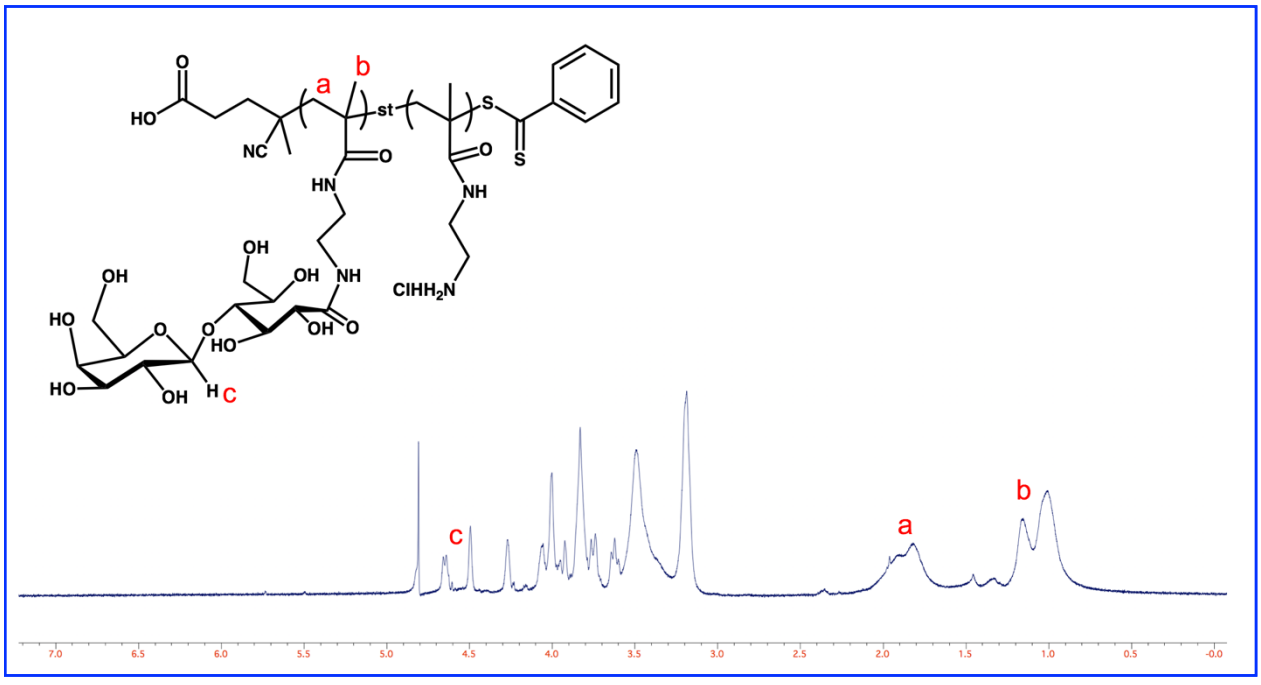

Figure 2S2. ^{1}H-NMR spectra in (D_2O) for Glycopolymer 1 P(LAEMA$_{20}$-*b*-AEMA$_{47}$).

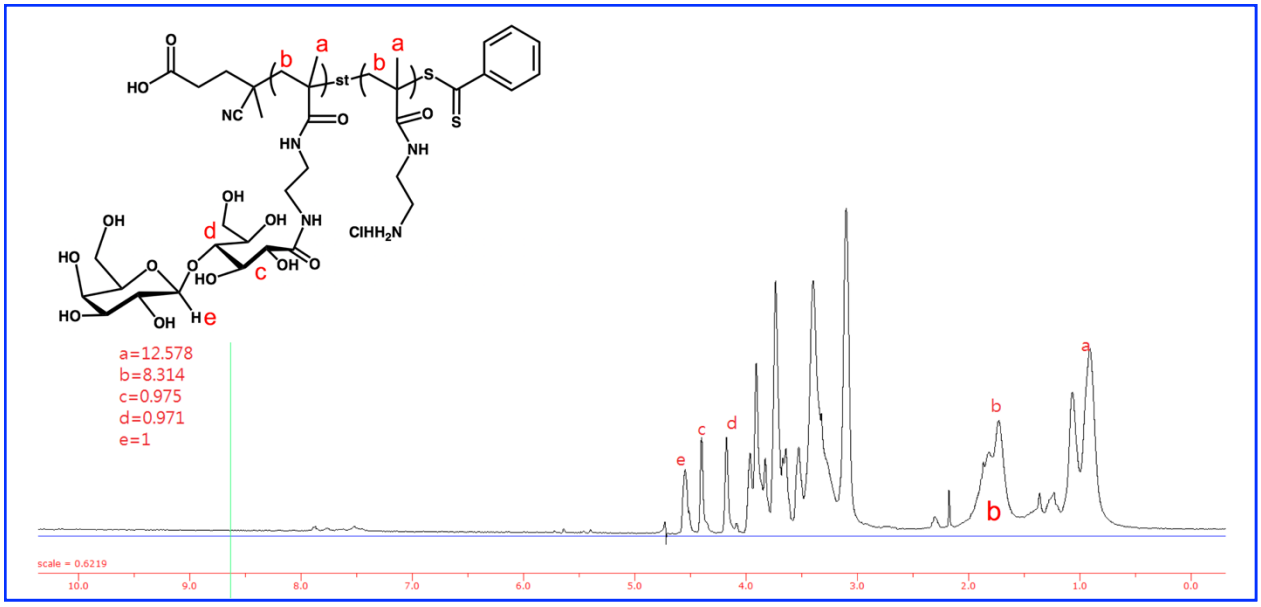

Figure 2S3. ^{1}H-NMR spectra in (D_2O) for Glycopolymer 2 P($AEMA_8$-*b*-$AEMA_{24}$).

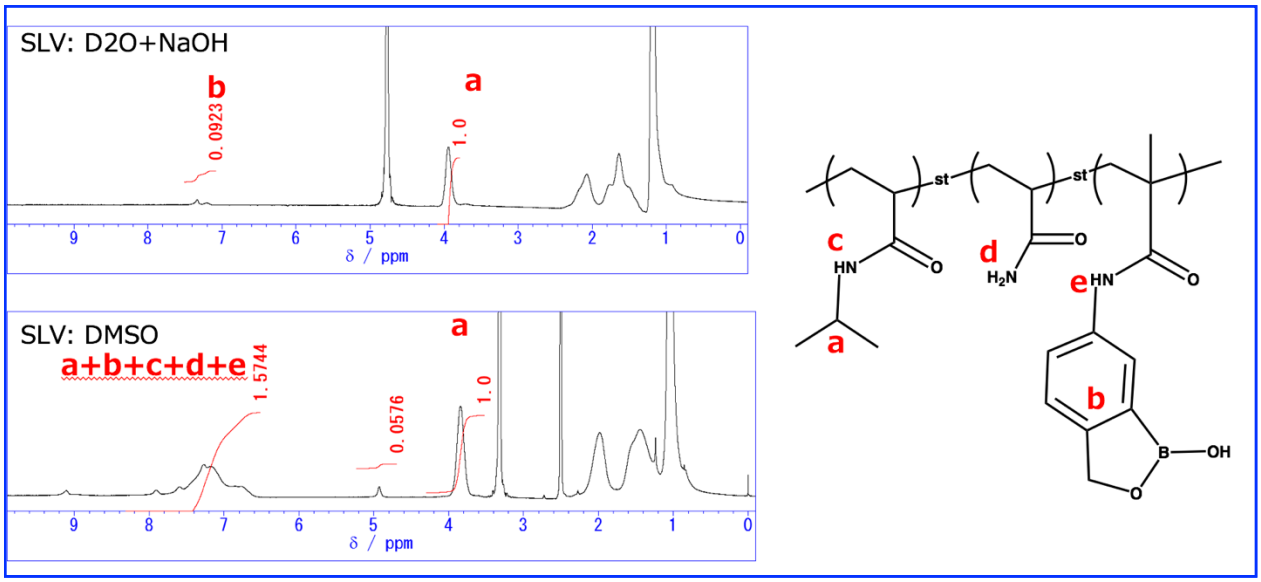

Figure 2S4. ^{1}H-NMR spectra in (D_2O) for pOxaborole P($NIPAAm_{294}$-*st*-AAm_{63}-*st*-$MAAmBO_9$).

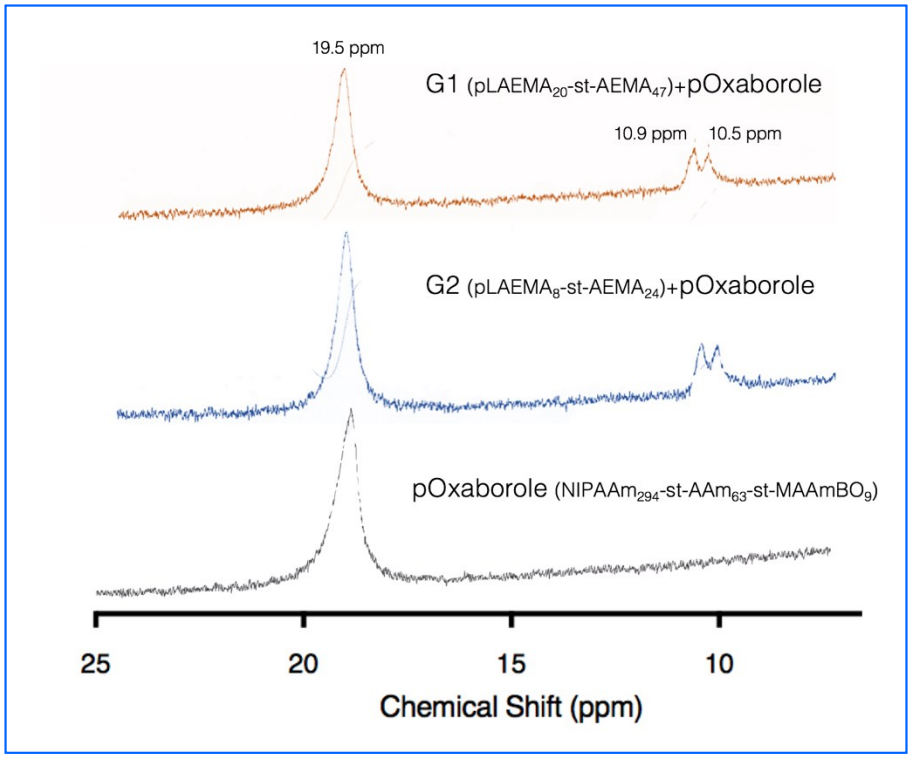

Figure 2S5. Boron NMR in D_2O of oxaborole-glycopolymer complexes. pOxaborole P(NIPAAm$_{294}$-st-AAm$_{63}$-st- MAAmBO$_9$) revealed a single ^{11}B peak at 19.5 ppm, the binding between pOxaborole and the glycopolymers was indicated by the two small peaks at 10.9 and 10.5 ppm.

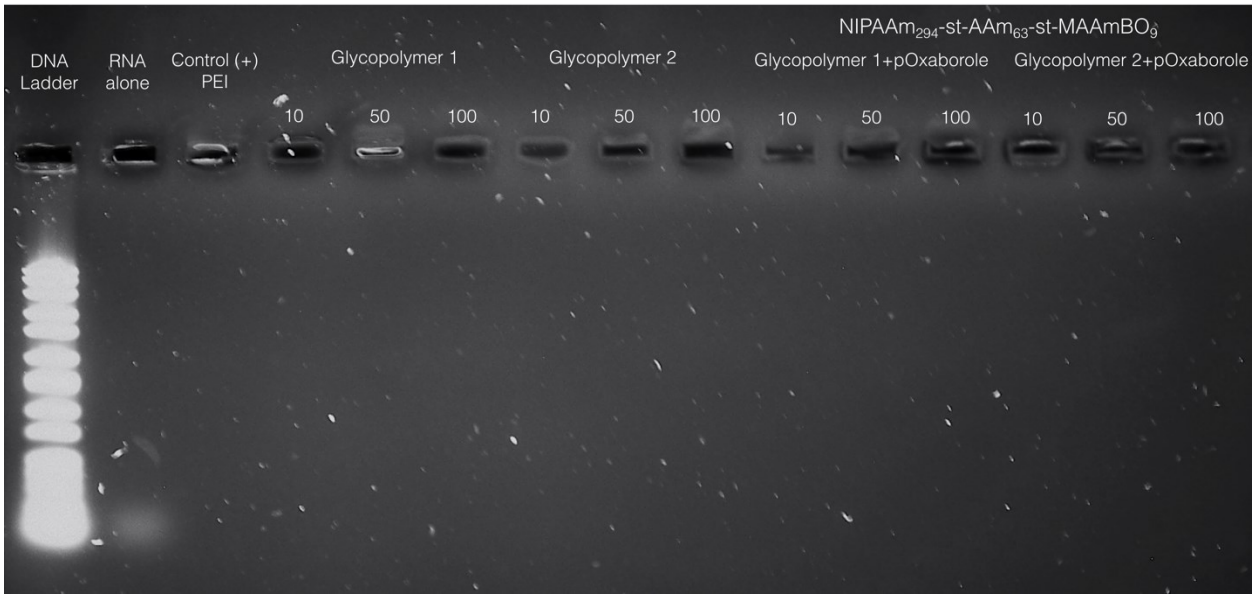

Figure 2S6. Agarose gel electrophoresis showing polyplex formation at various weight/weight ratios of oxaborole-glycopolymers with EGFR siRNA (133 ng).

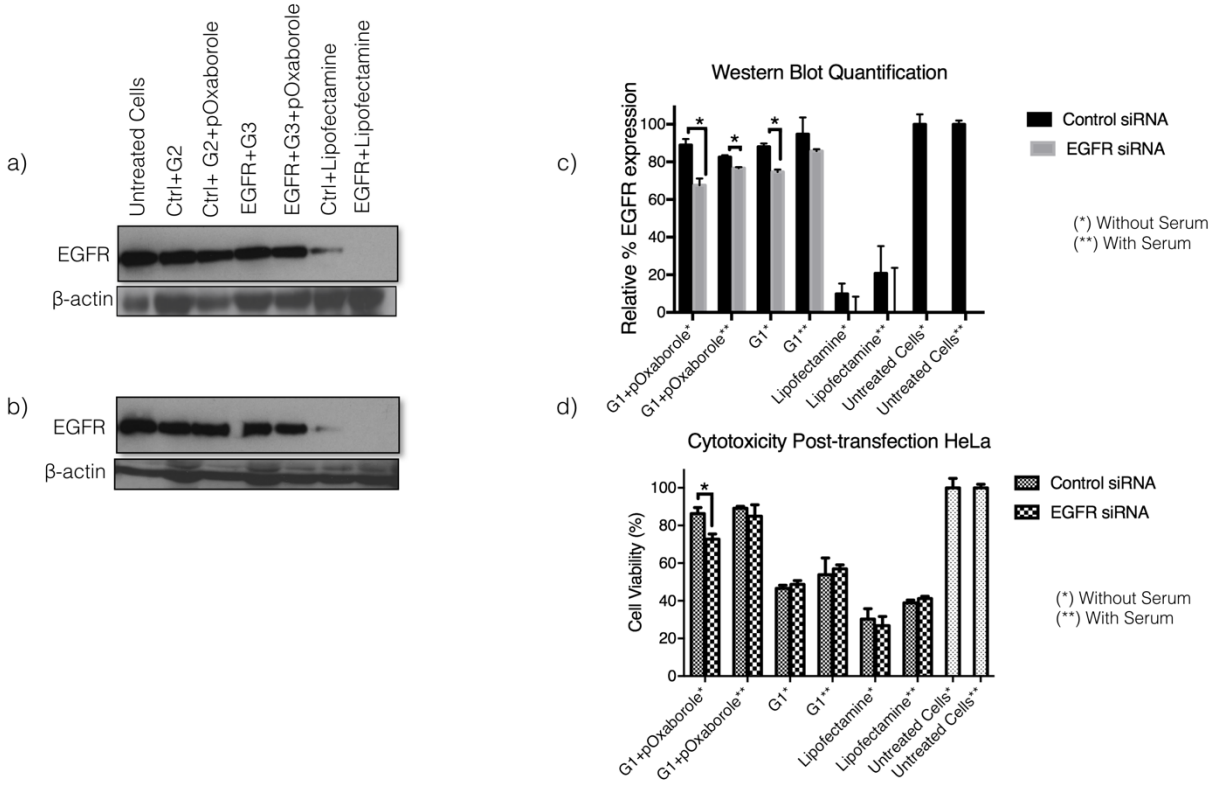

Figure 2S7. EGFR knockdown with G1 and G1+pOxaborole complex in HeLa cells in the presence (a) and absence (b) serum. HeLa cells were transfected with either control or EGFR siRNA for 48 h and cell lysates were subjected to immunoblot analysis using indicated antibodies. (c) Western Blot quantification was done by ImageJ analysis. (d) Cell viability was assessed by Janus Green assay 48h post-transfection, with error bars representing S.D. (versus control siRNA *P<0.01).

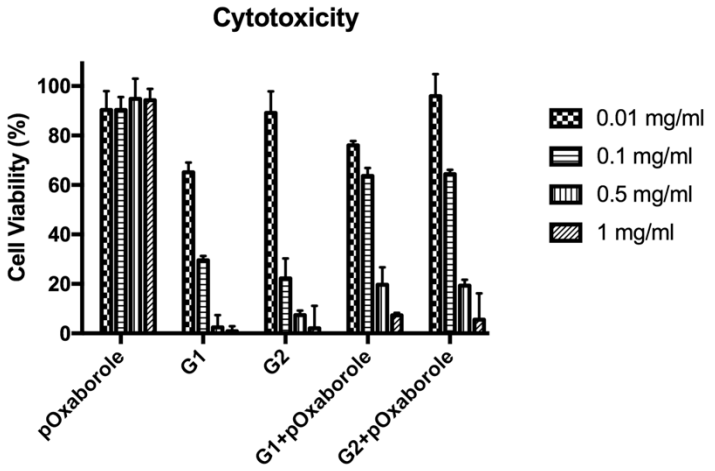

Polymer	IC_{50} (mg/ml)
Glycopolymer 1	0.02545
Glycopolymer 2	0.02052
pOxaborole	12.28
Glycopolymer 1+pOxaborole	0.1309
Glycopolymer 2+pOxaborole	0.1081

Figure 2S8. Glycopolymers and oxaborole-glycopolymers cytotoxicity in HeLa cells determined by MTT assay. IC50 were calculated using GraphPad Prism.

CHAPTER 3

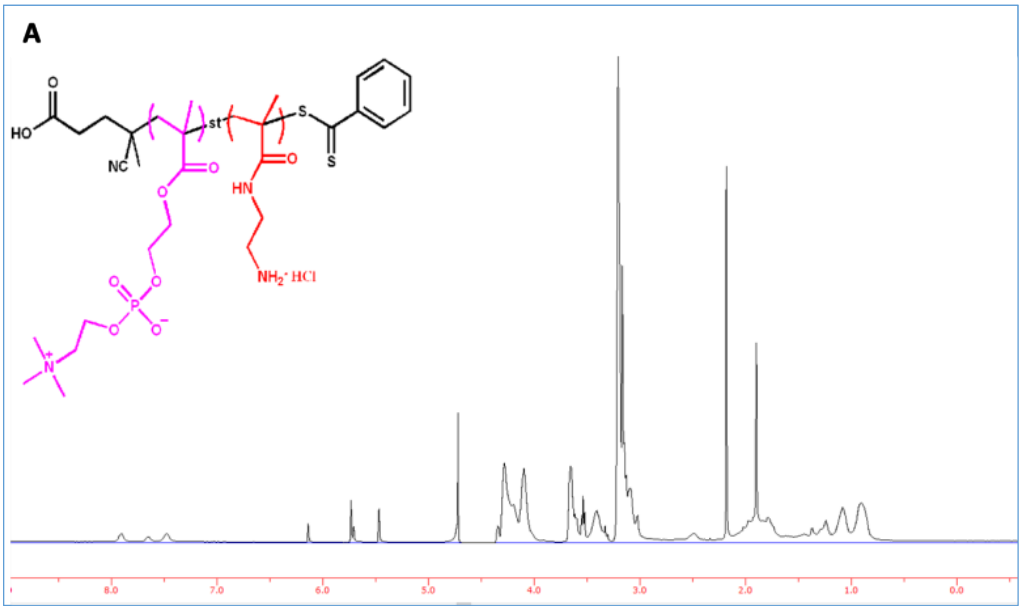

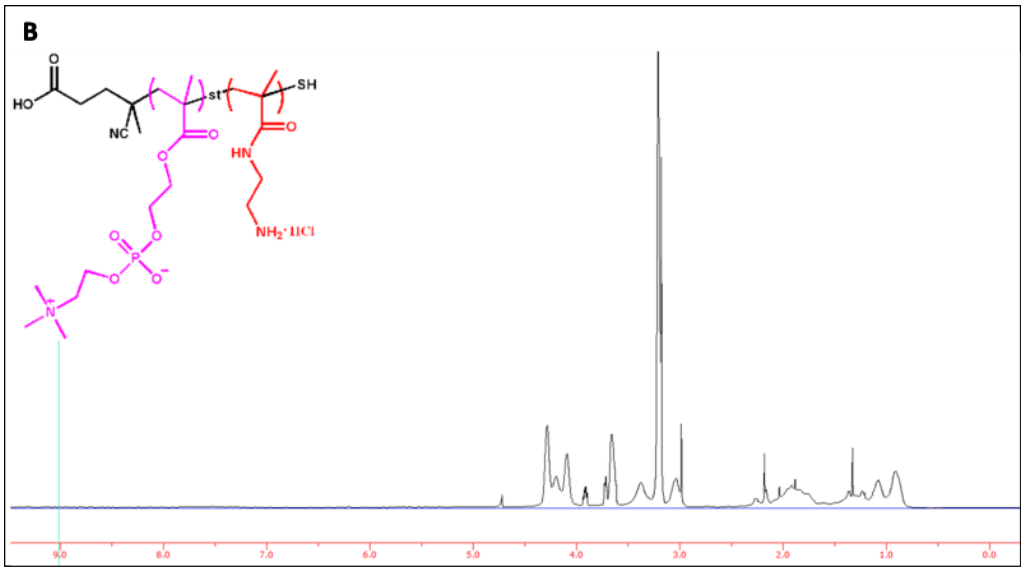

Figure 3S1. ^{1}H NMR spectrum of PMA (A), PMA-SH (B).

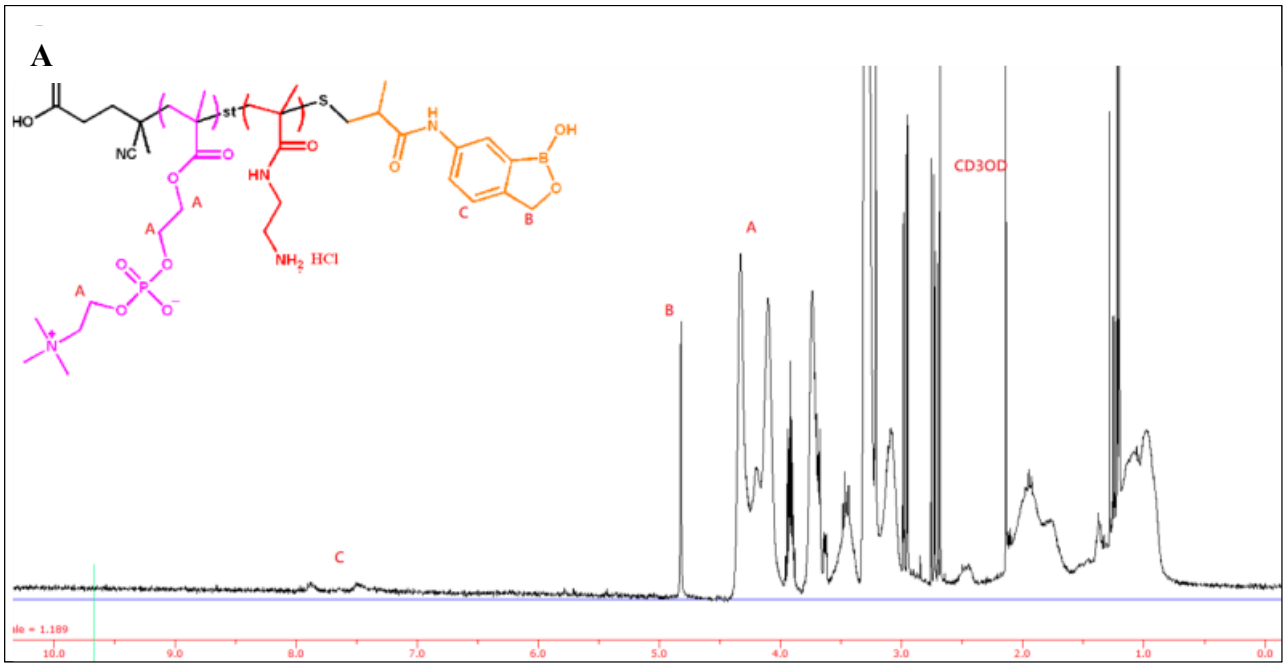

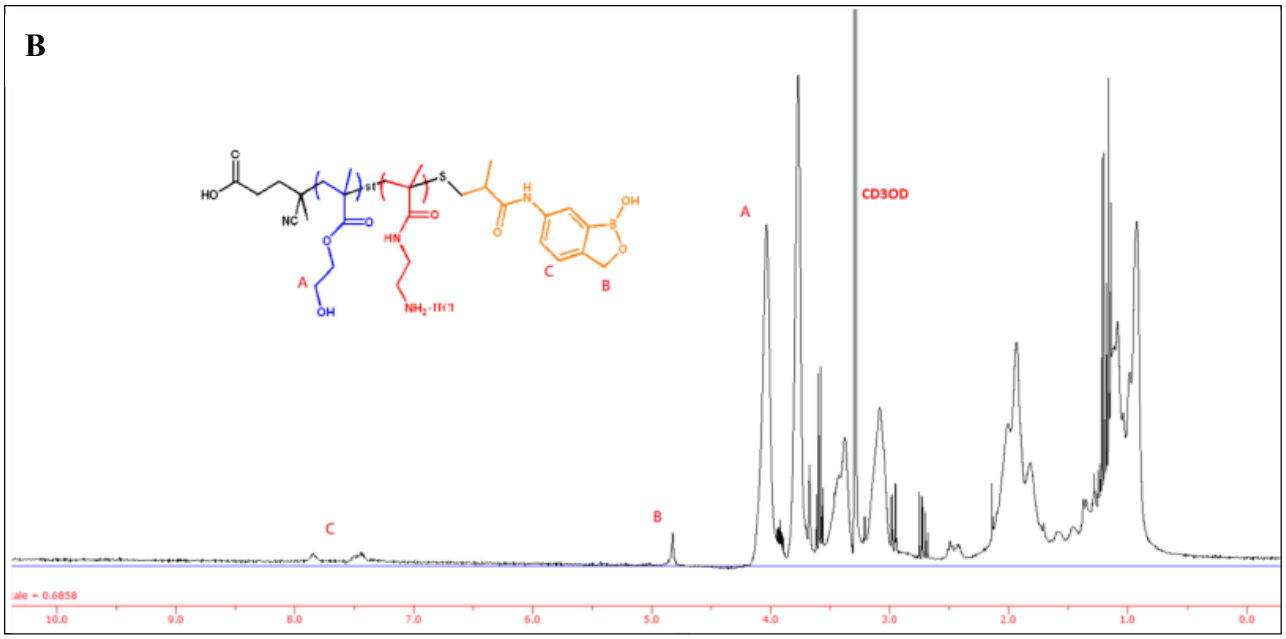

Figure 3S2. ^{1}H NMR spectrum of PMA-B (A) and PHA-B (B).

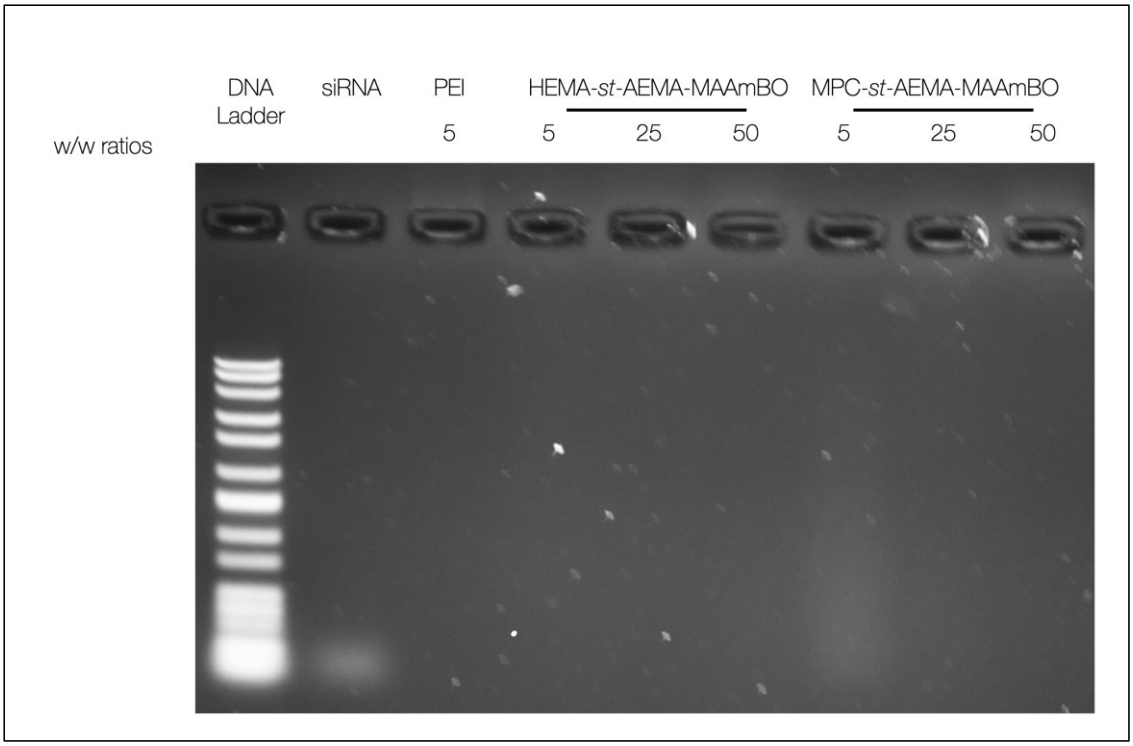

Figure 3S3. Agarose gel electrophoresis showing polyplex formation at various weight/weight ratios of sugar-benzoxaborole polymers with EGFR siRNA (133 ng).

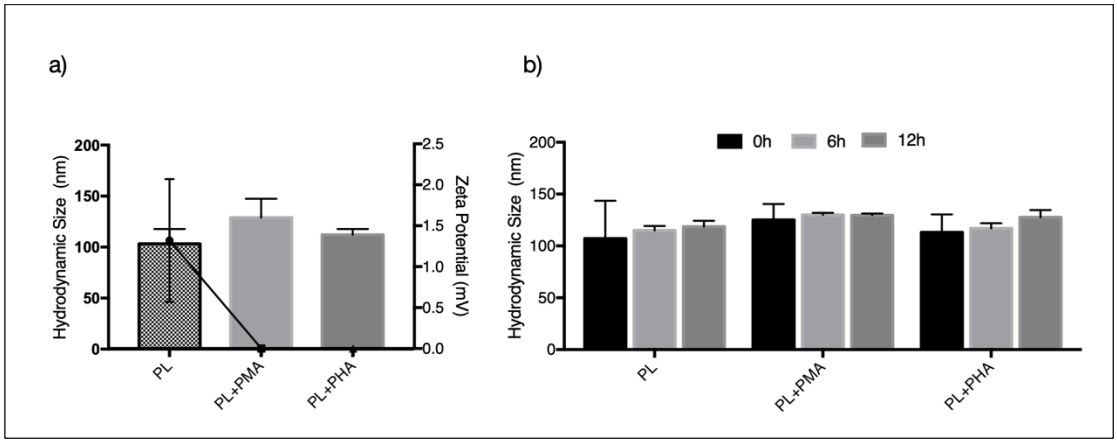

Figure 3S4. a) Hydrodynamic size and zeta potential of the polyplexes **b)** Polyplex stability is DMEM media + Serum after 12 h incubation.

CHAPTER 4

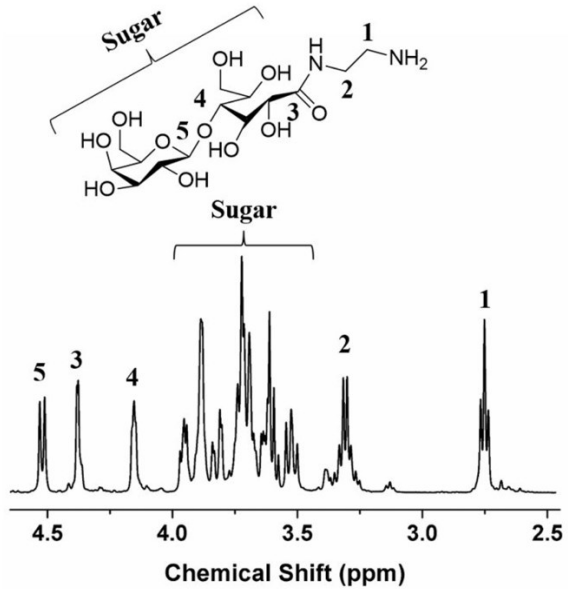

Figure 4S1. H NMR spectrum of Lac-NH_2 in D_2O.

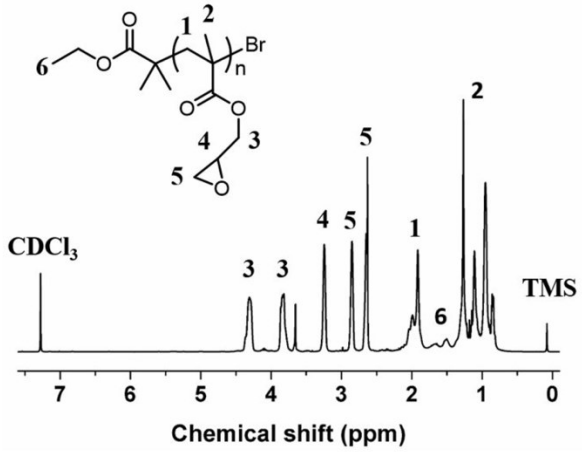

Figure 4S2. H NMR spectrum of PGMA in $CDCl_3$.

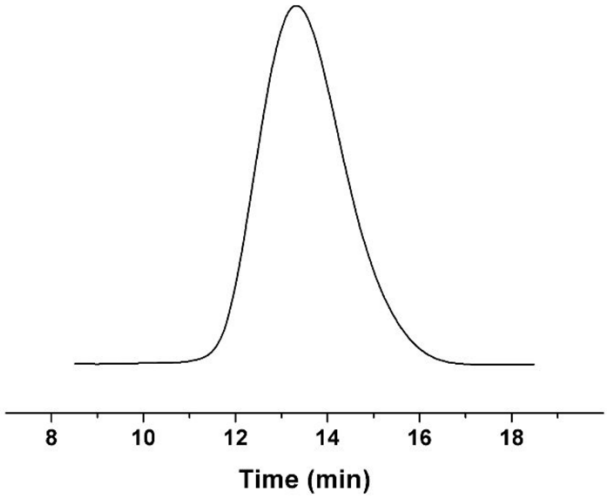

Figure 4S3. GPC trace of PGMA using DMF/10 mM LiBr as the mobile phase.

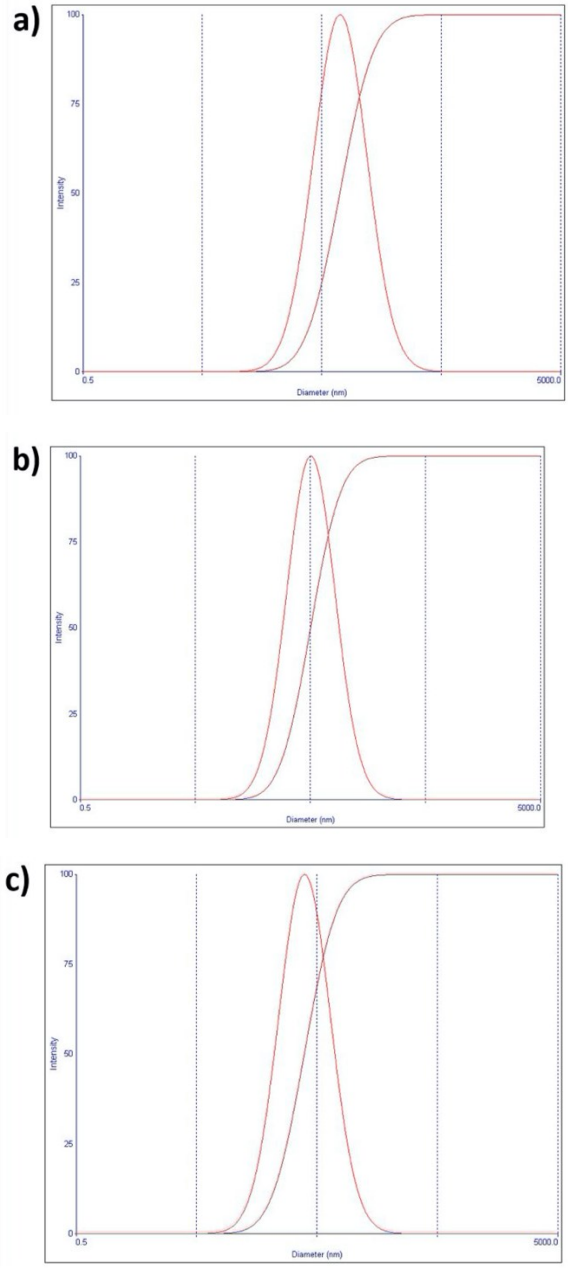

Figure 4S4. Size distribution (by intensity) of polyplexes formed from different cationic polymers: a) PGEA, b) PGEL-1, c) PGEL-2.

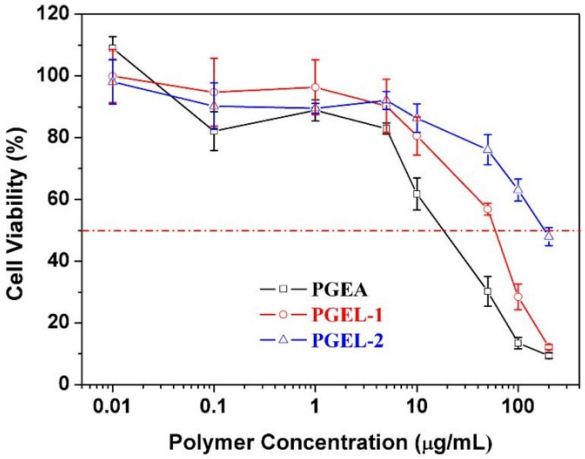

Figure 4S5. Cell viability of HeLa cells treated with different concentrations of PGEA, PGEL-1, and PGEL-2 for 48 h.

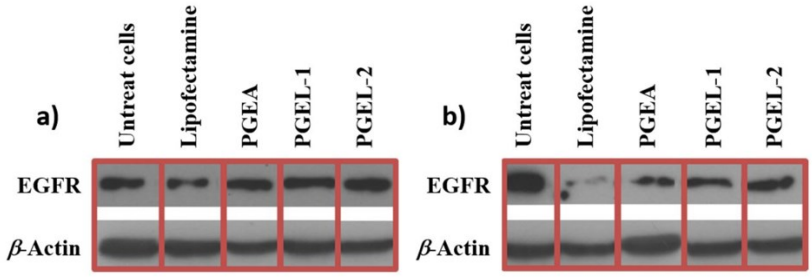

Figure 4S6. Western blot EGFR knockdown in the presence of serum in HeLa cells: a) Control siRNA, b) EGFR siRNA.

CHAPTER 5

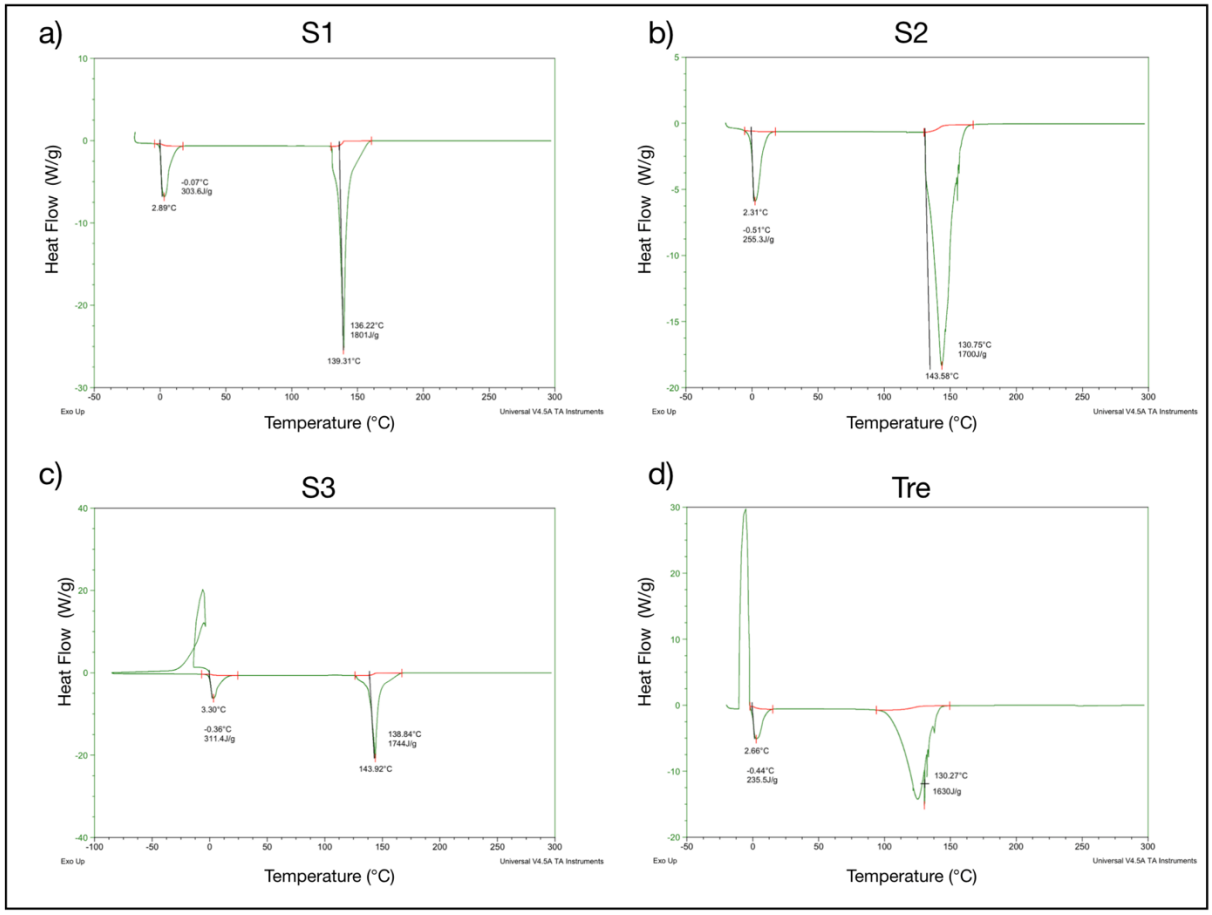

Figure 5S1. Effects on ice formation of the trehalose-based polymers. DSC thermograms of (a) **S1** , (b) **S2** (C) **S3** polymers and (d) pure Trehalose (**Tre**).

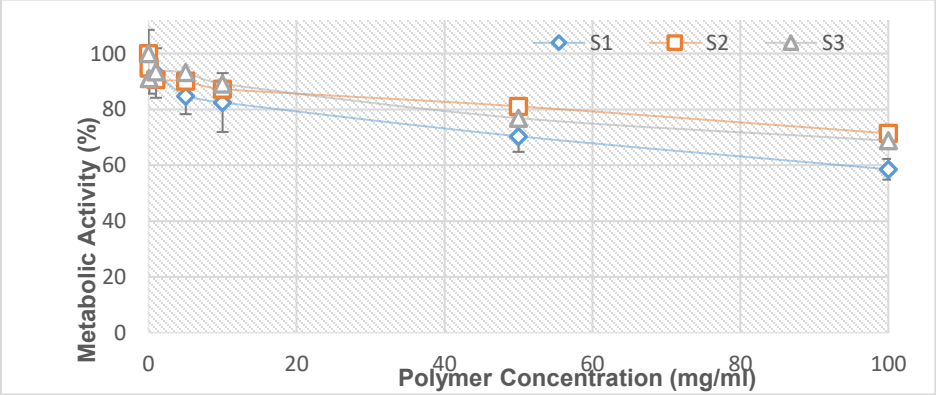

Figure 5S2. Cytotoxicity tests of the Poly(Tre-ECH) polymers by MTT assay. ~105 million HeLa cells were seeded on 96 well plates and left for 24 h to attach. Afterwards,

cells were treated with increasing concentrations of dissolved Tre-ECH polymers and incubated under at 37 °C for 24 h. 100 μM DMSO was used as vehicle control. Following treatment, MTT reagent was added; cells were incubated for 4 h, followed by the addition of 100 μL of lysis buffer (DMSO: 2-propanol = 1: 1). The plate was then read at 570 nm and percent metabolic activity was determined. Error bars represent standard error of the means.

CHAPTER 6

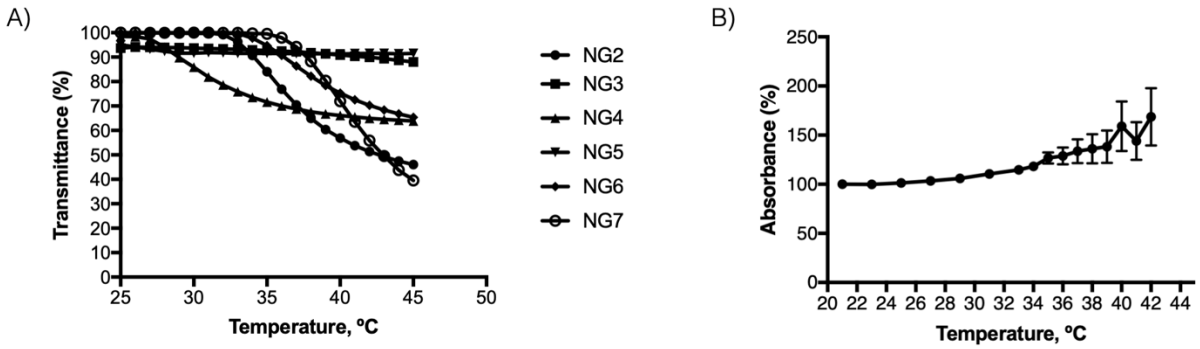

Figure 6S1. Scattered light intensity of different nanogels (NGs) as a function of temperature to determine the lower critical solution temperature (LCST) (b) **NG1** LSCT measure as absorbance percentage.

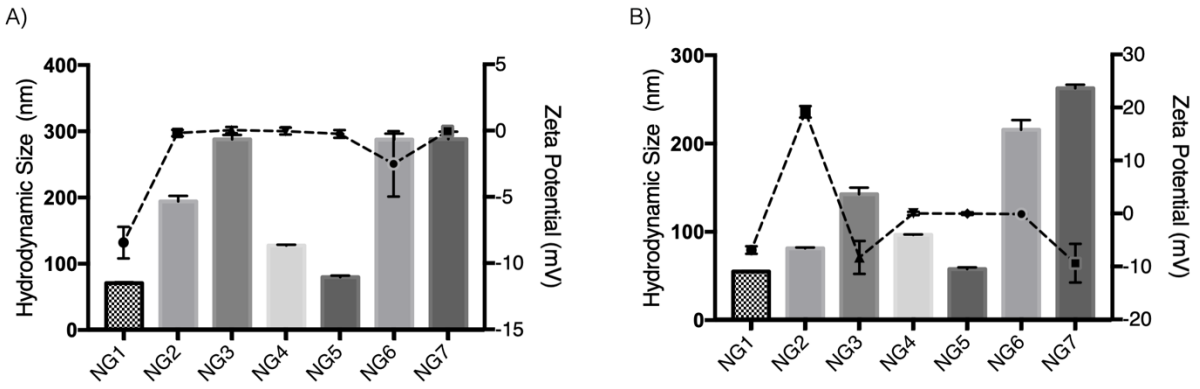

Figure 6S2. Hydrodynamic size and zeta potential characterization of the NGs. A) at 15 ^{o}C B) at 37 ^{o}C.

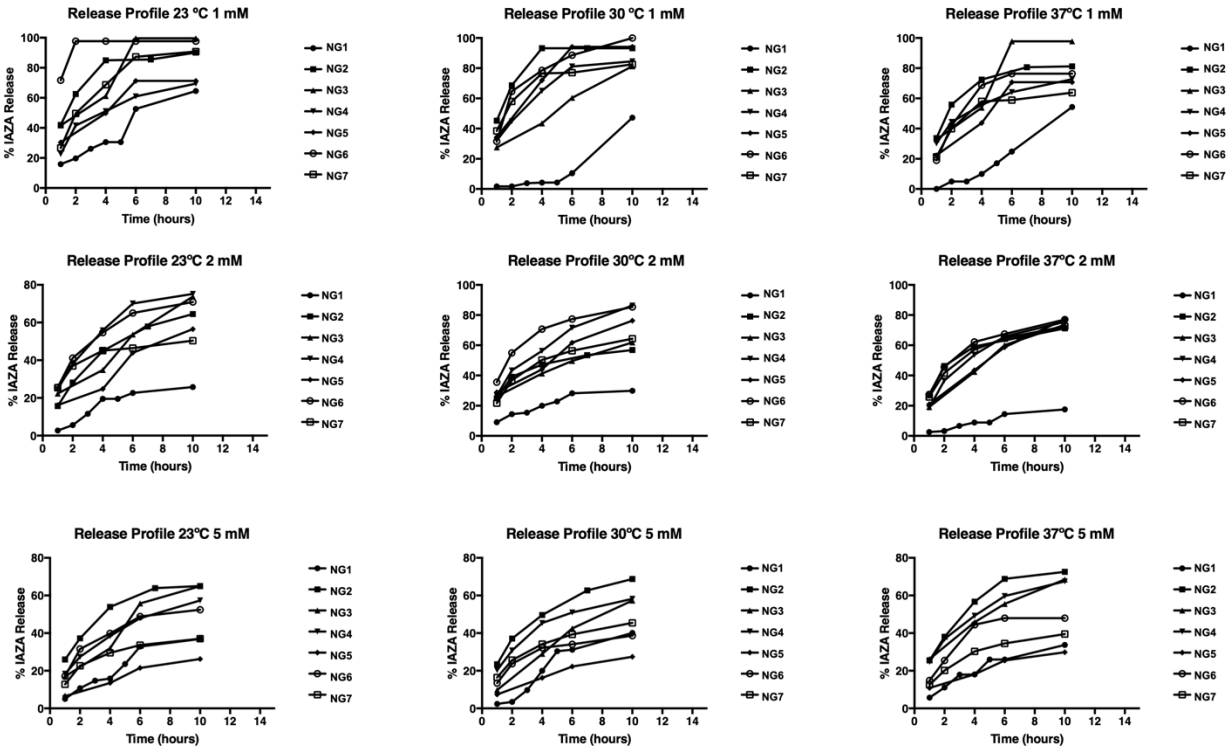

Figure 6S3. Release profile of encapsulated IAZA in different nanogels depending on temperature (23˚C, 30˚C and 37˚C) and concentrations (1mM, 2 mM, and 5 mM).

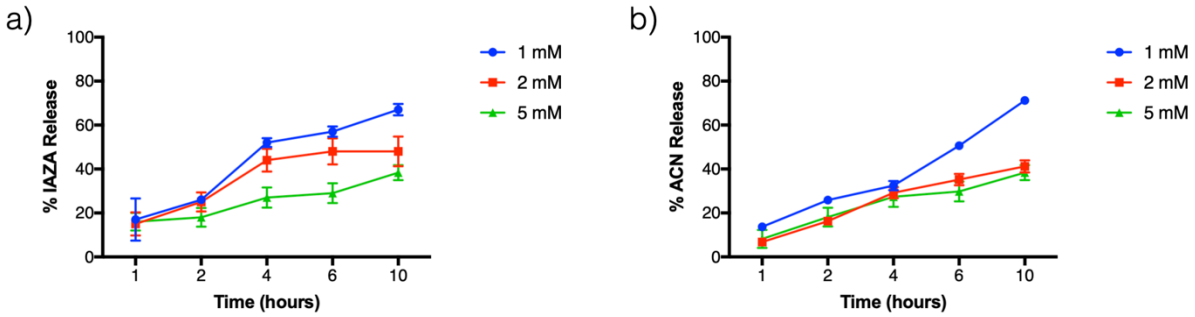

Figure 6S4. Release profile of encapsulated (a) IAZA and (b) ACN in modified FITC-labeled NG1 at 37 ˚C after 10 h.

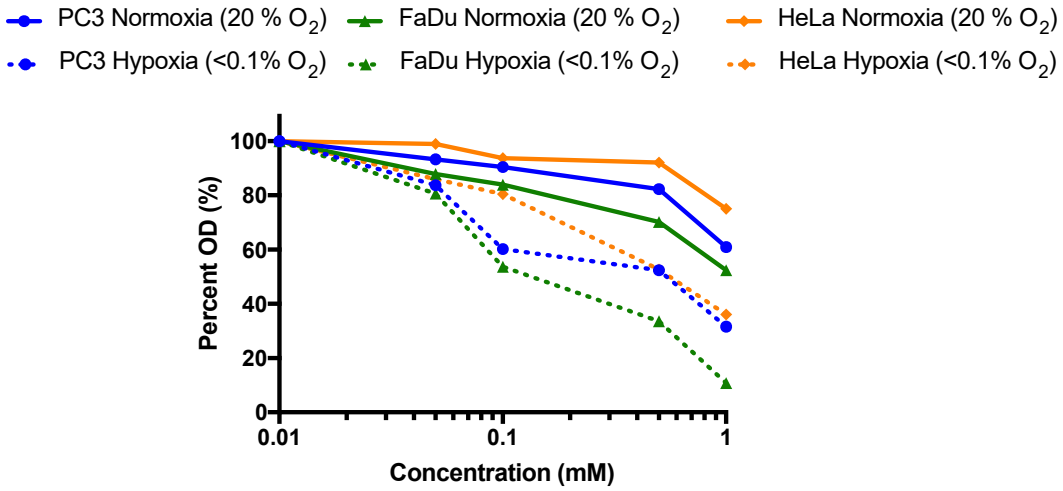

Figure 6S5. IAZA cytotoxicity under normoxia (20% O2) and hypoxia (<0.1% O2) conditions. ~2,000 cells were seeded on 96 well plates and left for 24 h to attach. Afterwards, cells were treated with increasing concentrations of IAZA, and incubated under normoxia (20% O_2) and hypoxia (<0.1% O_2) for 72 h. Following incubation, MTT

reagent was added; the formazan crystal formed was dissolved in 100 µL of dimethylsulfoxide: Isopropanol (1:1), and absorbance was measured at 570 nm using a Tecan Microplate reader. Untreated cells were used as a positive control, and the percentage of optical density (O.D.) was calculated with respect to the controls.

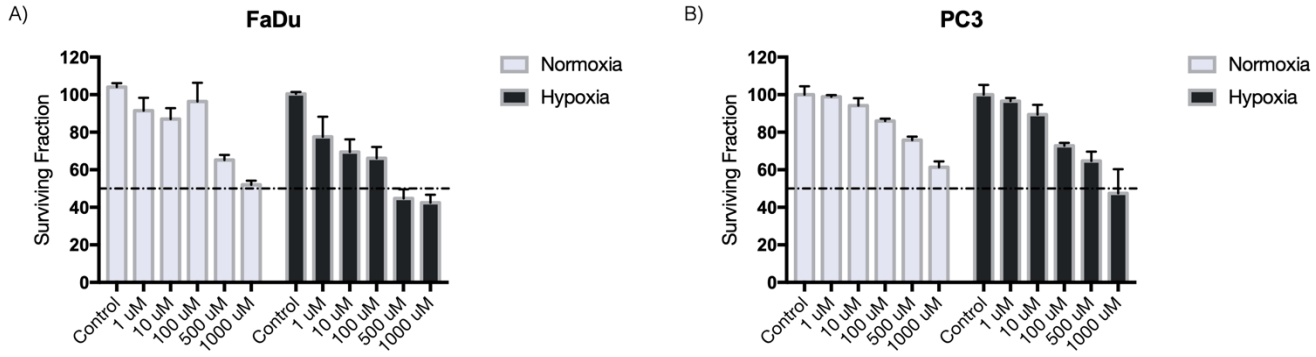

Figure 6S6. Colony formation assay in A) FaDu B) PC3 cells treated with either DMSO (control) (100 µM) or increasing concentration of IAZA (1 µM, 10 µM, 100 µM, 500 µM and 1000 µM) for 24 hours under normoxia and hypoxia (<1% O_2); cells were allowed to form colonies for 14 days, stained with crystal violet, counted and plotted as relative surviving fraction; error bars represent standard error of the means.